DISS. ETH NO. 21890

NOVEL COMPONENTS OF HUMAN PRERIBOSOMAL PARTICLES AND THEIR CONTRIBUTION TO RIBOSOME BIOGENESIS

A thesis submitted to attain the degree of

DOCTOR OF SCIENCES of ETH ZURICH

(Dr. sc. ETH Zurich)

Presented by

FRANZISKA WANDREY
MSc ETH in Biology, ETH Zurich

Born on May 7th, 1984
Citizen of Germany

Accepted on the recommendation of

Prof. Ulrike Kutay, examiner

Prof. Frédéric Allain, co-examiner

Prof. André Gerber, co-examiner

Prof. Pierre-Emmanuel Gleizes, co-examiner

2014

Summary

The production of ribosomes is one of the most energy consuming processes in a cell. In eukaryotes, ribosome biogenesis takes place in different cellular compartments and involves more than 200 non-ribosomal proteins, termed trans-acting factors. Most of these factors were identified in yeast, but their mechanistic function is still largely unknown. Even less is known about the composition and maturation pathway of preribosomal particles in human cells.
In this thesis, we set out to identify novel human trans-acting factors by tandem-affinity purification (TAP) of preribosomal particles and subsequent proteomic analysis by mass spectrometry. Thereby, we found two isoforms of casein kinase 1, CK1δ and CK1ε, to be components of pre-40S subunits. Chemical inhibition as well as siRNA-mediated depletion of both isoforms led to impairment of late 40S biogenesis steps, as detected by cytoplasmic recycling defects of the 40S trans-acting factors ENP1, PNO1, RIOK2, and RRP12. Notably, only co-inhibition or co-depletion of CK1δ and CK1ε led to this phenotype, suggesting their redundancy in this process. Additionally, CK1δ and CK1ε were required for cytoplasmic 18S rRNA maturation but not for export of pre-40S particles to the cytoplasm. Furthermore, *in vitro* kinase assays showed that the trans-acting factors ENP1 and LTV1 were phosphorylated on pre-40S subunits in a CK1-dependent manner. Taken together, these data led to the model that CK1δ and CK1ε are required for early cytoplasmic maturation steps of pre-40S, possibly for the release of LTV1 and ENP1 from these particles.
Using mass spectrometry analysis of pre-60S particles derived from TAP of human ZNF622, we identified NF45 and NF90 as novel components of pre-60S subunits. NF45 and NF90 form a heterodimeric complex and were previously shown to be involved in several cellular processes such as transcription, translation and antiviral response. We confirmed their association with pre-60S subunits by sucrose gradient assays as well as TAP using NF90 as bait. By using truncations and mutant forms of HASt-tagged NF90 in TAP experiments, we could show that binding of NF90 to pre-60S particles is dependent on the dsRBDs of NF90, whereas the ability to bind NF45 is disposable for association of NF90 to pre-60S. Localization studies

showed that NF90 and NF45 are nuclear proteins and enriched in nucleoli. Depletion of NF45 or NF90 by RNAi led to nuclear accumulation of pre-60S particles as well as reduced rRNA precursor levels. Furthermore, nucleolar shape and number was altered upon NF45 or NF90 depletion. Taken together, these data suggest that NF45 and NF90 are components of human pre-60S particles and play a role in early nuclear 60S biogenesis.

Zusammenfassung

Die Herstellung von Ribosomen ist einer der am meisten Energie verbrauchenden zellulären Prozesse. In Eukaryoten erfolgt die Biogenese von Ribosomen in verschiedenen zellulären Kompartimenten und benötigt mehr als 200 nichtribosomale Proteine, die sogenannten Biogenesefaktoren. Die meisten dieser Faktoren wurden in der Hefe *S. cerevisiae* identifiziert, ihre mechanistischen Funktionen sind jedoch noch weitestgehend unbekannt. Noch weniger weiss man allerdings über die Zusammensetzung und Maturation von ribosomalen Untereinheiten in menschlichen Zellen.

In dieser Doktorarbeit haben wir uns damit befasst, bisher unbekannte menschliche Biogenesefaktoren zu ermitteln, indem wir präribosomale Partikel mit Hilfe der Tandem-Affinitätsreinigungs(TAP)-Methode isoliert und ihre proteomische Zusammensetzung durch Massenspektrometrie analysiert haben. Dabei entdeckten wir, dass zwei Isoformen der Proteinkinase casein kinase 1, CK1δ und CK1ε, Bestandteile von Vorläufern der 40S Untereinheit (prä-40S) sind. Chemische Inhibition beider Isoformen sowie auch Herunterregulierung von beiden Isoformen mittels siRNAs führte zu einer Beeinträchtigung von späten 40S Biogeneseschritten, nachgewiesen durch einen Rezyklierungsdefekt der 40S Biogenesefaktoren ENP1, PNO1, RIOK2 und RRP12 im Zytoplasma. Bemerkenswert ist, dass nur gleichzeitige Hemmung oder Herunterregulierung beider Isoformen diesen Phänotyp hervorriefen, was auf eine Redundanz von CK1δ und CK1ε in diesem Prozess hinweist. Zusätzlich waren CK1δ und CK1ε für die Maturation der 18S rRNA im Zytoplasma notwendig, allerdings waren sie nicht für den Export von prä-40S Untereinheiten in das Zytoplasma erforderlich. Des Weiteren konnten wir mit Hilfe von *in vitro* Phosphorylierungsexperimenten zeigen, dass die Biogenesefaktoren ENP1 und LTV1, gebunden an prä-40S Partikel, in Abhängigkeit von CK1 phosphoryliert werden. Zusammenfassend führten diese Daten zu dem Modell, dass CK1δ und CK1ε notwendig für frühe Maturierungsschritte von prä-40S Partikeln im Zytoplasma und wahrscheinlich für die Ablösung von ENP1 und LTV1 von ebendiesen Partikeln verantwortlich sind.

Mittels massenspektrometrischer Untersuchungen von menschlichen prä-60S Partikeln, die durch TAP-Aufreinigungen des Biogenesefaktors ZNF622 gewonnen wurden, gelang es uns, die Proteine NF45 und NF90 als neue Komponenten von prä-60S Partikeln zu identifizieren. NF45 und NF90 bilden ein Heterodimer und ihnen wurde eine Rolle in verschiedenen zellulären Prozessen zugeschrieben, z.B. in der Transkription, Translation und antiviralen Abwehrreaktion. Wir bestätigten die Bindung von NF45 und NF90 an prä-60S Untereinheiten mit Hilfe von Saccharose-Gradient-Experimenten sowie mit TAP-Aufreinigungen von NF90. Indem wir verkürzte und mutierte Versionen von NF90 in TAP-Aufreinigungen verwendeten, konnten wir aufzeigen, dass die Bindung von NF90 an prä-60S Partikel abhängig von seinen dsRBDs (doppelsträngigen RNA Bindungsdomänen) ist, jedoch unabhängig von der Fähigkeit von NF90, an NF45 zu binden. Lokalisierungsstudien haben gezeigt, dass NF45 und NF90 nukleäre Proteine und insbesondere in Nucleoli angereichert sind. Herunterregulierung von NF45 oder NF90 durch RNAi führte zu einer Ansammlung von prä-60S Untereinheiten im Zellkern sowie zu reduzierten Mengen von unreifen rRNA Vorstufen. Weiterhin wurden nach Herunterregulierung von NF45 und NF90 eine veränderte Form und verringerte Anzahl von Nucleoli innerhalb der Zelle festgestellt. Zusammenfassend können wir aus diesen Daten schlussfolgern, dass NF45 und NF90 Bestandteile von menschlichen prä-60S Partikeln sind und eine Rolle in der Synthese von prä-60S Untereinheiten im Zellkern spielen.

Table of Contents

1. Introduction

Ribosomes consist of a small and a large subunit (in eukaryotes 40S and 60S subunits, respectively), which are composed of ribosomal RNA (rRNA) and ribosomal proteins. Their structure and function is highly conserved throughout all kingdoms of life. Ribosomes catalyze translation of mRNA into proteins, one of the fundamental processes in every organism. Therefore, most of the cellular resources and energy is utilized to produce new ribosomes. In a growing yeast cell, approximately 2000 ribosomes are synthesized per minute, and 60% of total transcription is used to produce new rRNA (Warner, 1999). It is therefore essential for the energy management of a cell that the biogenesis of such a sophisticated macromolecular complex takes place in a correct and timely fashion. While bacterial ribosomes are able to assemble *in vitro* by combining rRNA and ribosomal proteins without any accessory components (Traub and Nomura, 1969; Held et al., 1973), there are assembly factors *in vivo* that accelerate rRNA folding, processing and binding to ribosomal proteins (reviewed in (Shajani et al., 2011)). In eukaryotes, ribosome biogenesis takes places in different cellular compartments (reviewed in chapter 1.2) and requires the help of a plethora of trans-acting factors that associate with preribosomal particles at different steps during the maturation pathway and perform diverse enzymatic functions to ensure coordinated assembly.

This work led to the identification of novel trans-acting factors in human cells and investigated their contribution to ribosome biogenesis.
In the first part of the introduction, a closer look will be taken at the nucleolus and its properties during the cell cycle and in response to external stresses. This is followed by a general introduction of ribosome biogenesis in the budding yeast *Saccharomyces cerevisiae* and a comparison to the pathway in higher eukaryotes, in particular human cells. Finally, an overview of the NF45/NF90 complex and its known functions is given since a large part of this thesis covers findings of a novel role for this extensively studied complex.

1.1 The nucleolus – site of ribosome production

Nucleoli were first discovered as dark spots in blastocyst nuclei (Wagner, 1835) but it took more than 100 years to elucidate their role in ribosome biogenesis (reviewed in (Hadjiolov, 1985)). In eukaryotic cells, the nucleolar organizer regions (NOR) (McClintock, 1934), which contain the ribosomal DNA (rDNA) repeats (Miller and Beatty, 1969), cluster together with associated proteins to form nucleoli. There, transcription of rRNA by RNA polymerase I (POL I) and rRNA modification/processing take place in an organized manner (further reviewed in chapter 1.2.1). Mass spectrometry analysis created an overview of all proteins present in nucleoli; a nucleolar proteome database has been established, containing more than 4500 putative nucleolar proteins to date (Ahmad et al., 2009; Leung et al., 2006). This relatively high number is most likely on one hand due to the sensitivity of the detection method; on the other hand it has been reported that the nucleolar composition is varying and can fluctuate rapidly depending on cellular state and external cues (Phair and Misteli, 2000; Andersen et al., 2005; Olson and Dundr, 2005). Even under normal growth conditions, there is a high flux and exchange of proteins between nucleoli in the same nucleus (Muro et al., 2008). Furthermore, the nucleolus has additional functions apart from ribosome synthesis, which can explain the protein diversity within (reviewed in (Boisvert et al., 2007; Emmott and Hiscox, 2009)).

1.1.1 Organization of the nucleolus

The nucleolus in higher eukaryotes is composed of three compartments that can be distinguished by electron microscopy (EM): the inner fibrillar center (FC), the dense fibrillar component (DFC) and the granular component (GC) (Fig. 1.1) (Goessens, 1984; Hernandez-Verdun, 1986; Jordan, 1991).

The rDNA is clustered in the FC and POL I-dependent rRNA transcription takes place at the FC/DFC border. Proteins that are involved in the transcription process, such as the vertebrate-specific upstream binding factor UBF, (see chapter 1.2.1), are used to mark this nucleolar compartment. Interestingly, lower eukaryotes but also insects and turtles do not possess a FC (Knibiehler et al., 1984; Thiry and Lafontaine, 2005).

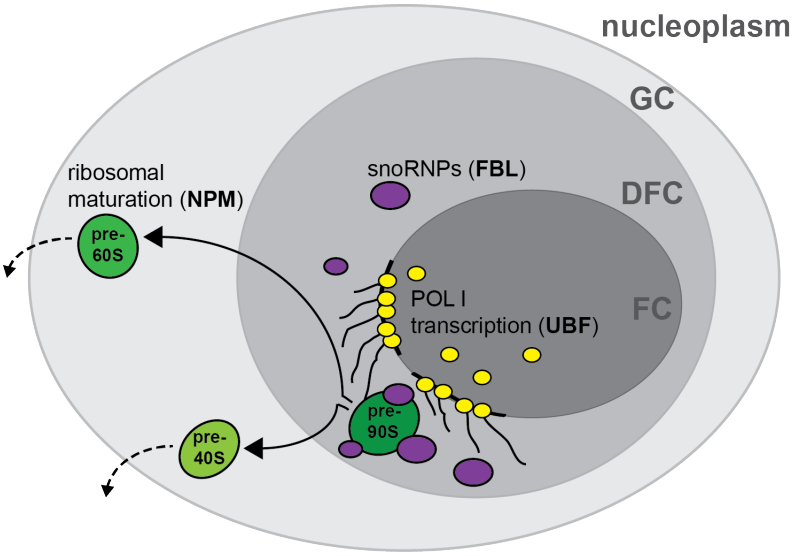

Figure 1.1
Scheme of nucleolar compartments
The three nucleolar compartments fibrillar center (FC), dense fibrillar component (DFC) and granular component (GC) are shown along with different steps in ribosome biogenesis.
Proteins used in this study as markers for the different components are shown in brackets.

In the DFC, the nascent rRNA transcript associates with ribosomal proteins and early assembly factors. At this stage, rRNA modification/processing occurs, mediated by small nucleolar ribonucleoproteins (snoRNPs) and trans-acting factors. Upon endonucleolytic cleavage of the rRNA precursor (see also chapter 1.2.1 for more details on rRNA modification and processing), the pre-60S and pre-40S particles, precursors of the large and small ribosomal subunits, respectively, are released into the GC. In this component, which received its name from granules observed by EM that presumably correspond to pre-60S subunits, additional trans-acting factors join the preribosomal particles. These factors accompany the preribosomal subunits to the nucleoplasm or even further to the cytoplasm.

1.1.2 Changes in nucleolar size and number

The size and number of nucleoli per cell generally reflect the activity of ribosome production. While nucleoli are small in differentiated cells and larger in dividing cells, their size can be increased even further in cancer cells ((Dubben, 1990; Derenzini et al., 2000; Belin et al., 2009), also reviewed in (Montanaro et al., 2008)). Also, the amount of nucleoli per nucleus varies by cell type and malignant cancers display more NORs and nucleoli (Shea and Leblond, 1966; Bratulic et al., 1996). Further, inhibition of POL I transcription leads to nucleolar disruption by segregation of FC, DFC, and GC (Puvion-Dutilleul et al., 1997; Hernandez-Verdun, 2006). This disruption can in turn

influence cell cycle progression by activation of the p53 pathway (discussed in detail in chapter 1.3).

Nucleoli assemble at several NORs after mitosis, but in early G1 phase in HeLa cells, nucleoli are fusing within a few minutes after contact and nucleolar number decreases (Savino et al., 2001; Yamauchi et al., 2007). This nucleolar fusion can be induced in *Xenopus laevis* oocytes using a microneedle. The fusion and the resulting spherical shape could be attributed to liquid droplet-like behavior of nucleoli and seems to be ATP dependent (Brangwynne et al., 2011). However, little is known about the fusion mechanism and the involved factors.

1.2 Ribosome biogenesis overview

The budding yeast *Saccharomyces cerevisiae* has been a model organism for ribosome biogenesis for decades and most of our knowledge on the synthesis of ribosomal subunits in eukaryotes derives from it. Ribosome biogenesis requires the action of all three RNA polymerases and requires the release of preribosomal particles from the nucleolus to the nucleoplasm and export to the cytoplasm (Fig. 1.2). The ribosome synthesis pathway involves over 200 trans-acting factors that, inter alia, drive ribosome assembly, rRNA modification and processing, subunit export through the nuclear pore complex (NPC) and perform regulatory functions to ensure accurate synthesis of ribosomes (reviewed in (Fromont-Racine et al., 2003; Tschochner and Hurt, 2003; Henras et al., 2008; Kressler et al., 2010; Thomson et al., 2013)). The importance of these trans-acting factors is highlighted by the fact that many of them are essential. While the inventory of yeast trans-acting factors has largely been discovered by the systematic biochemical purification of preribosomal particles at different steps of ribosome biogenesis followed by proteomic analysis (Bassler et al., 2001; Harnpicharnchai et al., 2001; Fatica et al., 2002; Grandi et al., 2002; Dragon et al., 2002; Nissan et al., 2002; Schäfer et al., 2003), the mechanistic role of many of these factors remains to be elucidated.

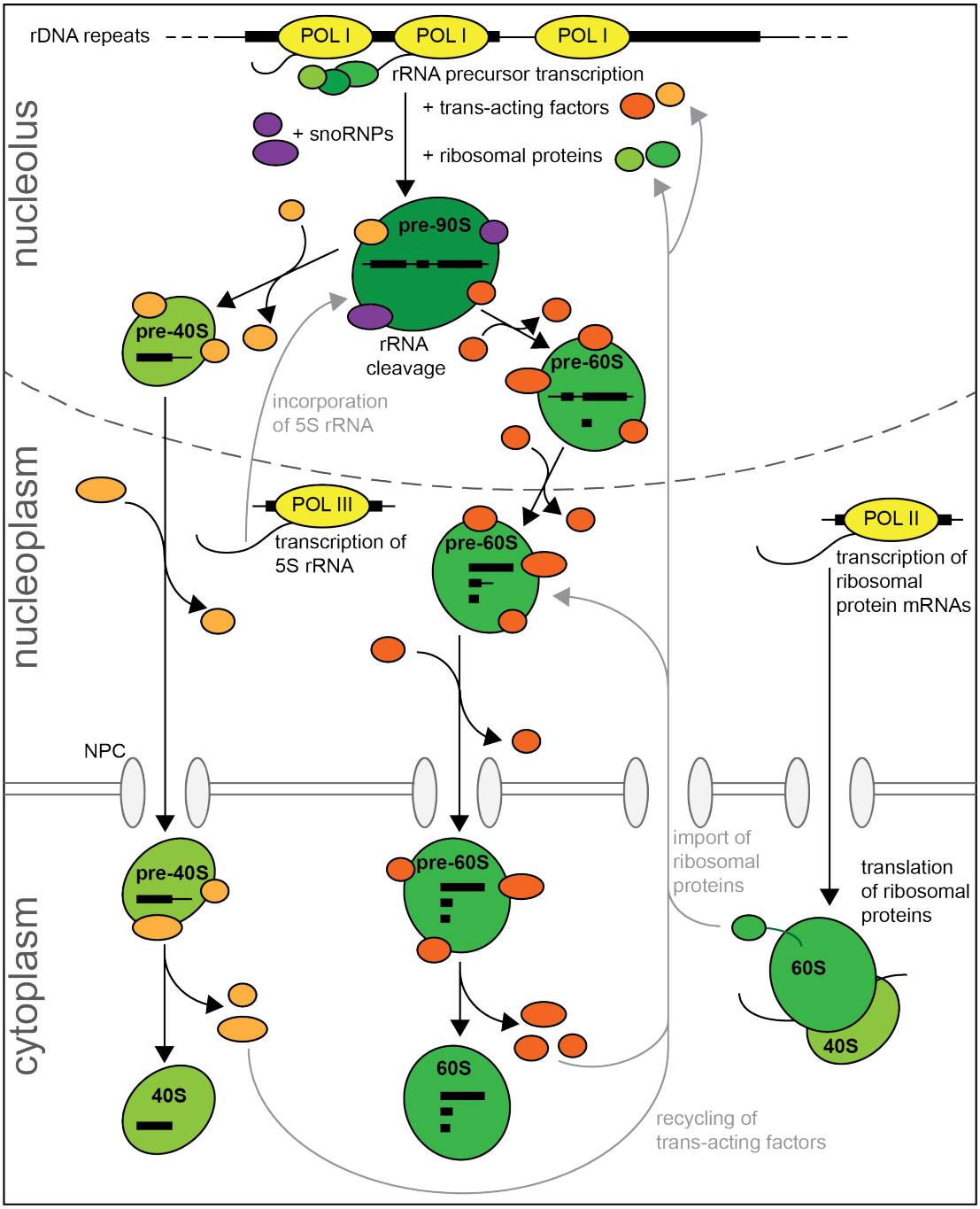

Figure 1.2
Overview of ribosome biogenesis in eukaryotes
Eukaryotic ribosome biogenesis starts in the nucleolus where a long rRNA precursor is transcribed by POL I. Binding of ribosomal proteins and trans-acting factors to the rRNA leads to the formation of a pre-90S particle. Cleavage of the rRNA precursor yields a pre-40S and pre-60S particle, which are further processed, assembled and exported through the NPC to the cytoplasm where final maturation steps occur in order to produce translational competent ribosomal subunits. Released trans-acting factors are recycled for another round of ribosome synthesis. POL II-transcribed mRNAs encoding ribosomal proteins are translated in the cytoplasm and ribsoomal proteins are imported into the nucleus for incorporation into preribosomal particles. For a more detailed description of the pathway, see text.

While ribosome biogenesis has been extensively studied in yeast, comparatively little is known about the pathway in higher eukaryotes. Although it is generally assumed that the core pathway is conserved, recent studies have shown that there are notable differences in ribosome synthesis in higher eukaryotes, which will be highlighted below.

1.2.1 Ribosome composition

The yeast 60S ribosomal subunit consists of three rRNA species: 25S, 5.8S and 5S rRNA, and 46 proteins (ribosomal proteins of the large subunit or RPL), whereas the 40S subunit contains the 18S rRNA and 33 proteins (ribosomal proteins of the small subunit or RPS) (Kressler et al., 2010). In humans, 60S consist of 28S, 5.8S and 5S rRNA and 48 RPL proteins, and 40S are made up of 18S rRNA and 34 RPS proteins. Together, they form the 80S ribosome, which can engage in translation.

The structures of the *S. cerevisiae* and human 80S ribosomes have been solved by cryo-electron microscopy (cryo-EM) (Spahn et al., 2001; Taylor et al., 2009; Anger et al., 2013), and a crystal structure of yeast 80S ribosomes at 3 Å resolution has been obtained (Ben-Shem et al., 2011). Recently, an effort has been undertaken to crystallize human 80S ribosomes for structural analysis (Khatter et al., 2014). Although the resolution was quite poor, this represents an important step towards a high-resolution structure of the human ribosome. Taken together, these structures, along with structural analysis of ribosomal subunits from other eukaryotic organisms in complex with trans-acting or translation initiation factors (Greber et al., 2012; Klinge et al., 2011; Weisser et al., 2013), have revealed that the overall composition and function of the ribosome is remarkably conserved. Yet, there are important differences that developed over the course of evolution. Compared to structures of their prokaryotic counterparts, eukaryotic ribosomes possess more ribosomal proteins with longer domain extensions as well as more than 20 stretches of additional rRNA called expansion segments. For example, these expansion segments comprise about 2500 extra nucleotides (nt) for human ribosomes compared to *E. coli* ribosomes (reviewed in (Wilson and Doudna Cate, 2012; Klinge et al., 2012; Melnikov et al., 2012). Even when comparing yeast and

human ribosomes, the expansion segments are more than thousand nt longer in the latter (Anger et al., 2013). Their function is debated and mostly unknown but it is suggested that these rRNA expansion segments possess a function in providing novel binding platforms for trans-acting and/or translation factors. Additionally, they could provide binding sites for proteins that interconnect ribosome biogenesis and other signaling pathways (Gao et al., 2005; Rabl et al., 2011). This might reflect that the higher complexity of eukaryotes or even multicellular organisms demands additional pathways to regulate the production of ribosomes.

A good example on how a change in ribosome composition can lead to specialization is the mitochondrial ribosome. Recently, the structure of the porcine (*Sus scrofa*) large mitochondrial ribosomal subunit was solved by cryo-EM, which showed that considerable remodeling led to a specification in translating the predominantly hydrophobic mitochondrial transmembrane proteins (Greber et al., 2014). Even within one organism or cell, heterogeneity of ribosome composition and post-translational modification has been suggested, perhaps conferring specialized activity to ribosome subpopulations (Xue and Barna, 2012).

1.2.2 rRNA transcription, modification and processing

rRNA transcription initiation and regulation

The rDNA in *S. cerevisiae* is organized in about 150 repeats of 9.1 kb rDNA genes, which are located on one chromosome. In humans, the five acrocentric chromosomes contain clusters of repeated 43 kb rDNA genes that are able to form NORs (Henderson et al., 1972; Gonzalez and Sylvester, 1995). The length of each cluster varies greatly between individuals from 50 kb to > 6 Mb (Stults et al., 2007). Also, not all rDNA repeats are transcriptionally active; about half of the rDNA genes are in a silent heterochromatic state (Conconi et al., 1989; Santoro and Grummt, 2001; Guetg and Santoro, 2012).

POL I transcription of rDNA in yeast yields polycistronic 35S rRNA precursors that contain the 18S, 5.8S and 25S rRNA species (Fig. 1.2 and 1.4). Each rDNA gene contains two upstream promoter elements to which transcription

factor complexes bind in order to initiate transcription. In yeast, the upstream element (UE) is bound by the upstream activity factor (UAF) complex, which triggers binding of the transcription core factor complex (CF) associated with the TATA box binding protein (TBP) to the core element (CE). This in turn leads to recruitment of POL I by Rrn3 (Peyroche et al., 2000) and transcription initiation (Fig. 1.3A) (reviewed in (Moss, 2004; Vannini, 2013)).

The process is similar in humans (Fig. 1.3B): the 47S rRNA precursor contains the 18S, 5.8S and 28S rRNA species (Fig 1.4). The UE is bound by an upstream binding factor (UBF) dimer, which is responsible for rDNA decondensation and transcriptional activation (Bell et al., 1988; Mais et al., 2005; Sanij et al., 2008; Sanij and Hannan, 2009). The CF analog SL1 along with TBP binds the CE and recruits POL I with the Rrn3 homolog TIF-1A (Fig. 1.3B) (Bodem et al., 2000; Miller et al., 2001).

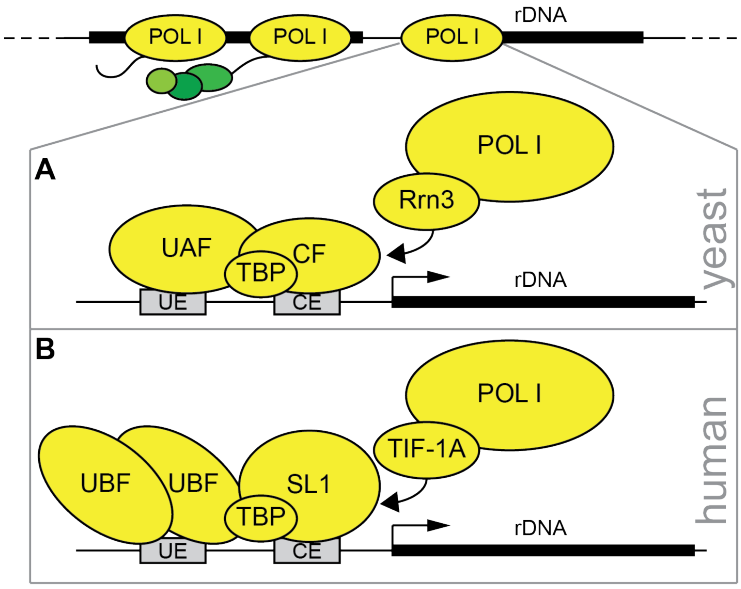

Figure 1.3
POL I transription initiation
The POL I transcription initiation complex in **(A)** yeast and **(B)** humans.
Two types of transcription factor complexes need to bind the rDNA promoter: the upstream transcription factor UAF/UBF binds the upstream element (UE) and the core transcription factor complex CF/SL1 associated with the TATA box binding protein (TBP) binds the core element (CE). This leads to the recruitment of POL I along with Rrn3/TIF-1A and initiation of rRNA transcription.

Not only POL I transcription is needed for ribosome synthesis. Ribosomal protein genes are transcribed by RNA polymerase II (POL II) (Fig. 1.2). It has been suggested that there is a crosstalk between POL I transcription activity and POL II transcription specifically of ribosome components (Laferté et al., 2006).

Moreover, the 5S rRNA, which is present in 60S subunits, is not encoded by the long rDNA precursor. In yeast, 5S rDNA is situated in a region between the rDNA repeats flanked by nontranscribed regions NTS1 and NTS2 (Nomura et al., 2004). It is transcribed by RNA polymerase III (POL III), which

is also responsible for transcription of tRNAs and the spliceosome component U6 small nuclear RNA. The rDNA encoding for 5S rRNA in higher eukaryotes is present in tandem repeats on a region that is neither linked to the 47S precursor rDNA nor part of NORs (Long and Dawid, 1980). Therefore, the 5S rRNA is transcribed by POL III in the nucleoplasm and has to be targeted to the nucleolus. 5S rRNA forms a complex with the ribosomal proteins RPL5 and RPL11 prior to incorporation into nascent ribosomes (Zhang et al., 2007). While it was assumed for a long time that the 5S-L5-L11 RNP is incorporated into pre-60S subunits after rRNA precursor cleavage (Warner and Soeiro, 1967), more recent data show that it is already associated with pre-90S particles (Zhang et al., 2007).

In response to external stimuli and intracellular signals, a cell can quickly adapt its growth and proliferation rate by regulating ribosome synthesis, mainly by signaling cascades that target the nucleolus and rRNA transcription. One pathway implicated in the regulation of POL I transcription is the target of rapamycin (TOR) pathway with the TORC1 (mTORC1 in mammalian cells) complex that serves as a central node in coordination of nutrient sensing and cell growth (Wullschleger et al., 2006; Lempiäinen and Shore, 2009). This complex contains the TOR kinase that, when active under favorable nutrient conditions, phosphorylates Rrn3/TIF-1A so that it can interact with and recruit the POL I complex to rDNA (Mayer et al., 2004). Furthermore, mTORC1 indirectly leads to phosphorylation of UBF, which is required for its interaction with rDNA (Hannan et al., 2003). TORC1 also upregulates POL II transcription of ribosomal protein genes in yeast through activation of the transcription factor Sfp1 (Marion et al., 2004).
In mammalian cells, the proto-oncogene c-Myc has been described to share properties of Sfp1: its overexpression leads to increased cell size and expression of ribosomal proteins (Kim et al., 2000; Jorgensen et al., 2004). Further, the transcription factor c-Myc stimulates POL I transcription of rRNA by binding and recruiting SL1 to rDNA and stabilizing the SL1/UBF association (Grandori et al., 2005; Arabi et al., 2005). POL III transcription of 5S rRNA is also upregulated by c-Myc (Felton-Edkins et al., 2003; Gomez-

Roman et al., 2003) as is the transcription of UBF (Poortinga et al., 2004) and certain trans-acting factors, such as higher eukaryote-specific nucleophosmin/ NPM, required in several 60S biogenesis steps (Zeller et al., 2001; Colombo et al., 2011) and Dyskerin (see below) (Schlosser et al., 2003). Taken together, c-Myc has been proposed as a master regulator of ribosome biogenesis. However, the specificity of its effect on ribosome biogenesis has recently been challenged by the findings that it acts as a pleiotropic if not universal activator of transcription (Lin et al., 2012; Nie et al., 2012). Notably, c-Myc expression is upregulated in many tumors. The oncogenic potential of c-Myc can be inhibited by RPL11 (Dai et al., 2007; Dai et al., 2010), which also plays a major role in activation of the tumor suppressor p53 (see chapter 1.3).

rRNA modification by snoRNPs

One of the first class of trans-acting factors to cotranscriptionally bind the rRNA precursor in the DFC of the nucleolus is the small nucleolar RNA (snoRNA) containing snoRNPs (see Fig. 1.1 and 1.2). There are about 75 snoRNPs in yeast (about 150 in humans) that modify and help in folding and processing of newly transcribed rRNA. The two main modifications accomplished by snoRNPs on rRNA are 2'-O-methylation and pseudouridylation, which are catalyzed by box C/D snoRNPs and H/ACA-containing snoRNPs, respectively (Cavaillé et al., 1996; Kiss-László et al., 1996; Ganot et al., 1997; Ni et al., 1997). The snoRNPs consist of a snoRNA, which guides the complex to the target rRNA sequence, and four core proteins. Box C/D snoRNAs are about 100 nt in length and associated with the core proteins Snu13 (15.5K/NHPX in humans), Nop56, Nop58 and the methyltransferase Nop1 (Fibrillarin/FBL in humans). For the ~200 nt H/ACA snoRNAs, the core proteins are Nhp2, Nop10, Gar1, and the catalytic subunit is Cbf5 (Dyskerin in humans) (Watkins and Bohnsack, 2012).

Many factors are involved in the biogenesis of snoRNPs, which need to be processed, assembled and transported from the nucleoplasm to the nucleolus (Lafontaine and Tollervey, 1998; Kiss et al., 2006). Additionally, there are several helicases involved that either facilitate binding of snoRNAs to rRNA or

snoRNA release after modification (Liang and Fournier, 2006). Interestingly, while most yeast snoRNA genes are monocistronic, most human snoRNA genes are located in introns of housekeeping genes required for ribosome biogenesis (Yang et al., 2006; Dieci et al., 2009).

The number of rRNA residues modified by these snoRNPs is not conserved between species (~100 modifications in yeast vs. ~200 in humans), but modified sites are found predominantly in functionally important regions such as the ribosomal A- and P-site and the intersubunit bridge (Decatur and Fournier, 2002; Decatur et al., 2007). While deletion of a single snoRNA does not display a strong phenotype, co-deletion of several snoRNAs leads to impaired translation and severe growth defects. Further, the methyltransferase Nop1/FBL is essential for development and survival (King et al., 2003; Newton et al., 2003; Tollervey et al., 1991). Therefore, although the specific role of these modifications has not yet been discovered, it is proposed that they collectively stabilize rRNA to support ribosome function. Furthermore, some snoRNPs, such as the U3 box C/D snoRNP and snR10 and snR30 box H/ACA snoRNPs, are also involved in rRNA processing (Hughes and Ares, 1991; Kass et al., 1990; Morrissey and Tollervey, 1993; Peculis and Steitz, 1993).

An often-fatal disease associated with snoRNP dysfunction in humans is X-linked dyskeratosis congenita (X-DC). A mutation in Dyskerin, the catalytic subunit of H/ACA snoRNPs, leads to impaired translation of internal ribosome entry site (IRES)-containing mRNAs. Some of these mRNAs encode tumor suppressors such as p27 and p53 (see also chapter 1.3), which could explain the high cancer susceptibility of X-DC patients (Bellodi et al., 2010a; Bellodi et al., 2010b; Yoon et al., 2006). Overexpression of the methyltransferase FBL also leads to tumorigenesis. It is thought that overmethylation of rRNA leads to a decrease in translational fidelity and changes in translation pattern (Marcel et al., 2013). Furthermore, FBL was recently shown to not only methylate RNA but also a glutamine residue on histone H2A specifically in nucleoli resulting in reduced POL I transcription (Tessarz et al., 2014).

One important rRNA modification that takes place independently of snoRNPs is the dimethylation of 18S rRNA. In yeast, Dim1 catalyzes the methylation of two adenines close to the 3' end of the 18S rRNA in the cytoplasm (Brand et al., 1977; Lafontaine et al., 1995). Although the presence of Dim1 is required for 18S rRNA processing (Lafontaine et al., 1995), expression of a catalytically inactive mutant blocked dimethylation but not rRNA processing (Lafontaine et al., 1995). It appears, however, that this modification is still essential for 40S function since 40S subunits lacking this modification are unable to catalyze translation *in vitro* (Lafontaine et al., 1995).

rRNA processing

The rRNA present in mature 40S and 60S subunits, except for the 5S rRNA, are transcribed as one polycistronic precursor, from which the external and internal transcribed spacers (ETS and ITS, respectively) have to be cut off during rRNA maturation. This involves a series of RNA cleavage and processing events that take place in the nucleolus, nucleoplasm and cytoplasm and is mediated by several endo- and exonucleases (Fig. 1.4). While many factors involved in specific rRNA processing steps have been identified in yeast, comparatively little is known about rRNA processing factors in human cells. It is questionable whether all of the respective human homologs perform the same task, especially since there are significant differences in the order of cleavage events, in the lengths of ETS/ITS, and precursor species (Fig. 1.4 and reviewed in (Mullineux and Lafontaine, 2012)). In yeast, the first processing steps of rRNA are carried out cotranscriptionally (Gallagher et al., 2004; Osheim et al., 2004). First, the 5'-ETS and 3'-ETS on both sides of the precursor are removed. Subsequently, endonucleolytic cleavage at site A_2 in the ITS1 catalyzed by Rcl1 (Horn et al., 2011) leads to separation of the pre-90S particle into pre-40S and pre-60S particles (Fig. 1.2 and 1.4). These first cleavage steps are dependent on the U3 snoRNP, which is part of the small subunit (SSU) processome (Bernstein et al., 2004; Dragon et al., 2002; Grandi et al., 2002).

In human cells, an alternative pathway exists where cleavage in the ITS1 precedes processing of the 5'ETS (Fig. 1.4B) (Hadjiolova et al., 1993;

Rouquette et al., 2005). Furthermore, the human 5'-ETS contains an additional cleavage site that is not present in yeast (Fig. 1.4B).

After these first cleavage steps, both preribosomal subunits undergo further rRNA processing events (Fig. 1.4). In yeast, pre-40S particles containing the 20S rRNA precursor after cleavage at site A_2 are exported to the cytoplasm without further nucleoplasmic rRNA processing steps. In the cytoplasm, the 3' end of the 20S rRNA is cleaved off at site D by the endonuclease Nob1 to yield mature 18S rRNA (Fig. 1.4A) (Fatica et al., 2003; Fatica et al., 2004; Lamanna and Karbstein, 2009).
In human cells, pre-40S particles undergo rRNA processing events in the nucleoplasm, which results in formation of the 18S-E rRNA precursor (Fig. 1.4B). The mechanism, which leads to 18S-E rRNA formation, is debated; endonucleolytic as well as exonucleolytic processing have been suggested, as well as both happening successively (Carron et al., 2011; Wang and Pestov, 2011; Preti et al., 2013). The 18S-E rRNA is then cleaved in the cytoplasm at site 3 to yield 18S rRNA, possibly by the Nob1 homolog, NOB1 (Rouquette et al., 2005).

Processing of the rRNA in the pre-60S particle takes place in the nucleus and is much more complex than in pre-40S particles because it involves several endonucleolytic cleavage steps as well as exonucleolytic trimming of ITS1 and ITS2 (Fig. 1.4) (reviewed in Henras et al., 2008). These steps are not strictly ordered and alternative pathways with a different order of processing steps are possible (Fig. 1.4).
Alternative 28S/5.8S rRNA processing pathways also exist in human cells and some similarities to yeast have been shown. For example, the PES1/BOP1/WDR12 (PeBoW) complex in humans was proposed to mediate cleavage of an early 28S rRNA precursor. Its yeast homolog, the Nop7/Erb1/Ytm1 complex, has previously been shown to play a role in 28S rRNA maturation (Hölzel et al., 2005; Miles et al., 2005; Strezoska et al., 2000). However, there are also considerable differences between humans and yeast in respect to rRNA processing events in pre-60S particles. For

example, while the MRP RNase is required for cleavage at the A_3 site in yeast (Lygerou et al., 1996), it does not seem to be required for ITS1 processing in human cells (Sloan et al., 2013b). Moreover, components of the RISC complex that do not possess a homolog in yeast have been suggested to be required for correct 5.8S rRNA production (Liang and Crooke, 2011).

A congenital disease associated with the failure of efficient ITS1 processing and ribosome assembly in humans is Diamond-Blackfan anemia (DBA), characterized by bone marrow failure and malformations (Lipton and Ellis, 2009; Ellis and Gleizes, 2011). Intriguingly, the disease is caused by mutations in genes for ribosomal proteins leading to haploinsufficiency (Boria et al., 2010). This demonstrates that, while ribosomal proteins are not the enzymes directly catalyzing rRNA processing steps, their presence is of utmost importance for efficient rRNA cleavage. It is likely that binding of ribosomal proteins to rRNA leads to structural changes that facilitate rRNA processing (O'Donohue et al., 2010; Preti et al., 2013).

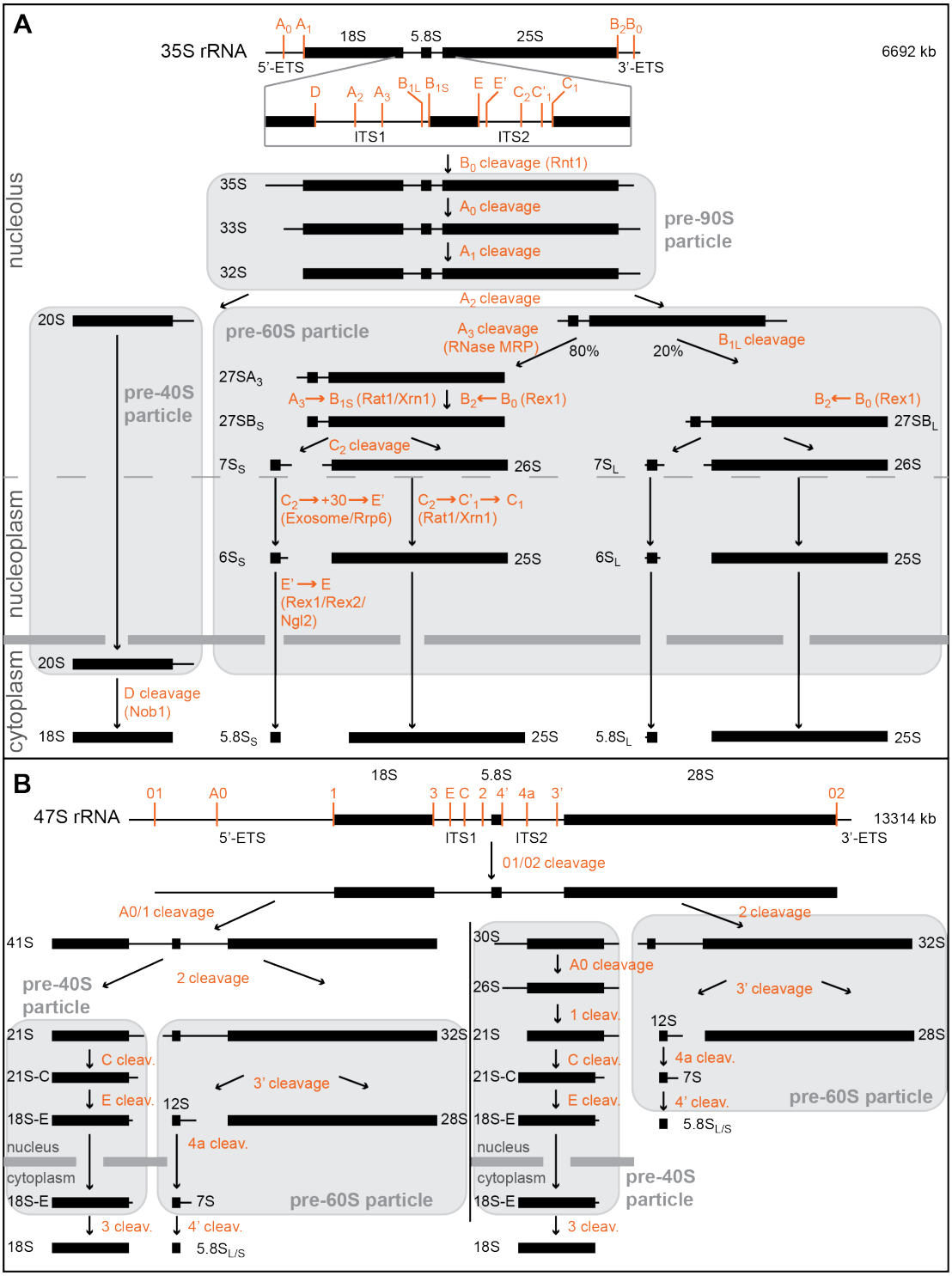

Figure 1.4
rRNA processing pathways in yeast and humans
Schematic representation of rRNA precursors and processing events in **(A)** yeast and **(B)** humans. The long polycistronic 35S/47S rRNA precursors are drawn to scale on top with the mature rRNA species as black boxes and lines depicting the external and internal transcribed spacers (ETS and ITS, respectively). Cleavage sites are indicated in orange and alternative cleavage pathways are shown below with processing factors indicated in orange where known. (adapted from Henras et al., 2008; Mullineux and Lafontaine, 2012)

1.2.3 Nuclear maturation steps

Concomitantly to POL I transcription of 35S/47S rRNA, mainly SSU ribosomal proteins and early 40S trans-acting factors assemble at the 5' end of the rRNA precursor to form a pre-90S particle (Fig. 1.2) (Grandi et al., 2002). After early rRNA modification and processing events (see chapter 1.2.2), the pre-90S particle separates into a pre-40S and pre-60S particle and many of the early trans-acting factors dissociate during that cleavage step. While the further maturation of pre-40S and pre-60S is largely independent, there are some factors that are required for maturation of both ribosomal subunits (Venema and Tollervey, 1999).

Pre-40S particles do not undergo many assembly steps in the nucleoplasm and are quickly exported through the NPC to the cytoplasm for final maturation. In contrast, many LSU ribosomal proteins and trans-acting factors bind and process pre-60S particles in the nucleus after 90S precursor cleavage. The composition of different yeast 60S precursor intermediates has been analyzed by tandem-affinity purification followed by mass spectrometry (Bassler et al., 2001; Harnpicharnchai et al., 2001; Fatica et al., 2002; Nissan et al., 2002; Saveanu et al., 2003; Woolford and Baserga, 2013). Several of the identified 60S trans-acting factors are helicases, GTPases, and AAA-ATPases, which suggests that several energy-dependent remodeling steps of pre-60S are governed by these enzymes in the nucleus. However, precise roles of these factors are largely unknown (Strunk and Karbstein, 2009). A mechanism of action has been proposed for the ATPase Rea1, which is associated with pre-60S in the nucleus, forming a tail visible in EM due to its large size of about 550 kDa (Galani et al., 2004; Nissan et al., 2004; Ulbrich et al., 2009). ATP hydrolysis by Rea1 leads to its dissociation along with other trans-acting factors, and thereby causes a structural rearrangement of pre-60S. This renders pre-60S particles competent for export, allowing the export adaptor protein Nmd3 to bind on a site that was previously occupied by the GTPase Nug2 (Matsuo et al., 2014).

In humans, the composition of only a few pre-60S particles is known so far (Yanagida et al., 2001; Fujiyama et al., 2002; Hayano et al., 2003; Wild et al., 2010). A systematic analysis of mammalian pre-60S particle composition at

different maturation steps has not yet been undertaken. This would certainly aid in identifying similarities and divergences from the yeast ribosome assembly pathway.

1.2.4 Nuclear export of preribosomal particles

One major task in the biogenesis of ribosomes is the export of preribosomal subunits from the nucleus to the cytoplasm. This export occurs through nuclear pore complexes (NPCs) embedded in the nuclear envelope. In growing yeast cells, one preribosomal particle is transported through each NPC approximately every three seconds (Warner, 1999). This is a tremendous task, considering that the large preribosomal particles, which have a hydrophilic surface, need to navigate through the hydrophobic FG-repeat meshwork in the nuclear pore efficiently and in a directed manner. In addition, only preribosomal subunits that have undergone the necessary nuclear maturation steps are permitted to export through the NPC. Thus, it is not unexpected that several factors have been proposed to aid in the export of preribosomal particles, as discussed below.

Export of preribosomal subunits in yeast

In order to identify proteins involved in preribosomal particle export in yeast, candidate factors were depleted or mutated and a visual readout was used to detect possible export impairments. Specifically, ribosomal subunits were either labeled with a fluorophore or rRNA precursors were detected by fluorescence *in situ* hybridization (FISH). A nuclear accumulation of fluorescent signal would implicate that preribosomal subunit export is disturbed. Using these methods, it has been shown that a number of nucleoporins (Nups), constituents of the NPC, as well as a functional Ran-GTPase cycle is needed for pre-40S (Gleizes et al., 2001; Moy and Silver, 1999; Moy and Silver, 2002) as well as pre-60S export (Gleizes et al., 2001; Hurt et al., 1999; Stage-Zimmermann et al., 2000). Furthermore, the exportin Crm1 that utilizes the Ran cycle for directional transport (see Fig. 1.5A) is essential for the export of both pre-40S and pre-60S particles (Gadal et al., 2001; Ho et al., 2000; Moy and Silver, 2002). Crm1 binds cargo molecules

that possess a leucine-rich nuclear export signal (NES) and facilitates their transport through the NPC by interacting with Nups.

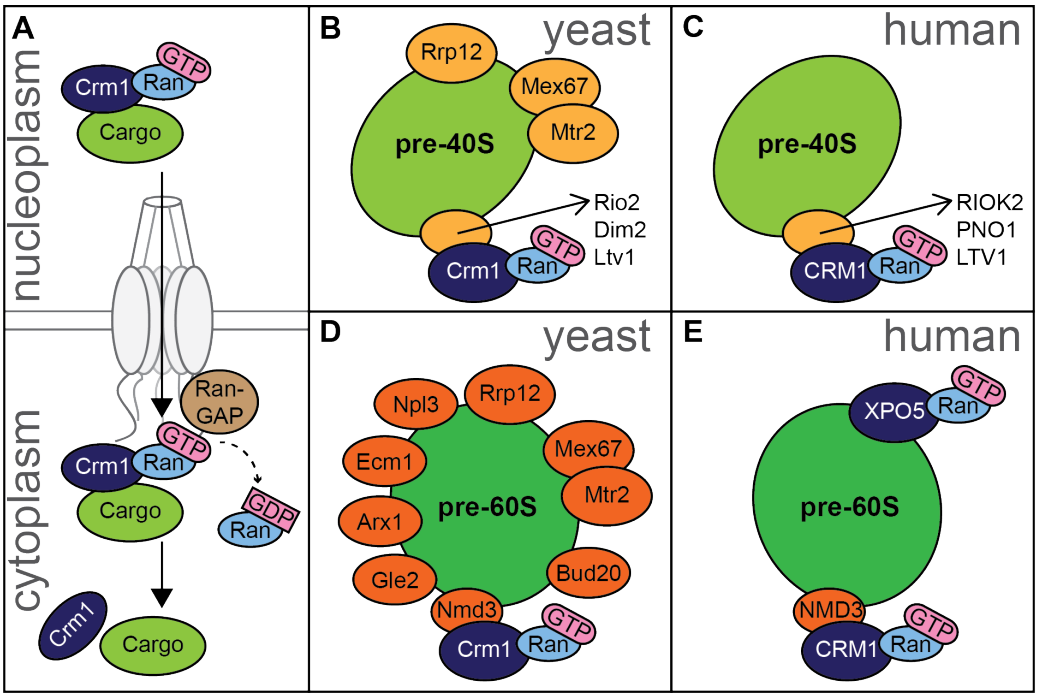

Figure 1.5
Nuclear export of preribosomes
(A) Scheme of Crm1-mediated export. Binding of the exportin Crm1 to its cargo is dependent on the association with Ran-GTP in the nucleoplasm. Crm1 directly interacts with the NPC and facilitates passage of its cargo. After transit through the NPC, hydrolysis of GTP to GDP activated by Ran-GAP leads to the dissociation of Crm1 and its cargo in the cytoplasm. Directionality of tranport is ensured by the asymmetric distribution of Ran-GTP. Figure adapted from (Tran et al., 2007).
(B)-(D) Scheme of trans-acting factors proposed to mediate export of pre-40S in yeast **(B)** and humans **(C),** and export of pre-60S in yeast **(D)** and humans **(E).**

For the export of pre-40S particles, three proteins have been suggested to serve as adaptors for Crm1 association since they are (a) components of pre-40S, (b) accumulate in the nucleus upon Crm1 inhibition using the Crm1 inhibitor leptomycin B (LMB) and (c) possess a potential NES (Fig. 1.5B): Dim2, Rio2 and Ltv1. Dim2 deletion leads to pre-40S accumulation in the nucleus, which cannot be rescued by a deletion of a putative NES (Vanrobays et al., 2008). However, since this mutation also led to rRNA processing defects, it is not clear whether the nuclear accumulation is due to diminished Crm1 binding (Vanrobays et al., 2008). Furthermore, there are conflicting data about a contribution of the kinase Rio2 to pre-40S export (Schäfer et al., 2003; Vanrobays et al., 2003) and Ltv1 deletion has only slight effects on pre-40S export (Seiser et al., 2006). So far, it has not been worked out whether

these proteins may function as Crm1 adaptors in a redundant manner, which could explain the less drastic phenotype of their single deletion compared to direct inhibition of Crm1.

For preribosomal particles of the large subunit, the trans-acting factor Nmd3 has been proposed to be the adaptor molecule through which Crm1 associates with pre-60S. Nmd3 is shuttling between the nucleus and the cytoplasm and an Nmd3 mutant lacking the C-terminal NES blocks export of pre-60S particles (Gadal et al., 2001; Ho et al., 2000). However, an Nmd3-dependent binding of Crm1 to pre-60S has not been demonstrated so far. Interestingly, artificial fusions between NES-deficient Nmd3 and Mtr2, Mex67 (see below) or even the tRNA exportin Los1 can rescue pre-60S export even when Crm1 is inhibited in the presence of LMB, suggesting a high flexibility in export mechanisms (Lo and Johnson, 2009).

Several other factors have been proposed to function together in mediating pre-60S export (summarized in Fig. 1.5D). The trans-acting factor Arx1 has been shown to interact with FG-repeat-containing Nups functioning as a nuclear export receptor (Bradatsch et al., 2007; Hung et al., 2008). However, Arx1 is not essential for pre-60S export, although it enhances the export defect upon deletion/mutation of other export factors. Furthermore, a cryo-EM structure of Arx1 bound to pre-60S revealed that the FG-repeat binding pocket of Arx1 faces the ribosomal exit tunnel (Greber et al., 2012). This would make it difficult, if not impossible, for Arx1 to interact with Nups while bound to pre-60S particles.

The Mex67—Mtr2 complex was first identified to act as a Ran cycle-independent export receptor for mRNAs (Segref et al., 1997; Santos-Rosa et al., 1998; Görlich and Kutay, 1999; Conti and Izaurralde, 2001) but it has been shown to also interact with pre-60S particles *in vivo* and 5S rRNA *in vitro*. Further, upon mutation of a positively charged loop in Mex67, which abolishes binding of the heterodimer to pre-60S particles, the export of pre-60S but not of mRNA is impaired (Yao et al., 2007). Recently, Mex67—Mtr2 has been shown to also interact with pre-40S and was suggested to play a role as well in pre-40S export (Faza et al., 2012).

Another trans-acting factor that is required for export of both ribosomal subunits is the HEAT-repeat protein Rrp12 (Oeffinger et al., 2004). It is associated with pre-40S and pre-60S, can interact with nucleoporins and its deletion leads to nuclear accumulation of both subunit precursors. Furthermore, Bud20, Gle2, Npl3 and Ecm1 were also suggested to contribute to pre-60S export by binding pre-60S as well as nucleoporins, but it is unknown whether they all act together on the same particle or whether their function is redundant (Altvater et al., 2012; Bassler et al., 2012; Hackmann et al., 2011; Occhipinti et al., 2013; Yao et al., 2010).

Taken together, many factors seem to facilitate the passage of preribosomal particles through the NPC. Considering the size of ribosomal subunits it is not surprising that a combination of factors that shield the particle surface and interact with Nups is needed for efficient export to the cytoplasm. Nevertheless, it has to be taken into account that a distinction cannot always be made between a genuine export defect and a defect in nuclear ribosomal maturation where the resulting aberrant particle does not reach export competence. Hence, the deletion of many ribosomal proteins leads to nuclear accumulation of preribosomal subunits but an indirect effect on export by an upstream disruption in the ribosome assembly pathway is the most likely explanation.

Preribosomal subunit export in higher eukaryotes

Like in yeast, export of ribosomal subunits in higher eukaryotes is dependent on CRM1/Exportin-1 and components of the NPC (Bernad et al., 2006; Thomas and Kutay, 2003; Trotta et al., 2003). The kinase RIOK2, the human homolog of Rio2, possesses an NES, binds CRM1 *in vitro* and contributes to pre-40S export. However, the relatively weak phenotype upon RIOK2 depletion implicates more than one CRM1 adaptor for pre-40S in human cells (Fig. 1.5C) (Zemp et al., 2009). For the human homolog of Dim2, PNO1, mutation of conserved residues in the putative NES did not diminish CRM1 binding *in vitro* (Thomas Wild, dissertation, ETH Zurich).

For pre-60S subunits, human NMD3 serves as an adaptor protein for CRM1 (Thomas and Kutay, 2003; Trotta et al., 2003). In contrast, the Arx1 homolog

PA2G4/EBP1 is associated with pre-60S (Squatrito et al., 2004) but does not bind FG-repeat nucleoporins (Bradatsch et al., 2007). Similarly, the loops needed for interaction of Mex67—Mtr2 with pre-60S are not conserved in the human homolog TAP—p15 (Fribourg and Conti, 2003; Senay et al., 2003).
Interestingly, in a candidate RNA interference (RNAi) screen to identify trans-acting factors involved in the human ribosome biogenesis pathway, exportin 5 (XPO5) was classified as a hit as its depletion led to nuclear accumulation of pre-60S. Follow-up analysis confirmed the involvement of XPO5 specifically in pre-60S export in human cells as well as in *Xenopus laevis* oocytes (Fig. 1.5E) (Wild et al., 2010). Notably, the yeast homolog Msn5 is not required for ribosome export, suggesting that the involvement of XPO5 is specific for higher eukaryotes (Moy and Silver 1999, Stage-Zimmermann et al., 2000).

1.2.5 Cytoplasmic maturation steps

After transport of preribosomal subunits to the cytoplasm, final maturation steps have to occur to yield translation-competent ribosomes (reviewed in (Zemp and Kutay, 2007)). Primarily, trans-acting factors have to be released from subunit precursors, which is achieved by energy-dependent remodeling steps that lead to changes in particle structure (further described below). These structural changes later enable the joining of mature 40S and 60S subunits as well as their association with mRNA and translation initiation/elongation factors. Conversely, lack of these structural rearrangements makes it impossible for immature or aberrant cytoplasmic ribosomal subunits to engage in translation.

60S subunit maturation in the cytoplasm

Similar to nuclear pre-60S maturation, most cytoplasmic 60S remodeling steps are catalyzed by NTPases, for instance Efl1, Drg1, Lsg1, and Ssa1/Ssa2 with its cofactor Jjj1. They, along with other factors (Fig. 1.6), catalyze the release of trans-acting factors from cytoplasmic pre-60S. An overview of cytoplasmic 60S maturation steps is given in Fig. 1.6, and several steps are described in more detail below.

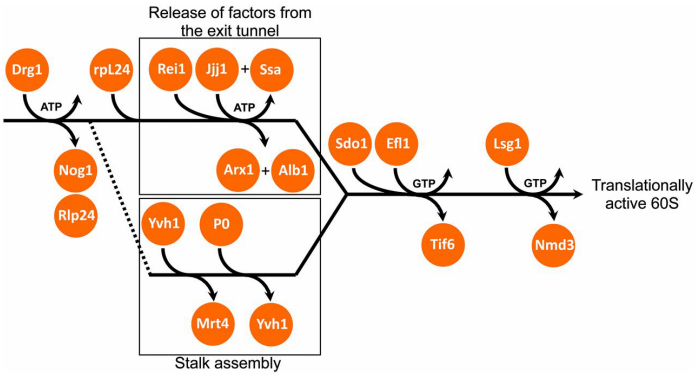

Figure 1.6
Cytoplasmic maturation steps of pre-60S subunits in yeast
Scheme of the trans-acting factor release from pre-60S in the cytoplasm. Upon ATP or GTP hydrolysis, dissociation of trans-acting factors from pre-60S leads to incorporation Rpl24 and P0. Note that the indicated order of action does not equate the order of association with pre-60S. Figure taken from (Woolford and Baserga, 2012).

Some of the trans-acting factors bound to pre-60S subunits are acting as placeholders for ribosomal proteins, which can only be incorporated into pre-60S upon release of these factors in the cytoplasm. For example, the trans-acting factor Rlp24 is a placeholder for the ribosomal protein Rpl24. In one of the first cytoplasmic maturation steps, the AAA-ATPase Drg1 catalyzes the release of Rp24, allowing the subsequent joining of Rpl24 (Pertschy et al., 2007; Lo et al., 2010; Kappel et al., 2012).

One main remodeling event that has to take place to render these pre-60S particles translation competent is the freeing of the polypeptide exit tunnel to allow the translocation of newly synthesized proteins. Cryo-EM and cross-linking studies revealed that the putative export factor Arx1 (see 1.2.4) binds close to the polypeptide tunnel exit (Bradatsch et al., 2012; Greber et al., 2012). The dissociation of Arx1 is promoted by the recruitment of the cytoplasmic factor Rei1 along with the ATPase Ssa1/Ssa2 and its cofactor Jjj1 (Fig. 1.6) (Demoinet et al., 2007; Lebreton et al., 2006; Meyer et al., 2010; Meyer et al., 2007).

An important feature that has to be assembled during late steps of 60S biogenesis is the stalk, a protrusion essential for translation factor recruitment during protein synthesis. The stalk is composed of the ribosomal proteins P0, P1 and P2 (Wahl and Möller, 2002). Incorporation of P0 is catalyzed by Yvh1, which removes the P0 placeholder Mrt4 (Fig. 1.6) (Kemmler et al., 2009; Lo et al., 2009).

As a last step in cytoplasmic 60S biogenesis, the trans-acting factor Tif6 and the export adaptor Nmd3 (see 1.2.4) have to dissociate from pre-60S. Both proteins are located at the 60S/40S interface and their release enables

subunit joining for translation initiation (Valenzuela et al., 1982; Gartmann et al., 2010; Sengupta et al., 2010). Tif6 is first phosphorylated by the kinase Hrr25, which is a prerequisite for its removal catalyzed by the GTPase Efl1 together with Sdo1 (Bécam et al., 2001; Senger et al., 2001; Menne et al., 2007; Basu et al., 2001; Ray et al., 2008). In parallel, the GTPase Lsg1 releases Nmd3 from pre-60S (Hedges et al., 2005; Kallstrom et al., 2003). Removal of Nmd3 additionally requires prior loading of the ribosomal protein Rpl10 onto pre-60S, facilitated by its binding partner Sqt1 (West et al., 2005).
Notably, depletion of many cytoplasmic 60S maturation factors leads to nuclear accumulation and rRNA processing defects of pre-60S. This can be explained by the fact that failure of trans-acting factor release sequesters these proteins in the cytoplasm. As a consequence, these factors are unavailable to newly synthesized pre-60S, which cannot mature further and accumulate in the nucleus.

In humans, several 60S cytoplasmic maturation steps appear to be conserved but only a few human homologs of yeast factors involved in this process have been investigated. For example, the cytoplasmic release of MRTO4, the Mrt4 homolog, is also dependent on ribosomal protein P0 and the Yvh1 homolog DUSP12. Additionally, when stalk assembly is disrupted, eIF6, the Tif6 homolog, partially mislocalizes to the cytoplasm, suggesting an inefficient release from pre-60S (Lo et al., 2010; Lo et al., 2009). Further, the Hrr25 homolog CK1 phosphorylates eIF6, regulating its subcellular localization (Biswas et al., 2011). Interestingly, the human homolog of Sdo1 is SBDS, a protein that is mutated in 90% of patients suffering from Shwachman-Bodian-Diamond syndrome (SDS), a pleiotropic disease associated with pancreatic insufficiency and leukemia predisposition (Boocock et al., 2003; Shimamura, 2006). This emphasizes the importance of efficient pre-60S maturation for cellular function.

40S subunit maturation in the cytoplasm

Analysis of late yeast pre-40S particles purified by Rio2-TAP revealed the presence of seven trans-acting factors that are stably associated with it: the

kinase and putative export adaptor Rio2, the export adaptor Ltv1 (see 1.2.4), the endonuclease Nob1 (see 1.2.2), its binding partner Dim2, the methylase Dim1 (see 1.2.2), the GTPase-like protein Tsr1 and Enp1 (Fig. 1.7) (Strunk et al., 2011). In contrast to cytoplasmic maturation of pre-60S particles, which mainly requires the action of ATP- and GTPases, the involvement of several kinases in releasing 40S trans-acting factors (see below) demonstrates the importance of phosphorylation events for 40S maturation. For instance, depletion or mutation of the kinase Rio2 leads to accumulation of 20S pre-rRNA in the cytoplasm (Geerlings et al., 2003; Vanrobays et al., 2003). Not only Rio2 but also the kinase Rio1 contributes to 18S processing and the release of 40S assembly factors in the cytoplasm. Notably, apart from autophosphorylation activity of Rio1 and Rio2, no other substrates of these kinases have been identified yet (Vanrobays et al., 2003; Vanrobays et al., 2001).

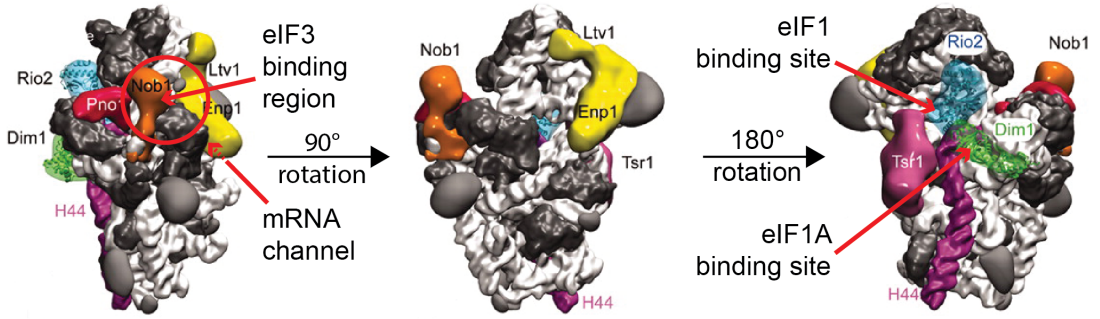

Figure 1.7
Positions of trans-acting factors on pre-40S particles
Cryo-EM structure of *S. cerevisiae* pre-40S with the trans-acting factors positioned on the particle. Additionally, mapped binding sites of the translation initiation factors eIF1, eiF1A and eIF3 are indicated, which are masked by different trans-acting factors. The mRNA channel formation is inhibited by the presence of Ltv1/Enp1. Figure adapted from (Strunk et al., 2011).

Another kinase is involved in the release of Ltv1 and Enp1 from pre-40S particles. These two trans-acting factors have been shown to form a trimeric complex together with the ribosomal protein Rps3. The kinase Hrr25, which is also involved in 60S maturation (see above), phosphorylates the Rps3/Enp1/Ltv1 subcomplex (Schäfer et al., 2006). This phosphorylation event is a prerequisite for dissociation of the subcomplex from pre-40S particles. Subsequent dephosphorylation of Rps3 by an unknown phosphatase has been suggested to lead to stable incorporation of Rps3 into pre-40S and the formation of the so-called “beak” structure. Interestingly, it

has been shown by cryo-EM that the Rps3/Enp1/Ltv1 complex is located close to the opening of the mRNA channel, which needs to be accessible in order for 40S subunits to become translationally competent (Fig. 1.7) (Strunk et al., 2011).

Cytoplasmic pre-40S subunits not only have to release their associated trans-acting factors for maturation, the rRNA also has to be cleaved at site D to yield mature 18S rRNA (see 1.2.2). Depletion of several cytoplasmic trans-acting factors affect this final rRNA processing step, although they are not directly involved in the cleavage mechanism. This suggests that rRNA processing is one of the last maturation steps to occur before 40S subunits join 60 subunits and acquire the ability to translate proteins (Fig. 1.8). The endonuclease Nob1 that catalyzes this cleavage is already associated with nuclear pre-40S particles that contain the 20S rRNA precursor and accompanies these particles to the cytoplasm (Fatica et al., 2003; Fatica et al., 2004; Pertschy et al., 2009). To prevent premature processing, the rRNA close to site D was suggested to adapt a fold that hinders cleavage in the nucleoplasm and changes conformation in the cytoplasm. This conformational switch renders the cleavage site accessible for the catalytic domain of Nob1, possibly by action of the GTPase Fun12 (Pertschy et al., 2009; Fatica et al., 2003; Lebaron et al., 2012). Notably, Nob1 and its binding partner Dim2 occupy a space on pre-40S that is overlapping with the binding site of the translation initiation factor eIF3, suggesting that they have to be released from pre-40S to allow translation initiation (Fig. 1.7) (Strunk et al., 2011).

Interestingly, immature 40S subunits have been suggested to be able to associate with mature 60S for an initial round of translation. However, these particles are less stable than their mature counterparts and are degraded (Soudet et al., 2010).

In human cells, RIOK1 and RIOK2, the homologs of Rio1 and Rio2, respectively, are also involved in cytoplasmic 40S maturation steps (Rouquette et al., 2005; Widmann et al., 2012; Wyler et al., 2011; Zemp et al., 2009). In particular, RIOK1 and RIOK2 were shown to be required for 18S-E to 18S rRNA processing as well as the release of several trans-acting factors

from pre-40S particles in the cytoplasm. The requirement of their kinase activity and/or presence differs for the release of certain trans-acting factors (Widmann et al., 2012), which led to a proposed order of action for RIOK1 and RIOK2 (Fig. 1.8). Additionally, the higher eukaryote-specific kinase RIOK3 was shown to be part of pre-40S particles and to play a role in 21S rRNA processing (Baumas et al., 2012; Widmann et al., 2012).

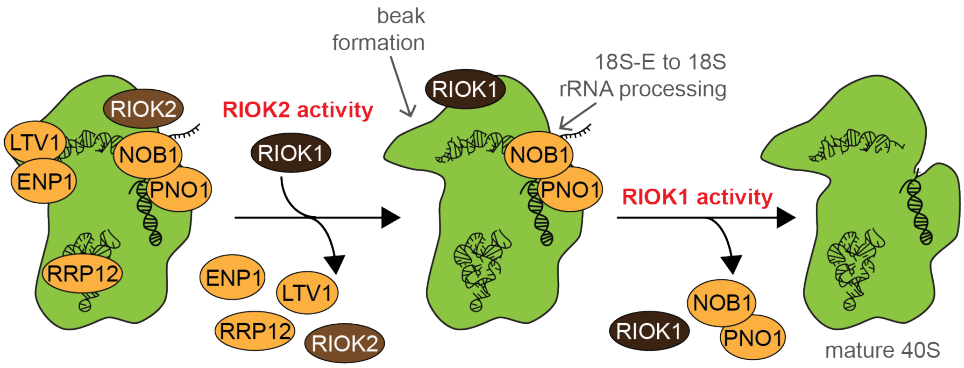

Figure 1.8
Model of the role of human RIOK1 and RIOK2 in cytoplasmic 40S maturation
Scheme of successive release of 40S trans-acting factors upon the activity of RIOK1 and RIOK2 in human cells. Analyses of the requirement of activity and/or presence of these kinases for the release of factors indicated that RIOK2 acts before RIOK1 (Zemp et al., 2009; Wyler et al., 2011; Widmann et al., 2012). Trans-acting factors, except for RIOK1 and RRP12, were placed on the particle according to (Strunk et al., 2011). Figure adapted from (Ivo Zemp, ETH Zurich, unpublished data).

TAP of different human pre-40S followed by proteomic analysis gave insight on human 40S precursor composition, and revealed a high conservation in the trans-acting factors present on these particles (Wyler et al., 2011). Direct binding of NOB1 to the Dim2 homolog PNO1 was also shown to be conserved (Widmann et al., 2012).

Nevertheless, functional differences between yeast and human homologs of 40S trans-acting factors have been demonstrated. For instance, when human TSR1 is depleted, pre-40S subunits accumulate in the nucleus whereas Tsr1 depletion in yeast leads to cytoplasmic pre-40S accumulation (Carron et al., 2011; Léger-Silvestre et al., 2004). Furthermore, human ENP1/BYSL depletion leads to accumulation of the 21S-C precursor, an equivalent was not observed in yeast so far (Carron et al., 2010). Further analysis is needed to compare function of other human 40S trans-acting factors to their yeast counterparts.

1.3 Linking ribosome biogenesis and the cell cycle - the p53 pathway and more

The transcription factor p53 is activated by malignancy-associated stress signals such as DNA damage, hypoxia, and viral infection and in return influences numerous fundamental cellular pathways leading to cell cycle arrest, cell senescence and apoptosis (reviewed in (Kruse and Gu, 2009; Vousden and Prives, 2009)), making it a crucial tumor suppressor. Consequentially, p53 is the most frequently mutated gene in human tumors (Hollstein et al., 1994). Moreover, in many tumors bearing wild type p53, induction of its activity is inhibited. Since cell growth is linked to the rate at which a cell is able to translate new proteins, it is conceivable that p53 influences ribosome production. Indeed, active p53 inhibits rRNA synthesis, as it has been shown that tumors with altered p53 function exhibit increased rRNA transcription rates (Treré et al., 2004). Vice versa, it has been shown that inhibition of ribosome biogenesis by deletion of *RPS6* in mice liver cells induces a cell cycle checkpoint that leads to G1 phase arrest, which was later shown to be true for the depletion of many ribosomal proteins (Volarevic et al., 2000). Shortly after, p53 was found to be a link between disturbed ribosome biogenesis and cell cycle control. Inhibition of POL I transcription as well as depletion (and sometimes overexpression) of many trans-acting factors leads to activation of p53. When p53 is inactivated in addition to trans-acting factor depletion, it rescues cell cycle arrest but not ribosome biogenesis defects (Hölzel et al., 2010; Kurki et al., 2004; Pestov et al., 2001).

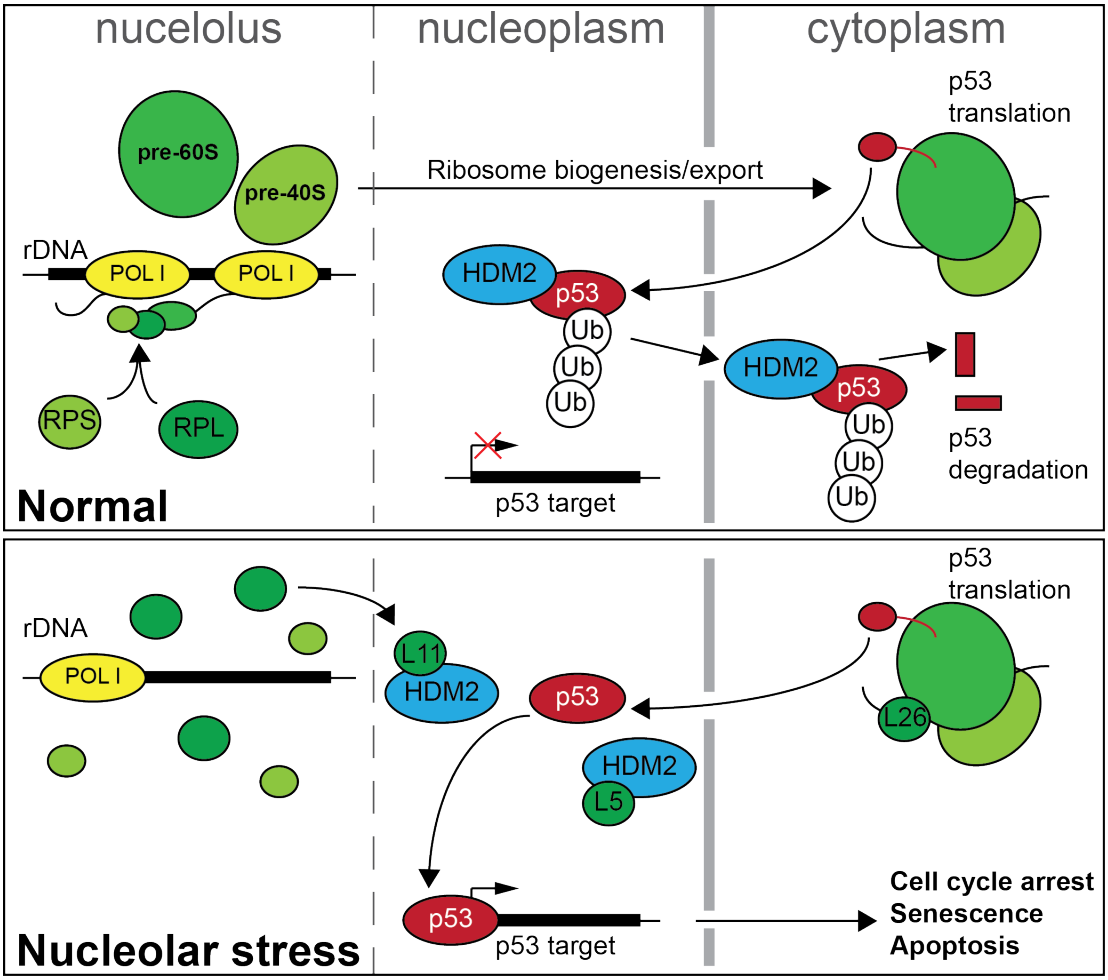

Figure 1.9
Overview of p53 activation upon nucleolar stress
(A) P53 protein levels are kept low by rapid turnover rates mediated by the E3 ligase HDM2. **(B)** Upon nucleolar stress and ribosome biogenesis disruption, free ribosomal proteins associate with HDM2 leading to p53 stabilization and activation, which in turn influences cell growth and division. Figure adapted from (Quin et al., 2014).

Under normal growth conditions, p53 is kept at low levels through ubiquitination by the E3 ligase HDM2 and subsequent proteasomal degradation (Fig. 1.9). Upon nucleolar stress and ribosome biogenesis defects, newly translated ribosomal proteins are not efficiently incorporated into preribosomes. In their free form, RPL5, RPL11, RPL23, RPS3, and RPS7 are able to bind and inhibit HDM2 in the nucleoplasm, leading to p53 stabilization and activation (reviewed (Chakraborty et al., 2011; Quin et al., 2014; Zhang and Lu, 2009)). The two main players appear to be RPL5 and RPL11, since RPL23 depletion still leads to p53 upregulation ((Dai et al., 2004) and Fig. 2.3.14). Moreover, RPS7-dependent activation of p53 is not consistent in all cell types (Zhu et al., 2009).

It has also been suggested that RPL5 and RPL11 act cooperatively to inhibit HDM2, even in a complex with 5S rRNA (Donati et al., 2013; Horn and Vousden, 2008; Sloan et al., 2013a). In addition, RPL26 regulates p53 levels by binding to the 3'UTR of p53 mRNA and selectively promoting its translation (Fig. 1.9) (Takagi et al., 2005). Furthermore, several nucleolar trans-acting factors, for instance NPM, nucleolin and nucleostemin, are also able to activate p53 by directly binding to HDM2 (Dai et al., 2008; Kurki et al., 2004; Saxena et al., 2006). The p53 activation/inhibition pathway is yet more complex due to additional players and regulatory feedback loops. For example, p53 enhances the transcription of its own inhibitor HDM2 (Barak et al., 1993; Wu et al., 1993).

Interestingly, although impairment of 40S biogenesis by RPS6 depletion leads to decreased general translation, the translation of a subset of mRNAs that possess a 5'-terminal oligopyrimidine tract (TOP) is enhanced (Fumagalli et al., 2009). Increased levels of RPL11, which is translated from a 5'TOP mRNA, would lead to p53 activation without disturbing 60S biogenesis and nucleolar integrity. All these mechanisms suggest that the interplay between ribosome biogenesis and p53 is tightly regulated to ensure a highly controlled impact on cell growth and proliferation. Unsurprisingly, there is a prevalence of ribosomal protein overexpression as well as errors in ribosome biogenesis regulation in many tumors (Amsterdam et al., 2004; Bilanges and Stokoe, 2007; Maggi and Weber, 2005; Montanaro et al., 2008).

Notably, *S. cerevisiae* does not possess a gene encoding for p53. However, when human wild type p53 is overexpressed in yeast, it leads to a slow growth phenotype. This is not the case when tumor-derived loss-of-function mutants of p53 are overexpressed. This suggests that human p53 can also act as a transcription factor and influence cell cycle progression in yeast (Nigro et al., 1992). Nevertheless, *S. cerevisiae* is able to delay cell cycle progression from G1 to S phase upon ribosome biogenesis defects through a p53-independent mechanism (Bernstein et al., 2007).

Several p53-independent pathways that link ribosome biogenesis errors and cell cycle arrest have been discovered in human cells as well (reviewed in

(Donati et al., 2012)). For instance, when ribosome biogenesis is disturbed, RPL11 binds to c-Myc (see 1.2.2), decreasing its transcription activation capacity. Furthermore, RPL11 binds to the mRNA of c-Myc thereby destabilizing the mRNA leading to its fast degradation (Dai et al., 2007). Another example is the depletion of the PeBoW complex member PES1 (see 1.2.2), which leads to p53-independent reduction of cyclin D1 expression and upregulation of the CDK inhibitor p27, blocking cell cycle progression (Li et al., 2009). Furthermore, RPS19 interacts with the kinase PIM1, which promotes p27 inactivation. When RPS19 levels decrease, PIM1 becomes instable and is degraded leading to p27 activation, which impairs cell proliferation (Iadevaia et al., 2010). Considering all these recently discovered links between ribosome biogenesis and cell cycle progression, the nucleolus emerged as an interesting and promising target for cancer therapies (Drygin et al., 2010; Quin et al., 2014).

1.4 Structure and function of the NF45/NF90 complex

The nuclear factor of activated T cells (NF-AT) was found to bind the interleukin-2 (IL-2) promoter and induce IL-2 expression when T cells are activated upon antigen exposure (Shaw et al., 1988; Yaseen et al., 1993). DNA affinity chromatography identified two proteins at the size of 45 and 90 kDa as components of this NF-AT complex (Corthésy and Kao, 1994; Kao et al., 1994), which were termed interleukin enhancer binding factor 2 and 3 (ILF2 and ILF3), or NF45 and NF90, respectively. NF45 and NF90 have in later studies been implicated in several other cellular pathways, which will be further discussed below.

1.4.1 NF45 and NF90 heterodimerize via their DZF domain

NF45 as well as NF90 possess an N-terminal domain termed domain associated with zinc fingers (DZF) (Fig. 1.10A), a domain which is found exclusively in metazoans. Recently, the crystal structure of the DZF domains of NF45 and NF90 in a heterodimeric complex has been solved (Wolkowicz and Cook, 2012). The dimerized DZF domains of NF45 and NF90, which are 30% identical, display a 2-fold rotational symmetry (Fig. 1.10B). Three

residues in NF90 (Glu312, Gln319, Arg323) required for complex formation with NF45 are conserved in the two related proteins SPNR and Zfr, which are able to bind to NF45 *in vitro* (Wolkowicz and Cook, 2012). This suggests that NF45 is able to form and function in different heterodimeric complexes, although this association has yet to be confirmed *in vivo*.

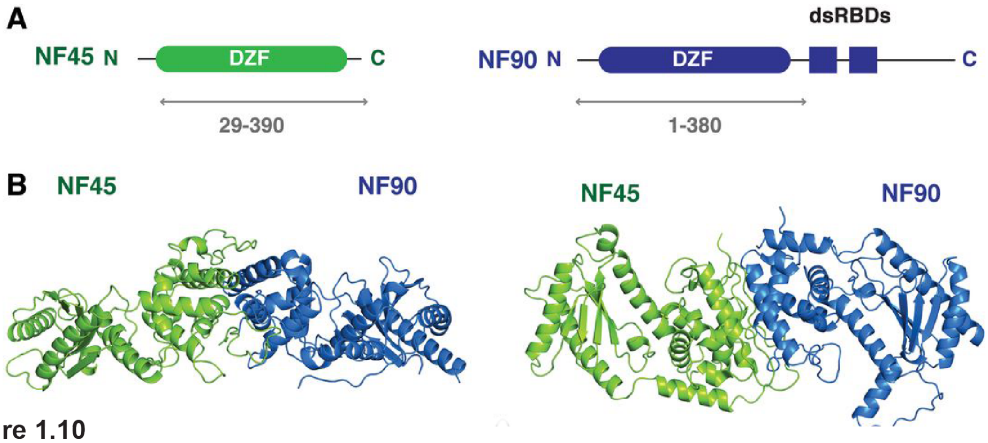

Figure 1.10
Structure of the NF45/NF90 heterodimer
(A) Schematic representation of the domains of NF45 and NF90. The protein fragments used for crystallization are marked with a grey bar.
(B) Structure overview of the NF45/NF90 heterodimer from the 'side' (left) and 'top' (right). (Figure taken from Wolkowicz and Cook, 2012)

Interestingly, the DZF domains of NF45 and NF90 possess structural similarities to template-free nucleotidyltransferases, enzymes that catalyze the addition of an NTP to the end of an oligonucleotide (Wolkowicz and Cook, 2012). The family of template-free nucleotidyltransferases includes TUTases, poly (A) polymerases, and CCA-adding enzymes of tRNAs (reviewed in (Betat et al., 2010; Guschina and Benecke, 2008)). However, not all residues important for nucleotidyltransferase activity are conserved in the DZF of NF45 and NF90. Moreover, no nucleotidyltransferase activity of NF45 and NF90 has been observed *in vitro* (Wolkowicz and Cook, 2012), which makes it unlikely that they are able to transfer nucleotides to an RNA substrate. Nevertheless, the fold of the DZF domain of NF45 allows for nucleotide binding *in vitro*, with a preference for ATP and UTP, while the DZF domain of NF90 is not able to bind any nucleotides due to a serine to leucine substitution in the binding pocket (Wolkowicz and Cook, 2012). Whether the ability of NF45 to bind nucleotides is merely an evolutionary artifact or whether it is essential for its cellular function remains to be investigated.

1.4.2 The double stranded RNA binding domains of NF90

In addition to the N-terminal DZF domain, NF90 possesses two double-stranded RNA binding domains (dsRBDs) in its C-terminal region (Fig. 1.10A). DsRBDs were first identified by sequence similarity in the *Drosphila* protein Staufen, human TRBP and *Xenopus laevis* RNA-binding protein (St Johnston et al., 1992). These 65-75 amino acid long domains usually display an α-β-β-β-α fold (Barraud et al., 2012; Bycroft et al., 1995; Kharrat et al., 1995; Nanduri et al., 1998) and are able to bind double stranded as well as structured RNA by interacting with the minor groove (reviewed in (Fierro-Monti and Mathews, 2000; Masliah et al., 2013)). In addition, dsRBDs can also play a role in protein dimerization (Cosentino et al., 1995; Patel and Sen, 1998; Romano et al., 1998) and nuclear localization (Doyle et al., 2013; Eckmann et al., 2001). Interestingly, NF90 interacts with other dsRBD containing proteins, namely ADAR1 (Nie et al., 2005) and the double-stranded RNA-dependent protein kinase PKR (Patel et al., 1999) although this interaction is likely mediated by concurrent RNA binding. Additionally, it has been shown that NF90 is indeed able to bind dsRNA (Langland et al., 1999; Patel et al., 1999) as well as VA RNA_{II}, a highly structured adenovirus RNA (Liao et al., 1998) via its dsRBDs. Furthermore, a new family of small non-coding RNAs was discovered to bind NF90 in cross-linking experiments. These RNA species were termed small NF90-associated RNAs (snaR) (Parrott and Mathews, 2007). Their function, however, remains to be elucidated.

Notably, NF90 possesses at least five differently spliced isoforms ((Duchange et al., 2000; Saunders et al., 2001); see also Fig. 2.3.4A) that all possess the DZF and dsRBD domains and differ only in the length of the C terminus. The C-terminally extended versions are termed NF110 in comparison to the shorter NF90 isoforms, corresponding to their mass in kDa. The NF90 isoforms, in complex with NF45, have been more extensively studied than the longer isoforms. The NF110 isoform is predominantly chromatin bound and thought to play a general role in gene transcription (Reichman and Mathews, 2003; Reichman et al., 2003) while the NF90 isoform is known to perform various cellular functions (see below).

1.4.3 Cellular functions of the NF45/ NF90 complex

In addition to transcription activation of IL-2 in activated T cells, the NF45/NF90 complex has also been implicated in transcriptional upregulation of IL13 in T cells by binding to DNase I-hypersensitive sites in the DNA of the IL13 promoter region (Kiesler et al., 2010). In general, it was found that the NF90 isoform could act as both an activator and a repressor of transcription (Reichman et al., 2002), but a DNA binding motif has not been identified so far.

DNA damage response

Apart from being a transcription factor and associating with promoter elements, the NF45/NF90 complex was shown to interact at promoters with Ku70 and Ku80, which can also modulate transcription (Giffin et al., 1996; Reichman et al., 2002; Shi et al., 2007). Additionally, both proteins are part of the DNA-dependent proteins kinase (DNA-PK) complex, which is required for DNA double strand break repair and telomere maintenance. This complex interacts with NF45/NF90 at sites of DNA damage and NF45/NF90 were shown to aid in nonhomologous end joining DNA break repair *in vivo* and in *vitro* (Shamanna et al., 2011; Ting et al., 1998).

Association with mRNA and involvement in translation

Not only nuclear functions of NF45/NF90 have been proposed: NF90 is able to shuttle between the nucleus and cytoplasm under certain cellular conditions and its subcellular distribution is dependent on the cell cycle stage and tissue type (Nepliouevа et al., 2010; Parrott et al., 2005). For example, NF90 relocalizes from the nucleus to the cytoplasm upon T cell activation to bind and stabilize the IL-2 mRNA (Shim et al., 2002). For this export step, NF90 needs to be phosphorylated by the serine/threonine kinase AKT (Pei et al., 2008). In general, NF90 was proposed to bind mRNA in the nucleus and regulate its export to the cytoplasm by retaining it in intranuclear foci and accompanying it to the cytoplasm. In addition, NF90 was suggested to regulate translation itself by influencing mRNA turnover and translation rates ((Kuwano et al., 2008; Pfeifer et al., 2008); reviewed in (Masuda et al., 2013)).

An effort has been undertaken to identify the mRNA classes bound to NF90 by RNA co-immunoprecipitation (IP)/micro-array (RIP-Chip) assays. They include mRNAs encoding histone proteins, proteins involved in oxidative phosphorylation and, interestingly, ribosomal proteins (Nepliouevaet al., 2010). However, the direct influence of NF90 on translation of these mRNAs remains to be elucidated.

NF45/NF90 have also been identified as components of cytoplasmic RNP granules that contain mature 40S particles and mRNA but lack 60S and are translationally silent (Jønson et al., 2007). These granules are thought to facilitate translocation of mRNA and associated factors. Similarly, murine ILF3 was shown to interact with Tau mRNA in mice neurons, and it was suggested that it accompanies these mRNAs during their translocation along the axon (Larcher et al., 2004).

Export of NF90 from the nucleus to the cytoplasm is mediated by the export receptor exportin-5 (XPO5), which is also responsible for pre-miRNA and, in vertebrates, pre-60S export and can contribute to tRNA export (Brownawell and Macara, 2002; Wild et al., 2010; Calado et al., 2002). However, association of NF90 with XPO5 is indirect and dependent on the presence of RNA (Calado et al., 2002). It was also shown that NF90 and XPO5 mutually increase their affinities for dsRNA targets which leads to more efficient export of target RNAs (Gwizdek et al., 2004).

Response to viral infection

As a defense mechanism against viral infection, the dsRBD-containing kinase PKR phosphorylates the translation initiation factor eIF2A, inhibiting general mRNA translation and thus preventing virus production (reviewed in (Dabo and Meurs, 2012)). PKR was also shown to interact with the NF45/NF90 complex and to phosphorylate NF90 upon viral infection (Langland et al., 1999; Parker et al., 2001; Patel et al., 1999). This leads to NF45 dissociation, while NF90 remains locked on viral transcripts preventing their translation (Harashima et al., 2010). Based on these findings, the NF45/NF90 complex has been suggested to function as an antiviral agent (Isken et al., 2003; Krasnoselskaya-Riz et al., 2002; Merrill and Gromeier, 2006; Shabman et al.,

2011; Wang et al., 2009). In some cases, however, the complex was proposed to enhance infection rates of Hepatitis C and dengue viruses, by binding to and changing the conformation of the viral RNAs (Gomila et al., 2011; Isken et al., 2007). It remains to be investigated how interaction of NF45/NF90 with viral RNA can have reverse effects depending on the type of virus.

Other functions of NF45/NF90

Furthermore, NF45/NF90 were also shown to negatively regulate miRNA biogenesis when overexpressed, mainly the processing of pri-miRNA into pre-miRNA ((Sakamoto et al., 2009); reviewed in Masuda et al., 2013). The NF45/NF90 complex has also been implicated to play a role in several other pathways such as splicing (Rigo et al., 2012), mitochondrial degradation (Higuchi et al., 2012), as well as cell growth and division (Guan et al., 2008). Recently, it has been shown that depletion of NF90 or NF45 leads to activation of p53 and increased expression of its downstream target p21 ((Shamanna et al., 2013) and Fig. 2.3.14).

Taken together, NF45 and NF90 are pleiotropic factors that have been implicated in many cellular pathways and it remains to be investigated in which pathways the NF45/NF90 complex is directly involved and which cellular phenotypes upon depletion are secondary or even tertiary effects. Nevertheless, it is a physiologically important complex, consistent as loss of NF45/NF90 is embryonic lethal (Pfeifer et al., 2008). Notably, the expression of NF45/NF90 is increased in different cancer types (Guo et al., 2012; Hu et al., 2013; Shim et al., 1998), which suggests that they might play an important regulatory role in cell growth and proliferation.

2. Results

Tandem affinity purification (TAP) of preribosomal particles in combination with mass-spectrometric analysis to identify the composition of pre-40S and pre-60S particles at various stages of ribosome biogenesis led to the identification of numerous trans-acting factors in *S. cerevisiae* (see chapter 1.2). To date, more than 200 trans-acting factors have been found; their mechanistic involvement in ribosome biogenesis, however, is still unknown for many maturation steps. Even less is known about the composition of preribosomes and trans-acting factor function in higher eukaryotes. Many factors seem to be conserved from yeast to humans. There are, however, considerable differences in the ribosome biogenesis pathway, e.g. in processing of preribosomal RNA (pre-rRNA) (Rouquette et al, 2005) and nuclear export of preribosomal particles (Wild et al, 2010). Furthermore, some trans-acting factors have already been described to play different roles in yeast vs. human ribosome biogenesis (Carron et al., 2011; Sloan et al., 2013). In order to expand our knowledge on human ribosome biogenesis we analyzed the composition of pre-40S and pre-60S particles purified by TAP. We then set out to characterize preribosomal particle-associated proteins that were previously not described as trans-acting factors in human cells, namely casein kinase 1 isoforms δ and ε (chapter 2.2) and NF45/NF90 (chapter 2.3). Apart from demonstrating their association with preribosomes, we investigated their influence on ribosome biogenesis by RNAi experiments and different biochemical methods.

Contributions

The experiments in this thesis were carried out by Franziska Wandrey with the following exceptions (all mentioned contributors were members of the Kutay lab at the time of the experiment):
Dr. Ivo Zemp performed the experiment for Fig. 2.2.5C and Fig. 2.2.2 except for the PNO1 readout in the lowest panel, which was performed by Franziska Wandrey. The experiment for Fig. 2.2.6B was carried out by Dr. Sanjana Rao together with Franziska Wandrey. Christian Montellese carried out the TAPs and Western blot for Figures 2.3.1 and 2.3.2B. Lukas Badertscher performed

the sucrose gradient experiment in Fig. 2.3.3 and Lukas Bammert carried out the FISH assay in Fig. 2.3.10B.

2.1 Characterization of the novel 40S trans-acting factor C21orf70

The human nucleolar 40S trans-acting factor NOC4L is a homolog of the *S. cerevisiae* protein Noc4, which is part of the SSU processome in nucleoli (Bernstein et al., 2004). HASt-tagged NOC4L expressed in HEK 293 cells was recently used as bait in TAP experiments followed by mass spectrometric analysis, which showed that HASt-NOC4L co-purifies early pre-40S particles. In addition, it led to the identification of a novel component of pre-40S: the previously uncharacterized protein C21orf70/FAM207A (Wyler et al., 2011). Upon siRNA-mediated depletion of C21orf70, pre-40S particles accumulated in the nucleoplasm of HeLa cells (Wyler et al., 2011), which suggests a role of C21orf70 in nuclear maturation steps or export of 40S subunits. In this thesis, we further characterized C21orf70 and confirmed its association with pre-40S.

2.1.1 C21orf70 is a nuclear protein enriched in nucleoli

In a first characterization step of C21orf70, we wanted to analyze its subcellular localization. Interestingly, C21orf70 has been previously identified as part of the nucleolar proteome (Leung et al., 2006; Ahmad et al., 2008). To confirm this, we generated a polyclonal peptide-specific antibody against C21orf70 to detect its localization in HeLa cells. In steady state, C21orf70 was enriched in nucleoli (Fig. 2.1.1). The specificity of the antibody was confirmed by depletion of C21orf70 with previously published siRNAs (Wyler et al., 2011). Upon knockdown of C21orf70, the nucleolar signal disappeared and only a weak nucleoplasmic background signal is detected (Fig. 2.1.1).

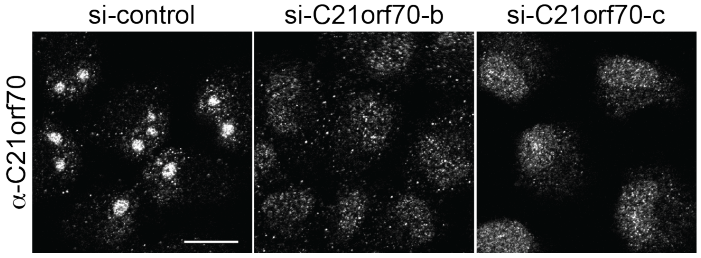

Figure 2.1.1
C21orf70 localizes to nucleoli
HeLa cells were treated with the indicated siRNAs for 48 h followed by immunofluorescence analysis with an antibody against C21orf70. Scale bar, 20 µm.

2.1.2 TAP of HASt-C21orf70 identifies CK1δ and CK1ε as novel components of pre-40S

C21orf70 has been identified as a component of pre-40S particles by NOC4L-TAP and sucrose gradient analysis (Wyler et al., 2011). To confirm this association, we cloned HASt-tagged C21orf70 that can be used for TAP. To first assess the subcellular localization of this construct, we generated a HeLa FRT cell line in which the expression of HASt-C21orf70 is tetracycline-dependent. HASt-C21orf70 localized to nucleoli comparable to the endogenous protein (Fig. 2.1.2A, see also Fig. 2.1.1).

To analyze a potential shuttling behavior of C21orf70, we treated the HASt-C21orf70-expressing cell line with siRNAs targeting the 40S trans-acting factors RIOK2, NOB1 and the ribosomal protein RPS3. It has previously been shown that disturbance of cytoplasmic 40S maturation steps led to impaired release of 40S trans-acting factors from pre-40S (Zemp et al., 2009). This resulted in cytoplasmic accumulation of 40S trans-acting factors such as ENP1/BYSL, which is nuclear in steady-state but accompanies preribosomal 40S particles from the nucleolus to the cytoplasm. If C21orf70 was associated with these late cytoplasmic pre-40S particles, it would display a similar behavior and accumulate in the cytoplasm. Upon downregulation of RIOK2, NOB1 or RPS3, ENP1 mislocalized to the cytoplasm, whereas HASt-C21orf70 remained nuclear (Fig. 2.1.2A). However, upon NOB1 depletion, HASt-C21orf70 partially relocalized to the nucleoplasm and appeared less enriched in nucleoli. This suggests that C21orf70 is not part of late, cytoplasmic pre-40S particles.

We then generated a HEK 293 cell line expressing HASt-C21orf70 in a tetracycline-inducible manner and performed TAP followed by SDS-PAGE. Mass spectrometric analysis (Fig. 2.1.2B) as well as Western blotting (Fig. 2.1.2C) revealed that TAP of HASt-C21orf70 co-purified pre-40S particles, which is demonstrated by the presence of several 40S trans-acting factors including NOC4L, ENP1, and RRP12, as well as RPS but not RPL proteins. Notably, the late joining ribosomal proteins RPS10 and RPS26 (O'Donohue et al., 2010) were not co-purified with HASt-C21orf70 (Fig. 2.1.2C), which indicates that HASt-C21orf70 is indeed associated with early pre-40S. This

notion is further supported by the co-purification of the early, nucleolar trans-acting factor NOC4L.

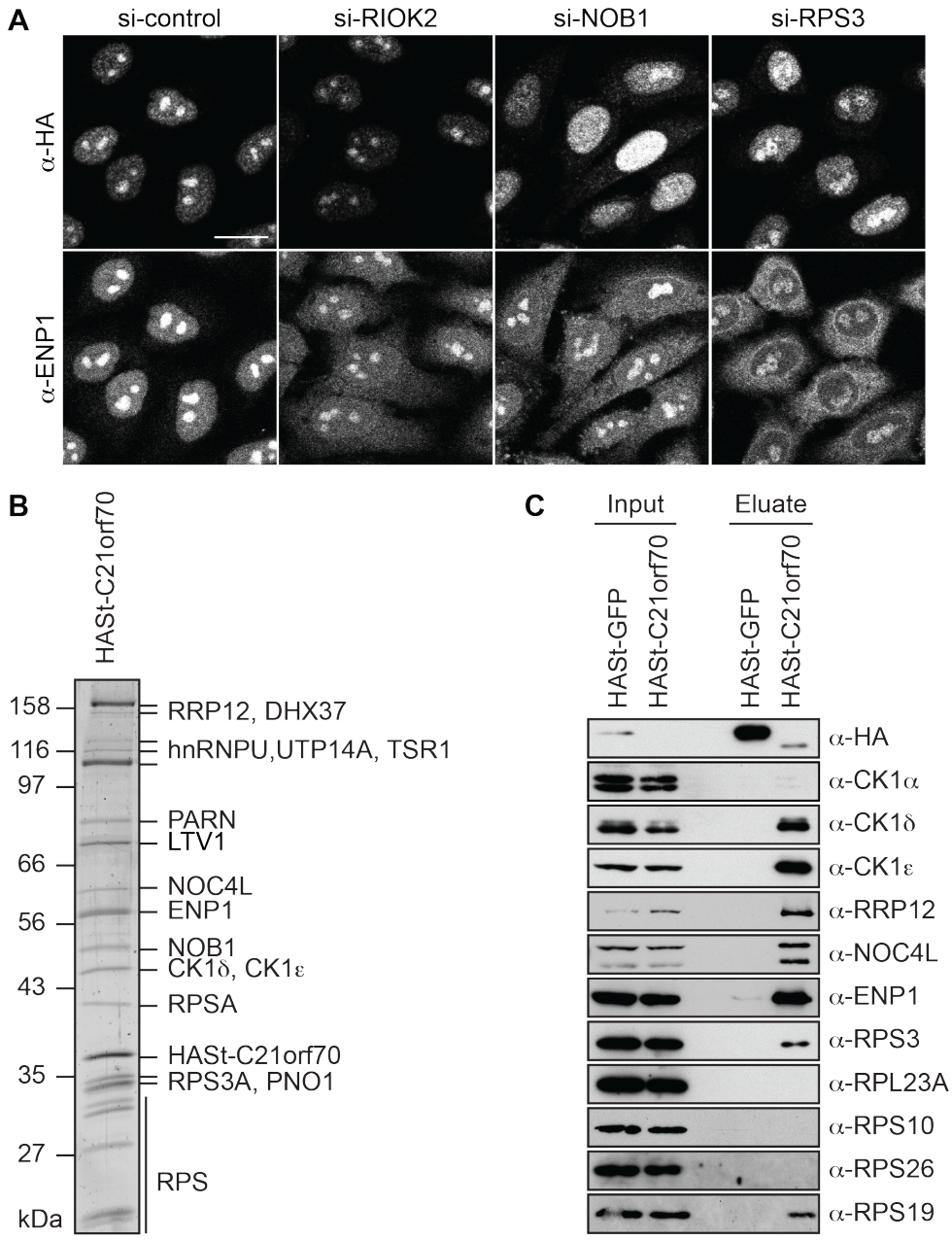

Figure 2.1.2
C21orf70 associates with early pre-40S particles
(A) HeLa cells expressing HASt-C21orf70 were treated with the indicated siRNAs for 72 h. Expression of HASt-C21orf70 was induced by the addition of tetracycline 24 h prior to fixation. Localization of HASt-C21orf70 (α-HA) and ENP1 was analyzed by co-immunofluorescence. Scale bar, 20 µm.
(B) Tandem affinity purification was performed from a HEK 293 FlpIn TRex cell line expressing HASt-C21orf70 in a tetracycline-inducible manner and analyzed by SDS-PAGE followed by Coomassie staining. Visible bands were cut out and subjected to mass spectrometric analysis. The major protein hits are listed on the right. HASt-C21orf70 co-purifies RPS as well as 40S trans-acting factors.
(C) TAP of HASt-C21orf70 using HASt-GFP as a negative control. Cleared cell extracts (Input) and eluted proteins (Eluate) were analyzed by SDS-PAGE followed by Western blotting using the indicated antibodies. CK1δ and CK1ε are co-purified with HASt-C21orf70.

Interestingly, we also detected two proteins in the mass spectrometry analysis of HASt-C21orf70 TAP that have so far not been identified as pre-40S components: the casein kinase 1 isoforms δ and ε (CK1δ and CK1ε, respectively) (Fig. 2.1.6B). We verified the association by Western blotting (Fig. 2.1.6C) and decided to investigate this further (see Chapter 2.2).
Taken together, these findings confirm C21orf70 as a component of early pre-40S particles.

2.2 CK1δ and CK1ε play a role in late 40S biogenesis

In mammals, there are seven isoforms of casein kinase 1 (CK1): α, β, γ1, γ2, γ3, δ, and ε. They play different roles in several cellular pathways such as cell proliferation (Peters et al., 1999), establishment of circadian rhythm (Lee et al., 2001), and cancer development (Knippschild et al., 1997). In *S. cerevisiae*, the serine/threonine kinase Hrr25 is a homolog of CK1 and has previously been demonstrated to be involved in biogenesis of both ribosomal subunits (see chapter 1.2.5). In mammalian cells, CK1 has been linked to 60S biogenesis by phosphorylation of the yeast Tif6 homolog eIF6 promoting its nuclear export (Basu et al., 2001; Biswas et al., 2011). Its direct effect on 60S maturation, however, remains to be elucidated.
We set out to investigate the involvement of CK1 in 40S biogenesis, in particular to find out which isoforms of CK1 are required and at which pre-40S maturation step they play a role.

2.2.1 Chemical inhibition of CK1 leads to late 40S biogenesis defects

After identifying CK1δ and CK1ε as components of pre-40S (Chapter 2.1.5), we tested whether inhibition of CK1 activity leads to defects in 40S biogenesis. For this, we treated cells with the CK1 inhibitor D4476 (Bain et al., 2007; Rena et al., 2004). D4476 has been shown to inhibit CK1δ (Rena et al., 2004) as well as CK1ε (Bryja et al., 2007), but it has not been systematically studied which other isoforms it might inhibit as well. Following the D4476 treatment, the localization of the 40S trans-acting factors PNO1 and ENP1 was analyzed by immunofluorescence (IF) since it has been previously shown that their mislocalization can indicate which step of 40S biogenesis is impaired (Zemp

et al., 2009; Wild et al., 2010). ENP1 as well as PNO1 are predominantly nuclear/nucleolar proteins at steady state (Fig. 2.2.1), but they have been shown to accompany pre-40S to the cytoplasm where they are released to shuttle back to the nucleus for another round of 40S maturation. Upon treatment of HeLa cells with D4476, ENP1 and PNO1 partially relocalize to the cytoplasm (Fig. 2.2.1), suggesting a defect in cytoplasmic 40S biogenesis.

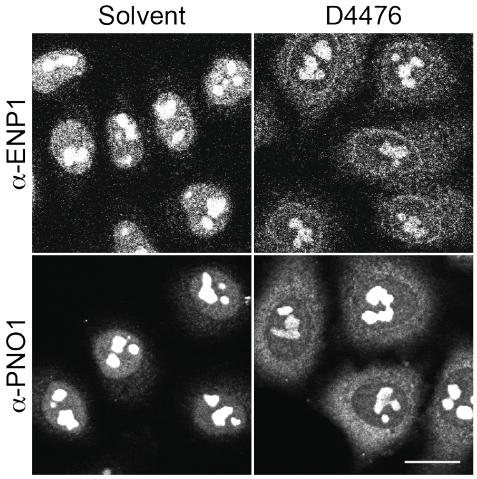

Figure 2.2.1
Inhibition of CK1 by D4476 leads to relocalization of 40S trans-acting factors to the cytoplasm
HeLa cells were either treated with solvent (DMSO) or D4476 (100 µM, 8 h), fixed and analyzed by immunofluorescence with the indicated antibodies. The 40S trans-acting factors ENP1 and PNO1 partially mislocalize to the cytoplasm upon D4476 treatment. Scale bar, 20 µm.

2.2.2 Co-depletion of CK1δ/ε leads to late 40S biogenesis defects

To further investigate the involvement of the different CK1 isoforms in 40S maturation, we turned to siRNA-mediated depletion of the individual CK1 isoforms as well as co-depletion experiments. Again, the localization of several 40S trans-acting factors visualized by immunofluorescence was used as a readout. Single knockdown of CK1 isoforms did not alter the localization of the investigated trans-acting factors (Fig. 2.2.2 and data not shown).

However, only co-depletion of CK1δ and CK1ε could reproduce the partial mislocalization of ENP1 and PNO1 as observed by D4476 treatment (Fig 2.2.2). Additionally, the localization of the 40S trans-acting factors NOC4L, RRP12 and RIOK2 was analyzed. While RRP12 partially relocalized to the cytoplasm similar to ENP1 and PNO1, NOC4L localization was not affected, most likely since it does not accompany pre-40S to the cytoplasm.

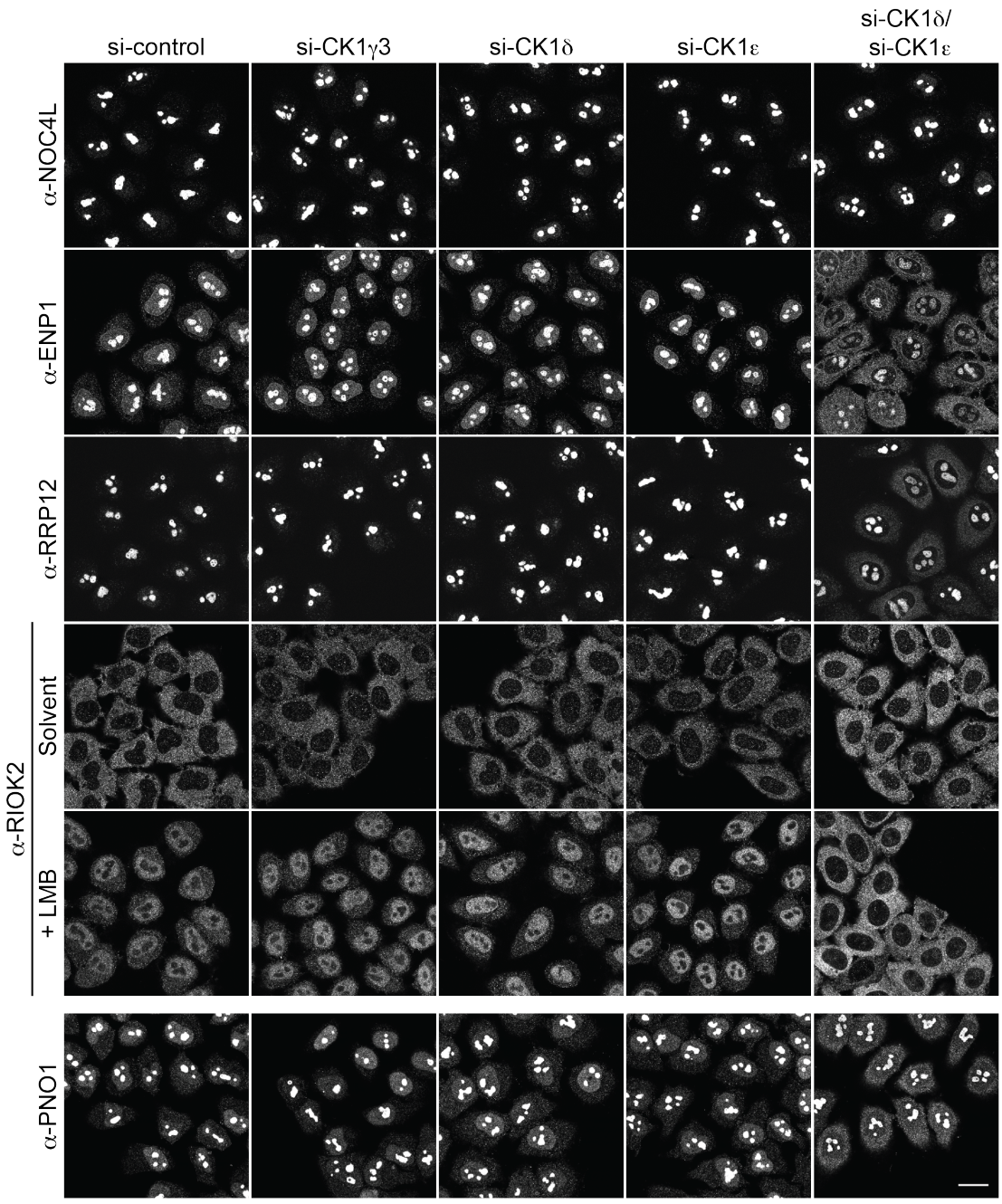

Figure 2.2.2
Co-depletion of CK1δ and CK1ε leads to cytoplasmic recycling defects of 40S trans-acting factors
HeLa cells were treated with the indicated siRNAs for 72 h. Cells were fixed and analyzed by immunofluorescence using the indicated antibodies. For RIOK2 localization analysis, cells were treated with solvent (ethanol) or leptomycin B (LMB) 1 h prior to fixation. Upon co-depletion of CK1δ and CK1ε, several 40S trans-acting factors mislocalize to the cytoplasm and RIOK2 is unable to relocalize to the nucleoplasm after LMB treatment. PNO1 localization was analyzed in an independent experiment. Scale bar, 20 µm.

The kinase RIOK2, cytoplasmic in steady state, did not change its localization upon CK1δ/ε co-depletion (Fig. 2.2.2). When HeLa cells were treated with leptomycin B (LMB), a small molecule inhibitor that blocks CRM1-dependent

export by binding to a cysteine residue in its central region (Kudo et al., 1999), RIOK2 accumulated in the nucleoplasm since it is a shuttling protein (Fig. 2.2.2; Zemp at al., 2009). However, upon combination of LMB treatment with CK1δ/ε co-depletion, RIOK2 failed to shuttle back to the nucleoplasm and remained cytoplasmic (Fig. 2.2.2), indicating the inhibition of trans-acting factor release from late pre-40S.

To support the apparent redundant function of CK1δ and CK1ε in cytoplasmic 40S biogenesis, we treated HeLa cells with different small molecule inhibitors of CK1. The inhibitors LH846 and PF4800567 preferentially target CK1δ and CK1ε, respectively (Lee et al., 2011; Walton et al., 2009), whereas PF670462 potently inhibits both isoforms (Badura et al., 2007). Treatment with LH846 or PF4800567 alone did not change the localization of ENP1 (Fig. 2.2.3). Upon combination of LH846 and PF4800567 treatment, ENP1 accumulated in the cytoplasm, comparable to D4476 treatment (Fig. 2.2.3) and siRNA-mediated co-depletion (Fig. 2.2.2). The same effect on ENP1 was observed when cells were treated with low concentrations of PF670462 (Fig. 2.2.3).

Taken together, co-inhibition as well as co-depletion of CK1δ and CK1ε leads to cytoplasmic 40S biogenesis defects by impairing trans-acting factor release from pre-40S particles.

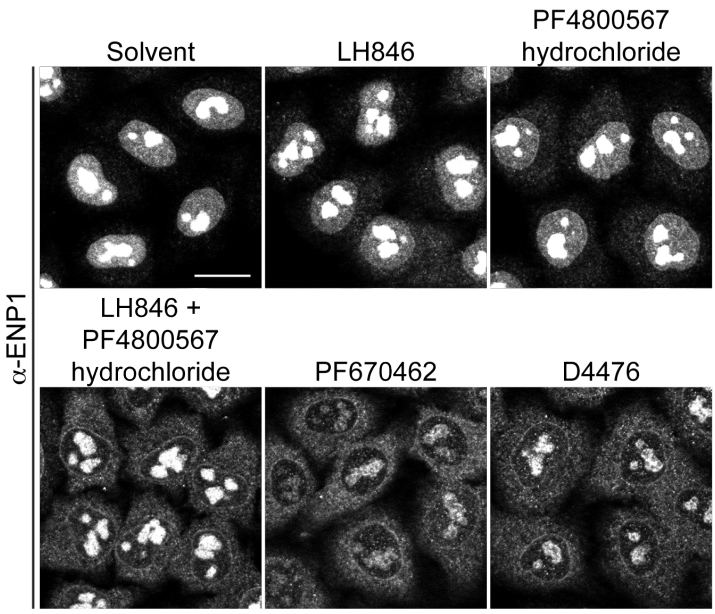

Figure 2.2.3
Coinhibition of CK1δ and CK1ε leads to cytoplasmic ENP1 accumulation
HeLa cells were treated with solvent (DMSO) or the indicated CK1 inhibitors for 6 h followed by fixation and immunofluorescence analysis using an anti-ENP1 antibody. Single inhibition of CK1δ (LH846) or CK1ε (PF4800567 hydrochloride) does not alter ENP1 localization, whereas inhibition of both (lower panel) leads to ENP1 accumulation in the cytoplasm. Scale bar, 20 µm.

2.2.3 The kinase activity of CK1ε is required for ENP1 recycling

CK1δ and CK1ε depletion by siRNA treatment and chemical inhibition of both isoforms led to the same phenotype. While the first method downregulates protein levels, the second merely inhibits protein function but keeps protein levels stable. To further investigate whether the presence of CK1 on the pre-40S particle is sufficient or whether kinase activity is needed for 40S biogenesis, we performed rescue experiments. For this, CK1δ and CK1ε were co-depleted by RNAi in HeLa cells followed by transient transfection of either wild type CK1ε or a kinase-dead mutant (D149A) (Fig. 2.2.4A). Transfected cells were scored for ENP1 localization, with three possible phenotypes: predominantly nuclear, predominantly cytoplasmic and an intermediate phenotype where ENP1 was localized evenly throughout the cell. Three independent experiments were quantified (Fig. 2.2.4B) and a partial but significant rescue could be observed upon CK1ε wild type transfection, whereas CK1ε(D149A) expression did not rescue ENP1 localization, indicating that kinase activity of CK1ε is required for ENP1 release from pre-40S.

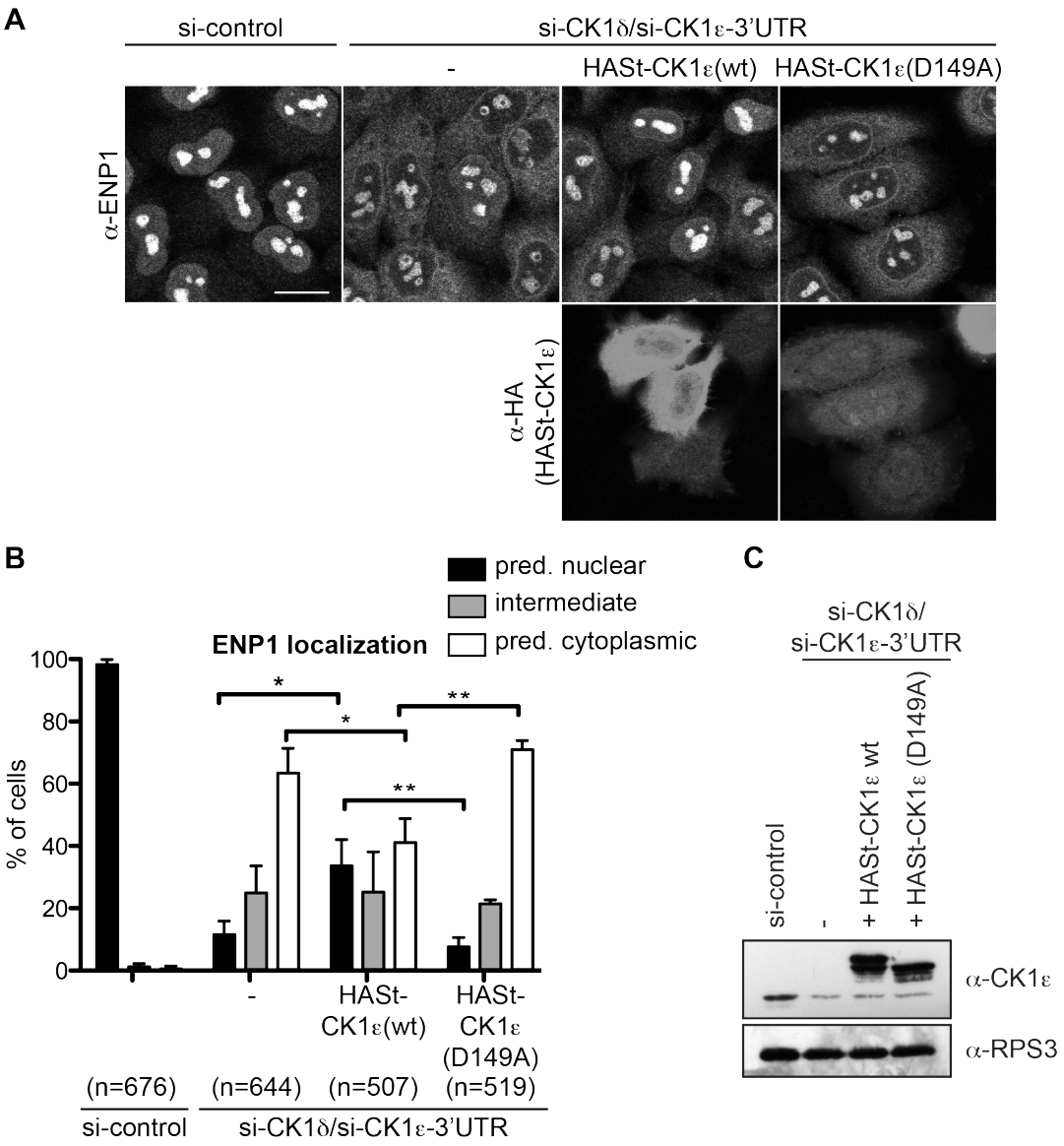

Figure 2.2.4
CK1ε wild type but not kinase-dead partially rescues ENP1 mislocalization
(A) HeLa cells were treated with the indicated siRNAs for 48 h. 24 h prior to fixing the cells, HASt-CK1ε wild type (wt) or HASt-CK1ε kinase-dead (D149A) was transiently transfected. Cells were analyzed by immunofluorescence with the indicated antibodies. Scale bar, 20 µm.
(B) Quantification of three independent rescue experiments. Cells were analyzed based on ENP1 localization and divided into three phenotypic classes: predominantly nuclear, intermediate and predominantly cytoplasmic localization. For cells transfected with HAST-CK1ε (wt) or (D149A), only cells displaying anti-HA IF signal were used in the analysis. The percentage of cells displaying a certain ENP1 localization per condition is shown with the standard deviation. An unpaired t-test was performed and significant differences of the means for rescued cells are marked with an asterisk (* equals P value <0.05; ** equals P value <0.01).
(C) Western blot analysis of one of the three independent experiments of (B) with the indicated antibodies to ensure efficient CK1ε downregulation and rescue construct expression.

2.2.4 CK1δ/ε are not required for pre-40S export but for pre-rRNA processing

It has previously been shown that when the *S. cerevisiae* CK1 homolog Hrr25 is depleted, 40S subunits accumulate in the nucleoplasm as visualized by the fluorescently labeled reporter protein Rps2-YFP (Schäfer et al., 2006), suggesting that Hrr25 is needed for nuclear export of pre-40S. So far, we only observed cytoplasmic defects of 40S biogenesis upon depletion/inhibition of CK1δ and CK1ε and thus wanted to test whether CK1 depletion also leads to nucleoplasmic accumulation of pre-40S. For this, we used a HeLa FRT TetR cell line expressing RPS2-YFP under a tetracycline-inducible promoter (Zemp et al., 2009), which allows for visualization of newly synthesized pre-40S subunits. In addition, we immunostained cells for ENP1 as an additional readout. Under control conditions, RPS2-YFP localized predominantly to the cytoplasm and nucleoli, but accumulated in the nucleoplasm upon depletion of the exportin CRM1 (Fig. 2.2.5A). However, neither single nor co-depletion of CK1δ and CK1ε led to nuclear accumulation of RPS2-YFP whereas ENP1 mislocalized to the cytoplasm upon CK1δ/ε co-depletion (Fig. 2.2.5A). This demonstrates that CK1δ and CK1ε are not required for nuclear 40S maturation steps or pre-40S export but rather for late cytoplasmic 40S biogenesis steps.

The maturation of the small ribosomal subunit in the cytoplasm does not only include the release of trans-acting factors but also involves a ribosomal RNA (rRNA) processing event during which the 18S-E pre-rRNA is cleaved at site 3 (site D in yeast) to yield the mature 18S rRNA. This step is very likely catalyzed by NOB1, the human homolog of the yeast endonuclease Nob1 (see chapter 1.2.2). Next, we investigated whether cytoplasmic rRNA processing is impaired upon CK1δ and CK1ε depletion. For this, fluorescence *in situ* hybridization (FISH) with a Cy5-labeled probe complementary to the 5' end of the ITS1 was used. This probe detects all 18S rRNA precursors but not the mature 18S rRNA (Fig. 2.2.5B). In HeLa cells treated with negative control siRNAs, the detected signal is predominantly nucleolar, whereas depletion of RIOK2 leads to accumulation of 18S-E pre-rRNA in the cytoplasm (Fig. 2.2.5C and Zemp et al., 2009). Similarly to RIOK2 depletion, upon co-

depletion of CK1δ and CK1ε an increased cytoplasmic signal of the Cy5-5'ITS1 probe was detected (Fig. 2.2.5C), indicating that CK1δ/ε are required for efficient site 3 cleavage in the cytoplasm.

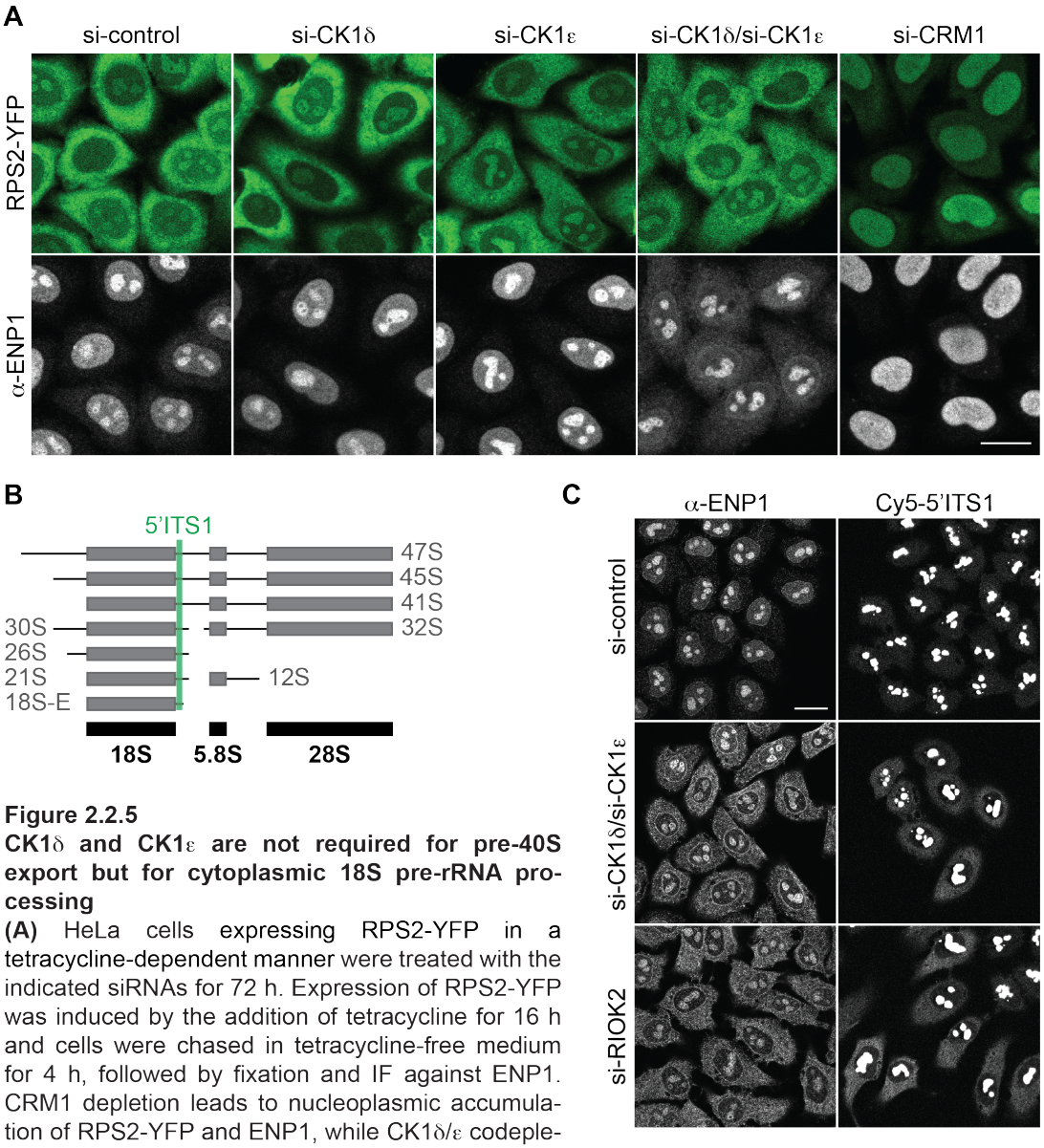

Figure 2.2.5
CK1δ and CK1ε are not required for pre-40S export but for cytoplasmic 18S pre-rRNA processing

(A) HeLa cells expressing RPS2-YFP in a tetracycline-dependent manner were treated with the indicated siRNAs for 72 h. Expression of RPS2-YFP was induced by the addition of tetracycline for 16 h and cells were chased in tetracycline-free medium for 4 h, followed by fixation and IF against ENP1. CRM1 depletion leads to nucleoplasmic accumulation of RPS2-YFP and ENP1, while CK1δ/ε codepletion only affects ENP1 localization. Scale bar, 20 µm.

(B) Scheme of human rRNA precursors. The main precursors are shown in grey, the three mature rRNA species are shown in black. The probe used for detection in (C) is depicted in green.

(C) HeLa cells were treated with the indicated siRNAs for 72 h, followed by fluorescence in situ hybridization (FISH) analysis using a Cy5 labeled 5'ITS1 probe or immunofluorescence using an anti-ENP1 antibody. Depletion of RIOK2 was used as a positive control. CK1δ and CK1ε co-depletion leads to cytoplasmic Cy5-5'ITS1 signal, indicating 18S-E pre-rRNA processing defects. Scale bar, 20 µm.

2.2.5 ENP1 and LTV1 are phosphorylated on pre-40S in a CK1-dependent manner

The chemical inhibition and RNAi experiments indicated that CK1δ and CK1ε are involved in cytoplasmic maturation steps of pre-40S subunits and that the kinase activity of CK1ε appears to be required for release of ENP1 from pre-40S. In *S. cerevisiae*, Hrr25 phosphorylates Ltv1, Enp1 and Rps3 on the preribosomal particle, which contributes to their release (Schäfer et al., 2006). To assess whether CK1 is able to phosphorylate proteins associated with human pre-40S subunits, we isolated 40S precursors by TAP using HASt-LTV1 as bait (Wyler et al., 2011), and confirmed association of CK1δ and CK1ε by Western blotting (Fig. 2.2.6A).

Next, we incubated LTV1-TAP particles with ^{32}P-γATP in the presence or absence of the CK1δ/ε inhibitor PF670462 and detected phosphorylation by autoradiography. PF670462 efficiently inhibited the ability of CK1δ and CK1ε to phosphorylate casein *in vitro* while not affecting autophosphorylation activity of RIOK2 (Fig. 2.2.6B). Of the proteins co-purified with HASt-LTV1, two major bands could be observed in the autoradiogram, which disappeared upon PF670462 treatment. Mass spectrometry analysis identified these bands as HASt-LTV1 and ENP1. For RPS3, only weak phosphorylation was observed. Taken together, these data show that phosphorylation of LTV1 and ENP1 is dependent on the activity of the pre-40S components CK1δ and CK1ε, which are required for cytoplasmic trans-acting factor release and 18S-E rRNA processing.

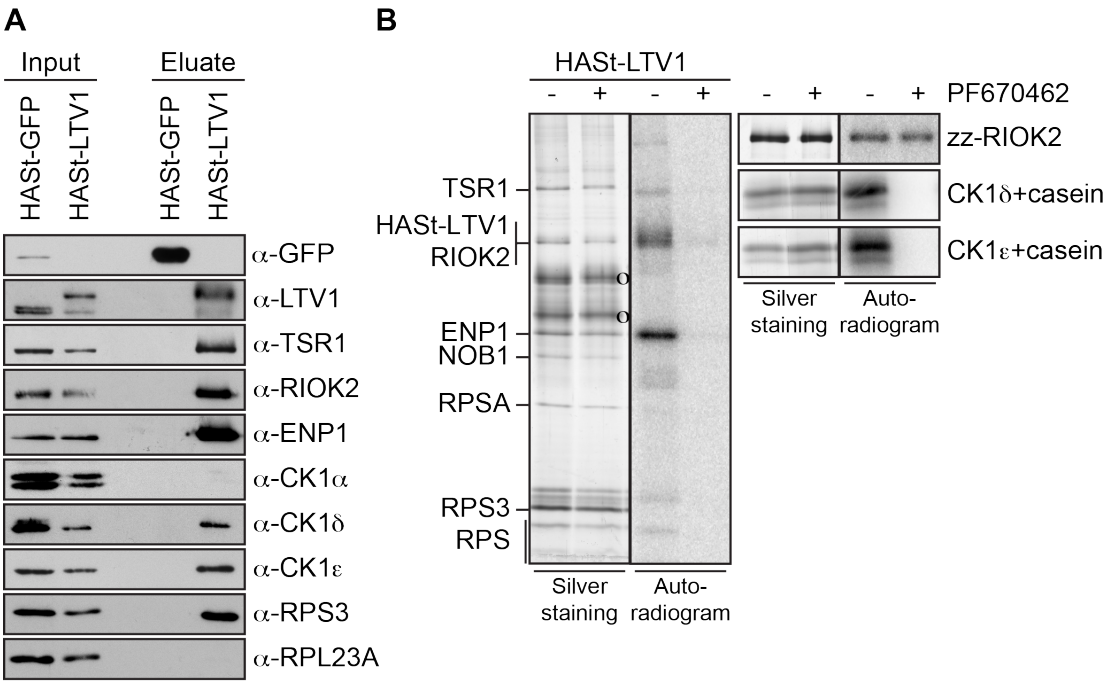

Figure 2.2.6
Phosphorylation of LTV1 and ENP1 on pre-40S is dependent on CK1
(A) TAP of HEK 293 FlpIn TRex cells expressing HASt-LTV1 in a tetracycline-dependent manner. Cleared cell lysate (Input) and eluted proteins (Eluate) were analyzed by SDS-PAGE followed by Western blotting using the indicated antibodies. HASt-GFP served as a negative control. CK1δ and CK1ε are co-purified with HASt-LTV1.
(B) TAP of HASt-LTV1 followed by addition of ^{32}P-γATP to the purified pre-40S particles in the presence or absence of the CK1δ/ε inhibitor PF670462 (5 µM) at 30°C for 20 min. Eluted proteins were analyzed by silver staining (left) and autoradiography (right). The identity of radioactively labeled protein bands was determined in a separate TAP experiment by mass spectrometry. Circles mark unspecific bands. For control reactions, purified zz-RIOK2 alone or casein with either CK1δ or CK1ε were incubated with ^{32}P-γATP in the presence or absence of PF670462 (5 µM) and analyzed as described above. HAST-LTV1 and ENP1 are phosphorylated, and their phosphorylation is reduced upon CK1 inhibition. Autophosphorylation of zz-RIOK2 was not affected by PF670462 treatment.

2.3 Identification and characterization of the novel 60S trans-acting factors NF45/NF90

2.3.1 Tandem affinity purification of human Rei1 co-purifies NF45 and NF90

In order to identify novel trans-acting factors in mammalian 60S ribosomal subunit biogenesis, we performed TAP of human 60S trans-acting factors followed by proteomic analysis of the purified particles by mass-spectrometry. This technique was already successfully used to analyze human pre-40S composition as well as to identify the previously uncharacterized, mammalian-specific 40S trans-acting factor C21orf70 and CK1δ/ε as novel pre-40S components (Wyler et al, 2011; Chapter 2.1.2).

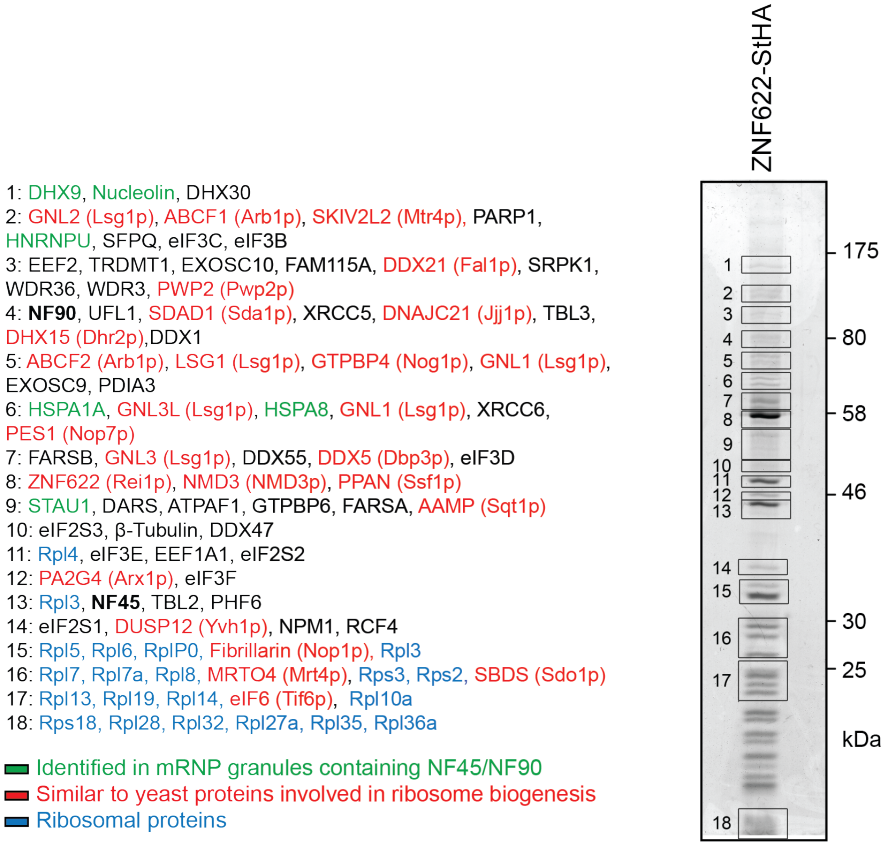

Figure 2.3.1
Mass spectrometric analysis of proteins co-purified with ZNF622-StHA
Pre-60S ribosomal particles were isolated by TAP using a ZNF622-StHA HEK 293 FlpIn TRex cell line. Expression of ZNF622-StHA was induced with tetracycline 24 h prior to harvesting the cells. The eluate was analyzed by SDS-PAGE followed by Coomassie staining. Protein bands were excised from the gel and subjected to mass spectrometric analysis. Proteins of which more than 4 peptides were detected are listed. NF90 (band 4) and NF45 (band 13) are present as the strongest and second strongest hit, respectively.

TAP of the human homolog of the budding yeast *S. cerevisiae* 60S trans-acting factor Rei1, ZNF622/ZPR9, co-purified pre-60S particles (Wild et al., 2010). We analyzed the associated proteins by mass-spectrometry. As expected, most of the detected proteins are ribosomal proteins of the large subunit (RPL) as well as human homologs of yeast 60S trans-acting factors (Fig. 2.3.1).

While *S. cerevisiae* Rei1 is characterized as a predominantly cytoplasmic protein, which plays a role in the release of Arx1 from pre-60S in the cytoplasm (see 1.2.5), ZNF622 additionally localizes to nucleoli, as observed by immunostaining of endogenous ZNF622 as well as transiently transfected ZNF622-StHA (Fig. 2.3.2A). To exclude that the detected nucleolar localization of ZNF622 is not an artifact of the antibody or overexpression of the transfected protein, we treated cells with the CRM1 inhibitor LMB. Endogenous as well as transiently transfected ZNF622-StHA accumulated in the nucleoplasm upon treatment of cells with LMB (Fig. 2.3.2A), which indicates a CRM1-dependent shuttling behavior of ZNF622. This suggests that ZNF622 joins pre-60S particles early during their maturation pathway in the nucleolus and accompanies them to the cytoplasm. Thus, the purified particles from the ZNF622 TAP would comprise a mixture of early and late pre-60S.

Interestingly, proteins that are not similar to any known yeast 60S trans-acting factors were also detected in the ZNF622 TAP. Two of these proteins were the Interleukin enhancer-binding factors 2 and 3 (ILF2 and ILF3, respectively), also termed NF45 and NF90, respectively.

Additionally, NF45 and NF90 were also present in TAPs of other 60S trans-acting factors, namely MRTO4 and PA2G4/EBP1. MTRO4 is the homolog of *S. cerevisiae* Mrt4, a placeholder for the ribosomal stalk protein RPLP0 ((Lo et al., 2009; Rodríguez-Mateos et al., 2009), see also 1.2.5). PA2G4 is the human homolog of Arx1p (Squatrito et al, 2004), which may act in yeast as a nuclear export receptor for pre-60S particles (Bradatsch et al, 2007, see also 1.2.4). Both proteins co-purified pre-60S along with NF45 and NF90 (data not shown).

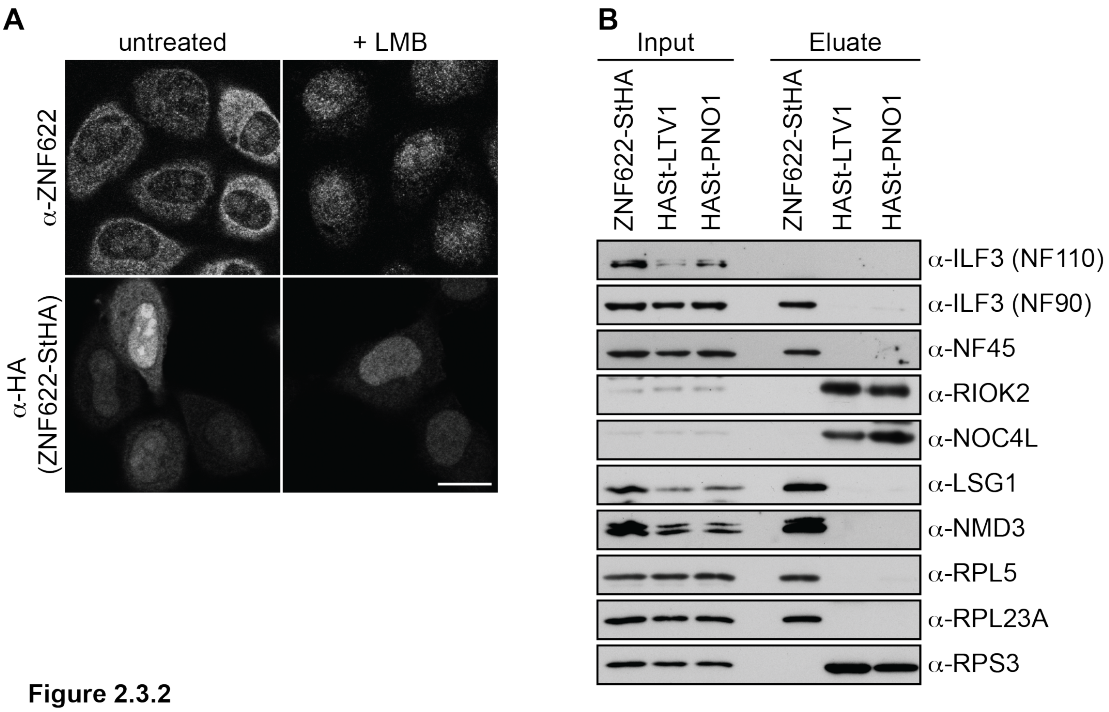

Figure 2.3.2
TAP of ZNF622-StHA co-purifies NF45 and NF90
(A) Comparison of the localization of the endogenous 60S trans-acting factor ZNF622 (upper panel) to transiently transfected ZNF622-StHA (lower panel). Proteins were detected by IF using the indicated antibodies. To study shuttling behavior, cells were treated with LMB to inhibit CRM1-mediated export. ZNF622 localizes predominantly to the cytoplasm in steady state, but is also present in nucleoli. After LMB treatment, ZNF622 accumulates in the nucleoplasm, which indicates shuttling behavior. Scale bar, 20 µm.
(B) TAP was performed from HEK 293 FlpIn TRex cell lines expressing the indicated HASt-tagged trans-acting factors in a tetracycline-inducible manner. Cleared cell extracts (Input) and eluted proteins (Eluate) were analyzed by SDS-PAGE followed by Western blotting using the indicated antibodies. NF45 and the ILF3 isoform NF90, but not NF110, copurify with ZNF622-StHA, whereas they are not associated with pre-40S particles (LTV1, PNO1).

To assess whether NF45 and NF90 specifically associate with pre-60S or whether they are also components of pre-40S ribosomal particles, we performed TAP of ZNF622 as well as the two 40S trans-acting factors LTV1 and PNO1 that purify pre-40S (Wyler et al., 2011). Western blot analysis shows that NF45 and NF90 are only present in the ZNF622 TAP but not in the LTV1 or PNO1 TAP (Fig. 2.3.2B). Notably, only the short isoform, called NF90 (see 1.4.2) but not the longer, C-terminally extended NF110 isoform (Fig. 2.3.4A) was co-purified with ZNF622.

2.3.2 NF45 and NF90 co-sediment with pre-60S

To further investigate the association of NF45 and NF90 with ribosomal particles, we performed sucrose gradient centrifugation of HeLa extract. The sedimentation behavior of 40S and 60S ribosomal subunits was visualized by

immunoblotting against RPS3 and RPL23A, respectively. In accordance with the ZNF622 TAP data, NF45 and NF90 partially co-migrated with 60S particles as it was the case for the 60S trans-acting factor LSG1 (Fig. 2.3.3). NF110 however was only detected near the top of the gradient, which suggests that it is only present as a free protein or in smaller complexes but does not associate with ribosomal subunits.

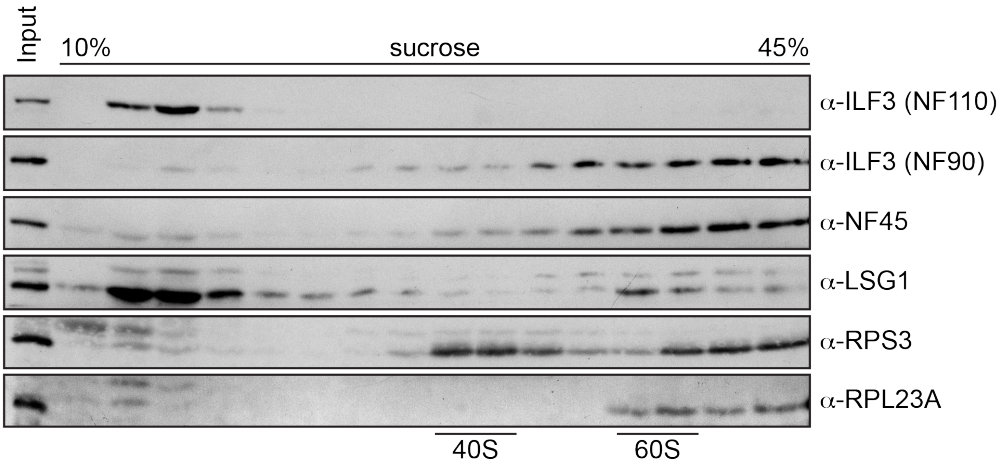

Figure 2.3.3
NF45 and NF90 co-sediment with (pre-)60S particles
Sucrose gradient analysis of sedimentation behavior of NF45 and NF90/NF110. Extract was prepared from HeLa cells and centrifuged on a 10-45% sucrose gradient. Samples of the extract (Input) and gradient fractions were analyzed by Western blotting using the indicated antibodies. Fractions containing pre-40S and pre-60S particles are indicated (40S and 60S, respectively). NF45 and NF90 but not NF110 are present in the same fractions as 60S particles.

2.3.3 Characterization of NF45 and NF90/NF110 localization

Since NF45 and NF90 but not NF110 appear to be associated with pre-60S particles, we wanted to characterize their subcellular localization. For this, we first performed cellular fractionation of HeLa cells and analyzed the presence of NF45 and NF90 in these fractions by immunoblotting. In steady state, NF45 and NF90 are nuclear proteins (Fig. 2.3.4B). Furthermore, immunofluorescence analysis showed that NF45 is predominantly localized to nucleoli and also NF90 displayed some nucleolar accumulation (Fig. 2.3.4C). Since the α-ILF3 antibody recognizes both NF90 and NF110 isoforms, we also used an antibody that specifically recognizes a peptide in the C-terminus of NF110 for IF analysis. NF110 is localized to the nucleoplasm and is not enriched in nucleoli (Fig. 2.3.4C).

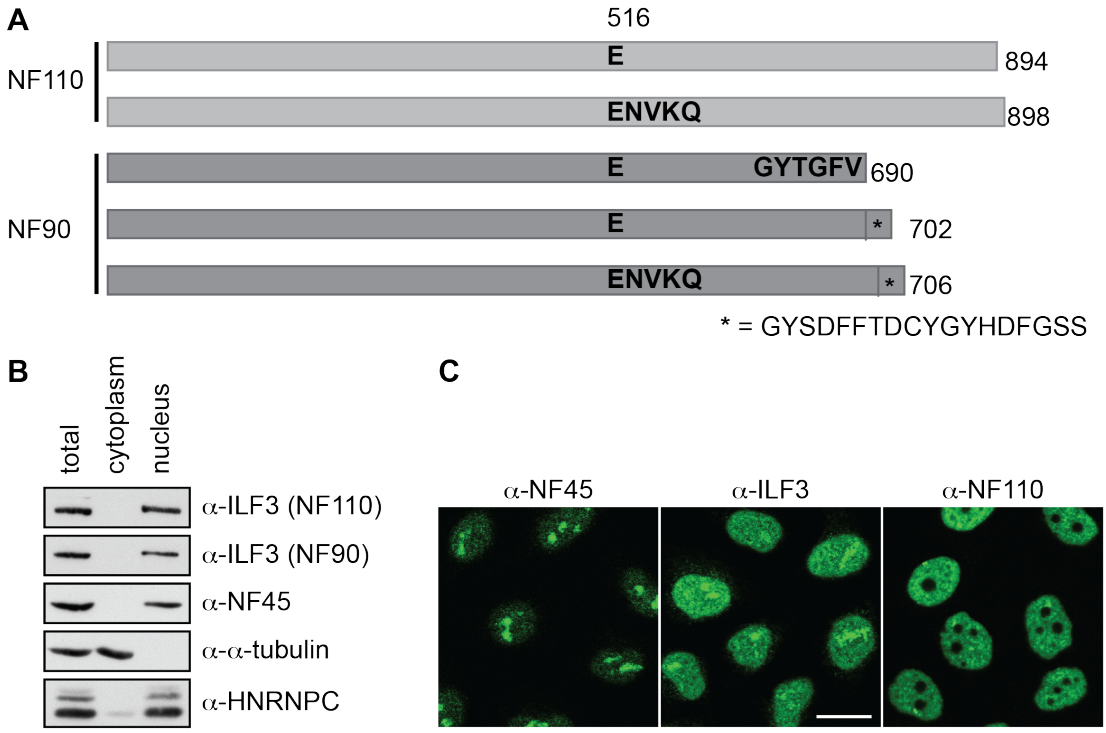

Figure 2.3.4
NF45 and NF90/NF110 are nuclear proteins
(A) Schematic representation of different human ILF3 isoforms. The two longer isoforms, termed NF110, only differ in a four amino acid (aa) insertion at aa 516. The shorter NF90 isoforms posess different C-termini and also differ in the aforementioned 4 aa insertion.
(B) HeLa cells were fractionated and analyzed by SDS-PAGE, followed by Western blotting with the indicated antibodies. NF45 and NF90/NF110 are exclusively present in the nuclear fraction.
(C) Immunofluorescence analysis of HeLa cells using antibodies recognizing either NF45, all ILF3 isoforms (α-ILF3) or specifically only the C-terminus of the two longer ILF3 isoforms (α-NF110). The antibody signal for NF45 and ILF3 is nucleoplasmic and enriched in nucleoli, while the NF110 isoforms localize to the nucleoplasm and are excluded from nucleoli. Scale bar, 20 μm.

To further distinguish NF90 and NF110 localization, N- and C-terminally HASt-tagged NF90 and NF110 (the longest of each isoform, see Fig. 2.3.4A) were generated and transiently transfected into HeLa cells. Localization of these constructs was detected by immunofluorescence. Nucleoli were visualized in the same cells by co-immunofluorescence with an antibody against the predominantly nucleolar 60S trans-acting factor RLP24/RSL24D1, a placeholder for its ribosomal protein homolog RPL24. While NF90 was mainly present in nucleoli, NF110 was distributed throughout the nucleoplasm (Fig. 2.3.5A). Only in cells overexpressing NF110-StHA, a slight nucleolar accumulation of NF110 could be observed in some cases.

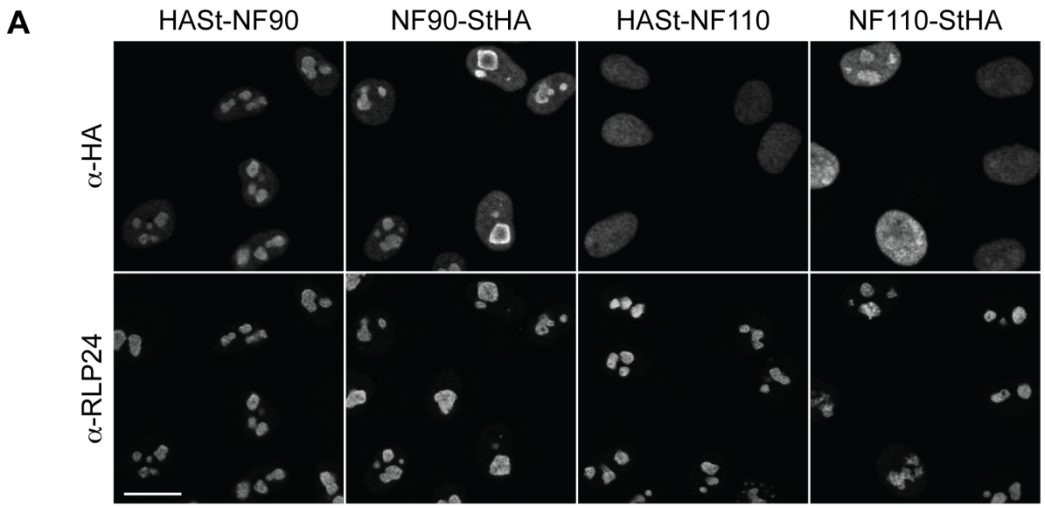

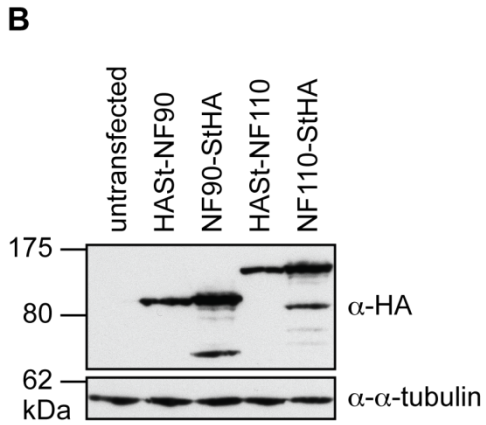

Figure 2.3.5
Different ILF3 isoforms show distinct localizations
(A) Transient transfection of HASt-tagged NF90 and NF110 into HeLa cells. Co-immunofluorescence analysis using the indicated antibodies was carried out to visualize localization of transfected constructs and nucleoli (α-RLP24). While NF90 is strongly enriched in nucleoli, NF110 is more evenly distributed throughout the nucleoplasm. Scale bar, 20 μm.
(B) Western blot analysis of (A) with the indicated antibodies was performed to ensure similar expression levels of the transfected constructs.

It has been previously reported that NF45 depletion affects NF90 levels and vice versa (Guan et al., 2008), most likely because heterodimerization stabilizes NF45/NF90 and the free proteins are more rapidly degraded. When we depleted NF45 in HeLa cells by siRNA treatment, we did not observe a strong decrease in NF90 levels. NF45, however, was significantly downregulated upon depletion of NF90/NF110 using an siRNA targeting both isoforms (si-NF90/110) (Fig. 2.3.6A).

Since we could not reproduce the previously described effect of NF45 depletion on NF90 levels, we wanted to analyze whether NF45 depletion could affect NF90 localization. For this, we generated a tetracycline-inducible HASt-NF90 expressing HeLa cell line and performed siRNA-mediated knockdown of NF45. Indeed, HASt-NF90 was no longer enriched in nucleoli when NF45 levels were reduced (Fig. 2.3.6B). This suggests that NF45 is needed for the correct nucleolar localization of NF90.

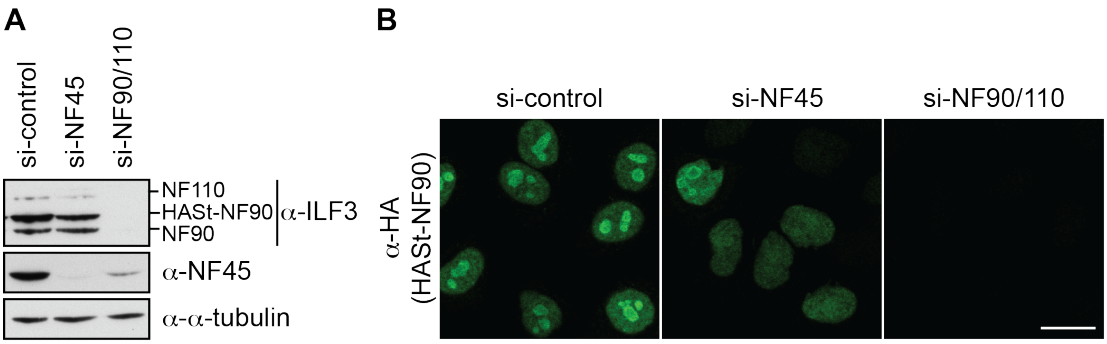

Figure 2.3.6
NF90/NF110 depletion affects NF45 levels and NF45 downregulation leads to NF90 mislocalization
HeLa FRT cells expressing HASt-NF90 in a tetracycline-dependent manner were treated with the indicated siRNAs for 72 h. Expression of HASt-NF90 was induced by the addition of tetracycline 24 h prior to fixation/harvesting.
(A) Western blot analysis with the indicated antibodies was performed to ensure efficient downregulation of NF45 and NF90/NF110. Notably, NF45 levels are also significantly reduced after NF90/NF110 depletion (last lane).
(B) Immunofluorescence analysis of (A). HASt-NF90 is less enriched at nucleoli after NF45 depletion. Scale bar, 20 μm.

To investigate whether the nucleolar localization of NF90 and NF45 is dependent on active ribosome biogenesis, we specifically inhibited RNA polymerase I (POL I)-dependent transcription by treating HeLa cells with a low concentration of actinomycin D (ActD) (Perry, 1963) and visualized NF45 localization by immunofluorescence. To distinguish the localization of the different ILF3 isoforms, we performed immunofluorescence with an antibody specifically recognizing NF110 and used the above-mentioned HASt-NF90 HeLa cell line to specifically detect the NF90 isoform. Interestingly, while NF45 was still present in the nucleolar remnants after ActD treatment shown by colocalization with RLP24 (Fig. 2.3.7A), NF90 was only present in the nucleoplasm and even partly excluded from nucleoli (Fig. 2.3.7B). This suggests that the NF45/NF90 heterodimer can no longer be retained in nucleoli after inhibition of POL I-dependent rRNA transcription.

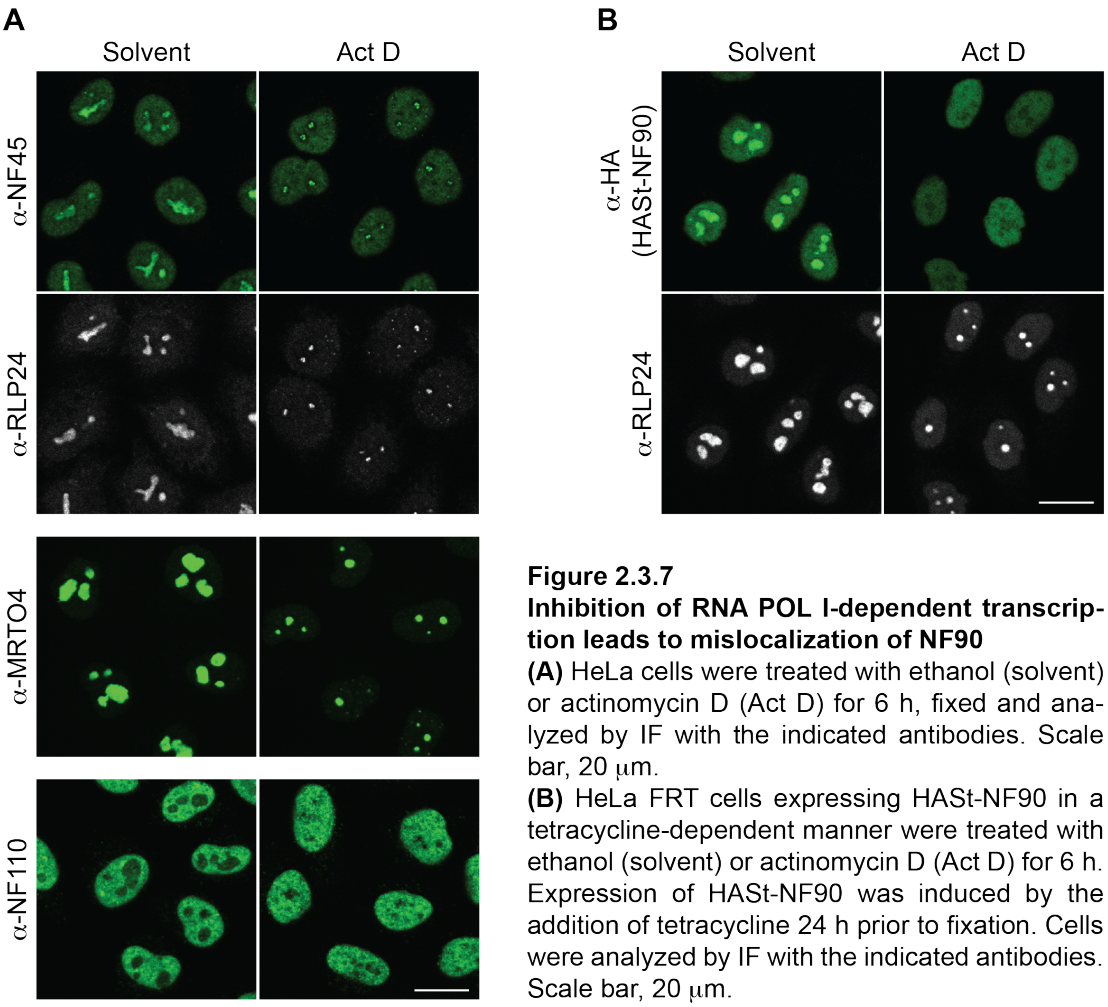

Figure 2.3.7
Inhibition of RNA POL I-dependent transcription leads to mislocalization of NF90
(A) HeLa cells were treated with ethanol (solvent) or actinomycin D (Act D) for 6 h, fixed and analyzed by IF with the indicated antibodies. Scale bar, 20 μm.
(B) HeLa FRT cells expressing HASt-NF90 in a tetracycline-dependent manner were treated with ethanol (solvent) or actinomycin D (Act D) for 6 h. Expression of HASt-NF90 was induced by the addition of tetracycline 24 h prior to fixation. Cells were analyzed by IF with the indicated antibodies. Scale bar, 20 μm.

2.3.4 NF45/NF90 depletion leads to 60S export defects and changes in nucleolar morphology

After establishing that the NF45/NF90 complex is a novel component of pre-60S particles, we set out to investigate whether depletion of NF45/NF90 influences 60S biogenesis. For this, a HeLa cell line expressing RPL29-GFP in a tetracycline-dependent manner was used (Wild et al., 2010) to observe newly synthesized (pre-)60S subunits. In cells treated with control siRNA, the reporter was mainly localized to the nucleolus and cytoplasm, and thus represents early, immature pre-60S and late pre-60S/mature 60S subunits, respectively. Upon depletion of either NF45 or NF90/NF110, the cytoplasmic signal was strongly reduced, and pre-60S particles accumulated in the nucleoplasm (Fig. 2.3.8A). This indicates either a 60S export defect or a nuclear 60S maturation defect prior to export. Interestingly, not only the localization of the fluorescent reporter changed upon knockdown of

NF45/NF90, but also the shape and size of nucleoli differs from control cells. There were fewer nucleoli per cell while they appeared bigger and more spherical. The same effect of NF45/NF90 depletion on nucleolar morphology was observed when the 60S trans-acting factor MRTO4 and the POL I transcriptional activator UBF were visualized by immunofluorescence (Fig. 2.3.8C) and likewise when FBL (Fig. 2.3.9A), NPM and RLP24 were used as nucleolar markers (data not shown).

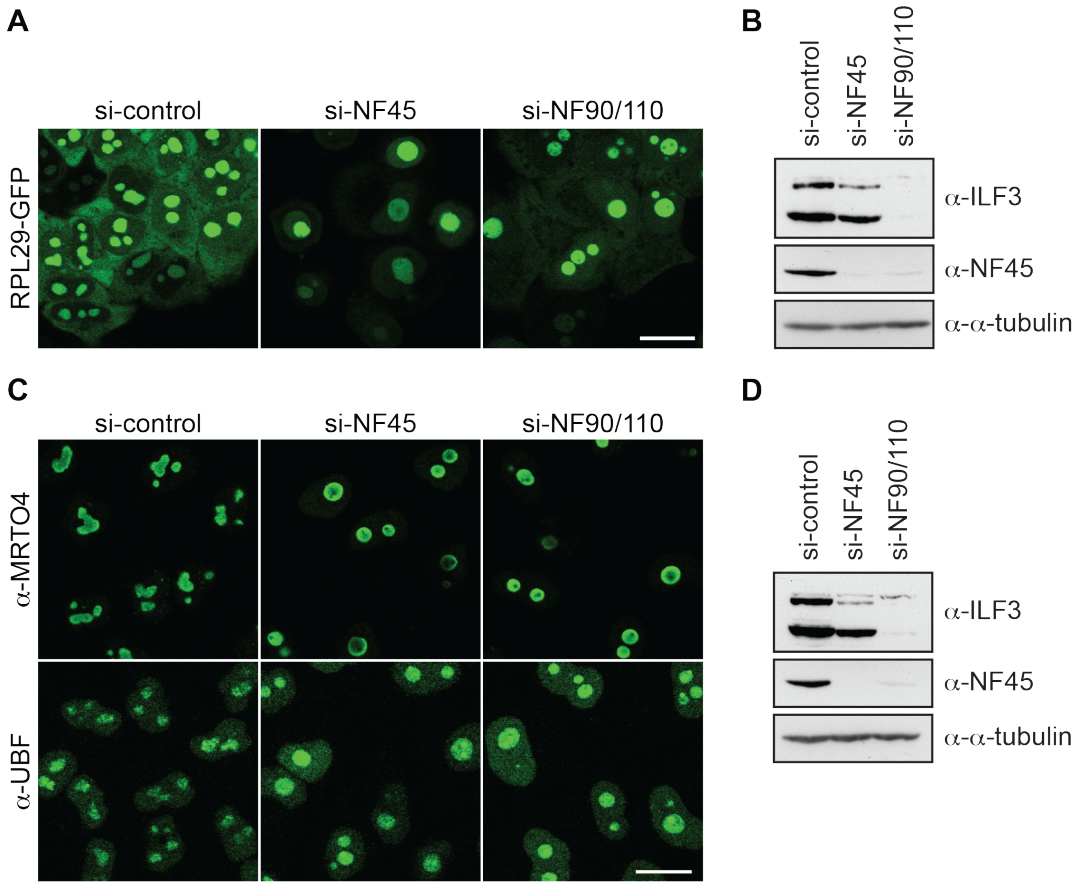

Figure 2.3.8
NF45 or NF90/NF110 depletion affects 60S biogenesis and leads to changed nucleolar morphology
(A) HeLa cells expressing RPL29-GFP in a tetracycline-inducible manner were treated the indicated siRNAs for 72 h. 20 h before fixation, cells were induced by the addition of tetracycline (tet). Cells were chased with tet-free medium for 5 h before fixation. Scale bar, 20 μm.
(B) Western blot analysis of (A) with the indicated antibodies was performed to ensure efficient downregulation.
(C) IF analysis of HeLa cells treated with the indicated siRNAs for 72 h. Cells were fixed and analyzed by immunostaining using the indicated antibodies. Scale bar, 20 μm.
(D) Western blot analysis of (C) using the indicated antibodies was performed to ensure efficient downregulation.

To verify whether this phenotype is specific for NF45/NF90 depletion or whether downregulation of other 60S trans-acting factors leads to the same effect, siRNA-mediated knockdown was carried out for other factors that play a role in 60S maturation, namely ZNF622, PES1, XPO5, and NPM. Depletion of the first two led to a very similar nucleolar phenotype observed by FBL immunostaining (Fig. 2.3.9A). Downregulation of XPO5 did not result in significant changes in nucleolar shape or size, while nucleoli were slightly smaller upon NPM depletion (Fig. 2.3.9A).

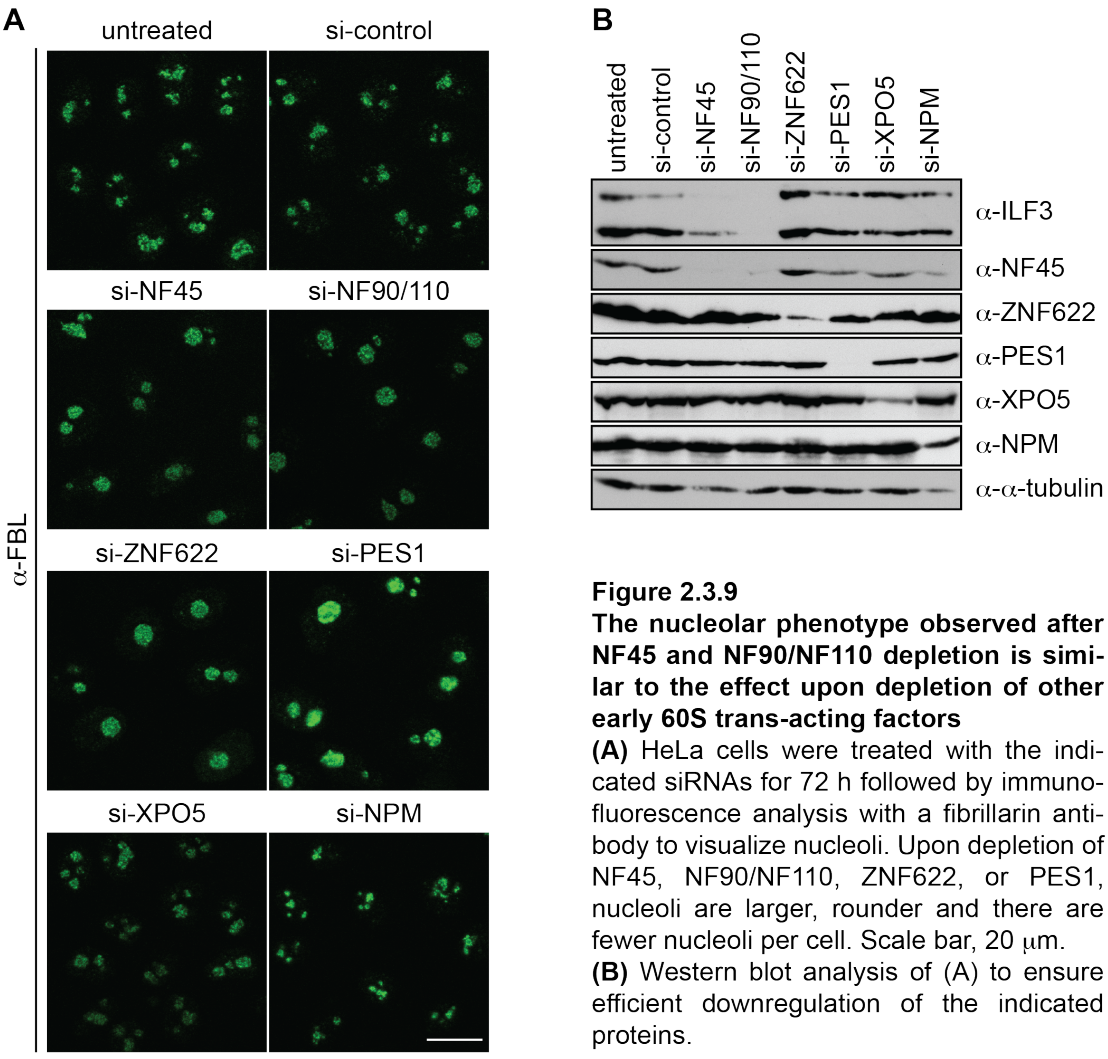

Figure 2.3.9
The nucleolar phenotype observed after NF45 and NF90/NF110 depletion is similar to the effect upon depletion of other early 60S trans-acting factors
(A) HeLa cells were treated with the indicated siRNAs for 72 h followed by immunofluorescence analysis with a fibrillarin antibody to visualize nucleoli. Upon depletion of NF45, NF90/NF110, ZNF622, or PES1, nucleoli are larger, rounder and there are fewer nucleoli per cell. Scale bar, 20 μm.
(B) Western blot analysis of (A) to ensure efficient downregulation of the indicated proteins.

Taken together, NF45/NF90 are required for efficient 60S biogenesis and their depletion leads to changes in nucleolar morphology, similar to the phenotype observed after depletion of certain other 60S trans-acting factors.

2.3.5 NF45/NF90 depletion does not significantly influence rRNA processing but leads to decreased rRNA precursor levels

The NF45/NF90 complex has first been described as a transcriptional activator of the interleukin 2 promoter (Yaseen et al., 1993; Corthesy et al., 1994). Taken together with the observation that NF45/NF90 localize to nucleoli where rRNA transcription occurs and their influence on nucleolar architecture (Chapter 2.3.4), we speculated that NF45/NF90 might play a role in POL I-mediated transcription of the long rRNA precursor. To examine this, HeLa cells were depleted for NF45 and/or NF90/NF110 and rRNA precursors were visualized by FISH using a fluorescently labeled probe that specifically binds to the 5' end of the external transcribed spacer 1 (5'ETS1), thus labeling only the earliest, nucleolar 47S rRNA precursor (Fig. 2.3.10A).

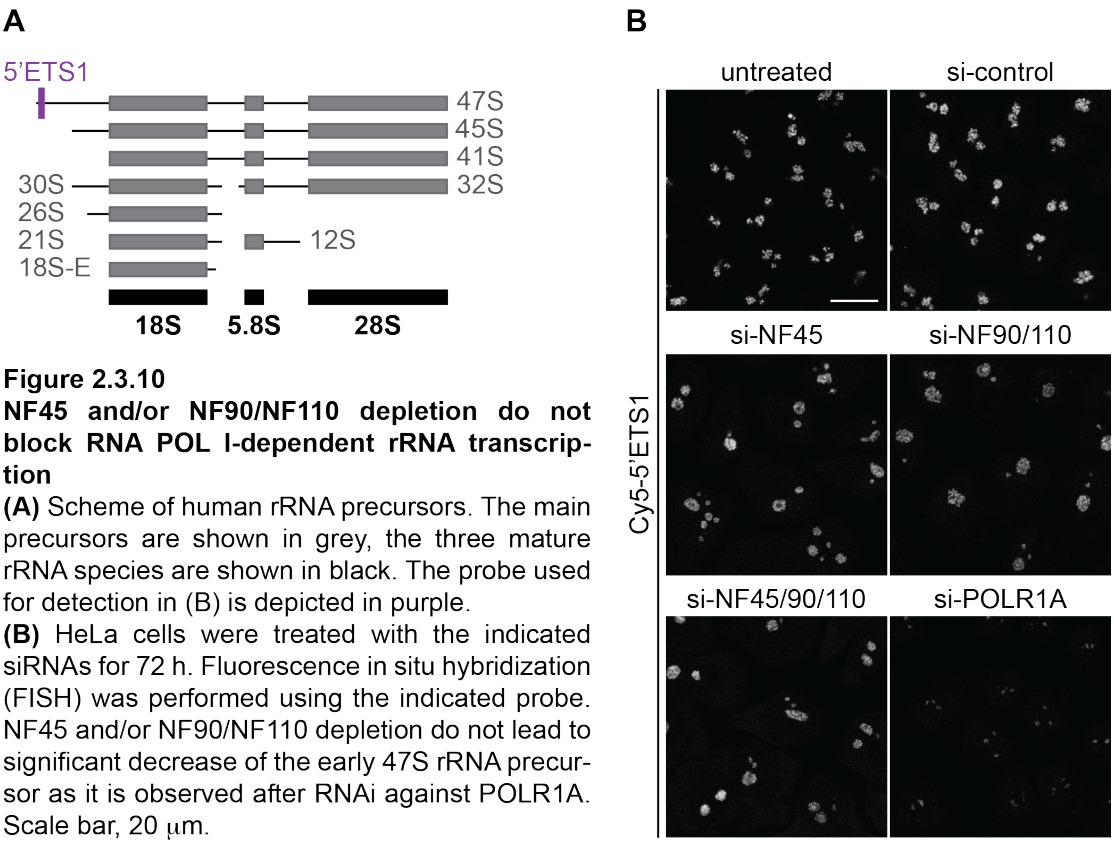

Figure 2.3.10
NF45 and/or NF90/NF110 depletion do not block RNA POL I-dependent rRNA transcription
(A) Scheme of human rRNA precursors. The main precursors are shown in grey, the three mature rRNA species are shown in black. The probe used for detection in (B) is depicted in purple.
(B) HeLa cells were treated with the indicated siRNAs for 72 h. Fluorescence in situ hybridization (FISH) was performed using the indicated probe. NF45 and/or NF90/NF110 depletion do not lead to significant decrease of the early 47S rRNA precursor as it is observed after RNAi against POLR1A. Scale bar, 20 μm.

Cells depleted for NF45/NF90 did not show a significant reduction in fluorescent signal as compared to knockdown of the POL I subunit POLR1A, which blocks rRNA transcription (Fig. 2.3.10B). This indicates that NF45/NF90 are not required for 47S rRNA transcription. However, subtle differences in

signal intensity would be hard to detect due to changes in nucleolar size and numbers.

One of the biggest remodeling events in ribosome biogenesis is the multistep pathway of rRNA processing, in which successive cleavage of the 47S rRNA precursor leads to the mature 18S, 28S and 5.8S rRNAs (reviewed in Mullineux and Lafontaine, 2012, see also chapter 1.2.2). Although only few trans-acting factors possess endo- or exonucleolytic activity, depletion of many trans-acting factors leads to a block or impairment in the assembly pathway, which inhibits downstream rRNA processing events.
To investigate whether NF45/NF90 might be involved in pre-rRNA processing, pre-rRNAs of HeLa cells were analyzed by Northern blotting upon depletion of NF45/NF90 using probes that detect different precursors of 18S and 28S rRNA (pictured in Fig. 2.3.11B, previously described in Rouquette et al., 2005). While depletion of the large ribosomal subunit protein RPL11 led to strong accumulation of 32S pre-rRNA and reduction of mature 28S rRNA, this was not the case for NF45/NF90 downregulation (Fig. 2.3.11A) although NF45/NF90 depletion was efficient (Fig. 2.3.11C) and cells displayed the large nucleoli phenotype as observed by FBL immunofluorescence analysis (Fig. 2.3.11D). However, general rRNA precursor levels seemed to be reduced compared to mature 28S or 18S rRNA, especially when NF45 and NF90/NF110 were co-depleted (Fig. 2.3.11A). To verify this, we measured and quantified the ratio of the 47/45S precursor to mature 28S rRNA from three independent Northern experiments. Upon NF45 and NF90/NF110 depletion, 47/45S rRNA levels were significantly reduced compared to 28S rRNA (Fig. 2.3.12), which could indicate that NF45/NF90 contribute to 47S production or stability.

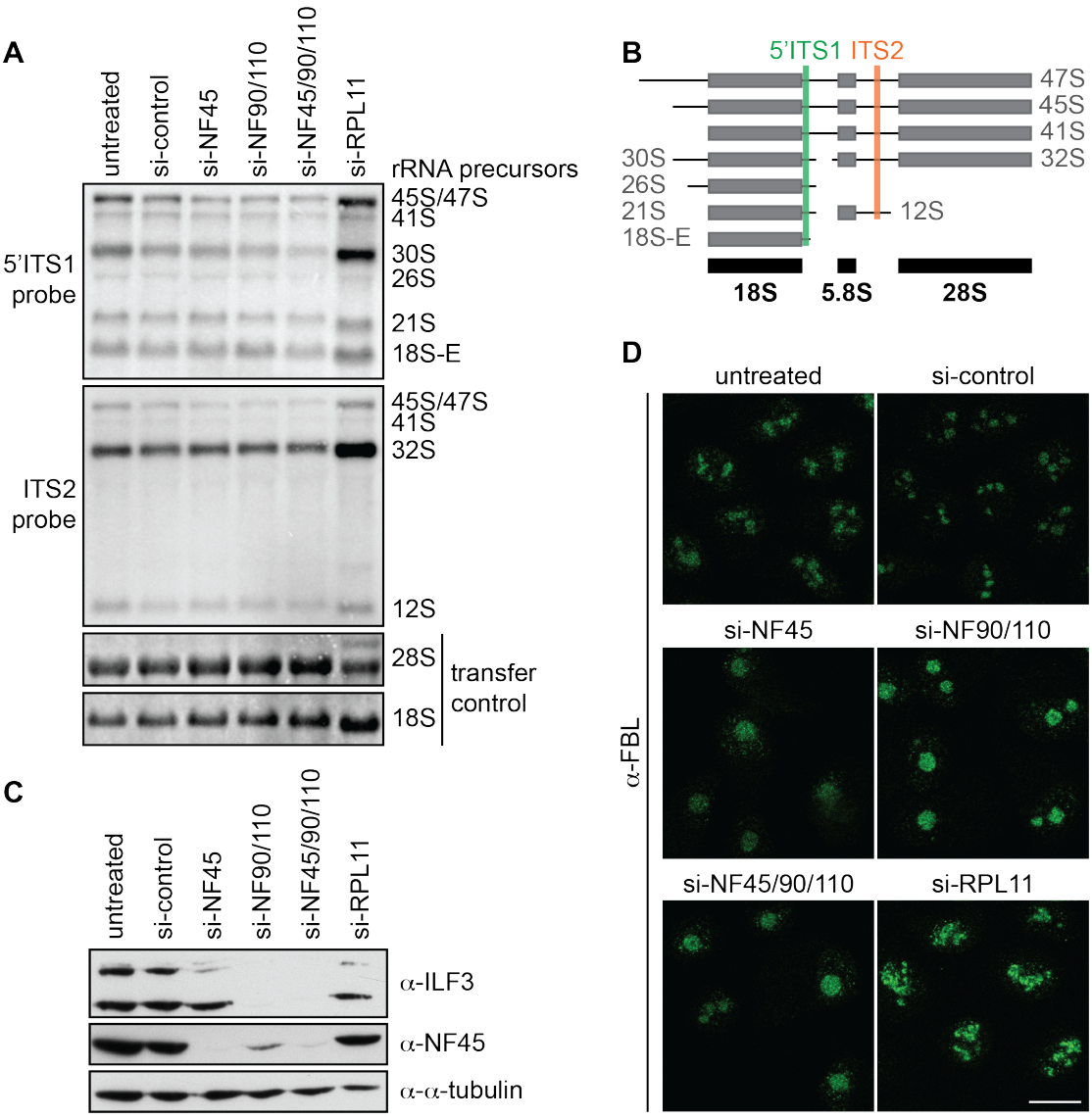

Figure 2.3.11
NF45 and NF90/NF110 depletion does not influence pre-rRNA processing
(A) HeLa cells were treated with the indicated siRNAs for 72 h. RNA was extracted, separated by agarose gel electrophoresis and analyzed by Northern blotting using the indicated probes. NF45 and/or NF90/NF110 depletion does not lead to accumulation of rRNA precursors as it is the case upon depletion of RPL11 (positive control).
(B) Scheme of human rRNA precursors. The main precursors are shown in grey, the three mature rRNA species are shown in black. The two probes used for detection in (A) are depicted in color.
(C) Western blot analysis of (A) with the indicated antibodies was performed to ensure efficient depletion of NF45 and NF90/NF110.
(D) siRNA treated cells from (A) were fixed and analyzed by immunostaining against FBL. Downregulation of NF45 and/or NF90/NF110 leads to larger nucleoli and also to fewer nucleoli per cell, while RPL11 depletion leads to more dispersed nucleolar staining. Scale bar, 20 μm.

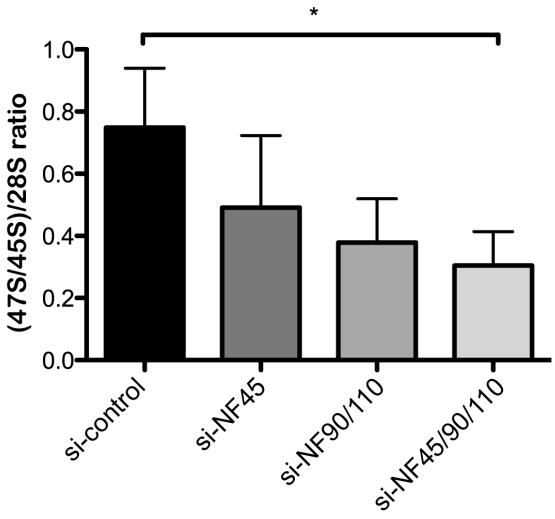

Figure 2.3.12
NF45/NF90/NF110 depletion leads to decreased 47/45S rRNA precursor levels compared to mature 28S rRNA
Three independent Northern blot experiments were carried out as in Figure 2.3.11 and the bands corresponding to 45S/47S pre-rRNA as well as 28S rRNA were quantified using ImageJ. The calculated ratios were normalized to untreated cells and are shown with their standard deviation. Codepletion of NF45 and NF90/NF110 leads to a significant (P value < 0.05) reduction of 45S/47S over 28S rRNA.

One possible explanation for not observing rRNA precursor accumulation is that NF45/NF90 depletion does not block rRNA processing but merely delays it. The overall amount of each rRNA precursor present in cells in steady-state might not be significantly altered, while the processing rate is slowed down.

To observe changes in rRNA processing kinetics, we performed a pulse-chase radiolabeling experiment. Newly synthesized RNA was labeled by incubating the cells in ^{33}P-containing medium followed by chase periods of different lengths in label-free medium. The cells incorporate ^{33}P into rRNA upon transcription and one can follow the processing intermediates at different time points. While PES1 depletion led to a kinetic delay in appearance of 28S rRNA and accumulation of the 47S/45S precursors, the depletion of NF45 or NF90 did not significantly delay the production of mature rRNA (Fig. 2.3.13B).

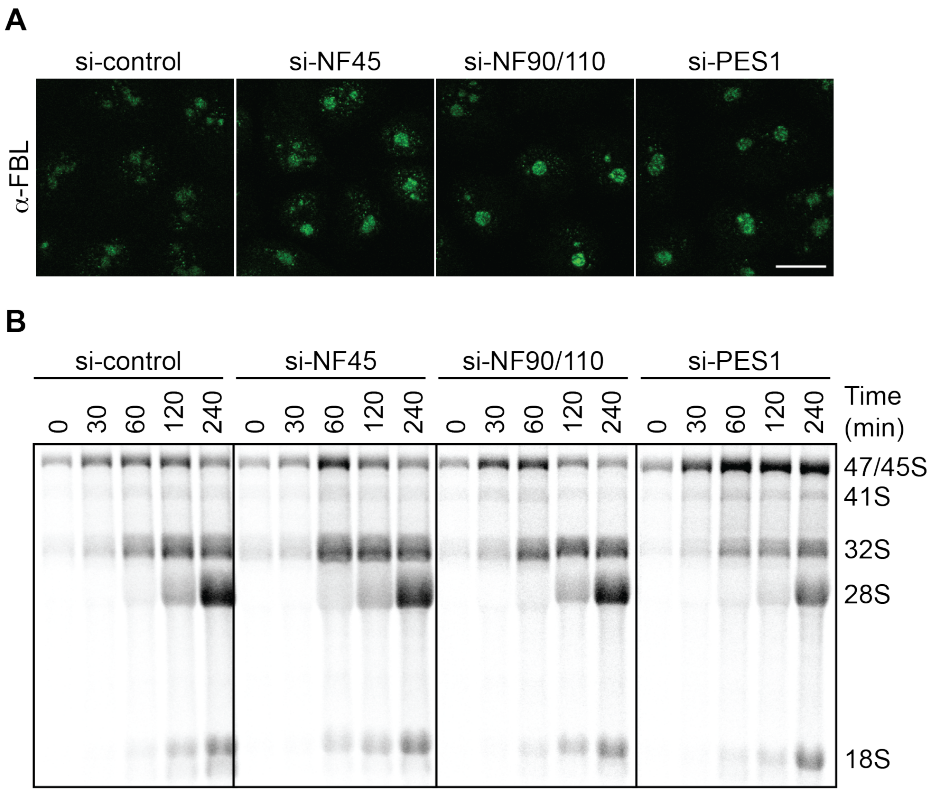

Figure 2.3.13
NF45 or NF90/NF110 depletion does not influence pre-rRNA processing kinetics
(A) HeLa cells were treated with the indicated siRNAs for 72 h. Cells were fixed and analyzed by immunostaining against fibrillarin (FBL). Downregulation of NF45, NF90/NF110 and PES1 leads to larger and fewer nucleoli per cell. Scale bar, 20 μm.
(B) Pulse-chase analysis of (A). Cells were incubated in phosphate-free medium for 1 h and then, ^{33}P-labeled phosphate was added for 1 h. The medium was exchanged with regular medium containing unlabeled phosphate for the indicated chase times. Cells were harvested and the extracted RNA was subjected to agarose gel electrophoresis and the radioactive signal was detected on a phosphoimager screen. Depletion of NF45 and NF90/NF110 does not affect rRNA production or pre-rRNA processing kinetics, while less 28S rRNA is produced and the 47/45S rRNA precursors accumulate upon PES1 depletion.

2.3.6 NF45/NF90 depletion leads to increased p53 levels

Recently, it has been shown that NF90/NF45 depletion leads to an increase in p53 levels as well as p21 levels in HeLa cells (Shamanna et al, 2013). HeLa cells possess wild-type p53, but they are modified by Human papillomavirus (HPV) infection, which introduced DNA from the virus into the genome, and express E6 oncoprotein, which promotes p53 degradation (Scheffner et al., 1990). We wanted to test whether NF45/NF90 depletion leads to p53/p21 upregulation in the human osteosarcoma U2OS cell line, which possesses wild-type p53 but the expression of which is downregulated by overexpression of the E3-ligase HDM2 (Flørenes et al., 1994). Knockdown of NF45 and/or

NF90 led to a modest increase of p53 levels and a strong increase in expression of the downstream effector p21 (Fig. 2.3.14). This effect was reversed by co-depletion of RPL11, which, as a free protein, binds and inhibits HDM2, leading to p53 stabilization ((Lohrum et al., 2003); see also chapter 1.3). Interestingly, NF45 and NF90 levels were increased upon depletion of RPL23, which also leads to increased p53 and p21 levels. The effect of NF45/NF90 RNAi on p53 levels suggests that upon downregulation of NF45 and/or NF90 60S biogenesis is affected leading to a free pool of RPL11, which results in p53 stabilization and activation.

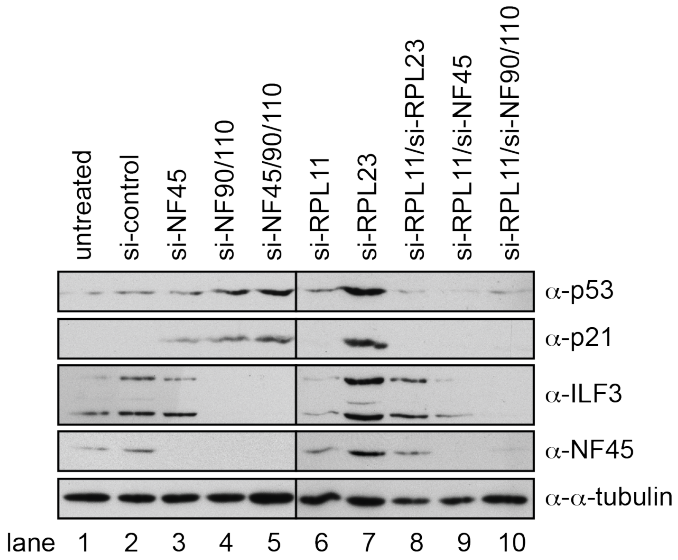

Figure 2.3.14
p53 levels are elevated upon depletion of NF45 and NF90/NF110
U2OS cells were treated with the indicated siRNAs for 72 h. Protein levels were analyzed by SDS-PAGE followed by Western blotting using the indicated antibodies. Upon depletion of NF45 and/or NF90/NF110, p53 levels increase and p21 expression is induced (lane 3-5). Co-depletion of RPL11 with NF45 or NF90/NF110 inhibits the increase of p53/p21 levels (lane 9, 10)

2.3.7 NF45/NF90 are not required for XPO5 loading on pre-60S

The NF45/NF90 complex has been shown to regulate miRNA maturation and export (Sakamoto et al., 2009) which is dependent on exportin-5 (XPO5) (Lund et al., 2004). Interestingly, recent data has demonstrated that XPO5 is required for pre-60S export in vertebrate cells (Wild et al, 2010). It is intriguing to speculate that NF45/NF90 mediate the association of XPO5 to pre-60S because firstly, it has been shown that NF90 binds to XPO5 (Brownawell et al., 2002), secondly, depletion of NF45 or NF90 leads to nuclear accumulation of an RPL29-GFP reporter (Fig. 2.3.8), and thirdly, NF90 is only present in

vertebrates which would make it an ideal candidate for this higher eukaryote-specific process.

To test this hypothesis, we performed TAP from HEK 293 cells expressing MRTO4-StHA to purify pre-60S. These preribosomal particles were incubated with HeLa cell extract devoid of tRNA and ribosomes, in the presence or absence of RanQ69L-GTP (Fig. 2.3.15A). XPO5 is associated with pre-60S in a Ran-GTP-dependent manner, as it has been shown previously (Fig. 2.3.15B; Wild et al, 2010). When NF45 and NF90 were depleted prior to TAP of MRTO4-StHA, neither binding of XPO5 nor of CRM1 to pre-60S was diminished suggesting that NF45/NF90 do not play a role in exportin loading onto pre-60S.

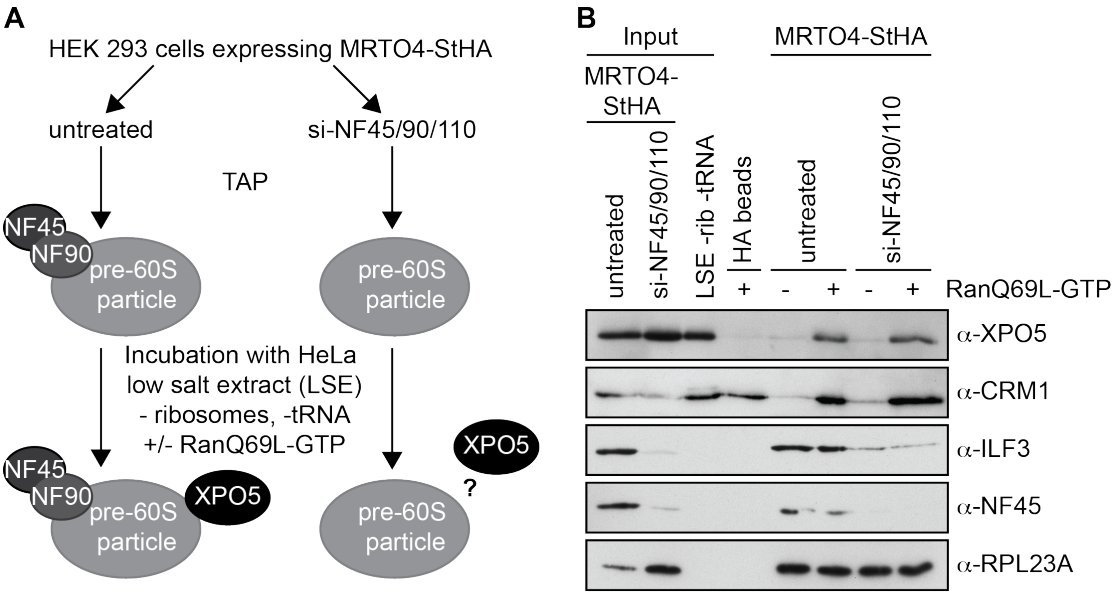

Figure 2.3.15
Co-depletion of NF45 and NF90/NF110 does not influence the ability of XPO5 to associate with pre-60S particles
(A) Schematic representation of the experimental setup. Cells were either left untreated or treated with siRNAs against NF45 and NF90/NF110 for 72 h. 24 h prior to harvesting, expression of MRTO4-StHA was induced with tetracycline. TAP was performed but instead of the second elution step, purified particles bound to anti-HA beads were incubated with HeLa low salt extract with or without the addition of RanQ69L-GTP (10 μM). Particles were eluted with SDS buffer and analyzed by SDS-PAGE. Figure adapted from (Wild et al., 2010)
(B) Western blot analysis of the binding assay described in (A) with the indicated antibodies. XPO5 binding to pre-60S particles is not diminished in cells depleted of NF45 and NF90/NF110.

2.3.8 Tandem affinity purification of NF90 co-purifies pre-60S

To confirm the association of the NF45/NF90 complex with pre-60S subunits, we investigated whether NF90 is able to co-purify pre-60S when used as bait in TAP. For this, a HEK 293 cell line expressing HASt-NF90 in an inducible manner was generated. Tandem affinity purification of HASt-NF90 co-purified NF45, RPL proteins and 60S trans-acting factors, but no 40S trans-acting factors as shown by Western blot analysis (Fig. 2.3.16B).

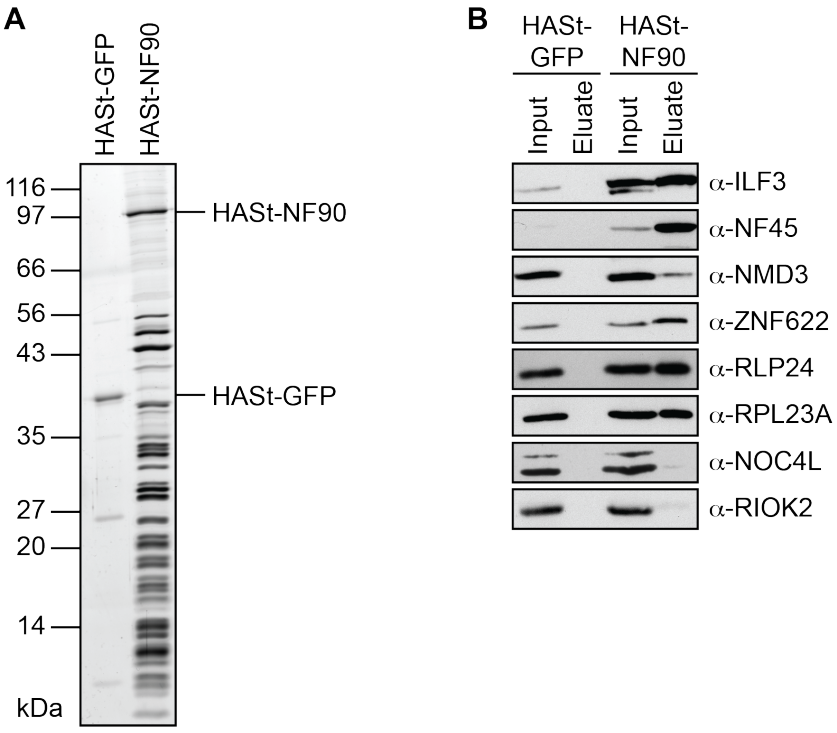

Figure 2.3.16
Tandem affinity purification of HASt-NF90 purifies pre-60S ribosomal particles
TAP was carried out using HEK 293 FlpIn TRex cells expressing either HASt-GFP as a negative control or HASt-NF90 in a tetracycline-inducible manner.
(A) Analysis of eluted proteins by SDS-PAGE followed by silver staining.
(B) Western blot analysis of the TAP experiment in (A) with the indicated antibodies. NF90 copurifies NF45, ribosomal proteins of the 60S subunit as well as 60S, but not 40S trans-acting factors.

The HASt-NF90 TAP was also analyzed by mass spectrometry. TAP of HASt-NF90 co-purified several previously described interaction partners of the NF45/NF90 complex, such as IGF2BP1/IMP1 (Jønson et al., 2007), ADAR1 (Nie et al., 2005) and PRMT1 (Tang et al., 2000). In addition, ribosomal proteins as well as 60S trans-acting factors were enriched in the TAP of NF90 (Fig. 2.3.17). This substantiates the association of NF45/NF90 with pre-60S.

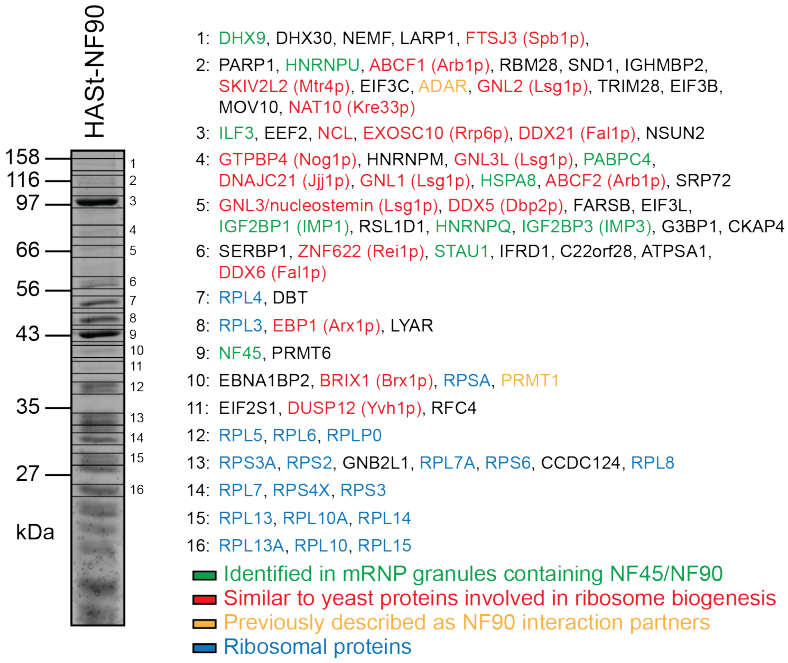

Figure 2.3.17
Mass spectrometric analysis of proteins associated with HASt-NF90
TAP was performed from HEK 293 FlpIn TRex cells with HASt-NF90 as bait. The eluted proteins were analyzed by SDS-PAGE followed by Coomassie staining. The marked bands were excised from the gel and analyzed by mass spectrometry. For each band, proteins are sorted according to the number of peptides found. Only proteins with at least 8 peptides present in the analysis are listed.

2.3.9 The dsRBDs of NF90 are required for binding of the NF45/NF90 complex to pre-60S

After establishing that NF90 is indeed able to co-purify pre-60S, we wanted to investigate further how NF90 interacts with preribosomal subunits. NF90 possesses an N-terminal DZF domain (domain associated with zinc fingers), through which it is forming a heterodimeric complex with the DZF domain of NF45 (Wolkowicz and Cook, 2012). At amino acids 371-394 of NF90, a bipartite NLS can be found (Reichman et al, 2002), followed by two double-stranded RNA binding domains (dsRBDs) (Fig. 2.3.18). It is conceivable that NF90 interacts directly with rRNA via its dsRBDs. Another mode of binding to pre-60S could be mediated through its binding partner NF45, since depletion of NF45 leads to mislocalization of NF90 to the nucleoplasm (Fig. 2.3.6).

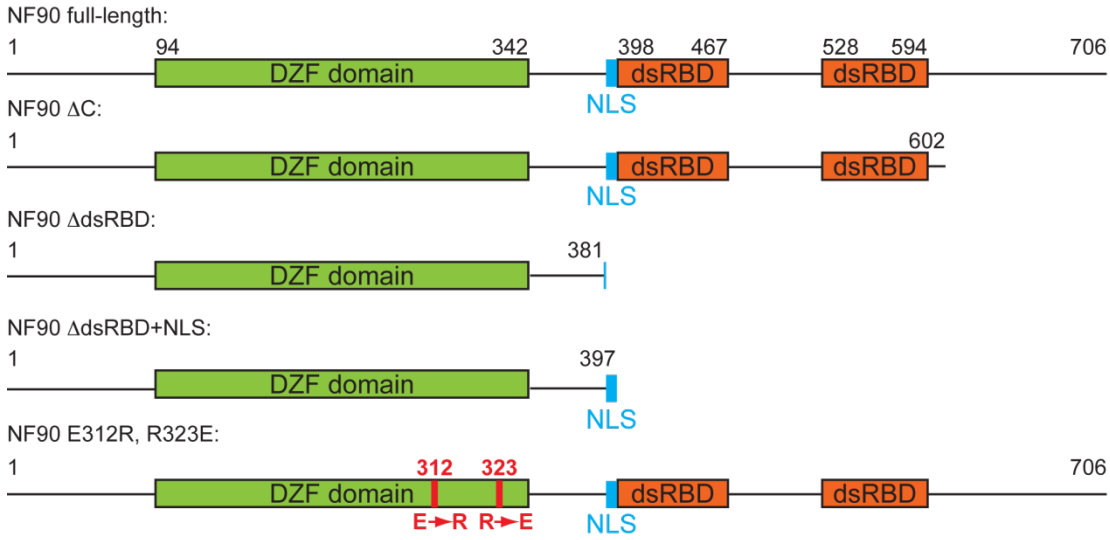

Figure 2.3.18
Generation of NF90 truncations to study dsRBD contribution to pre-60S binding
NF90 truncations and mutant used for generation of TAP cell lines. The beginning and end of domains are indicated with the amino acid number.

To test which domain of NF90 is responsible for binding to pre-60S, we cloned truncation constructs of NF90 missing the C-terminus but that still possess (ΔC) or lack both dsRBDs (ΔdsRBD) (Fig. 2.3.18). To determine their subcellular localization, the HASt-tagged constructs were transiently transfected into HeLa cells and detected by immunofluorescence using an anti-HA antibody. While the full-length and the ΔC HASt-NF90 constructs, like endogenous NF90 (Fig. 2.3.19A), were localized to the nucleus and are enriched in nucleoli, HASt-NF90ΔdsRBD was displaced from nucleoli and localized to the nucleoplasm and cytoplasm (Fig. 2.3.19A). This might be partly due to the fact that the NLS of NF90 is also missing in the ΔdsRBD mutant. However, it was still able to partly localize to the nucleoplasm, which could be due to diffusion, since the truncation is considerably smaller than full-length NF90 (Fig. 2.3.18) or by binding to another NLS-containing protein. An NF90 truncation that lacks the dsRBDs but contains the NLS (ΔdsRBD+NLS) (Fig. 2.3.18) completely localized to the nucleoplasm but was still displaced from nucleoli (Fig. 2.3.19A). Taken together, the dsRBDs of NF90 appear to be required for the nucleolar localization of NF90.

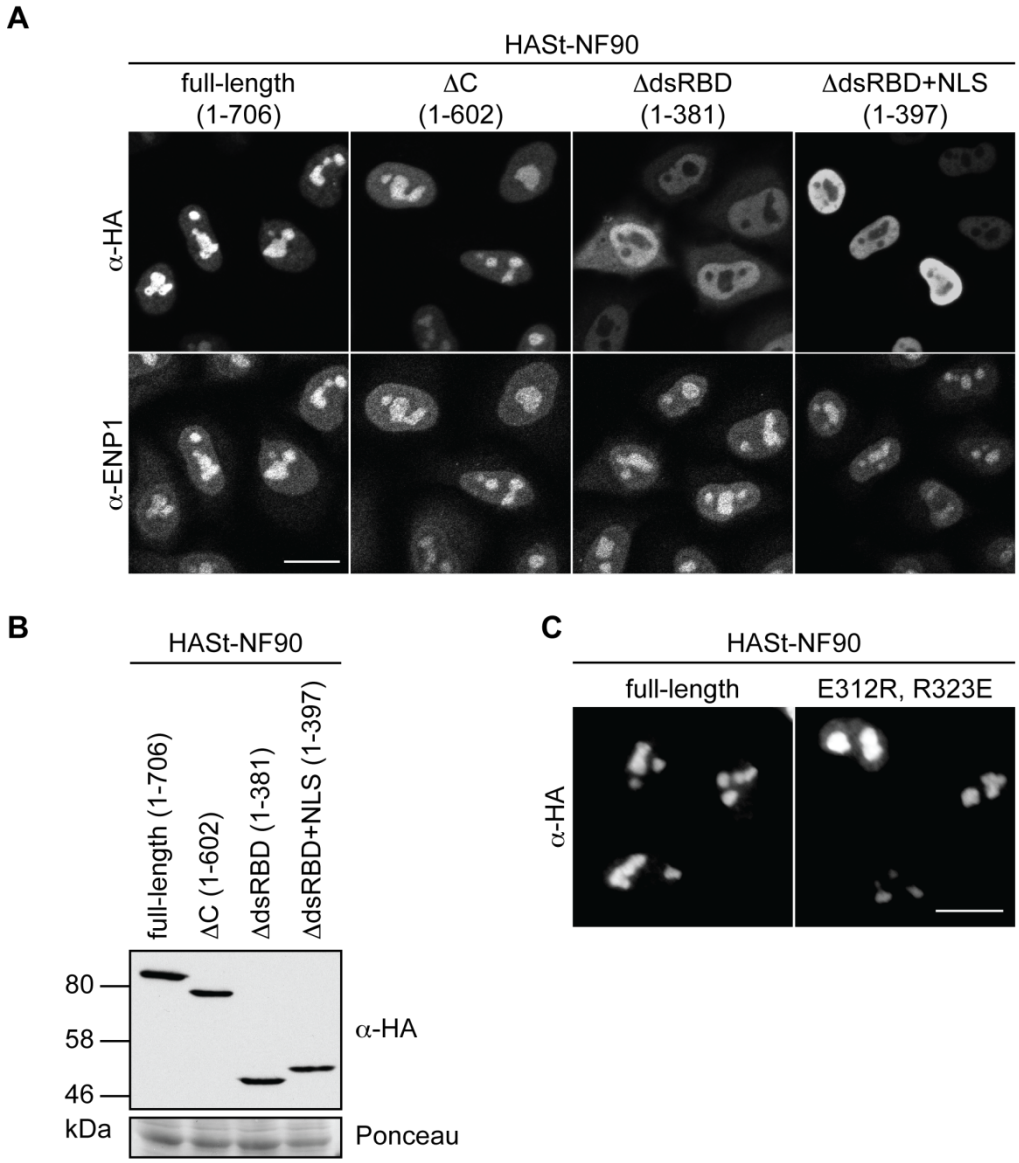

Figure 2.3.19
The dsRBDs of NF90 are required for nucleolar localization
(A) Comparison of transiently transfected HASt-NF90 constructs localization in HeLa cells. Proteins were detected by IF using the indicated antibodies. ENP1 localization was detected by co-IF to visualize nucleoli. Full-length HASt-NF90 as well as HASt-NF90 missing 104 amino acids at the C-terminus localize predominantly to nucleoli. The HASt-NF90 truncations that do not possess the two dsRBD domains are excluded from nucleoli. Scale bar, 20 μm.
(B) Western blot analysis of (A) with an anti-HA antibody to ensure comparable expression levels of transiently transfected constructs. A protein band visible on the membrane after Ponceau staining was used as a loading control.
(C) Comparison of transiently transfected HASt-NF90 full-length wild type and mutant (E312R, R323E) in HeLa cells. Localization of proteins was detected with an anti-HA antibody. The mutant localizes similarly to wild type NF90. Scale bar, 20 μm.

To assess the influence of NF45 binding, we also generated an NF90 construct where binding to NF45 is abolished. For this, we mutated two out of three conserved amino acids at the dimerization interface to amino acids of

the opposite charge (E312R, R323E; analogous to the D308R, R319E mutation in NF45 in Wolkowicz and Cook, 2012). The transiently transfected mutant localized to nucleoli comparable to wild-type HASt-NF90 (Fig. 2.3.19C).

To further analyze which of these truncations can still associate with pre-60S, we generated HEK 293 cell lines expressing these HASt-NF90 truncations/mutants in a tetracycline-dependent manner and performed TAP. While the HASt-NF90ΔC truncation was still able to co-purify pre-60S comparable to full-length HASt-NF90 (Fig. 2.3.20A and B), HASt-NF90ΔdsRBD only co-purified NF45 but did not associate with pre-60S (Fig. 2.3.20A and B). The same is true for HASt-NF90ΔdsRBD+NLS. This indicates that the dsRBD domains of NF90 are required for binding to pre-60S. Interestingly, the NF45 binding-deficient mutant of NF90, HASt-NF90(E312R, R323E), was still able to associate with pre-60S, but its ability to bind NF45 was abolished as predicted (Fig. 2.3.20A and B). Taken together, this suggests that binding of the NF90 to pre-60S is mediated through the dsRBD of NF90 and is not dependent on NF45.

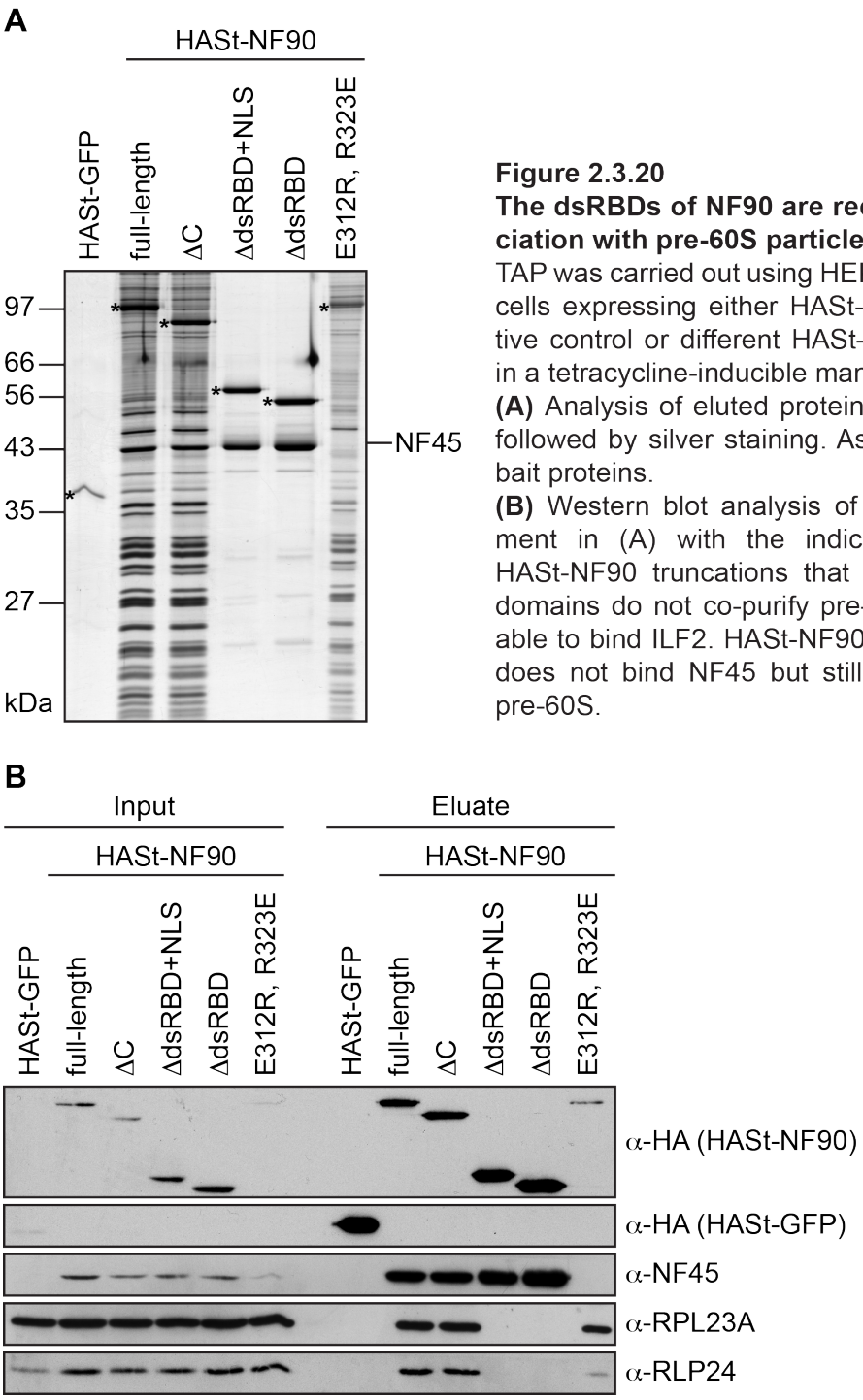

Figure 2.3.20
The dsRBDs of NF90 are required for association with pre-60S particles
TAP was carried out using HEK 293 FlpIn TRex cells expressing either HASt-GFP as a negative control or different HASt-NF90 constructs in a tetracycline-inducible manner.
(A) Analysis of eluted proteins by SDS-PAGE followed by silver staining. Asterisks mark the bait proteins.
(B) Western blot analysis of the TAP experiment in (A) with the indicated antibodies. HASt-NF90 truncations that lack the dsRBD domains do not co-purify pre-60S but are still able to bind ILF2. HASt-NF90(E312R, R323E) does not bind NF45 but still associates with pre-60S.

3. Discussion

Understanding the complex pathway of ribosome biogenesis is not only important because it is such an essential and conserved process. Severe genetically inherited diseases as well as many types of cancer are associated with aberrant or misregulated ribosome production. Most of our knowledge on ribosome biogenesis stems from the model organism *S. cerevisiae*. In this study, we set out to broaden our horizon on the composition of human pre-40S and pre-60S particles by TAP followed by mass spectrometry analysis. As a result, we identified and characterized several novel trans-acting factors and investigated on their role in ribosome biogenesis.

3.1 Characterization of C21orf70, a putative export adaptor for pre-40S

In this work, we further characterized C21orf70, a protein that was first identified as being associated with early pre-40S particles by TAP of HASt-NOC4L coupled with mass spectrometry (Wyler et al., 2011). We confirmed this association with TAP using C21orf70 as bait, which co-purifies pre-40S (Fig. 2.1.2). Upon depletion of C21orf70, 40S trans-acting factors as well as an inducible RPS2-YFP reporter accumulate to the nucleoplasm similar to CRM1 depletion (Wyler et al., 2011). This speaks for either an early maturation defect in the nucleus, which results in aberrant pre-40S that do not reach export competence or an inhibition of CRM1-mediated export.

The nuclear export of both preribosomal particles is dependent on the exportin CRM1 (Gadal et al., 2001; Ho et al., 2000; Moy and Silver 2002; Bernad et al., 2006; Thomas and Kutay et al., 2003; Trotta et al., 2003). For pre-60S subunits, Nmd3 has been shown to act as an adaptor protein in yeast and human cells (Ho et al., 2000; Gadal et al., 2001; Thomas and Kutay et al., 2003; Trotta et al., 2003) whereas the adaptor protein(s) that mediate CRM1 association to 40S have not been identified to date (see 1.2.4). Several candidates that possess putative NES have been suggested (Zemp et al. 2009; Thomas Wild, dissertation, ETH Zurich), however, most of them do not lead to a 40S export defect upon depletion comparable to CRM1 depletion. This could be due to a redundant function of these putative export adaptor proteins, with several copies of CRM1 mediating transport of one pre-40S

particle through the NPC. This is conceivable considering that several factors have been proposed to contribute to pre-60S export as well (Ho et al., 2000; Bradatsch et al., 2007; Yao et al., 2007; Oeffinger et al., 2004; Bassler et al., 2012; Occhipinti et al., 2013; Hackmann et al., 2011; Yao et al., 2010).

Through *in vitro* binding assays using recombinant proteins we could demonstrate that C21orf70 directly binds CRM1 in a Ran-GTP dependent manner, presumably through two NES (Fig. 5.3). We also identified an N-terminal NES of C21orf70 through point mutations that abolished CRM1 binding (Fig. 5.4). The C-terminus however was still able to bind CRM1 when the putative NES was deleted. A possibility is that the truncated protein is misfolded, which leads to exposed hydrophobic residues on the surface that can interact with CRM1 and are hidden in the correctly folded full-length protein. It remains to be investigated whether there is a second NES in the C-terminus that is functional in the full-length protein. Once the sequences in C21orf70 that contribute to CRM1 binding are identified, a C21orf70 mutant could be generated that is still a component of pre-40S particles but interaction with CRM1 is abolished. This mutant could be used in rescue experiments to analyze C21orf70 contribution to 40S export *in vivo*.

Altogether, C21orf70 is a good candidate for a CRM1 export adaptor because (a) it is a component of pre-40S particles, (b) depletion of C21orf70 leads to nuclear accumulation of pre-40S and (c) it directly binds to CRM1 *in vitro*. To further support this hypothesis, it is of importance to show that C21orf70 indeed is a shuttling protein. Localization studies using immunofluorescence showed that C21orf70 is localized to the nucleus and enriched in nucleoli at steady state (Fig. 4.1). Furthermore, experiments with C21orf70 truncations fused to GST-GFP showed that C21orf70 is actively imported and possesses two sequence regions that could function as NLS (Fig. 5.1). However, it needs to be demonstrated that these regions alone can promote import of an unrelated protein to confirm their NLS function.

Depletion of late 40S trans-acting factors, e.g. RIOK2, that lead to impaired release of assembly factors from cytoplasmic pre-40S (Zemp et al., 2009) did not result in cytoplasmic accumulation of C21orf70. Thus, an export of

C21orf70 to the cytoplasm could so far not be demonstrated *in vivo* (Fig. 2.1.2A). Nevertheless, the release of an export adaptor could be further upstream than the cytoplasmic maturation steps that are blocked by these depletions and would not be detectable with this method. A different approach, such as a heterokaryon assay (Schmidt-Zachmann et al., 1993) could give insight on nucleocytoplasmic shuttling behavior of C21orf70.

So far, it cannot be ruled out that C21orf70 might function in a nuclear 40S maturation step that renders pre-40S particles export competent and that the observed export defect is a secondary effect. Therefore, changes of pre-40S particle composition upon C21orf70 depletion could give insight on its function in 40S biogenesis. Specifically, an *in vitro* CRM1 binding experiment in the absence or presence of C21orf70, analogous to what has been done for exportin binding to pre-60S in Figure 2.3.17 and (Wild et al., 2010) using purified pre-40S particles, e.g. derived from an ENP1 TAP, could clarify the contribution of C21orf70 to CRM1 binding to pre-40S.

Basic Local Alignment Search Tool (BLAST) analysis of the C21orf70 amino acid sequence revealed homology to Slx9 in *S. cerevisiae*. Slx9 was first proposed to be involved in DNA damage repair and replication, because it was identified by a synthetic lethality screen with the DNA helicase Sgs1 present at DNA replication forks (Ooi et al., 2003). It was also shown to play a role in 40S biogenesis, in particular in ITS1 rRNA processing (Bax et al., 2006). Surprisingly, it was proposed that Slx9 is specific to yeast and does not possess a homolog in higher eukaryotes (Bax et al., 2006). Recently, involvement of Slx9 in pre-40S export and genetic interaction with the 40S transport receptor Mex67—Mtr2 was suggested (Faza et al., 2012). Since the human homolog of Mex67—Mtr2, TAP—p15, does not possess the two loops that are required for interaction with pre-40S (Fribourg and Conti, 2003; Faza et al., 2012), a conserved function of Mex67—Mtr2 in human pre-40S export is highly unlikely.

Taken together, we have investigated a previously uncharacterized factor that plays an important role in pre-40S biogenesis in human cells. Further experiments will elucidate whether C21orf70 is involved in pre-40S export or in nuclear 40S maturation steps.

3.2 CK1δ and CK1ε are 40S trans-acting factors

Cytoplasmic maturation steps of 40S particles require the action of several kinases (see 1.2.5) and disruption of their activity leads to recycling defects and thus cytoplasmic accumulation of 40S trans-acting factors, which can be observed via immunofluorescence (Zemp et al. 2009, Widmann et al., 2012). In addition to the known kinases involved in human 40S biogenesis, we have identified two casein kinase 1 (CK1) isoforms, CK1δ and CK1ε, as novel components of pre-40S particles by mass spectrometry and Western blot analysis of C21orf70 and LTV1 TAPs (Figs. 2.1.6 and 2.2.6).

Chemical inhibition of CK1 by the compound D4476 led to partial relocalization of the 40S trans-acting factors PNO1 and ENP1 to the cytoplasm (Fig. 2.2.1). Furthermore, the effect of inhibition by D4476 could be reproduced by co-depletion of CK1δ and CK1ε, which led to cytoplasmic accumulation of ENP1, PNO1, RRP12 and delayed nuclear import of RIOK2 after LMB treatment (Fig. 2.2.2). Notably, single knockdown, as well as co-depletion of either CK1δ or CK1ε with other CK1 isoforms did not result in mislocalization of trans-acting factors. This is in accordance with mass spectrometry data from the C21orf70 TAP, where only the two isoforms CK1δ and CK1ε were found.

It is conceivable that CK1δ and CK1ε play redundant roles in 40S biogenesis since they are highly similar proteins, with 98% of their kinase domain being identical (Fish et al., 1995). However, CK1δ and CK1ε have also been shown to play different roles, for example in circadian rhythm (Etchegaray et al., 2009). The assumption that they function redundantly in 40S biogenesis was supported by the employment of additional small molecule inhibitors that preferentially target one or the other isoform. When combined, a recycling defect of ENP1 was observed similar to D4476 inhibition and co-depletion of the two isoforms (Fig 2.2.3). It remains to be elucidated whether both isoforms are present on the same preribsomal particle or whether they mutually exclude binding of the other isoform. This could be achieved by purifying pre-40S by TAP or immunoprecipitation of one CK1 isoform and observing whether the other isoform is co-purified along with these particles.

To assess the contribution of the kinase activity of CK1 on 40S biogenesis, we performed rescue experiments (Fig. 2.2.4). The kinase-dead mutant of CK1ε was unable to restore normal ENP1 localization upon knockdown of CK1δ and CK1ε, whereas wild type CK1ε partially rescued ENP1 localization. Therefore, not only the presence of CK1δ or CK1ε is needed on the pre-40S particles but also the kinase activity plays a role in small subunit biogenesis. This is in agreement with the effect of CK1 inhibitor treatment on 40S maturation. The inhibitor does not alter CK1 levels but merely abolishes its enzymatic function. That the rescue with wild type CK1ε is only partial, could be explained by the observation that overexpression of CK1ε in HeLa cells has a dominant-negative effect on ENP1 localization (data not shown). This indicates that CK1 protein levels need to be tightly regulated for correct function in 40S biogenesis.

In budding yeast it was shown that Hrr25, a CK1 homolog, contributes to 40S biogenesis by phosphorylating Enp1, Ltv1 and Rps3 on the preribosomal particle, leading to dissociation of the Enp1/Ltv1/Rps3 subcomplex in the cytoplasm (Schafer et al., 2006). This is a prerequisite for stable incorporation of Rps3 into pre-40S after its dephosphorylation by a so far unknown phosphatase. This incorporation is suggested to lead to a structural rearrangement of the pre-40S subunit, in particular the formation of a protrusion called “beak”, which is composed of helix 33 of the 18S rRNA close to the binding site of Rps3. In addition, release of Ltv1 and Enp1 exposes the opening of the mRNA channel, which is suggested to be required for translation competence (Strunk et al., 2011). We could show by kinase assays on purified pre-40S that ENP1 and LTV1 are phosphorylated on the particle, whereas only very minor phosphorylation was observed for RPS3 (Fig. 2.2.6). Furthermore, these phosphorylation events can be inhibited by a CK1δ/ε-specific inhibitor that does not target RIOK2, another kinase present on these particles. Whether and how the phosphorylation of ENP1/LTV1 and possibly RPS3 leads to dissociation of these proteins from pre-40S remains to be investigated. Also, it cannot be ruled out that phosphorylation of RPS3 on purified pre-40S particles leads to its reduced binding affinity. This would result in loss of RPS3 in the washing steps following the kinase assay, which

could explain the low levels of RPS3 phosphorylation observed in the experiment. The CK1-dependent phosphorylation of ENP1 and LTV1 on pre-40S demonstrates that functional similarities exist between CK1δ/ε and Hrr25.

In our experiments, we could confirm a conserved function for CK1δ/ε in trans-acting factor phosphorylation and release from cytoplasmic pre-40S particles. However, we did not observe nuclear accumulation of an RPS2-YFP reporter after CK1δ and CK1ε depletion (Fig. 2.2.5A), as it has been reported for Hrr25 depletion in yeast (Schafer et al., 2006). This suggests at least a partial change in the functional output of these kinases in ribosome biogenesis in the course of evolution, as in mammalian cells CK1δ and CK1ε appear to only play a role in cytoplasmic 40S maturation.

Inhibition or depletion of CK1δ and CK1ε leads to recycling defects of several 40S trans-acting factors located on different sides of pre-40S particles (Strunk et al., 2011). However, it is unlikely that CK1δ and CK1ε are directly involved in the simultaneous release of all of these factors but rather facilitate their later release through the aforementioned conformation changes, rendering them accessible for enzymes that catalyze their release. The RIO kinases have been described to play a role in cytoplasmic trans-acting factor recycling as well (Rouquette et al., 2005; Zemp et al., 2009; Widmann et al., 2012; Baumas et al., 2012). Activity of CK1δ and CK1ε appears to be needed for the release of all investigated shuttling trans-acting factors, whereas the presence but not the activity of RIOK1 and RIOK2 suffices for the release of certain factors (Table 3.1). This presumably places CK1δ and CK1ε activity upstream of RIOK1 and RIOK2 in the cytoplasm (Fig. 3.1).

		CK1δ/ε	RIOK2	RIOK1
release of	RRP12	activity	activity	NO
	ENP1	activity	presence	presence
	LTV1	activity	activity	presence
	PNO1	activity	activity	activity
	NOB1	activity	activity	activity
	RIOK2	activity	-	presence
	RIOK1	n.a.	NO	-
rRNA processing		activity	activity	activity

Table 3.1
Contribution of different kinases to cytoplasmic 40S trans-acting factor release and 18S-E to 18S rRNA processing.
Data are compiled from (Zemp et al., 2009; Wyler et al., 2011; Widmann et al., 2012), and this study.

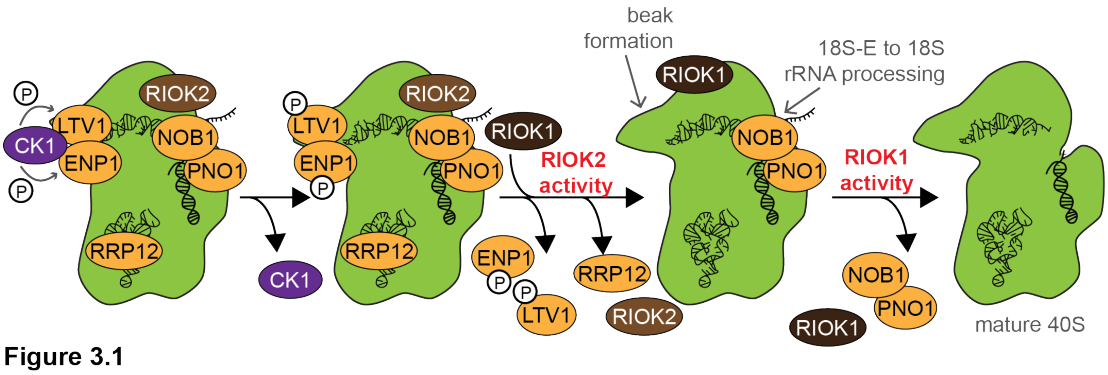

Figure 3.1
Model of the role of human CK1, RIOK1 and RIOK2 in cytoplasmic 40S maturation
Extended model of Figure 1.8. CK1δ or CK1ε (CK1) phosphorylate LTV1 and ENP1 on pre-40S particles, which leads to their release. This event is suggested to take place before the release of the other factors, since the activity of CK1 is needed for the release of all investigated factors (see Table 3.1).

However, there are still several open questions concerning the model above. Is RRP12 released before or after RIOK1 joins the particle? Is LTV1 released together with ENP1 (as pictured in Fig. 3.1) or in a later step since RIOK2 activity is needed for LTV1 release but not for ENP1 release (Table 3.1)? Is the association of CK1δ/ε and RIOK1 with pre-40S mutually exclusive? To answer some of these questions, proteomic analysis of pre-40S particles, derived from TAP of different cytoplasmic trans-acting factors, might give insight in the order of trans-acting factor release.

The higher eukaryote-specific kinase RIOK3 is not pictured in the above model (Fig. 3.1). However, it has been described to associate with late cytoplasmic pre-40S, as it was co-purified by immunoprecipitation of NOB1 and RIOK1 TAP (Widmann et al., 2012). More data is needed to incorporate RIOK3 into this model, in particular on RIOK3 kinase activity requirement for different steps in 40S biogenesis.

Seemingly contradictory to the cytoplasmic action of CK1δ and CK1ε is their association with early, nuclear pre-40S purified by the nuclear protein C21orf70, although shuttling of C21orf70 cannot be ruled out at this point (see 3.1). CK1δ and CK1ε are localized throughout the cell and nucleocytoplasmic shuttling behavior was reported for CK1δ (reviewed in (Gross and Anderson, 1998; Knippschild et al., 2005; Cheong and Virshup, 2011)), supporting a possible association with nuclear pre-40S. If CK1δ and CK1ε are already associated with nuclear pre-40S, is has to be ensured that phosphorylation of ENP1/LTV1 is not taking place prior to export, since nucleoplasmic beak

formation was suggested to hinder passage through the NPC. Premature phosphorylation could be avoided by blocking the accessibility of substrates by steric hindrance through an unfavorable conformation or binding of additional factors that have to be released in the cytoplasm. A similar mechanism was proposed for the endonuclease Nob1 that can only cleave 18S-E pre-rRNA in the cytoplasm after a conformational switch in the rRNA (Fatica et al., 2003; Lebaron et al., 2012; Pertschy et al., 2009). Furthermore, a priming phosphorylation on the substrate is required for CK1 phosphorylation efficiency (Flotow et al., 1990), which could also be used as a regulatory mechanism to inhibit phosphorylation of CK1 substrates in the nucleoplasm.

The casein kinase family has also been shown to be involved in numerous cellular processes, such as circadian rhythm (reviewed in Knippschild et al., 2005). Recently, a study showed that the circadian clock affects ribosome biogenesis through transcriptional control (Jouffe et al., 2013). It will be interesting to investigate how CK1δ and CK1ε provide a possible link between these different pathways. Moreover, CK1δ and CK1ε were shown to phosphorylate and thereby stabilize p53 upon cellular stress, and a regulatory feedback loop exists between p53 and CK1δ, further intertwining ribosome biogenesis and cell cycle control (Knippschild et al., 1997).

Overall, we have identified two CK1 isoforms as novel components of human pre-40S particles. Further characterization demonstrated that they play an important and most likely redundant role in cytoplasmic 40S biogenesis.

3.3 Identification and characterization of NF45 and NF90 as novel 60S trans-acting factors

3.3.1 NF45 and NF90 are components of pre-60S particles

The protein composition of human preribosomal particles at different stages of maturation has not been fully explored to date. For pre-40S particles, an effort has been made to identify associated proteins by TAP of different pre-40S-associated baits coupled with mass spectrometry analysis, which led to the

identification of previously unknown 40S trans-acting factors (Wyler et al., 2011; this study).

To further advance the knowledge about human pre-60S composition, we purified pre-60S particles using ZNF622-StHA as bait and identified the associated proteins by mass spectrometry. ZNF622 is the human homolog of yeast Rei1, a 60S trans-acting factor needed for the release of Arx1 from pre-60S particles in the cytoplasm (Lebreton et al. 2006; Meyer et al. 2010). However, while Rei1 localizes to the cytoplasm (Iwase and Toh-e, 2004), ZNF622 also displays nuclear localization at steady state and accumulates in the nucleus upon LMB treatment (Fig. 2.3.2A). Thus, it could be expected that the ZNF622 TAP purifies a combination of nuclear and cytoplasmic pre-60S particles. Indeed, many copurified proteins were homologs of nuclear and/or cytoplasmic yeast 60S trans-acting factors (Fig. 2.3.1). In addition, NF45 and NF90, a short isoform of ILF3, were associated with the ZNF622 TAP, which have previously not been described as pre-60S components. Notably, there are no yeast homologs of these proteins as NF45 and NF90 are only present in metazoans or vertebrates, respectively. The association of NF45 and NF90 was specific for pre-60S particles since neither NF45 nor NF90 were detected in TAPs copurifying pre-40S subunits (Fig. 2.3.2.A). Furthermore, NF45 and NF90 comigrated with 60S particles in sucrose gradient analysis while the longer isoform of ILF3, NF110, was only present as a free protein or in smaller complexes (Fig. 2.3.3). The association could be further confirmed by TAP of HASt-NF90, which copurified NF45 as well as pre-60S particles, demonstrated by the presence of RPL proteins as well as several 60S trans-acting factors (Fig. 2.3.17).

It is not surprising that NF45 is strongly enriched in the NF90 TAP, since the two proteins were shown to form a heterodimeric complex (Wolkowicz and Cook, 2012). TAP of HASt-NF90 additionally copurified previously described interaction partners such as ADAR1 (Nie et al., 2005) and PRMT1 (Tang et al., 2000). In contrast to the ZNF622 TAP, there were also several RPS proteins present in the NF90 TAP, although 40S trans-acting factors were not enriched. An explanation for this is that the NF45/NF90 complex was shown to be part of cytoplasmic RNP granules that contain mature 40S but not 60S ribosomal

subunits (Jonson et al., 2007). Supporting this hypothesis, the protein IMP1 that was used as bait to purify these RNP granules was also co-purified in the NF90 TAP (Fig. 2.3.17).

The interaction between NF90 and pre-60S was further characterized by using NF90 truncations and mutants as bait for TAP experiments (Fig. 2.3.20). NF90 lacking its dsRBDs only copurifies NF45 but cannot bind pre-60S. Conversely, NF90 harboring a mutation in the DZF domain, which abolishes NF45 binding, is still able to copurify pre-60S. This indicates that the NF45/NF90 complex associates with pre-60S via the dsRBDs of NF90.
In collaboration with the Landthaler laboratory (Max Delbrück Center for Molecular Medicine, Germany), Photoactivatable-Ribonucleoside-Enhanced Crosslinking and Immunoprecipitation (PAR-CLIP) assays were carried out in order to elucidate the rRNA binding site of NF90. These experiments identified a binding sequence in the 5'ETS, between the cleavage sites A0 and 1 on the pre-rRNA (data not shown), suggesting that NF90 associates with very early preribosomal particles prior to ITS1 or ITS2 cleavage that yields pre-40S and pre-60S particles (Fig. 1.4B). This appears conflicting with the TAP data, which indicated that NF90 was part of pre-60S and did not bind to early 40S trans-acting factors such as NOC4L (Fig. 2.3.16B). However, it cannot be excluded that NF90 is already associated with early ribosomal precursors, since crosslinking, as performed in PAR-CLIP experiments, could stabilize possibly transient interactions and thus facilitate the extraction of intact nucleolar particles, which are not purified by TAP. Alternatively, the 5'ETS might adapt a flexible conformation enabling it to interact and stay associated with the pre-60S part of the preribosomal particle after ITS1/ITS2 cleavage. Further purification experiments such as NF90 TAP in combination with protein cross-linking could help to identify ribosomal proteins close to the binding site of NF90 in order to elucidate its binding site on the ribosome.
Taken together, we characterized the composition of human pre-60S particles bound to ZNF622 by mass spectrometry. Thereby we found that NF45 and a short isoform of ILF3, NF90, are components of pre-60S. Additional TAP

assays revealed that binding of NF45/NF90 to pre-60S is dependent on the dsRBDs of NF90.

3.3.2 Localization studies of NF45 and NF90/NF110

It has been previously reported that NF45 and NF90 are part of the nucleolar proteome (Ahmad et al., 2008; Jarboui et al, 2011). We showed by cell fractionation and immunofluorescence that, in steady state, NF45 and NF90/NF110 are nuclear proteins (Fig. 2.3.4). We also confirmed that NF45 as well as a HASt-tagged NF90 isoform were enriched in nucleoli, the site of rRNA transcription, whereas endogenous NF110 was nucleoplasmic and excluded from nucleoli (Fig. 2.3.4 and 2.3.5). Only in cells overexpressing HASt-tagged NF110, enrichment in nucleoli could be observed in a fraction of all cells (Fig. 2.3.5). In accordance to the localization data, only NF90 was detected to associate with pre-60S (see above), while NF110 was only present as free protein or in smaller complexes. It was previously reported that NF110 is predominantly chromatin-associated and involved in POL II transcription (Reichman and Mathews, 2003; Reichman et al., 2003), which could explain the different localization.

A nucleocytoplasmic shuttling behavior of NF90 has been previously reported upon cellular stress such as viral infection (Liao et al., 1998) and T cell activation (Shim et al., 2002). Therefore, in a next step, we investigated possible changes in NF45/NF90 localization. Upon inhibition of POL I transcription by treatment with low concentrations of actinomycin D, HASt-NF90 is displaced from nucleoli (Fig. 2.3.7). Relocalization to the nucleoplasm after treatment with actinomycin D has been observed for several nucleolar proteins involved in ribosome biogenesis such as NPM (Chan, 1992) and ENP1 (Miyoshi et al., 2007). Surprisingly, NF45 stays localized to nucleolar remnants after actinomycin D treatment (Fig. 2.3.7), suggesting that binding to NF90 was disturbed.

We were not able to observe an effect of NF90/NF110 depletion on NF45 localization due to the strong decrease of NF45 protein levels upon NF90/NF110 downregulation (Fig. 2.3.6A). Previously, it has been demonstrated that NF90 depletion leads to reduced NF45 levels and vice

versa (Guan et al., 2008). We could only observe a minor reduction of NF90 levels (Fig. 2.3.6A) but observed a displacement of HASt-NF90 from nucleoli upon depletion of NF45 (Fig. 2.2.6B). This indicates that the presence of NF45 is required for nucleolar localization of NF90. Surprisingly, an NF90 DZF mutant that is not able to bind NF45 (Fig. 3.2.20) is still able to localize to nucleoli (Fig. 3.2.19C), presenting an NF45-independent localization of NF90 to nucleoli. While these data seem to be conflicting, it has to be noted that in the first case, NF45 is depleted from cells while it is still present in the latter experiment. Therefore, although interaction with the NF90 mutant is not possible, NF45 might still fulfill a function that targets NF90 to preribosomes in the nucleolus. It would also be conceivable that the functional DZF domain of NF90 is sequestered by another factor in the nucleoplasm when NF45 is depleted, which would not be the case for the DZF mutant. It would be interesting to test whether NF45 depletion affects the localization of the NF90 mutant. Furthermore, the dsRBDs of NF90 are required for its nucleolar localization (Fig. 3.2.19A), consistent with the hypothesis that NF90 associates with pre-60S in the nucleolus via its dsRBDs.

Overall, these data suggest that the dsRBDs of NF90 and ongoing POL I transcription of rRNA by POL I are needed for nucleolar localization of the NF45/NF90 complex.

3.3.3 Effects of NF45/NF90 depletion on 60S biogenesis

Not only does the NF45/NF90 complex associate with pre-60S, the depletion of either NF45 or NF90/NF110 also leads to defects in 60S biogenesis as observed by nuclear accumulation of an RPL29-GFP reporter (Fig. 2.3.8A). The accumulation of RPL29-GFP in the nucleus is not due to impaired exportin binding since the association of CRM1 or XPO5 with pre-60S was not diminished upon NF45/NF90 knockdown (Fig. 2.3.15B). This suggests that a nuclear step of 60S biogenesis is disturbed, leading to aberrant pre-60S particles that are not export competent.

NF45/NF90 were first described as transcriptional activators of IL-2 expression upon T cell activation (Shaw et al., 1988; Yaseen et al., 1993). Therefore, it would stand to reason that this complex also plays a role in POL

I rRNA transcription. POL I-mediated rRNA transcription did not appear to be negatively affected after NF45/NF90 depletion as observed by FISH using a probe that only detects the long 47S rRNA precursor before cleavage at site 01 takes place (Fig. 2.3.10B). However, subtle changes in rRNA levels cannot be detected with this method, especially due to additional changes in nucleolar size and number (see below). Northern blot analysis of rRNA precursors after NF45/NF90 depletion showed that, although lack of accumulation of a certain rRNA precursor did not indicate specific rRNA processing defects, a general decrease of 47/45S rRNA precursors levels compared to mature 28S rRNA was observed (Figs. 2.3.11 and 2.3.12). This can either be explained by a slightly impaired POL I-mediated transcription or a more rapid degradation of newly produced, possibly aberrant, and thus instable preribosomal particles. The latter seems to be more likely, since production of new 47/45S rRNA precursors did not appear to be impaired in pulse-chase experiments (Fig 2.3.13). Nevertheless, a minor transcription impairment would perhaps not be clearly observable.

In addition to the nuclear accumulation of pre-60S particles, knockdown of NF45 or LF3 leads to another, quite striking phenotype: a changed nucleolar architecture with fewer, larger and more spherical nucleoli. A similar phenotype was observed after the knockdown of the 60S trans-acting factors ZNF622 and PES1 (Fig. 2.3.9). Depletion of XPO5, which leads to an export defect of pre-60S particles, did not result in changed nucleolar shape, which suggests that a later effect on 60S biogenesis does not cause this phenotype. An increase of spherical-shaped nucleoli was recently also observed after RPS6 but not RPL11 depletion (Louvet et al., 2013). It would be interesting to dissect which ribosomal proteins and trans-acting factors lead to this phenotype and to further characterize the change in nucleolar shape and size by IF and EM to visualize nucleolar component changes.
What causes this drastic change of nucleolar shape and number? One possible explanation is that reduced POL I transcription and/or 60S biogenesis leads to recruitment of additional factors to nucleoli and nucleolar fusion to counteract the deficiency.

It is intriguing to speculate that nucleolar fusion is caused by activation of the homologous recombination pathway in order to bring together different rDNA copies to repair DNA double strand break damage. The predominant pathway used to repair this type of DNA damage is the nonhomologous end joining (NHEJ) pathway, mediated by DNA-dependent protein kinase (DNA-PK), which competes with homologous recombination (Allen et al., 2002; Pierce et al., 2001). NF45 and NF90 were reported to aid in NHEJ and to interact with DNA-PK, facilitating DNA-PK binding to DNA *in vitro* (Ting et al., 1998; Shamanna et al., 2011). Upon depletion of NF45 or NF90, NHEJ would be disturbed and homologous recombination takes over as the main DNA double strand damage pathway, leading to nucleolar fusion. Further experiments, such as verification of increased homologous recombination events after NF45/NF90 depletion, are needed to support this hypothesis.

It cannot be excluded that the change in nucleolar number is not directly due to a ribosome biogenesis defect but is rather a secondary effect due to a cell cycle defect. It has been reported that nucleoli fuse in G1 phase (Savino et al., 2001; Yamauchi et al., 2007). An arrest in G1-S phase transition could thus explain the single nucleolus per cell. The NF45/NF90 complex has previously been described to play a role in cell cycle progression, although they have been implicated in cytokinesis rather than in G1-S phase transition (Guan et al., 2008). If there is a G1 phase arrest of NF45/NF90-depleted cells, it is likely mediated by p53. NF45/NF90 depletion results in an increase in p53 levels and activation as observed by increased expression of p21, a CDK1 inhibitor that blocks S phase entry (Fig. 2.3.14). Furthermore, RPS6 depletion, which leads to a similar effect on nucleoli (Louvet et al., 2013), has been reported to cause p53 activation and G1 arrest in mice liver cells (Volarevic et al., 2000). A co-depletion experiment of NF45/NF90 and p53 could be performed in order to elucidate whether nucleolar changes after NF45/NF90 depletion are caused by a p53-dependent cell cycle arrest. This would be a first step to investigate which effect of NF45/NF90 depletion is directly linked to ribosome biogenesis.

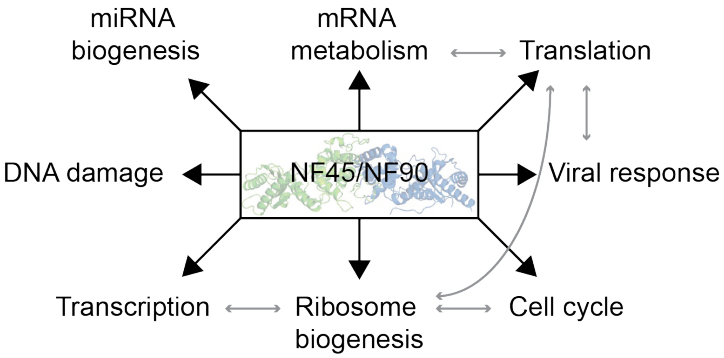

Figure 3.2
NF45/NF90 are involved in many different cellular processes
Scheme of pathways in which the NF45/NF90 complex was proposed to be involved. Grey arrows indicate potential crosstalks between different pathways.

To summarize, we have identified the NF45/NF90 complex as a novel, vertebrate-specific component of pre-60S particles. Furthermore, depletion of NF45 and NF90 leads to 60S biogenesis defects as well as an alteration in nucleolar shape and number. Their specific mechanistic function in 60S biogenesis, however, remains to be elucidated.

NF45 and NF90 have been implicated in many cellular pathways and proposed to interact with several different proteins involved in various cellular processes (Fig. 3.2). It will be a challenge to unravel which of the effects observed after NF45/NF90 depletion are direct and which are of a secondary nature.

4. Materials and Methods

4.1 Materials

4.1.1 Antibodies used in this study

Antibody	Source	Species	Dilution	Reference
α-C21orf70	Raised against a C-terminal peptide of C21orf70	rabbit	1: 200 (IF) 1: 500 (WB)	-
α-CK1α	Commercial (Abcam), ab108296	rabbit	1:500 (WB)	-
α-CK1δ	Commercial (Abcam), AF12G4	mouse	1:1000 (WB)	-
α-CK1ε	Commercial (BectonDickinson), 610445	mouse	1: 500 (WB)	-
α-CRM1	Raised against a CRM1 peptide	rabbit	1:2000 (WB)	Lund et al., 2004
α-ENP1	Raised against recombinant His-ENP1	rabbit	1:15,000 (IF) 1: (WB)	Zemp et al., 2009
α-FBL	Commercial (Santa Cruz), sc-166001	Mouse	1:300 (IF)	-
α-GFP	Raised against recombinant His-GFP	rabbit	1:2000 (WB)	-
α-HA	Commercial (Roche) 3F10	rat	1:200 (IF)	-
α-HA	Commercial (Covance), MMS-101P	mouse	1:3000 (IF) 1:3000 (WB)	-
α-HNRNPC	Monoclonal antibody 4F4	mouse	1:1000 (WB)	-
α-ILF3	Commercial (Santa Cruz), sc-136197	mouse	1:100 (WB) 1:100 (IF)	-
α-LSG1	Raised against recombinant His-LSG1	rabbit	1:3000 (WB)	-
α-LTV1	Raised against recombinant His-LTV1	rabbit	1:2000 (WB)	Zemp et al., 2009
α-MRTO4	Commercial (Santa Cruz), sc-81856	mouse	1:300 (IF) 1:200 (WB)	-
α-NF110	Commercial (GeneTex), GTX62243	rabbit	1:100 (IF) 1: 1000 (WB)	-
α-NF45	Commercial (Santa Cruz), sc-365283	mouse	1:100 (WB) 1:100 (IF)	-
α-NMD3	Raised against an NMD3 peptide	rabbit	1: 10,000(WB) 1:1000(IF)	Zemp et al., 2009
α-NOC4L	Raised against recombinant His-NOC4L	rabbit	1: 5000 (WB) 1:2000 (IF)	Wyler et al., 2011
α-NPM	Commercial (Sigma), B0556	mouse	1: 20,000(WB) 1:4000 (IF)	-
α-p21	Commercial (Santa Cruz), sc-756	rabbit	1:200 (WB)	-
α-p53	Commercial (BectonDickinson), 554293	mouse	1:250 (WB)	-
α-PES1	Commercial (Abcam), ab88543	mouse	1:1000 (WB)	-
α-PNO1	Raised against recombinant His-PNO1	rabbit	1:1000 (WB) (3^{rd} bleed) 1:2000 (IF)	Zemp et al., 2009
α-RIOK2	Raised against recombinant His-RIOK2	rabbit	1:5000 (WB) 1:5000 (IF)	Zemp et al., 2009
α-RLP24	Raised against recombinant His-RLP24	rabbit	1:2500 (WB) 1:5000 (IF)	Zemp et al., 2009
α-RPL5	Commercial (Abcam), ab86863	rabbit	1:2000 (WB) 1: 100 (IF)	-
α-RPL23A	Raised against an RPL23A peptide	rabbit	1:200 (WB) (2^{nd} bleed)	(Pool et al., 2002)

α-RPS3	Raised against recombinant His-RPS3	rabbit	1:1000 (WB) (3rd bleed)	Zemp et al., 2009
α-RPS10	Commercial (Abcam), ab151550	rabbit	1:1000 (WB)	-
α-RPS19	Raised against recombinant His-RPS19	rabbit	1:1000 (WB)	Wyler et al., 2011
α-RPS26	Commercial (Abcam), ab104050	rabbit	1:500	-
	(table continued on next page)			
α-RRP12	Raised against a peptide of RRP12	rabbit	1:1000 (WB) 1:2000 (IF)	Wyler et al., 2011
α-α-tubulin	Commercial (Sigma)	mouse	1:10,000 (WB)	-
α-TSR1	Raised against an N-terminal part of TSR1 (aa 1-245)	rabbit	1:10,000 (WB)	-
α-UBF	Commercial (Santa Cruz), sc-13125	mouse	1:1000 (WB) 1:500 (IF)	-
α-XPO5	Raised against an XPO5 peptide	rabbit	1:2000 (WB)	Lund et al., 2004
α-ZNF622	Commercial (Santa Cruz), sc-100980	mouse	1:200 (WB) 1: 250 (IF)	-

Table 4.1 List of primary antibodies used in this study

Antibody	Source	Species	Dilution
α-mouse HRP	Commercial (Sigma), A-9044	rabbit	1:5000
α-rabbit HRP	Commercial (Sigma), A-9169	goat	1:10'000
α-rabbit Alexa Fluor 488	Commercial (Molecular Probes), A11008	goat	1:400
α-rabbit Alexa Fluor 633	Commercial (Molecular Probes), A21070	goat	1:200
α-mouse Alexa Fluor 488	Commercial (Molecular Probes), A11001	goat	1:400
α-mouse Alexa Fluor 633	Commercial (Molecular Probes), A21052	goat	1:200
α-mouse Alexa Fluor 488 cross-adsorbed*	Commercial (Molecular Probes), A11029	goat	1:200
α-rat Alexa Fluor 633	Commercial (Molecular Probes), A21094	goat	1:200

Table 4.2 List of secondary antibodies used in this study

*This secondary antibody was used in co-immunofluorescence experiments in combination with α-rat Alexa Fluor 633 to decrease cross-reactivity.

4.1.2 Plasmids and primers used in this study

Construct	vector (Resist.)	Primers	Restriction sites
C21orf70-GST-GFP	pK7-GST-GFP (Amp)	f: CGCGAAGCTTATGGGGAAAGTGAGGG r: GGGGGTCGACGAGCTGGCCGCCATCTTC	HindIII/ SalI
C21orf70 (11-230)-GST-GFP	pK7-GST-GFP (Amp)	f: CCCCAAGCTTATGGTGCACCAGGCTGCCGTG r: GGGGGTCGACGAGCTGGCCGCCATCTTC	HindIII/ SalI
C21orf70 (100-230)-GST-GFP	pK7-GST-GFP (Amp)	f: CCCCAAGCTTATGACCGTTTTGCCCAAGAAG r: GGGGGTCGACGAGCTGGCCGCCATCTTC	HindIII/ SalI
C21orf70 (113-230)-GST-GFP	pK7-GST-GFP (Amp)	f: CCCCAAGCTTATGGAGCAATGGTTGCAG r: GGGGGTCGACGAGCTGGCCGCCATCTTC	HindIII/ SalI
C21orf70 (137-230)-GST-GFP	pK7-GST-GFP (Amp)	f: CGCGAAGCTTATGGCCACGGTGGTGGTGGG r: GGGGGTCGACGAGCTGGCCGCCATCTTC	HindIII/ SalI
zz-C21orf70	pQEzz60 (Amp)	f: GGGGCCATGGGGAAAGTGAGGGGG r: CCCCGGATCCGAGCTGGCCGCCATCTTC	NcoI/ BamHI
zz-C21orf70 (1-141)	pQEzz60 (Amp)	f: GGGGCCATGGGGAAAGTGAGGGGG r: CGCGGGATCCCACCACCACCGTGGCCCTC	NcoI/ BamHI
zz-C21orf70 (142-230)	pQEzz60 (Amp)	f: GCGCCCATGGGGGACCTGCACCCTCTC r: CCCCGGATCCGAGCTGGCCGCCATCTTC	NcoI/ BamHI

zz-C21orf70 (158-230)	pQEzz60 (Amp)	f: CGCGCCATGGAGGCTGGCAGCCGGCGCC r: CCCCGGATCCGAGCTGGCCGCCATCTTC	NcoI/ BamHI
zz-C21orf70 (142-230) (L144A, L147A)	pQEzz60 (Amp)	f (long primer containing the mutation): GCGCCC ATGGGGGACGCGCACCCTGCCAGGGATGCCCTG r: CCCCGGATCCGAGCTGGCCGCCATCTTC	NcoI/ BamHI
HASt-C21orf70	pcDNA5/ FRT/TO/ nTAPG (Amp)	f: CGGCGGATCCAATGGGGAAAGTGAGGG r: CCCCGTCGACTCAGAGCTGGCCGCCATCTTC	BamHI/ XhoI (vect.), SalI (ins.)
HASt-CK1ε	pcDNA5/FRT/TO/nTAPG (Amp)	f: GGGCGGTACCGATGGAGCTACGTGTGGGG r: ATTAGCGGCCGCTCACTTCCCGAGATGGTC	KpnI/ NotI
HASt-CK1ε (D149A)	pcDNA5/FRT/TO/nTAPG (Amp)	f: GGGCGGTACCGATGGAGCTACGTGTGGGG r: ATTAGCGGCCGCTCACTTCCCGAGATGGTC	KpnI/ NotI
HASt-NF90	pcDNA5/FRT/TO/nTAPG (Amp)	f: CCGGGGATCCAATGCGTCCAATGCGAATTTTTG r: GCGCGCGGCCGCCTAGGAAGACCCAAAATCATG	BamHI/ NotI
NF90-StHA	pcDNA5/FRT/TO/cTAPG (Amp)	f: CCGGGGATCCAATGCGTCCAATGCGAATTTTTG r: GCGCGCGGCCGCGGAAGACCCAAAATCATGATAG	BamHI/ NotI
HASt-NF110	pcDNA5/FRT/TO/nTAPG (Amp)	f: GCGCGGTACCGATGCGTCCAATGCGAATTTTTG r: GCGCGCGGCCGCTCTGTACTGGTAGTTCATG	KpnI/ NotI
NF110-StHA	pcDNA5/FRT/TO/cTAPG (Amp)	f: GCGCGGTACCGATGCGTCCAATGCGAATTTTTG r: GCGCGCGGCCGCTCTGTACTGGTAGTTCATG	KpnI/ NotI
HASt-NF90 ΔC	pcDNA5/FRT/TO/nTAPG (Amp)	f: CCGGGGATCCAATGCGTCCAATGCGAATTTTTG r: GCGCGCGGCCGCCTAGGCATCAAGGGCGAGAGGG	KpnI/ NotI
HASt-NF90 ΔdsRBD	pcDNA5/FRT/TO/nTAPG (Amp)	f: CCGGGGATCCAATGCGTCCAATGCGAATTTTTG r: GCGCGCGGCCGCCTACTTCTCCTCCCCGTCCTC	KpnI/ NotI
HASt-NF90 ΔdsRBD+NLS	pcDNA5/FRT/TO/nTAPG (Amp)	f: CCGGGGATCCAATGCGTCCAATGCGAATTTTTG r: GCGCGCGGCCGCCTATGCCTTCTCCTCTTTCTTCTG	KpnI/ NotI

Table 4.3 List of constructs and respective primers used in this study

Construct	Template	Primers
zz-C21orf70(1-141)(L67A, L69A)	zz-C21orf70 (1-141)	s: GGTGCAGAAGGCGGAGGCGGACGTGAGGAGTGTC as: GACACTCCTCACGTCCGCCTCCGCCTTCTGCACC
zz-C21orf70 (142-230) (L155A, L157A)	zz-C21orf70 (142-230)	s: CCTGCCCGAGCTGGCGGGGGCCGAGGCTGGCAGC as: GCTGCCAGCCTCGGCCCCCGCCAGCTCGGGCAGG
zz-C21orf70 (142-230) (L144A, L147A, L155A, L157A)	zz-C21orf70 (142-230) (L144A, L147A)	s: CCTGCCCGAGCTGGCGGGGGCCGAGGCTGGCAGC as: GCTGCCAGCCTCGGCCCCCGCCAGCTCGGGCAGG
HASt-NF90 (E312R, R323E)	HASt-NF90	E312R: s: CTAGACAGACAGCAACGGAGAGATATCACACAGAGTGCG as: CGCACTCTGTGTGATATCTCTCCGTTGCTGTCTGTCTAG E323R: s: GTGCGCAGCACGCACTGGAGCTCGCTGCCTTCGGCCAGC as: GCTGGCCGAAGGCAGCGAGCTCCAGTGCGTGCTGCGCAC

Table 4.4 List of QuikChange primers used in this study

4.1.3 Cell lines used in this study

Cell line name	Derived from	Resistance
HeLa Kyoto		-
HeLa RPS2-YFP	HeLa FRT TetR H2B mRED (Klebig et al., 2009; Wild et al., 2010)	Puromycin and hygromycin
HeLa RPL29-GFP	HeLa FRT TetR H2B mRED (Klebig et al., 2009; Wild et al., 2010)	Puromycin and hygromycin
U2OS		-
HEK 293 HASt-C21orf70	HEK 293 FlpIn TRex (Invitrogen)	Hygromycin and blasticidin
HEK 293 ZNF622-StHA	HEK 293 FlpIn TRex (Invitrogen) (Wild et al., 2010)	Hygromycin and blasticidin
HEK 293 MRTO4-StHA	HEK 293 FlpIn TRex (Invitrogen) (Wild et al., 2010)	Hygromycin and blasticidin
HEK 293 HASt-LTV1	HEK 293 FlpIn TRex (Invitrogen) (Wyler et al., 2011)	Hygromycin and blasticidin
HEK 293 HASt-PNO1	HEK 293 FlpIn TRex (Invitrogen) (Wyler et al., 2011)	Hygromycin and blasticidin
HEK 293 HASt-GFP	HEK 293 FlpIn TRex (Invitrogen) (Wyler et al., 2011)	Hygromycin and blasticidin
HEK 293 HASt-NF90	HEK 293 FlpIn TRex (Invitrogen)	Hygromycin and blasticidin
HEK 293 HASt-NF90 ΔC	HEK 293 FlpIn TRex (Invitrogen)	Hygromycin and blasticidin
HEK 293 HASt-NF90 ΔdsRBD	HEK 293 FlpIn TRex (Invitrogen)	Hygromycin and blasticidin
HEK 293 HASt-NF90 ΔdsRBD+NLS	HEK 293 FlpIn TRex (Invitrogen)	Hygromycin and blasticidin
HEK 293 HASt-NF90 (E312R, R323E)	HEK 293 FlpIn TRex (Invitrogen)	Hygromycin and blasticidin
HeLa FRT 8.14	Kind gift from Thomas Mayer (University of Konstanz, Germany)	
HeLa FRT HASt-NF90	HeLa FRT 8.14	Hygromycin
HeLa FRT HASt-C21orf70	HeLa FRT 8.14	Hygromycin

Table 4.5. List of Cell lines used in this study

4.1.4 Oligonucleotides used in this study

siRNA	Sequence (sense strand, 5'-3')	Reference	Manufacturer
AllStars	negative control (si-control)		Qiagen
si-C21orf70-b	CAAUAAAUGGCUCUGUGAA	Wyler et al., 2011	Sigma
si-C21orf70-c	GCAGCAGGGAGAGCAACAA	Wyler et al., 2011	Sigma
si-CK1γ3	GAATATGACTGGATTGGTA		Microsynth
si-CK1δ	CCATCGAAGTGTTGTGTAA		Microsynth
si-CK1ε	ACATCGAGAGCAAGTTCTA		Microsynth
si-CK1ε-3'UTR	CCCGTTCTCCTGTGTCTACTA		Qiagen
si-CRM1	UGUGGUGAAUUGCUUAUAC	Zemp et al., 2009	Microsynth
si-NF45	CTCCATAGAAGTGTCATTCCA		Qiagen
si-NF90/110	GTGGAGGTTGATGGCAATTCA		Qiagen
si-NOB1	GCCCAGAGATCATGCATTT		Microsynth
si-NPM	AAAGGTGGTTCTCTTCCCAAA		Qiagen
si-PES1	CCGGCTCACTGTGGAGTTCAT		Qiagen
si-POLR1A	AAGGATGTAGTTCTGATTCGA		Qiagen
si-RIOK2	GGAUCUUGGAUAUGUUUAA	Zemp et al., 2009	Microsynth
si-RPL11	GGUGCGGGAGUAUGAGUUA		Sigma
si-RPL23	GUGGUCAUUCGACAACGAU		Sigma
si-RPS3	GCAAGAUGGCAGUGCAAAU		Microsynth
si-XPO5	AGAUGCUCUGUCUCGAAUU	Wild et al., 2010	Qiagen
si-ZNF622	CAGGCACATATGAATGACAAA		Qiagen

Table 4.6 List of siRNAs used in this study

Probe	Sequence	Reference	Manufacturer
Cy5-5'ETS1	5′-CGGAGGCCCAACCTCTCC GACGACAGGTCGCCAGAGGAC AGCGTGTCAGC-3'	(Granneman et al., 2004)	Microsynth
Cy5-5'ITS1	5′-CCTCGCCCTCCGGGCTCC GTTAATGATC-3′	Rouquette et al., 2005	Microsynth
5'ITS1	5′-CCTCGCCCTCCGGGCTCC GTTAATGATC-3′	Rouquette et al., 2005	Microsynth
ITS2	5′-GCGCGACGGCGGACGA CACCGCGGCGTC-3′	Rouquette et al., 2005	Microsynth

Table 4.7 List of FISH and Northern blot probes used in this study

4.2 Molecular cloning

4.2.1 Source of coding sequences and amplification

The coding sequence of C21orf70 was amplified from cDNA. Casein kinase 1 epsilon (CK1ε) wild type and kinase-dead (D149A) were amplified from plasmids kindly provided by I. Zemp (pEGFP-C1-hCSNK1e#8 and pEGFP-C1-hCSNK1e(D149A)#2, respectively). The NF90 cDNA was ordered from Source BioScience (Nottingham, UK). A plasmid containing the coding sequence of NF110 was a kind gift from A. Cook (WTCCB, Edinburgh, UK).
All coding sequences were amplified from the aforementioned plasmids by polymerase chain reaction (PCR) using Pwo polymerase (Roche).

4.2.2 DNA gel electrophoresis

DNA was separated by size on a 1% Agarose gel in 0.5x TAE buffer containing 0.25x GelRed Nucleic Acid stain (Biotium). Prior to loading, DNA was mixed with Orange G buffer (1x final concentration) and the electrophoresis was carried out in 0.5x TAE buffer at 90 V. The DNA was visualized by UV light, excised from the gel and purified using the QIAEX II gel extraction kit (Qiagen) according to the manufacturer's protocol.

50x TAE buffer	2 M Tris-base, 50 mM EDTA pH 8, 5.75% acetic acid
5x Orange G buffer	50% glycerol, 25 mM EDTA pH 8, 0.4% Orange G

4.2.3 Restriction enzyme digest of PCR products and vectors

Purified PCR products or 5 µg of vector were subjected to digestion by restriction enzymes. 30 U restriction enzymes in their respective buffer were incubated with the DNA at 37°C for 3 h. Inserts were then purified using the QIAEX II gel extraction kit (Qiagen) according to the manufacturer's protocol. Digested vectors were dephosphorylated as described below before purification. All restriction enzymes used for this study and the respective vectors/inserts for which they were used are listed in table 4.3.
Analytical digests were performed to determine whether clones contained the transformed plasmid with an insert of the correct size. For this, about 2 µg

DNA was incubated at 37°C for 1 h with 5 U of the corresponding restriction enzymes in the according buffer and subsequently analyzed by DNA gel electrophoresis (4.2.2).

4.2.4 Dephosphorylation of vectors

After restriction enzyme digest and prior to ligation, vectors were dephosphorylated to inhibit self-ligation. For this, 10 U of calf intestinal alkaline phosphatase (CIP) was added to the restriction digest followed by incubation for 1 h at 37°C. Subsequently, the vector was purified using the QIAEX II gel extraction kit (Qiagen) according to the manufacturer's protocol.

4.2.5 Ligation of DNA

The digested vector and insert, in a molar ratio of approximately 1:4, were ligated for 1 h at RT with 20 U T4 DNA ligase (Thermo Fischer Scientific) in its corresponding buffer in 10 µl total volume prior to transformation into bacteria.

4.2.6 Heat-shock transformation of *E.coli*

To introduce plasmid DNA into *E. coli* for amplification, heat-shock competent XL1 blue *E. coli* cells were mixed with either 5 µl of the ligation reaction or 1 µg of plasmid DNA, incubated for 5 min on ice and transferred to 42°C for 90 s followed by incubation on ice for 10 min. Recovery was performed by adding 1 ml LB medium to the cells and incubation at 37°C for 45 min.

Cells were pelleted by centrifugation (6000 rpm, 5 min, RT), resuspended in 100 µl LB, plated on selective LB/Agar plates, and incubated at 37°C overnight. For cloning of C21orf70 constructs in the pQEzz60 vector, 2% glucose was added to the plates to suppress protein expression, since prolonged expression of C21orf70 led to reduced growth of the bacteria.

For midiprep cultures, 500 µl of recovered bacteria solution was added to 100 ml LB containing the appropriate antibiotic and incubated on a shaker at 37°C overnight.

4.2.7 Transformation by electroporation of *E.coli*

For recombinant expression of proteins, BLR(pRep4) *E. coli* cells were transformed with pQEzz60 plasmids containing the construct of interest. 0.5 µg DNA was added to 50 µl cells incubated on ice for 5 min and transferred to an electroporation cuvette. After electroporation (2.5 kV, 200 Ω, 25 µF), cells were recovered in 1 ml LB without antibiotics for 45 min at 37°C, then added to 250 ml DYT containing the appropriate antibiotics and incubated overnight at 37°C before the protein expression protocol was carried out (see 4.3.1). Note that for expression of C21orf70 constructs, glucose (2% final concentration) was added to the DYT medium for overnight incubation to suppress protein expression, since prolonged expression of C21orf70 led to significantly reduced cell growth.

4.2.8 Site directed mutagenesis

For insertion of point mutations into a plasmid, a modified protocol of the QuikChange mutagenesis kit (Strategene) was used. Primers were of 25-45 nt length, designed to contain the nucleotide mutation, and to have a melting temperature (T_m) of >78°C (with the following formula to calculate the T_m: T_m=81.5 + 0.41(%GC) - 674/N - % mismatch, where N is the amount of bases in the primer). 50 µl reaction mixture contained 100 ng template plasmid, 125 µg of the sense and antisense primer (all templates and the respective primers are listed in table 4.4), 400 µM dNTPs, 3% DMSO, and 5 U Pwo polymerase (Roche) in the corresponding 1x buffer. The following PCR program was used:

Time	Temperature
30 s	95°C
30 s	95°C
1 min	55°C
1 min/ 1kb	72°C
repeat step 2-4	18 times
7 min	72°C
Until end	4°C

Table 4.8. QuikChange PCR program

The PCR product was analyzed by DNA gel electrophoresis (see 4.2.2) along with the template plasmid to verify that amplification has taken place. The corresponding band was excised from the gel and purified using the QIAEX II gel extraction kit (Qiagen) according to the manufacturer's protocol. The purified DNA was incubated with 10 U of the restriction enzyme DpnI in its corresponding buffer (NEB) for 1 h at 37°C to digest the template DNA. The restriction digest product was directly transformed into XL1 blue *E. coli* cells (see 4.2.6).

4.2.9 DNA purification

For small scale DNA purification, minipreps were carried out from a 4 ml overnight culture at 37°C of LB containing the corresponding antibiotic inoculated from a previously transformed (see 4.2.6) XL1 blue *E. coli* colony. The GeneJET Plasmid Miniprep Kit (Fermentas/Thermo Fischer Scientific) was used according to the manufacturer's protocol.
Midipreps were performed from a 100 ml bacteria culture using the NucleoBond Xtra Midi kit according to the manufacturer's protocol.

4.2.10 DNA sequencing

Sanger sequencing of all constructs in table 4.3 and 4.4 was performed by Microsynth (Balgach, Switzerland).

4.3 Protein techniques

4.3.1 Protein expression

Transformed BLR(pRep4) *E. coli* cells (see 4.2.7) were grown in 250 ml DYT medium containing 2% Glucose (only for expression of C21orf70 constructs) and the corresponding antibiotics overnight at 37°C on a shaker. The culture was diluted with 750 ml DYT containing the corresponding antibiotics and further incubated at 37°C until it reached an OD_{600} of about 1.3-1.5. Subsequently, the culture was diluted with 500 ml ice-cold LB medium containing the corresponding antibiotics and incubated at the expression temperature (usually 25°C) for 30 min. Expression was induced by the addition of IPTG (1 mM final concentration) and incubation at the expression

temperature for 4 h. To prevent protein degradation, PMSF (175 mg PMSF in 15 ml ethanol) was added to the culture and cells were harvested by centrifugation (15 min, 4500 rpm, 4°C). The pellet was resuspended in 35 ml lysis buffer and lysed by sonication. The cell lysate was cleared by ultracentrifugation (1 h, 55,000 rpm, 4°C, Beckman Ti70 rotor), supplemented with 250 mM sucrose and shock-frozen in liquid nitrogen for storage at -80°C.

DYT medium	1% (w/v) bacto tryptone, 1% (w/v) yeast extract, 0.5% (w/v) NaCl
LB medium	1% (w/v) bacto tryptone, 0.5% (w/v) yeast extract, 1% (w/v) NaCl
Lysis buffer	50 mM Tris/HCl pH 7.4, 700 mM NaCl, 3 mM $MgCl_2$, 5% Glycerol

4.3.2 Ni-NTA protein purification

The cleared lysate containing the recombinantly expressed protein (see 4.3.1) was supplemented with 20 mM Imidazol and 2 mM β-mercaptoethanol and loaded on a column containing 3 ml Ni-NTA slurry previously washed with equilibration buffer. After loading the lysate twice, the column was washed with 25 ml wash buffer. Bound protein was eluted with elution buffer and the collected elution factions were analyzed by amido black staining (see 4.3.3) and sodium dodecyl sulfate polyacrylamide gel electrophoresis (SDS-PAGE; see 4.3.6).

Equilibration buffer	50 mM Tris/HCl pH 7.4, 700 mM NaCl, 3 mM $MgCl_2$, 5% Glycerol, 20 mM Imidazol, 2 mM β-mercaptoethanol
Wash buffer	50 mM Tris/HCl pH 7.4, 700 mM NaCl, 3 mM $MgCl_2$, 5% Glycerol, 20 mM Imidazol
Elution buffer	60% wash buffer, 40% 1 M Imidazol

4.3.3 Amido black staining

For detection of proteins in elution fractions, 1 µl of each fraction was spotted on a nitrocellulose membrane (GE Healthcare) and amido black staining solution was added. The membrane was destained with dH_2O after 3 min.

Amido black staining solution	2% (v/v) acetic acid, 0.1% (w/v) naphtol blue black, 1% (w/v) SDS

4.3.4 Buffer exchange

For buffer exchange of purified protein samples, a PD-10 column (Amersham Bioscience) was used according to the manufacturer's protocol. Collected elution factions were analyzed by amido black staining (see 4.3.3).

4.3.5 Protein gel electrophoresis

To separate proteins according to their molecular size, SDS-PAGE was used. Proteins were denatured by the addition of SDS sample buffer and subsequent heating (95°C, 10 min) and loaded on a polyacrylamide gel of suitable percentage. After electrophoresis at 45 mA for 1 h in 1x electrophoresis buffer, proteins were detected by either Coomassie staining (4.3.6), silver staining (4.3.7) or Western blotting (4.3.8).

2x SDS sample buffer	75 mM Tris/HCl pH 6.8, 20% glycerine, 4% SDS, 50 mM DTT, and little bromophenole blue until solution dark blue
10x electro-phoresis buffer	25 mM Tris-base, 133 mM glycine, 1% SDS

4.3.6 Coomassie staining

After SDS-PAGE (see 4.3.5), the gel was incubated for 2 min in 3% acetic acid and protein bands were visualized by addition of Coomassie staining solution for 45 min. To destain the gel, it was heated in dH_2O and incubated at RT while shaking for 3 h.

For colloidal Coomassie staining, proteins in the gel were fixed in fixation solution for 15 min, followed by washing three times with dH_2O for 5 min each. Colloidal Coomassie staining solution was added and the gel was incubated

for at least 1 h up to overnight before washing with dH_2O for 10 min to remove excess dye.

Coomassie staining solution	1% (w/v) Coomassie G250, 40% (v/v) methanol
Fixation solution	50% methanol, 7% acetic acid
Colloidal Coomassie staining solution	0.12% Coomassie brilliant blue G-250, 10% ammonium sulfate, 10% phosphoric acid, 20% methanol

4.3.7 Silver staining

For silver staining, the gel was incubated after SDS-PAGE (4.3.5) in fixation solution for 1 h, followed by incubation in buffer 2 for 1 h up to overnight. After washing three times for 10 min with dH_2O, the gel was incubated in silver staining solution for 30 min. The gel was washed briefly in dH_2O and developer solution was added under constant shaking until staining of the protein bands reached the desired intensity. The reaction was stopped by the addition of 50 mM EDTA pH 8.0.

Fixation solution	30% (v/v) ethanol, 15% (v/v) acetic acid
Silver staining buffer 2	0.5 M NaOAc, 12 mM $Na_2S_2O_3$, 0.125% glutaraldehyde, 25% ethanol
Silver staining solution	0.1% $AgNO_3$, 0.011% formaldehyde
Developer solution	12.5 g Na_2CO_3, 0.011% formaldehyde in 500 ml dH_2O

4.3.8 Western blot analysis

After SDS-PAGE (see 4.3.5), proteins were transferred from the gel to a nitrocellulose membrane (GE Healthcare) using the Trans-Blot SD Semi-Dry Transfer Cell (Bio-Rad). The transfer was carried out for 1 h in transfer buffer at a constant current of (area of membrane in cm^2)x1.1 mA. The membrane was blocked in 10% dry milk in TBT buffer for 30 min and incubated with the

primary antibody in 4% dry milk in TBT buffer for 1 h at RT up to overnight at 4°C. The membrane was washed three times for 10 min in 4% dry milk in TBT buffer and incubated with the appropriate secondary antibody coupled to horseradish peroxidase in 4% dry milk in TBT buffer for 30 min at RT (a list of all primary and secondary antibodies used in this study, their source and the concentration at which they were used can be found in table 4.1 and 4.2). The membrane was then washed for 5 min with 4% dry milk in TBT buffer and twice for 5 min with TBT buffer. The membrane was then incubated in the chemiluminescence solution for 1 min and the light emitted by the reaction was detected using Super RX films (Fujifilm).

Transfer buffer	2.5 mM Tris-base, 13.3 mM glycine, 0.1% SDS, 20% methanol
TBT buffer	150 mM NaCl, 6 mM Tris-base, 20 mM Tris-HCl, 0.1% (v/v) Tween-20
Chemiluminescence solution	100 mM Tris/HCl pH 8.5, 1.25 mM luminol, 68 µM p-coumaric acid, 0.01% H_2O_2

4.3.9 Ponceau S staining

After semi-dry transfer of proteins to the membrane (4.3.8), the membrane was incubated in Ponceau S staining solution for 3 min to ensure equal transfer and loading of samples. Excess dye was washed away with dH_2O and the membrane was scanned before incubation in blocking solution.

Ponceau S staining solution	0.3% Ponceau S, 3% Trichloroacetic acid

4.3.10 Mass spectrometry analysis

After colloidal Coomassie staining (4.3.6), proteins bands of interest were excised from the gel and analyzed by mass spectrometry by Jens Pfannstiel (Universität Hohenheim, Germany).

4.4 Cell culture methods

4.4.1 Maintenance of cells

All cell lines (a complete list of all cell lines used in this study is listed in table 4.5) were grown in DME medium (Sigma) supplemented with 10% fetal bovine serum (PAA) and 100 µg/ml penicillin/streptomycin (PAA) (DMEM +/+) at 37°C and 5% CO_2.

4.4.2 Transient transfection of cells

To transiently express a protein of interest, HeLa cells were grown in 6-well plates (Greiner) in 2 ml DMEM +/+ on coverslips for microscopy. Per well, 3 µl X-tremeGENE 9 DNA Transfection Reagent (Roche) was mixed with 97 µl DMEM without FBS and penicillin/streptomycin (DMEM -/-) and incubated at RT for 5 min. 1 µg DNA was added to the mix, further incubated for 25 min at RT, and the mixture was added to the cells, which were then incubated at 37°C, 5% CO_2 for 24 h.

4.4.3 Stable cell line generation

For stable incorporation of a gene of interest into the genome, HEK 239 FlpIn TRex cells or HeLa FRT 8.14 were transfected (see 4.2.2) with 0.1 µg pcDNA5/FRT/TO plasmid containing the tagged construct and 0.9 µg pOG44 plasmid (Invitrogen), which encodes the Flp Recombinase for integration of a gene at the Flp Recombinase Target (FRT) site in these cell lines. 24 h after transfection, cells were detached with PBS/0.5 mM EDTA and seeded in a 10 cm plate containing DMEM +/+. The medium was exchanged 24 h later to DMEM +/+ containing 400 µg/ml hygromycin (Invitrogen) for HeLa FRT 8.14 cells or 100 µg/ml hygromycin and 15 µg/ml blasticidin (Invitrogen) for HEK 293 FlpIn TRex cells in order to select for transfected cells. Cells were kept under selection for two weeks until colonies were visible. HEK 293 FlpIn TRex colonies were pooled yielding a polyclonal TAP cell line. For HeLa FRT 8.14 cell lines, single colonies were picked and selected based on expression levels and homogeneity.

4.4.4 Tetracycline-induction of protein expression

To induce expression of a stably incorporated construct (see 4.3.3), cells were treated with tetracycline in DMEM +/+ 24 h prior to harvesting/fixation. For TAP experiments, 0.5 µg/ml tetracycline was used for HEK 293 FlpIn TRex cells. HeLa FRT 8.14 cells were induced with 25 ng/ml tetracycline. RPS2-YFP and RPL29-GFP cell lines were induced with 125 ng/ml tetracycline for 16 h followed by a chase period with DMEM+/+ without tetracycline for 4 h.

4.4.5 Inhibitor treatment of cells

Leptomycin B: CRM1-mediated export was inhibited by the addition of 20 nM Leptomycin B (LMB, LC laboratories) to HeLa cells in DMEM +/+ for 1 h.

Actinomycin D: At low concentrations, actinomycin D (ActD) specifically inhibits POL I (Perry, 1963). HeLa cells were treated with 0.1 µg/ml ActD in DMEM +/+ for 6 h prior to fixation.

CK1 inhibitors:

D4476: To inhibit CK1 activity, HeLa cells were treated with 100 µM D4476 (Tocris) for 8 h. To increase solubility of the inhibitor, 2 µl of 100 mM D4476 was preincubated with 3 µl X-tremeGENE 9 DNA Transfection Reagent (Roche) and 6 µl DMEM -/- for 5 min at RT before adding the mixture to the cells grown in a 6-well in 2 ml DMEM +/+ (Rena et al., 2004).

LH846: LH846 (Tocris) preferentially inhibits CK1δ (IC_{50} of 290 nM vs. 1.3 µM for CK1ε). It was added to HeLa cells grown in 2 ml DMEM -/- at a final concentration of 7.5 µM for 6 h.

PF4800567 hydrochloride: PF4800567 (Tocris) preferentially inhibits CK1ε (IC_{50} of 32 nM vs. 711 nM for CK1δ). It was added to HeLa cells grown in 2 ml DMEM -/- at a final concentration of 1.5 µM for 6 h.

PF670462: PF670462 (Tocris) is a potent and selective inhibitor for CK1δ and CK1ε (IC_{50} of 7.7 nM and 14 nM, respectively). It was added to HeLa cells grown in 2 ml DMEM -/- at a final concentration of 1 µM for 6 h.

4.4.6 RNAi

For targeted knockdown of a specific protein *in vivo*, cells were treated with siRNAs at a final concentration of 9 nM for 72 h unless otherwise stated. For HeLa K and HeLa FRT Tet H2B-mRED derived cell lines (see table 4.5) grown in one 6-well, the siRNA was premixed with 200 µl Opti-MEM (Gibco) and 2 µl INTERFERin (Polyplus Transfection), incubated at RT for 15 min and added to the well. For HeLa FRT 8.14 and HEK 239 FlpIn TRex derived cell lines (see table 4.5) grown in one 6-well, the siRNA was premixed with 100 µl Opti-MEM and 1 µl Lipofectamine RNAiMAX Reagent (Invitrogen) and incubated at RT for 10 min prior to addition to the cells.
A list of all siRNAs used in this study is compiled in table 4.6.

4.4.7 CK1 rescue experiment

HeLa K cells were treated with 9 nM si-CK1δ and si-CK1ε-3'UTR siRNAs for 48 h (see 4.6.6). 24 h prior to fixation, cells were transiently transfected (see 4.2.2) with a plasmid encoding either HASt-CK1ε wild type or kinase-dead (D149A) to rescue the depletion phenotype. Localization of ENP1 and presence of HASt-CK1ε was detected by co-immunofluorescence (4.8.2).
For quantification of the rescue experiment, cells were divided into three groups: cells that display normal nuclear localization of ENP1 ("nuclear"), cells where ENP1 partially mislocalizes to the cytoplasm ("cytoplasmic") and an intermediate phenotype, where ENP1 levels are approximately the same for nucleoplasm and cytoplasm ("intermediate"). For transfected cells, only cells that were positive for HASt-CK1ε expression were scored. An unpaired t-test was performed using Prism (GraphPad software) for values from three independent experiments to investigate the statistical significance.

4.5 Biochemical assays

4.5.1 Cell fractionation

HeLa cells were grown on a 10 cm plate to 80-90% confluency. Cells were detached with PBS/0.5 mM EDTA, pelleted (2000 g, 5 min, 4°C) and resuspended in 400 µl wash buffer. After centrifugation (2000 g, 5 min, 4°C), the cell pellet was resuspended in 400 µl lysis buffer and a "total" sample was

taken. The cells were incubated on ice for 30 min and forced five times through a 27 G needle for lysis. The nuclei were pelleted by centrifugation (2000 g, 5 min, 4°C) and a “cytoplasm” sample was taken from the supernatant. The pellet was washed two times with lysis buffer before resuspension in 400 µl SDS buffer from which the “nucleus” sample was taken. All samples were taken as follows: 30 µl protein sample + 60 µl SDS buffer.

Wash buffer 10 mM Tris/HCl pH 7.4, 10 mM KCl, 2 mM $MgCl_2$

Lysis buffer 10 mM Tris/HCl pH 7.4, 10 mM KCl, 2 mM $MgCl_2$
1 mM EGTA, 1 mM DTT, 40 µg/ml PMSF, 10 µg/ml Aprotinin, 2 µg/ml Pepstatin A

4.5.2 Sucrose gradient analysis

HeLa cells were grown in 2 wells of a 6-well plate (NUNC) to confluency and harvested by detachment with PBS/0.5 mM EDTA, followed by centrifugation (700 g, 3 min, 4°C). The cells were lysed with lysis buffer and cleared by centrifugation (16,000 g, 5 min, 4°C). Protein concentration in the lysate was determined by the Bradford protein assay. A linear 10-45% sucrose gradient was generated in TLS55 tubes using a BioComp Gradient Master with time/angle/speed settings of 55 sec/85°/22 and 400 µg extract was loaded on top of the gradient. After centrifugation in a TLS55 rotor in an Optima TLX ultracentrifuge (Beckmann Coulter) (55,000 rpm, 1 h 50 min, 4°C, decel 7), 150 µl fractions were taken from the top of the gradient followed by TCA precipitation of proteins. Fractions were analyzed by SDS-PAGE (4.3.5) followed by Western blotting (4.3.8).

Lysis buffer 50 mM Hepes/KOH pH7.5, 100 mM KCl, 3 mM $MgCl_2$, 0.5% NP-40, 1mM DTT, 1 mM PMSF, 1 µg/ml Pepstatin A, 10 µg/ml Leupeptin, 10 µg/ml Aprotinin

Gradient buffer 50 mM Hepes/KOH pH7.5, 100 mM KCl, 3 mM $MgCl_2$

4.5.3. CRM1 binding assay

For each bait protein, 80 µl IgG sepharose slurry (40 µl beads, GE healthcare) was equilibrated in wash buffer and the recombinantly expressed zz-tagged bait proteins (see 4.3.1) were added in equimolar amounts to the beads. Bacterial lysate containing the zz-6xHis tag served as negative control. The IgG beads were incubated with the bait proteins on an overhead shaker for 2 h at 4°C and subsequently washed three times with wash buffer to remove unbound proteins. CRM1 (3.25 µM), BSA (160 µg/ml) and either RanQ69L-GTP (7 µM) or the equivalent volume of wash buffer was added to each sample in a total volume of 100 µl and incubated on ice for 2 h while mixed by pipetting every 15 min. The IgG beads were washed with wash buffer three times, transferred to MoBiCol columns (MoBiTec), washed once with 50 mM Tris/HCl pH 7.4, 5 mM $MgCl_2$ and eluted with SDS sample buffer without DTT. Prior to analyzing the samples by SDS-PAGE, DTT was added to the sample (30 mM final concentration).

Wash buffer 50 mM Tris/HCl pH 7.4, 175 mM KOAc, 2 mM $MgCl_2$, 0.001% Triton X-100

4.5.4 Tandem affinity purification (TAP)

HEK 293 FlpIn TRex cells were harvested by centrifugation (5 min, 700 g, 4°C) and taken up in 1 ml NP-40 lysis buffer per 10 cm plate. The cells were lysed by douncing (20 strokes), the lysate was cleared by centrifugation (4500 g, 12 min, 4°C) and added to 20 µl StrepTactin beads (IBA) per 10 cm plate of cells. After 30 min incubation at 4°C while rotating, the beads were washed three times with buffer 2 and eluted three times with 300 µl buffer 2 containing 2.5 mM desthiobiotin (Sigma). The eluate was added to 15 µl HA-Agarose/10 cm plate and incubated for 1 h at 4°C while rotating. After washing twice with buffer 2 and once with 50 mM Tris/HCl, pH 7.4, 2 mM $MgCl_2$, the HA-Agarose beads were transferred to MoBiCol columns (MoBiTec) and bound proteins were eluted using SDS sample buffer without DTT. Prior to analyzing the samples by SDS-PAGE, DTT was added to the sample (30 mM final concentration).

NP-40 lysis buffer 10 mM Tris/HCl pH 7.4, 100 mM KCl, 2 mM $MgCl_2$,0.5 mM NAF, 0.1 mM $NaVO_4$, 1 µg/ml Pepstatin A, 10 µg/ml Leupeptin, 10 µg/ml Aprotinin, 1 mM DTT, 0.5% NP-40

Buffer 2 10 mM Tris/HCl pH 7.4, 100 mM KCl, 2 mM $MgCl_2$,0.5 mM NAF, 0.1 mM $NaVO_4$, 1 µg/ml Pepstatin A, 10 µg/ml Leupeptin, 10 µg/ml Aprotinin

4.5.5 Exportin binding to pre-60S particles assay

MRTO4-StHA expressing HEK 293 FlpIn TRex cells were induced 24 h prior to harvesting with tetracycline (0.5 µg/ml). TAP was carried out (see 4.5.4), but instead of a direct elution after the second binding step, the anti-HA Agarose beads were washed twice with wash buffer. HeLa extract depleted of ribosomes and tRNAs (described in Wild et al., 2010), and either RanQ69L-GTP (10 µM) or buffer was added to the beads to a total volume of 100 µl and incubated at 4°C for 1 h. The anti-HA Agarose beads were washed twice with wash buffer and bound proteins were eluted with SDS sample buffer without DTT. Prior to analyzing the samples by SDS-PAGE, DTT was added to the sample (30 mM final concentration).

Wash buffer 50 mM Tris/HCl pH 7.5, 150 mM KCH_3CO_2, 1 mM $MgCl_2$

4.5.6 Kinase assay on pre-40S particles

Tandem affinity purification of HASt-LTV1 expressing HEK 293 FlpIn TRex cells was performed (see 4.5.4) except that purified complexes were not eluted from the HA agarose beads. The buffer was exchanged to 50 mM Tris/HCl pH 7.6, 50 mM NaCl and 5 mM $MgCl_2$, and 5 µM of the CK1δ/ε inhibitor PF670462 or solvent control (DMSO) was added. 1 µCi ^{32}P-γATP was added per reaction, followed by incubation at 30°C for 20 min. Proteins were eluted with SDS sample buffer without DTT. DTT was added after the elution (30 mM final concentration) and samples were analyzed by SDS-PAGE (see 4.3.5) followed by silver staining (see 4.3.7). The gel was dried and exposed on a Phosphoimager screen for 24 h. For control reactions, 0.9 µg recombinant zz-RIOK2 or 0.2 µg casein was incubated with 5 units (2.5 ng) rat CK1δ (NEB) or 10 ng CK1ε (SignalChem) in 10 µl reactions containing

1 µCi ^{32}P-γATP in Tris/HCl pH 7.6, 50 mM NaCl and 5 mM $MgCl_2$ for 20 min at 30°C. SDS sample buffer was added and the samples were analyzed as above.

4.6 Antibody generation and purification

A complete list of all antibodies used in this study can be found in table 4.1. The peptide-specific antibody against C21orf70 was generated for this study. A C-terminal C21orf70 peptide purchased from NeoMPS (France) was used to immunize two rabbits for antibody generation. Final bleeds of both rabbits were tested by Western blot analysis (4.3.8) against HeLa cell extract and the more specific antibody was purified (see 4.6.2).

4.6.1 Antigen coupling

To couple peptide antigens via their cysteine residues to SulfoLink beads (Thermo Fischer Scientific), 7 mg of the peptide was first dissolved in 450 µl ddH_2O by vortexing. 50 µl of 1 M Hepes pH 8.0 was added to facilitate dissolving of peptides and the solution was diluted to 1 ml volume with ddH_2O. To test whether the dissolved peptides were reduced, 2.5 µl of the solution was added to 45 µl of a 1:10 dilution of Ellman's reagent in 0.5 M Phosphate buffer pH 7.0. A bright yellow color indicated that the peptides were indeed in a reduced state.

2 ml SulfoLink bead slurry was equilibrated on a column with 50 mM Hepes pH 8.0, followed by addition of the peptide solution and incubation at RT for 2 h while rotating. Binding of peptides was confirmed by amido black staining (see 4.3.3) of input vs. flow-through samples.

The column was washed as follows:

1. 20 ml 50 mM Hepes pH 8.0
2. 10 ml 50 mM cysteine (1.75 g cysteine, 200 ml dH_2O and 2.5 ml 5 M NaOH), of which 5 ml were used for washing the column. The remaining 5 ml were added to the SulfoLink beads and the column was closed and incubated for 15 min at RT.
3. 10 ml dH_2O
4. 10 ml wash buffer
5. 10 ml dH_2O

6. 10ml 0.2 M Glycine pH 2.2
7. 10 ml dH_2O
8. 10 ml TBT buffer
9. 20 ml wash buffer
10. 10 ml wash buffer, 0.05% NaN_3

The column was stored in wash buffer containing 0.05% NaN_3 at 4°C.

Wash buffer 50 mM Tris/HCl pH 7.5, 150 mM NaCl

TBT buffer 150 mM NaCl, 6 mM Tris-base, 20 mM Tris-HCl, 0.1% (v/v) Tween-20

4.6.2 Antibody affinity purification

For affinity purification of the C21orf70 antibody, the final bleed serum was used. 40 ml of the serum was supplemented with 5 mM EDTA pH 8.0 and 0.1 mg/ml PMSF. The serum was loaded three times onto a column containing the peptide antigen bound to a SulfoLink resin (4.6.1). After washing with 10 ml wash buffer, 50 ml TBT and 50 ml wash buffer, the bound antibody was eluted with 10 ml 0.1 M Glycin pH 2.2 into a centrifugation tube for a Sorvall SS-34 rotor (Thermo Fischer Scientific) containing 0.5 ml 2 M Tris/HCl pH 8.8. To precipitate the antibody, 21 ml $(NH_4)_2SO_4$ was added and the solution was incubated on ice for 30 min. The antibody was pelleted by centrifugation (11,000 rpm, 50 min, 4°C, Sorvall SS-34 rotor) and resuspended in 2 pellet volumes of supernatant. Half of the precipitate was stored at 4°C, the other half was buffer exchanged to wash buffer, supplemented with 250 mM sucrose, and shock-frozen in liquid nitrogen for long term storage at -80°C.

Wash buffer 50 mM Tris/HCl pH 7.5, 150 mM NaCl

TBT buffer 150 mM NaCl, 6 mM Tris-base, 20 mM Tris-HCl, 0.1% (v/v) Tween-20

4.8 Immunolocalization and microscopy methods

4.8.1 Fixation/permeabilization of cells

HeLa cells grown on glass coverslips were briefly washed in PBS and fixed in 4% paraformaldehyde (PFA) in PBS for 15 min at RT. After washing twice for 5 min in PBS, cells were either directly mounted on glass slides using VectaShield (Vector labs), if fluorescent proteins were expressed, or permeabilized in 1x detergent solution for 5 min at RT in the case of immunofluorescence analysis.

For immunofluorescence analysis using the anti-NF45 antibody, cells were fixed/permeabilized by incubation in a 1:1 mixture of methanol/acetone at -20°C for 10 min. For immunofluorescence using the anti-ILF3 antibody, cells were fixed in 4% PFA for 15 min at RT followed by permeabilization in acetone for 5 min at -20°C.

1x detergent solution	0.1% Triton X-100, 0.02% SDS in PBS

4.8.2 Immunofluorescence

Fixed and permeabilized cells were preincubated in 2% BSA in PBS for 10 min at RT followed by incubation in blocking solution for 30 min. The primary antibody diluted in blocking solution was added to the coverslip and incubated for 1 h (all antibodies used in this study with their appropriate dilution for immunofluorescence are listed in table 4.1). After washing three times for 4 min each in 2% BSA in PBS, the cells were incubated in the secondary antibody (see table 4.2) diluted in blocking solution for 30 min. Cells were washed three times for 4 min each in 2% BSA in PBS, briefly incubated in 1x detergent solution and fixed in 4% PFA in PBS for 15 min, washed for 5 min in PBS and mounted on glass slides using VectaShield (Vector labs).

Blocking solution	10% goat serum, 2% BSA in PBS
1x detergent solution	0.1% Triton X-100, 0.02% SDS in PBS

4.8.3 Fluorescence in situ hybridization (FISH)

To detect rRNA precursors in HeLa cells, FISH was used. For this, cells were grown on coverslips and fixed in 4% PFA in PBS for 30 min at RT. To

permeabilize the cells, they were incubated in 70% ethanol overnight at 4°C. After rehydration by incubation in 2x SSC pH 7.0/10% formamide twice for 5 min each at RT, cells were incubated in FISH hybridization buffer for 5 h at 37°C. The sequence of the DNA probe used in this study is shown in table 4.7. Cells were washed twice in 2x SSC pH 7.0, 10% formamide for 30 min each at 37°C, rinsed once for 5 min in PBS, and incubated in 0.1 µg/ml DAPI in PBS for 10 min. After washing for 5 min in PBS, cells were mounted using VectaShield (Vector labs).

2x SSC	300 mM NaCl, 30 mM $Na_3C_6H_5O_7$
FISH hybridization buffer	10% formamide, 2x SSC, 0.5 µg/ml tRNA, 10% dextran sulfate, 50 µg/ml BSA, 10 mM ribonucleoside vanadyl complexes, 0.5ng/ml DNA probe

4.8.4 Microscopy

Pictures of cells were taken at the Light Microscopy Center, ETH Zurich, using a Leica SP1 confocal scanning system. For FISH experiments, a Leica SP2 confocal scanning system was used. Images were processed using Adobe Photoshop CS4 (Adobe). For FISH experiments using the 5'ITS1 probe, images were processed in parallel using γ-correction (setting 0.75).

4.9 RNA methods

4.9.1 Isolation of total RNA from mammalian cells

Cells were harvested by detaching with PBS/0.5 mM EDTA followed by centrifugation (5 min, 700 g, 4°C). The total RNA was extracted using the RNeasy mini kit (Qiagen) according to the manufacturer's protocol. RNA concentration was measured using a NanoVue Plus spectrophotometer (GE healthcare).

4.9.2 Agarose-formaldehyde gel electrophoresis

RNA species were separated by Agarose-Formaldehyde gel electrophoresis. The composition of the gel is shown in table 4.9. For Northern blot analysis, an Owl A5 Tank (Thermo Fischer Scientific) with 350 ml gel volume was used.

For pulse-chase analysis, a Sub-Cell GT Cell tank (BioRad) with 150 ml gel volume was used. The electrophoresis was carried out in 50 mM Hepes pH 7.8 at constant 75 V for 4 h.

Total	**350 ml**	**150 ml**
Agarose	4.2 g	1.8 g
0.5 M Hepes pH 7.8	35 ml	15 ml
H_2O	262 ml	113 ml
37% Formaldehyde	56 ml	24 ml

Table 4.9. Agarose-formaldehyde gel composition

4.9.3 Northern blot analysis

After gel electrophoresis (see 4.9.2) of 3 µg/lane of total RNA isolated from cells (see 4.9.1), diluted in RNA formaldehyde loading buffer (1x final concentration), the gel was stained with 3x GelRed (Biotium) in ddH_2O for 1 h. The gel was then washed as follows: 10 min in ddH_2O, 15 min in 75 mM NaOH, 20 min in 0.5M Tris/HCl pH 7.0, 1.5 M NaCl, and 10 min in 10x SSC. The RNA was then transferred to a positively charged nylon membrane (Amersham Hybond-N^+, GE Healthcare) via capillary transfer in 10x SSC overnight at RT. The membrane was dried and crosslinked using a UV Stratalinker (Stratagene) and a picture was taken with a UV transilluminator to verify transfer efficiency. After incubation of the membrane in 15 ml hybridization buffer at 65°C for 1 h, the ^{32}P-labeled probe (see 4.9.4, for the sequences of probes used see table 4.7) was added to the hybridization buffer. The membrane was then hybridized for 1 h at 65°C and overnight at 37°C. Next, the membrane was washed three times in 2x SSC for 5 min each at 25°C, wrapped in Saran Wrap and exposed on a Phosphoimager screen for 24 h up to several days.

2x RNA formaldehyde loading buffer	36% formamide, 12% formaldehyde, 0.8x Hepes, 0.05% Xylene cyanol, 0.05% Bromphenol blue, 20% Gycerol

10x SSC	1.5 M NaCl, 150 mM $Na_3C_6H_5O_7$
hybridization buffer	50% formamide, 5x SSPE pH 7.4, 5x Denhardt's solution, 1% SDS, 200 µg/ml DNA MB-grade from fish sperm (Roche)
20x SSPE pH 7.4	3.0 M NaCl, 0.2 M NaH_2PO_4, 0.02 M EDTA
10x Denhardt's solution	2% Ficoll 400, 2% Poly-vinyl-pyrrolidone, 2% BSA fraction V

4.9.4 5'-end labeling of oligonucleotides

The DNA probes used for Northern blotting are shown in table 4.7. 200 ng of the probe was incubated with 30 µCi ^{32}P-γATP and 10 U T4 polynucleotide kinase (Roche) and its corresponding buffer in a total volume of 15 µl for 1 h at 37°C followed by enzyme inactivation at 65°C for 20 min. The probe was diluted to 50 µl and purified using a MicroSpin G-50 column (GE Healthcare).

4.9.5 Pulse-chase labeling of RNA

For radioactive labeling of newly synthesized rRNA in HeLa cells, a protocol based on (Pestov et al., 2008) was used.

HeLa cells treated with siRNAs were grown in 6-wells (see 4.4.6) for 72 h and incubated in phosphate-free DMEM (Invitrogen) with 10% FBS for 1 h at 37°C. The medium was exchanged for 900 µl phosphate-free DMEM containing ^{33}P-phosphoroc acid (20 µCi/ml) and cells were incubated for 1 h at 37°C. The cells were briefly washed in DMEM +/+ and 1 ml DMEM +/+ was added per well for different chase periods (0/30/60/120/240 min) before harvesting. Cells were washed in 500 µl PBS, detached with 500 µl PBS/0.5 mM EDTA and centrifuged (3500 rpm, 5 min, RT). Cell pellets were kept at 4°C until all samples of all time points were collected. The RNA was isolated from cells using the Qiagen RNeasy mini kit according to the manufacturer's protocol. RNA samples were mixed with RNA formaldehyde loading buffer (1x final concentration), incubated at 95°C for 5 min and Agarose-formaldehyde gel electrophoresis (see 4.9.2) was performed. The gel was vacuum dried for 75 min at 50°C and exposed on a Phosphoimager screen for 24 h.

5. Appendix

5.1 C21orf70 possesses a bipartite NLS

The localization of proteins to the nucleus after translation in the cytoplasm occurs by two mechanisms: proteins smaller than approximately 50 kDa can diffuse freely through nuclear pore complexes (NPCs). Larger proteins need to be actively imported by binding to nuclear import receptors via their nuclear localization signal (NLS), a stretch of basic amino acids (different NLS consensus sequences are reviewed in (Xu et al., 2010). Also, small proteins that need to quickly and efficiently translocate into the nucleus, such as ribosomal proteins and histones, contain an NLS and are actively imported.

To test whether C21orf70 possesses an NLS for active import, we transiently transfected HeLa cells with N-terminal truncations of C21orf70 fused to GST-GFP. Endogenous C21orf70 has a molecular weight of 25 kDa and would thus be able to freely enter the nucleus by diffusion; the molecular weight of C21orf70-GST-GFP equals approximately 75 kDa, which is larger than the threshold for diffusion through the NPC allowing us to investigate whether a potential NLS in C21orf70 leads to import of the GST-GFP fusion. Furthermore, GST-GFP dimerizes (Walker et al., 1993), further increasing the size and mass of the molecule to be transported across the NPC. GST-GFP alone was localized to the cytoplasm, whereas C21orf70-GST-GFP was nuclear and strongly enriched in nucleoli (Fig. 5.1A), which speaks for active import via an import receptor. Furthermore, when the first ten amino acids of C21orf70 were deleted (C21orf70(11-230)-GST-GFP), import into the nucleus became less efficient, as observed by an increased cytoplasmic GFP signal (Fig. 5.1A). The localization was similar when the first 99 amino acids of C21orf70 were deleted (C21orf70(100-230)-GST-GFP in Fig. 5.1A). However, the import defect was exacerbated when amino acids 100-113 of C21orf70 are additionally deleted (C21orf70(113-230)-GST-GFP in Fig. 5.1A). Both of these amino acid stretches, which appear to contribute to import of C21orf70, are rich in the basic amino acids Lysine (K) and Arginine (R) (Fig. 5.1C). This suggests that C21orf70 possesses a composite NLS for active import into the nucleus.

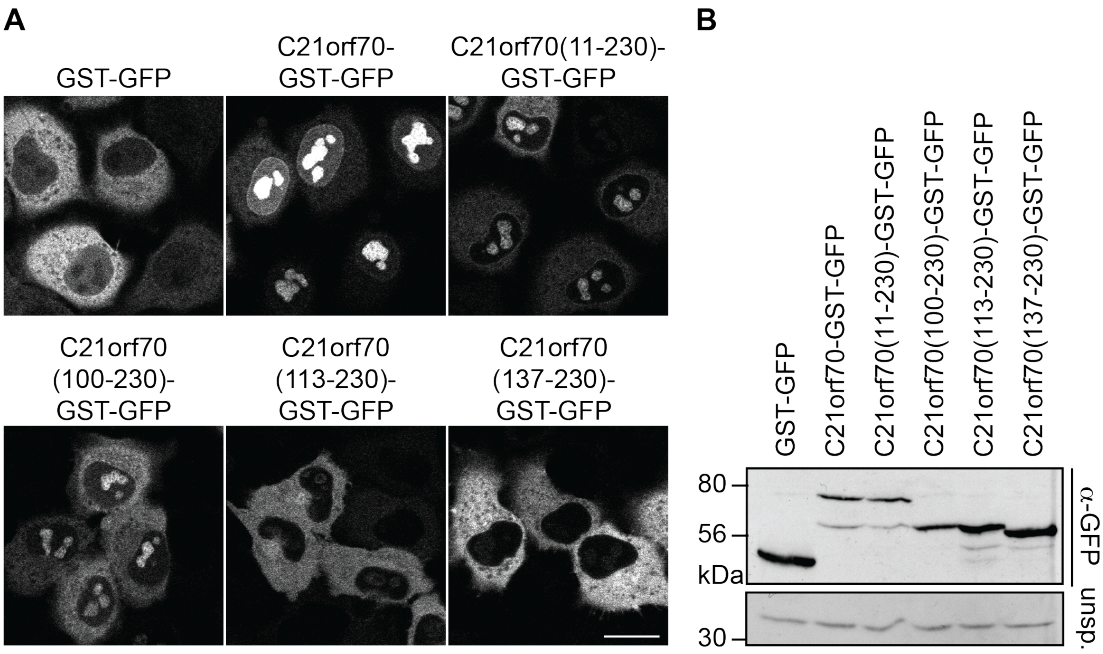

C

```
1   MGKVRGLRARVHQAAVRPKGEAAPGPAPPAPEATPPPASAAGKDWAFINT
51  NIFARTKIDPSALVQKLELDVRSVTSVRRGEAGSSARSVPSIRRGAEAKT
101 VLPKKEKMKLRREQWLQKIEAIKLAEQKHREERRRRATVVVGDLHPLRDA
151 LPELLGLEAGSRRQARSRESNKPRPSELSRMSAAQRQQLLEEERTRFQEL
201 LASPAYRASPLVAIGQTLARQMQLEDGGQL
```

Figure 5.1
Two regions in C21orf70 contribute to its nuclear localization
(A) HeLa cells were transiently transfected with C21orf70-GST-GFP fusion constructs. The numbers of the N-terminal truncation constructs indicate which amino acids of the full-length protein are contained. Scale bar, 20 µm.
(B) Western blotting of (A) was performed with an antibody against GFP to ensure comparable expression levels and correct construct length. An unspecific band (unsp.) served as a loading control.
(C) Amino acid sequence of C21orf70. The two regions that contribute to its nuclear localization based on (A) (amino acids 1-10, 101-113) are marked in green.

5.2 C21orf70 directly binds CRM1 *in vitro*

Depletion of C21orf70 in HeLa cells leads to nucleoplasmic accumulation of 40S trans-acting factors as well as of an RPS2-YFP reporter, similar to the phenotype observed upon CRM1 knockdown, albeit less severe (Wyler et al., 2011). Interestingly, RNAi against CRM1 leads to a moderate but highly reproducible increase in C21orf70 protein levels (Fig. 5.2). Notably, there are two bands observed upon immunoblotting against C21orf70, since it is expressed in two isoforms that differ in length by 15 amino acids. Upon CRM1 depletion, the levels of both isoforms are increased, which could indicate a functional interaction between CRM1 and C21orf70.

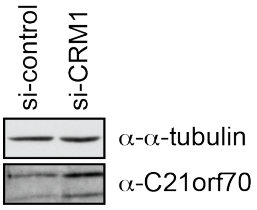

Figure 5.2
C21orf70 protein levels are increased upon CRM1 depletion
HeLa cells were treated with the indicated siRNAs for 48 h, harvested and analyzed by Western blotting using the indicated antibodies.

Export of human 60S as well as 40S preribosomal subunits is dependent on the exportin CRM1 (see 1.2.4). For 40S subunits, the adaptor protein(s) mediating CRM1 binding have been unknown so far, although there are several candidates that possess a nuclear export signal (NES) and associate with pre-40S: RIOK2 (Zemp et al., 2009), PNO1, LTV1 (Dissertation Thomas Wild, ETH Zurich), and NOB1 (data not shown). However, depletion of these proteins mostly leads to inhibition of late cytoplasmic 40S maturation steps although some export defect can be observed for an RPS2-YFP reporter upon RIOK2 or NOB1 depletion (Zemp et al., 2009 and data not shown). It is likely that more than one 40S trans-acting factor contributes to 40S export.

To further examine the possibility of C21orf70 serving as an adaptor protein for pre-40S export and to investigate whether C21orf70 and CRM1 are able to interact directly, we performed *in vitro* CRM1 binding assays with zz-C21orf70 fusion proteins of either full-length C21orf70 or its N- or C-terminal half (amino acids 1-141 or 142-230, respectively) recombinantly expressed and purified from *E. coli*. These proteins were immobilized on IgG beads and incubated with CRM1 with or without RanQ69L-GTP, a GTP hydrolysis deficient mutant of Ran. Full-length as well as both halves of C21orf70 are able to directly bind CRM1 in a Ran-GTP dependent manner (Fig. 5.3A, left panel). This implies that two NESs in C21orf70 contribute to CRM1 binding. Two point mutations in the putative NES in the N-terminal half of C21orf70 (L67A, L69A) abolish CRM1 binding (Fig. 5.3A, right panel).

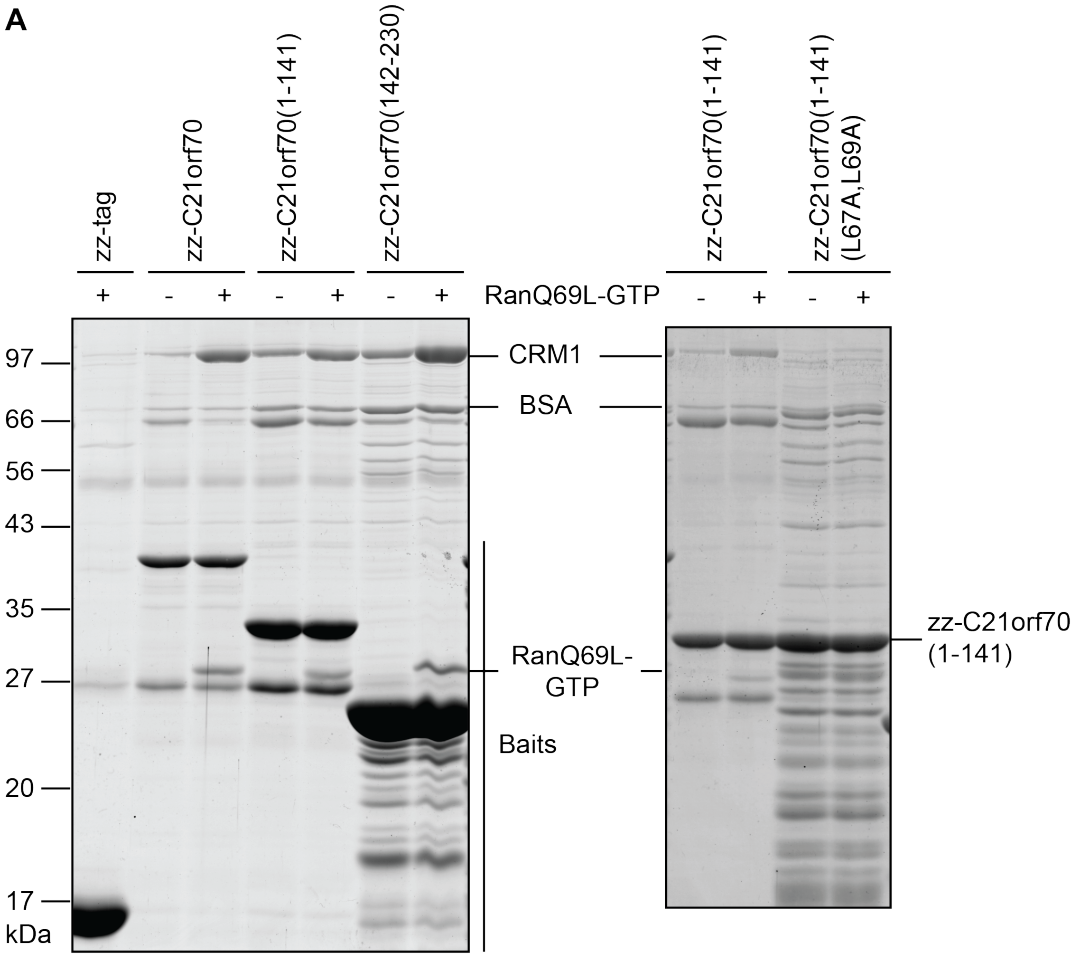

B

1 MGKVRGLRARVHQAAVRPKGEAAPGPAPPAPEATPPPASAAGKDWAFINT
51 NIFARTKIDPSALVQKLELDVRSVTSVRRGEAGSSARSVPSIRRGAEAKT
101 VLPKKEKMKLRREQWLQKIEAIKLAEQKHREERRRRATVVVGDLHPLRDA
151 LPELLGLEAGSRRQARSRESNKPRPSELSRMSAAQRQQLLEEERTRFQEL
201 LASPAYRASPLVAIGQTLARQMQLEDGGQL

Figure 5.3
C21orf70 is able to directly bind CRM1 *in vitro*
(A) Different zz-C21orf70 constructs were expressed in and purified from *E. coli*, immobilized on IgG beads and incubated with CRM1 in the presence or absence of RanQ69L-GTP. The zz-tag alone was used as a negative control. Eluted proteins were analyzed by SDS-PAGE followed by Coomassie staining. The full-length protein as well as the N- and C-terminal part of C21orf70 are able to bind CRM1 (left panel). The binding ability of C21orf70(1-141) to CRM1 is abolished when the residues L67 and L69 are mutated to A (right panel).
(B) Amino acid sequence of C21orf70. The identified NES is marked in green and mutated residues from (A) are marked in red.

For the C-terminal half, around amino acid 150, there is a hydrophobic patch, which is typical for a NES (la Cour et al., 2004) (Fig. 5.4B). Surprisingly, when four leucines in this region were mutated to alanine (L144A, L147A, L155A, L157A), the fragment was still able to bind CRM1 *in vitro* (Fig. 5.4A). Moreover, a fragment of amino acids 158-230 of C21orf70 also bound CRM1

(Fig. 5.4A). Thus, the NES in the C terminus of C21orf70 remains to be identified.

A

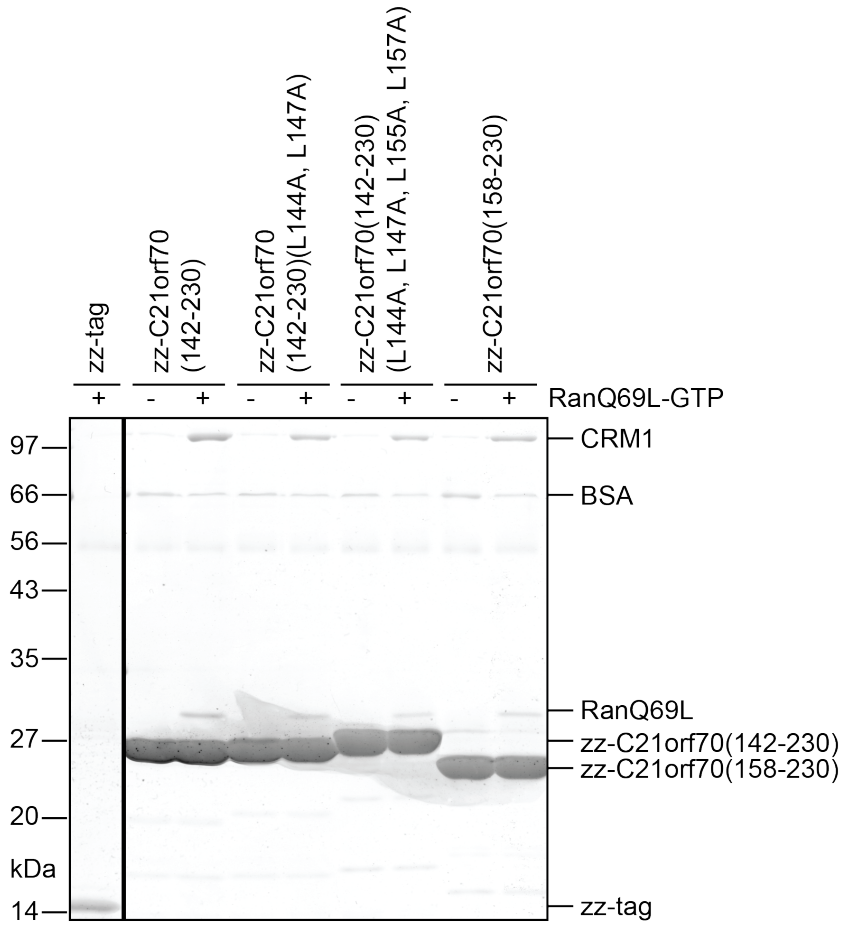

B

142 GDLHPLRDA
151 LPELLGLEAGSRRQARSRESNKPRPSELSRMSAAQRQQLLEEERTRFQEL
201 LASPAYRASPLVAIGQTLARQMQLEDGGQL

Figure 5.4
The C-terminal half of C21orf70 binds CRM1 *in vitro*
(A) Different zz-C21orf70(142-230) mutants were expressed in and purified from *E. coli*, immobilized on IgG beads and incubated with CRM1 in the presence or absence of RanQ69L-GTP. The zz-tag alone was used as a negative control. Eluted proteins were analyzed by SDS-PAGE followed by Coomassie staining. All C21orf70 constructs were still able to bind CRM1 *in vitro*. Vertical line separates lanes from the same gel.
(B) Amino acid sequence of C21orf70(142-230), the mutated residues from (A) are marked in red.

6. References

Ahmad, Y., F.-M. Boisvert, P. Gregor, A. Cobley, and A.I. Lamond. 2009. NOPdb: Nucleolar Proteome Database--2008 update. *Nucleic acids research*. 37:D181-184.

Allen, C., A. Kurimasa, M.A. Brenneman, D.J. Chen, and J.A. Nickoloff. 2002. DNA-dependent protein kinase suppresses double-strand break-induced and spontaneous homologous recombination. *Proceedings of the National Academy of Sciences of the United States of America*. 99:3758-3763.

Altvater, M., Y. Chang, A. Melnik, L. Occhipinti, S. Schütz, U. Rothenbusch, P. Picotti, and V.G. Panse. 2012. Targeted proteomics reveals compositional dynamics of 60S pre-ribosomes after nuclear export. *Molecular systems biology*. 8:628.

Amsterdam, A., K.C. Sadler, K. Lai, S. Farrington, R.T. Bronson, J.A. Lees, and N. Hopkins. 2004. Many ribosomal protein genes are cancer genes in zebrafish. *PLoS biology*. 2:E139.

Andersen, J.S., Y.W. Lam, A.K.L. Leung, S.-E. Ong, C.E. Lyon, A.I. Lamond, and M. Mann. 2005. Nucleolar proteome dynamics. *Nature*. 433:77-83.

Anger, A.M., J.-P. Armache, O. Berninghausen, M. Habeck, M. Subklewe, D.N. Wilson, and R. Beckmann. 2013. Structures of the human and Drosophila 80S ribosome. *Nature*. 497:80-85.

Arabi, A., S. Wu, K. Ridderstråle, H. Bierhoff, C. Shiue, K. Fatyol, S. Fahlén, P. Hydbring, O. Söderberg, I. Grummt, L.-G. Larsson, and A.P.H. Wright. 2005. c-Myc associates with ribosomal DNA and activates RNA polymerase I transcription. *Nature cell biology*. 7:303-310.

Badura, L., T. Swanson, W. Adamowicz, J. Adams, J. Cianfrogna, K. Fisher, J. Holland, R. Kleiman, F. Nelson, L. Reynolds, K. St Germain, E. Schaeffer, B. Tate, and J. Sprouse. 2007. An inhibitor of casein kinase I epsilon induces phase delays in circadian rhythms under free-running and entrained conditions. *The Journal of pharmacology and experimental therapeutics*. 322:730-738.

Bain, J., L. Plater, M. Elliott, N. Shpiro, C.J. Hastie, H. McLauchlan, I. Klevernic, J.S.C. Arthur, D.R. Alessi, and P. Cohen. 2007. The selectivity of protein kinase inhibitors: a further update. *The Biochemical journal*. 408:297-315.

Barak, Y., T. Juven, R. Haffner, and M. Oren. 1993. mdm2 expression is induced by wild type p53 activity. *The EMBO journal*. 12:461-468.

Barraud, P., B.S.E. Heale, M.A. O'Connell, and F.H.-T. Allain. 2012. Solution structure of the N-terminal dsRBD of Drosophila ADAR and interaction studies with RNA. *Biochimie*. 94:1499-1509.

Bassler, J., P. Grandi, O. Gadal, T. Lessmann, E. Petfalski, D. Tollervey, J. Lechner, and E. Hurt. 2001. Identification of a 60S preribosomal particle that is closely linked to nuclear export. *Molecular cell*. 8:517-529.

Bassler, J., I. Klein, C. Schmidt, M. Kallas, E. Thomson, M.A. Wagner, B. Bradatsch, G. Rechberger, H. Strohmaier, E. Hurt, and H. Bergler. 2012. The conserved Bud20 zinc finger protein is a new component of the ribosomal 60S subunit export machinery. *Molecular and cellular biology*. 32:4898-4912.

Basu, U., K. Si, J.R. Warner, and U. Maitra. 2001. The Saccharomyces cerevisiae TIF6 gene encoding translation initiation factor 6 is required for 60S ribosomal subunit biogenesis. *Molecular and cellular biology*. 21:1453-1462.

Baumas, K., J. Soudet, M. Caizergues-Ferrer, M. Faubladier, Y. Henry, and A. Mougin. 2012. Human RioK3 is a novel component of cytoplasmic pre-40S pre-ribosomal particles. *RNA biology*. 9:162-174.

Bax, R., H.A. Raué, and J.C. Vos. 2006. Slx9p facilitates efficient ITS1 processing of pre-rRNA in Saccharomyces cerevisiae. *RNA (New York, NY)*. 12:2005-2013.

Bécam, A.M., F. Nasr, W.J. Racki, M. Zagulski, and C.J. Herbert. 2001. Ria1p (Ynl163c), a protein similar to elongation factors 2, is involved in the biogenesis of the 60S subunit of the ribosome in Saccharomyces cerevisiae. *Molecular genetics and genomics : MGG*. 266:454-462.

Belin, S., A. Beghin, E. Solano-Gonzàlez, L. Bezin, S. Brunet-Manquat, J. Textoris, A.-C. Prats, H.C. Mertani, C. Dumontet, and J.-J. Diaz. 2009. Dysregulation of ribosome biogenesis and translational capacity is associated with tumor progression of human breast cancer cells. *PloS one*. 4:e7147.

Bell, S.P., R.M. Learned, H.M. Jantzen, and R. Tjian. 1988. Functional cooperativity between transcription factors UBF1 and SL1 mediates human ribosomal RNA synthesis. *Science*. 241:1192-1197.

Bellodi, C., N. Kopmar, and D. Ruggero. 2010a. Deregulation of oncogene-induced senescence and p53 translational control in X-linked dyskeratosis congenita. *The EMBO journal*. 29:1865-1876.

Bellodi, C., O. Krasnykh, N. Haynes, M. Theodoropoulou, G. Peng, L. Montanaro, and D. Ruggero. 2010b. Loss of function of the tumor suppressor DKC1 perturbs p27 translation control and contributes to pituitary tumorigenesis. *Cancer research*. 70:6026-6035.

Ben-Shem, A., N. Garreau de Loubresse, S. Melnikov, L. Jenner, G. Yusupova, and M. Yusupov. 2011. The structure of the eukaryotic ribosome at 3.0 Å resolution. *Science*. 334:1524-1529.

Bernad, R., D. Engelsma, H. Sanderson, H. Pickersgill, and M. Fornerod. 2006. Nup214-Nup88 nucleoporin subcomplex is required for CRM1-mediated 60 S preribosomal nuclear export. *The Journal of biological chemistry*. 281:19378-19386.

Bernstein, K.A., F. Bleichert, J.M. Bean, F.R. Cross, and S.J. Baserga. 2007. Ribosome biogenesis is sensed at the Start cell cycle checkpoint. *Molecular biology of the cell*. 18:953-964.

Bernstein, K.A., J.E.G. Gallagher, B.M. Mitchell, S. Granneman, and S.J. Baserga. 2004. The small-subunit processome is a ribosome assembly intermediate. *Eukaryotic cell*. 3:1619-1626.

Betat, H., C. Rammelt, and M. Mörl. 2010. tRNA nucleotidyltransferases: ancient catalysts with an unusual mechanism of polymerization. *Cellular and molecular life sciences : CMLS*. 67:1447-1463.

Bilanges, B., and D. Stokoe. 2007. Mechanisms of translational deregulation in human tumors and therapeutic intervention strategies. *Oncogene*. 26:5973-5990.

Biswas, A., S. Mukherjee, S. Das, D. Shields, C.W. Chow, and U. Maitra. 2011. Opposing action of casein kinase 1 and calcineurin in nucleo-cytoplasmic shuttling of mammalian translation initiation factor eIF6. *The Journal of biological chemistry*. 286:3129-3138.

Bodem, J., G. Dobreva, U. Hoffmann-Rohrer, S. Iben, H. Zentgraf, H. Delius, M. Vingron, and I. Grummt. 2000. TIF-IA, the factor mediating growth-dependent control of ribosomal RNA synthesis, is the mammalian homolog of yeast Rrn3p. *EMBO reports*. 1:171-175.

Boisvert, F.M., S. van Koningsbruggen, Navascués J, and L. AI. 2007. The multifunctional nucleolus. *Nat Rev Mol Cell Biol.* 8:574-585.

Boocock, G.R.B., J.A. Morrison, M. Popovic, N. Richards, L. Ellis, P.R. Durie, and J.M. Rommens. 2003. Mutations in SBDS are associated with Shwachman-Diamond syndrome. *Nature genetics*. 33:97-101.

Boria, I., E. Garelli, H.T. Gazda, A. Aspesi, P. Quarello, E. Pavesi, D. Ferrante, J.J. Meerpohl, M. Kartal, L. Da Costa, A. Proust, T. Leblanc, M. Simansour, N. Dahl, A.-S. Fröjmark, D. Pospisilova, R. Cmejla, A.H. Beggs, M.R. Sheen, M. Landowski, C.M. Buros, C.M. Clinton, L.J. Dobson, A. Vlachos, E. Atsidaftos, J.M. Lipton, S.R. Ellis, U. Ramenghi, and I. Dianzani. 2010. The ribosomal basis of Diamond-Blackfan Anemia: mutation and database update. *Human mutation*. 31:1269-1279.

Bradatsch, B., J. Katahira, E. Kowalinski, G. Bange, W. Yao, T. Sekimoto, V. Baumgärtel, G. Boese, J. Bassler, K. Wild, R. Peters, Y. Yoneda, I. Sinning, and E. Hurt. 2007. Arx1 functions as an unorthodox nuclear export receptor for the 60S preribosomal subunit. *Molecular cell*. 27:767-779.

Bradatsch, B., C. Leidig, S. Granneman, M. Gnädig, D. Tollervey, B. Böttcher, R. Beckmann, and E. Hurt. 2012. Structure of the pre-60S ribosomal subunit with nuclear export factor Arx1 bound at the exit tunnel. *Nature structural & molecular biology*. 19:1234-1241.

Brand, R.C., J. Klootwijk, T.J. Van Steenbergen, A.J. De Kok, and R.J. Planta. 1977. Secondary methylation of yeast ribosomal precursor RNA. *European journal of biochemistry / FEBS*. 75:311-318.

Brangwynne, C.P., T.J. Mitchison, and A.A. Hyman. 2011. Active liquid-like behavior of nucleoli determines their size and shape in Xenopus laevis oocytes. *Proceedings of the National Academy of Sciences of the United States of America*. 108:4334-4339.

Bratulic, M., Z. GrabareviC, B. ArtukoviC, and D. Capak. 1996. Number of Nucleoli and Nucleolar Organizer Regions per Nucleus and Nucleolus -- Prognostic Value in Canine Mammary Tumors. *Veterinary Pathology*. 33:527-532.

Brownawell, A.M., and I.G. Macara. 2002. Exportin-5, a novel karyopherin, mediates nuclear export of double-stranded RNA binding proteins. *The Journal of cell biology*. 156:53-64.

Bryja, V., G. Schulte, and E. Arenas. 2007. Wnt-3a utilizes a novel low dose and rapid pathway that does not require casein kinase 1-mediated phosphorylation of Dvl to activate beta-catenin. *Cellular signalling*. 19:610-616.

Bycroft, M., S. Grünert, A.G. Murzin, M. Proctor, and D. St Johnston. 1995. NMR solution structure of a dsRNA binding domain from Drosophila staufen protein reveals homology to the N-terminal domain of ribosomal protein S5. *The EMBO journal*. 14:3563-3571.

Calado, A., N. Treichel, E. Müller, A. Otto, and U. Kutay. 2002. Exportin-5-mediated nuclear export of eukaryotic elongation factor 1A and tRNA. *EMBO J*. 21:6216-6224.

Carron, C., M.-F. O'Donohue, V. Choesmel, M. Faubladier, and P.-E. Gleizes. 2011. Analysis of two human pre-ribosomal factors, bystin and hTsr1, highlights differences in evolution of ribosome biogenesis between yeast and mammals. *Nucleic acids research*. 39:280-291.

Cavaillé, J., M. Nicoloso, and J.-P. Bachellerie. 1996. Targeted ribose methylation of RNA in vivo directed by tailored antisense RNA guides. *Nature*. 383:732-735.

Chakraborty, A., T. Uechi, and N. Kenmochi. 2011. Guarding the 'translation apparatus': defective ribosome biogenesis and the p53 signaling pathway. *Wiley interdisciplinary reviews. RNA*. 2:507-522.

Chan, P.K. 1992. Characterization and cellular localization of nucleophosmin/B23 in HeLa cells treated with selected cytotoxic agents (studies of B23-translocation mechanism). *Experimental cell research*. 203:174-181.

Cheong, J.K., and D.M. Virshup. 2011. Casein kinase 1: complexity in the family. *The international journal of biochemistry & cell*

Colombo, E., M. Alcalay, and P.G. Pelicci. 2011. Nucleophosmin and its complex network: a possible therapeutic target in hematological diseases. *Oncogene*. 30:2595-2609.

Conconi, A., R.M. Widmer, T. Koller, and J.M. Sogo. 1989. Two different chromatin structures coexist in ribosomal RNA genes throughout the cell cycle. *Cell*. 57:753-761.

Conti, E., and E. Izaurralde. 2001. Nucleocytoplasmic transport enters the atomic age. *Current opinion in cell biology*. 13:310-319.

Corthésy, B., and P.N. Kao. 1994. Purification by DNA affinity chromatography of two polypeptides that contact the NF-AT DNA binding site in the interleukin 2 promoter. *The Journal of biological chemistry*. 269:20682-20690.

Cosentino, G.P., S. Venkatesan, F.C. Serluca, S.R. Green, M.B. Mathews, and N. Sonenberg. 1995. Double-stranded-RNA-dependent protein kinase and TAR RNA-binding protein form homo- and heterodimers in vivo. *Proceedings of the National Academy of Sciences of the United States of America*. 92:9445-9449.

Dabo, S., and E.F. Meurs. 2012. dsRNA-dependent protein kinase PKR and its role in stress, signaling and HCV infection. *Viruses*. 4:2598-2635.

Dai, M.-S., R. Sears, and H. Lu. 2007. Feedback regulation of c-Myc by ribosomal protein L11. *Cell cycle (Georgetown, Tex)*. 6:2735-2741.

Dai, M.-S., X.-X. Sun, and H. Lu. 2008. Aberrant expression of nucleostemin activates p53 and induces cell cycle arrest via inhibition of MDM2. *Molecular and cellular biology*. 28:4365-4376.

Dai, M.-S., X.-X. Sun, and H. Lu. 2010. Ribosomal protein L11 associates with c-Myc at 5 S rRNA and tRNA genes and regulates their expression. *The Journal of biological chemistry*. 285:12587-12594.

Dai, M.-S., S.X. Zeng, Y. Jin, X.-X. Sun, L. David, and H. Lu. 2004. Ribosomal protein L23 activates p53 by inhibiting MDM2 function in response to ribosomal perturbation but not to translation inhibition. *Molecular and cellular biology*. 24:7654-7668.

Decatur, W.A., and M.J. Fournier. 2002. rRNA modifications and ribosome function. *Trends in biochemical sciences*. 27:344-351.

Decatur, W.A., X.h. Liang, D. Piekna Przybylska, and M.J. Fournier. 2007. Identifying Effects of snoRNA–Guided Modifications on the Synthesis and Function of the Yeast Ribosome. Vol. 425. Elsevier. 283-316.

Demoinet, E., A. Jacquier, G. Lutfalla, and M. Fromont-Racine. 2007. The Hsp40 chaperone Jjj1 is required for the nucleo-cytoplasmic recycling of preribosomal factors in Saccharomyces cerevisiae. *RNA (New York, NY)*. 13:1570-1581.

Derenzini, M., D. Trerè, A. Pession, M. Govoni, V. Sirri, and P. Chieco. 2000. Nucleolar size indicates the rapidity of cell proliferation in cancer tissues. *The Journal of pathology*. 191:181-186.

Dieci, G., M. Preti, and B. Montanini. 2009. Eukaryotic snoRNAs: a paradigm for gene expression flexibility. *Genomics*. 94:83-88.

Donati, G., L. Montanaro, and M. Derenzini. 2012. Ribosome biogenesis and control of cell proliferation: p53 is not alone. *Cancer research*. 72:1602-1607.

Donati, G., S. Peddigari, C.A. Mercer, and G. Thomas. 2013. 5S ribosomal RNA is an essential component of a nascent ribosomal precursor complex that regulates the Hdm2-p53 checkpoint. *Cell reports*. 4:87-98.

Doyle, M., L. Badertscher, L. Jaskiewicz, S. Güttinger, S. Jurado, T. Hugenschmidt, U. Kutay, and W. Filipowicz. 2013. The double-stranded RNA binding domain of human Dicer functions as a nuclear localization signal. *RNA (New York, NY)*. 19:1238-1252.

Dragon, F., J.E.G. Gallagher, P.A. Compagnone-Post, B.M. Mitchell, K.A. Porwancher, K.A. Wehner, S. Wormsley, R.E. Settlage, J. Shabanowitz, Y. Osheim, A.L. Beyer, D.F. Hunt, and S.J. Baserga. 2002. A large nucleolar U3 ribonucleoprotein required for 18S ribosomal RNA biogenesis. *Nature*. 417:967-970.

Drygin, D., W.G. Rice, and I. Grummt. 2010. The RNA polymerase I transcription machinery: an emerging target for the treatment of cancer. *Annual review of pharmacology and toxicology*. 50:131-156.

Dubben, H.H. 1990. Different nucleolar antigen expression in resting and proliferating human lymphocytes as studied by fluorescence microscopy and flow cytometry. *Cell and tissue kinetics*. 23:89-97.

Duchange, N., J. Pidoux, E. Camus, and D. Sauvaget. 2000. Alternative splicing in the human interleukin enhancer binding factor 3 (ILF3) gene. *Gene*. 261:345-353.

Eckmann, C.R., A. Neunteufl, L. Pfaffstetter, and M.F. Jantsch. 2001. The human but not the Xenopus RNA-editing enzyme ADAR1 has an atypical nuclear localization signal and displays the characteristics of a shuttling protein. *Molecular biology of the cell*. 12:1911-1924.

Ellis, S.R., and P.-E. Gleizes. 2011. Diamond Blackfan anemia: ribosomal proteins going rogue. *Seminars in hematology*. 48:89-96.

Emmott, E., and J.A. Hiscox. 2009. Search Results | EMBOr. *EMBO reports*.

Etchegaray, J.-P., K.K. Machida, E. Noton, C.M. Constance, R. Dallmann, M.N. Di Napoli, J.P. DeBruyne, C.M. Lambert, E.A. Yu, S.M. Reppert, and D.R. Weaver. 2009. Casein kinase 1 delta regulates the pace of the mammalian circadian clock. *Molecular and cellular biology*. 29:3853-3866.

Fatica, A., A.D. Cronshaw, M. Dlakić, and D. Tollervey. 2002. Ssf1p prevents premature processing of an early pre-60S ribosomal particle. *Molecular cell*. 9:341-351.

Fatica, A., M. Oeffinger, M. Dlakić, and D. Tollervey. 2003. Nob1p is required for cleavage of the 3' end of 18S rRNA. *Molecular and cellular biology*. 23:1798-1807.

Fatica, A., D. Tollervey, and M. Dlakić. 2004. PIN domain of Nob1p is required for D-site cleavage in 20S pre-rRNA. *RNA (New York, NY)*. 10:1698-1701.

Faza, M.B., Y. Chang, L. Occhipinti, S. Kemmler, and V.G. Panse. 2012. Role of Mex67-Mtr2 in the nuclear export of 40S pre-ribosomes. *PLoS genetics*. 8:e1002915.

Felton-Edkins, Z.A., N.S. Kenneth, T.R.P. Brown, N.L. Daly, N. Gomez-Roman, C. Grandori, R.N. Eisenman, and R.J. White. 2003. Direct regulation of RNA polymerase III transcription by RB, p53 and c-Myc. *Cell cycle (Georgetown, Tex)*. 2:181-184.

Fierro-Monti, I., and M.B. Mathews. 2000. Proteins binding to duplexed RNA: one motif, multiple functions. *Trends in biochemical sciences*. 25:241-246.

Fish, K.J., A. Cegielska, M.E. Getman, G.M. Landes, and D.M. Virshup. 1995. Isolation and characterization of human casein kinase I epsilon (CKI), a novel member of the CKI gene family. *The Journal of biological chemistry*. 270:14875-14883.

Flørenes, V.A., G.M. Maelandsmo, A. Forus, A. Andreassen, O. Myklebost, and O. Fodstad. 1994. MDM2 gene amplification and transcript levels in human sarcomas: relationship to TP53 gene status. *Journal of the National Cancer Institute*. 86:1297-1302.

Flotow, H., P.R. Graves, A.Q. Wang, C.J. Fiol, R.W. Roeske, and P.J. Roach. 1990. Phosphate groups as substrate determinants for casein kinase I action. *The Journal of biological chemistry*. 265:14264-14269.

Fribourg, S., and E. Conti. 2003. Structural similarity in the absence of sequence homology of the messenger RNA export factors Mtr2 and p15. *EMBO reports*. 4:699-703.

Fromont-Racine, M., B. Senger, C. Saveanu, and F. Fasiolo. 2003. Ribosome assembly in eukaryotes. *Gene*. 313:17-42.

Fujiyama, S., M. Yanagida, T. Hayano, Y. Miura, T. Isobe, F. Fujimori, T. Uchida, and N. Takahashi. 2002. Isolation and proteomic characterization of human Parvulin-associating preribosomal ribonucleoprotein complexes. *The Journal of biological chemistry*. 277:23773-23780.

Fumagalli, S., A. Di Cara, A. Neb-Gulati, F. Natt, S. Schwemberger, J. Hall, G.F. Babcock, R. Bernardi, P.P. Pandolfi, and G. Thomas. 2009. Absence of nucleolar disruption after impairment of 40S ribosome biogenesis reveals an rpL11-translation-dependent mechanism of p53 induction. *Nature cell biology*. 11:501-508.

Gadal, O., D. Strauss, J. Kessl, and B. Trumpower. 2001. Nuclear export of 60s ribosomal subunits depends on Xpo1p and requires a nuclear export sequence-containing factor, Nmd3p, that associates with the large subunit *Mol Cell Biol* 21(10):3405-15

Galani, K., T.A. Nissan, E. Petfalski, D. Tollervey, and E. Hurt. 2004. Rea1, a dynein-related nuclear AAA-ATPase, is involved in late rRNA processing and nuclear export of 60 S subunits. *The Journal of biological chemistry*. 279:55411-55418.

Gallagher, J.E.G., D.A. Dunbar, S. Granneman, B.M. Mitchell, Y. Osheim, A.L. Beyer, and S.J. Baserga. 2004. RNA polymerase I transcription and pre-rRNA processing are linked by specific SSU processome components. *Genes & development*. 18:2506-2517.

Ganot, P., M.L. Bortolin, and T. Kiss. 1997. Site-Specific Pseudouridine Formation in Preribosomal RNA Is Guided by Small Nucleolar RNAs. *Cell*. 89(5):799-809

Gao, H., M.J. Ayub, M.J. Levin, and J. Frank. 2005. The structure of the 80S ribosome from Trypanosoma cruzi reveals unique rRNA components. *Proceedings of the National Academy of Sciences of the United States of America*. 102:10206-10211.

Gartmann, M., M. Blau, J.-P. Armache, T. Mielke, M. Topf, and R. Beckmann. 2010. Mechanism of eIF6-mediated inhibition of ribosomal subunit joining. *The Journal of biological chemistry*. 285:14848-14851.

Geerlings, T.H., A.W. Faber, M.D. Bister, J.C. Vos, and H.A. Raué. 2003. Rio2p, an evolutionarily conserved, low abundant protein kinase essential for processing of 20 S Pre-rRNA in Saccharomyces cerevisiae. *The Journal of biological chemistry*. 278:22537-22545.

Giffin, W., H. Torrance, D.J. Rodda, G.G. Préfontaine, L. Pope, and R.J. Hache. 1996. Sequence-specific DNA binding by Ku autoantigen and its effects on transcription. *Nature*. 380:265-268.

Gleizes, P.E., J. Noaillac-Depeyre, I. Léger-Silvestre, F. Teulières, J.Y. Dauxois, D. Pommet, M.C. Azum-Gelade, and N. Gas. 2001. Ultrastructural localization of rRNA shows defective nuclear export of preribosomes in mutants of the Nup82p complex. *The Journal of cell biology*. 155:923-936.

Goessens, G. 1984. Nucleolar structure. *International review of cytology*. 87:107-158.

Gomez-Roman, N., C. Grandori, R.N. Eisenman, and R.J. White. 2003. Direct activation of RNA polymerase III transcription by c-Myc. *Nature*. 421:290-294.

Gomila, R.C., I. Martin, Glover W, and L. Gehrke. 2011. NF90 Binds the Dengue Virus RNA 3′ Terminus and Is a Positive Regulator of Dengue Virus Replication. *PloS one*. 6:e16687.

Gonzalez, I.L., and J.E. Sylvester. 1995. Complete sequence of the 43-kb human ribosomal DNA repeat: analysis of the intergenic spacer. *Genomics*. 27:320-328.

Görlich, D., and U. Kutay. 1999. Transport between the cell nucleus and the cytoplasm. *Annual review of cell and developmental biology*. 15:607-660.

Grandi, P., V. Rybin, J. Bassler, E. Petfalski, D. Strauss, M. Marzioch, T. Schäfer, B. Kuster, H. Tschochner, D. Tollervey, A.C. Gavin, and E. Hurt. 2002. 90S pre-ribosomes include the 35S pre-rRNA, the U3 snoRNP, and 40S subunit processing factors but predominantly lack 60S synthesis factors. *Molecular cell*. 10:105-115.

Grandori, C., N. Gomez-Roman, Z.A. Felton-Edkins, C. Ngouenet, D.A. Galloway, R.N. Eisenman, and R.J. White. 2005. c-Myc binds to human ribosomal DNA and

stimulates transcription of rRNA genes by RNA polymerase I. *Nature cell biology*. 7:311-318.

Granneman, S., J. Vogelzangs, R. Lührmann, W.J. van Venrooij, G.J.M. Pruijn, and N.J. Watkins. 2004. Role of pre-rRNA base pairing and 80S complex formation in subnucleolar localization of the U3 snoRNP. *Molecular and cellular biology*. 24:8600-8610.

Greber, B.J., D. Boehringer, A. Leitner, P. Bieri, F. Voigts-Hoffmann, J.P. Erzberger, M. Leibundgut, R. Aebersold, and N. Ban. 2014. Architecture of the large subunit of the mammalian mitochondrial ribosome. *Nature*. 505:515-519.

Greber, B.J., D. Boehringer, C. Montellese, and N. Ban. 2012. Cryo-EM structures of Arx1 and maturation factors Rei1 and Jjj1 bound to the 60S ribosomal subunit. *Nature structural & molecular biology*. 19:1228-1233.

Gross, S.D., and R.A. Anderson. 1998. Casein kinase I: spatial organization and positioning of a multifunctional protein kinase family. *Cellular signalling*. 10:699-711.

Guan, D., N. Altan-Bonnet, A.M. Parrott, C.J. Arrigo, Q. Li, M. Khaleduzzaman, H. Li, C.-G. Lee, T. Peery, and M.B. Mathews. 2008. Nuclear factor 45 (NF45) is a regulatory subunit of complexes with NF90/110 involved in mitotic control. *Molecular and cellular biology*. 28:4629-4641.

Guetg, C., and R. Santoro. 2012. Formation of nuclear heterochromatin: the nucleolar point of view. *Epigenetics : official journal of the DNA Methylation Society*. 7:811-814.

Guo, Y., P. Fu, H. Zhu, E. Reed, S.C. Remick, W. Petros, M.D. Mueller, and J.J. Yu. 2012. Correlations among ERCC1, XPB, UBE2I, EGF, TAL2 and ILF3 revealed by gene signatures of histological subtypes of patients with epithelial ovarian cancer. *Oncology reports*. 27:286-292.

Guschina, E., and B.-J. Benecke. 2008. Specific and non-specific mammalian RNA terminal uridylyl transferases. *Biochimica et biophysica acta*. 1779:281-285.

Gwizdek, C., B. Ossareh-Nazari, A.M. Brownawell, S. Evers, I.G. Macara, and C. Dargemont. 2004. Minihelix-containing RNAs mediate exportin-5-dependent nuclear export of the double-stranded RNA-binding protein ILF3. *The Journal of biological chemistry*. 279:884-891.

Hackmann, A., T. Gross, C. Baierlein, and H. Krebber. 2011. The mRNA export factor Npl3 mediates the nuclear export of large ribosomal subunits. *EMBO reports*. 12:1024-1031.

Hadjiolov, A.A. 1985. The nucleolus and ribosome biogenesis. *Springer-Verlag*.

Hadjiolova, K.V., M. Nicoloso, S. Mazan, A.A. Hadjiolov, and J.P. Bachellerie. 1993. Alternative pre-rRNA processing pathways in human cells and their alteration by cycloheximide inhibition of protein synthesis. *European journal of biochemistry / FEBS*. 212:211-215.

Hannan, K.M., Y. Brandenburger, A. Jenkins, K. Sharkey, A. Cavanaugh, L. Rothblum, T. Moss, G. Poortinga, G.A. McArthur, R.B. Pearson, and R.D. Hannan. 2003. mTOR-dependent regulation of ribosomal gene transcription requires S6K1 and is mediated by phosphorylation of the carboxy-terminal activation domain of the nucleolar transcription factor UBF. *Molecular and cellular biology*. 23:8862-8877.

Harashima, A., T. Guettouche, and G. Barber. 2010. Phosphorylation of the NFAR proteins by the dsRNA-dependent protein kinase PKR constitutes a novel mechanism of translational regulation and cellular defense. *Genes Dev.* 24:2640-2653.

Harnpicharnchai, P., J. Jakovljevic, E. Horsey, T. Miles, J. Roman, M. Rout, D. Meagher, B. Imai, Y. Guo, C.J. Brame, J. Shabanowitz, D.F. Hunt, and J.L. Woolford. 2001. Composition and functional characterization of yeast 66S ribosome assembly intermediates. *Molecular cell*. 8:505-515.

Hayano, T., M. Yanagida, Y. Yamauchi, T. Shinkawa, T. Isobe, and N. Takahashi. 2003. Proteomic analysis of human Nop56p-associated pre-ribosomal ribonucleoprotein complexes. Possible link between Nop56p and the nucleolar protein treacle responsible for Treacher Collins syndrome. *The Journal of biological chemistry*. 278:34309-34319.

Hedges, J., M. West, and A.W. Johnson. 2005. Release of the export adapter, Nmd3p, from the 60S ribosomal subunit requires Rpl10p and the cytoplasmic GTPase Lsg1p. *The EMBO journal*. 24:567-579.

Held, W.A., S. Mizushima, and M. Nomura. 1973. Reconstitution of Escherichia coli 30 S ribosomal subunits from purified molecular components. *The Journal of biological chemistry*. 248:5720-5730.

Henderson, A.S., D. Warburton, and K.C. Atwood. 1972. Location of ribosomal DNA in the human chromosome complement. *Proceedings of the National Academy of Sciences of the United States of America*. 69:3394-3398.

Henras, A.K., J. Soudet, M. Gérus, S. Lebaron, M. Caizergues-Ferrer, A. Mougin, and Y. Henry. 2008. The post-transcriptional steps of eukaryotic ribosome biogenesis. *Cellular and molecular life sciences : CMLS*. 65:2334-2359.

Hernandez-Verdun, D. 1986. Structural organization of the nucleolus in mammalian cells. *Methods and achievements in experimental pathology*. 12:26-62.

Hernandez-Verdun, D. 2006. Nucleolus: from structure to dynamics. *Histochemistry and cell biology*. 125:127-137.

Higuchi, T., S. Sakamoto, Y. Kakinuma, S. Kai, K.-I. Yagyu, H. Todaka, E. Chi, S. Okada, T. Ujihara, K. Morisawa, M. Ono, Y. Sugiyama, W. Ishida, A. Fukushima, M. Tsuda, Y. Agata, and T. Taniguchi. 2012. High expression of nuclear factor 90 (NF90) leads to mitochondrial degradation in skeletal and cardiac muscles. *PloS one*. 7:e43340.

Ho, J., G. Kallstrom, and A.W. Johnson. 2000. Nmd3p is a Crm1p-dependent adapter protein for nuclear export of the large ribosomal subunit. *The Journal of cell biology*.

Hollstein, M., K. Rice, M.S. Greenblatt, T. Soussi, R. Fuchs, T. Sørlie, E. Hovig, B. Smith-Sørensen, R. Montesano, and C.C. Harris. 1994. Database of p53 gene somatic mutations in human tumors and cell lines. *Nucleic acids research*. 22:3551-3555.

Hölzel, M., M. Orban, J. Hochstatter, M. Rohrmoser, T. Harasim, A. Malamoussi, E. Kremmer, G. Längst, and D. Eick. 2010. Defects in 18 S or 28 S rRNA processing activate the p53 pathway. *The Journal of biological chemistry*. 285:6364-6370.

Hölzel, M., M. Rohrmoser, M. Schlee, T. Grimm, T. Harasim, A. Malamoussi, A. Gruber-Eber, E. Kremmer, W. Hiddemann, G.W. Bornkamm, and D. Eick. 2005. Mammalian WDR12 is a novel member of the Pes1-Bop1 complex and is required for ribosome biogenesis and cell proliferation. *The Journal of cell biology*. 170:367-378.

Horn, D., S. Mason, and K. Karbstein. 2011. Rcl1 protein, a novel nuclease for 18 S ribosomal RNA production. *J Biol Chem*. 286:34082-34087.

Horn, H.F., and K.H. Vousden. 2008. Cooperation between the ribosomal proteins L5 and L11 in the p53 pathway. *Oncogene*. 27:5774-5784.

Hu, Q., Y.-Y. Lu, H. Noh, S. Hong, Z. Dong, H.-F. Ding, S.-B. Su, and S. Huang. 2013. Interleukin enhancer-binding factor 3 promotes breast tumor progression by regulating sustained urokinase-type plasminogen activator expression. *Oncogene*. 32:3933-3943.

Hughes, J., and J. Ares, M. 1991. Depletion of U3 small nucleolar RNA inhibits cleavage in the 5'external transcribed spacer of yeast pre-ribosomal RNA and impairs formation of 18S ribosomal RNA. *The EMBO journal*.

Hung, N.-J., K.-Y. Lo, S.S. Patel, K. Helmke, and A.W. Johnson. 2008. Arx1 is a nuclear export receptor for the 60S ribosomal subunit in yeast. *Molecular biology of the cell*. 19:735-744.

Hurt, E., S. Hannus, B. Schmelzl, D. Lau, D. Tollervey, and G. Simos. 1999. A novel in vivo assay reveals inhibition of ribosomal nuclear export in ran-cycle and nucleoporin mutants. *The Journal of cell biology*. 144:389-401.

Iadevaia, V., S. Caldarola, L. Biondini, A. Gismondi, S. Karlsson, I. Dianzani, and F. Loreni. 2010. PIM1 kinase is destabilized by ribosomal stress causing inhibition of cell cycle progression. *Oncogene*. 29:5490-5499.

Isken, O., M. Baroth, C.W. Grassmann, S. Weinlich, D.H. Ostareck, A. Ostareck-Lederer, and S.-E. Behrens. 2007. Nuclear factors are involved in hepatitis C virus RNA replication. *RNA (New York, NY)*. 13:1675-1692.

Isken, O., C.W. Grassmann, R.T. Sarisky, M. Kann, S. Zhang, F. Grosse, P.N. Kao, and S.-E. Behrens. 2003. Members of the NF90/NFAR protein group are involved in the life cycle of a positive-strand RNA virus. *The EMBO journal*. 22:5655-5665.

Iwase, M., and A. Toh-e. 2004. Ybr267w is a new cytoplasmic protein belonging to the mitotic signaling network of Saccharomyces cerevisiae. *Cell structure and function*. 29:1-15.

Jønson, L., J. Vikesaa, A. Krogh, L.K. Nielsen, T.v. Hansen, R. Borup, A.H. Johnsen, J. Christiansen, and F.C. Nielsen. 2007. Molecular composition of IMP1 ribonucleoprotein granules. *Molecular & cellular proteomics : MCP*. 6:798-811.

Jordan, E.G. 1991. Interpreting nucleolar structure: where are the transcribing genes? *Journal of cell science*. 98 (Pt 4):437-442.

Jorgensen, P., I. Rupes, J.R. Sharom, L. Schneper, J.R. Broach, and M. Tyers. 2004. A dynamic transcriptional network communicates growth potential to ribosome synthesis and critical cell size. *Genes & development*. 18:2491-2505.

Kallstrom, G., J. Hedges, and A. Johnson. 2003. The putative GTPases Nog1p and Lsg1p are required for 60S ribosomal subunit biogenesis and are localized to the nucleus and cytoplasm, respectively. *Molecular and cellular biology*. 23:4344-4355.

Kao, P.N., L. Chen, G. Brock, J. Ng, J. Kenny, A.J. Smith, and B. Corthésy. 1994. Cloning and expression of cyclosporin A- and FK506-sensitive nuclear factor of activated T-cells: NF45 and NF90. *The Journal of biological chemistry*. 269:20691-20699.

Kappel, L., M. Loibl, G. Zisser, I. Klein, G. Fruhmann, C. Gruber, S. Unterweger, G. Rechberger, B. Pertschy, and H. Bergler. 2012. Rlp24 activates the AAA-ATPase Drg1 to initiate cytoplasmic pre-60S maturation. *The Journal of cell biology*. 199:771-782.

Kass, S., K. Tyc, J.A. Steitz, and B. Sollner-Webb. 1990. The U3 small nucleolar ribonucleoprotein functions in the first step of preribosomal RNA processing. *Cell*. 60:897-908.

Kemmler, S., L. Occhipinti, M. Veisu, and V.G. Panse. 2009. Yvh1 is required for a late maturation step in the 60S biogenesis pathway. *The Journal of cell biology*. 186:863-880.

Kharrat, A., M.J. Macias, T.J. Gibson, M. Nilges, and A. Pastore. 1995. Structure of the dsRNA binding domain of E. coli RNase III. *The EMBO journal*. 14:3572-3584.

Khatter, H., A.G. Myasnikov, L. Mastio, I.M.L. Billas, C. Birck, S. Stella, and B.P. Klaholz. 2014. Purification, characterization and crystallization of the human 80S ribosome. *Nucleic acids research*. (Epub)

Kiesler, P., P.A. Haynes, L. Shi, P.N. Kao, V.H. Wysocki, and D. Vercelli. 2010. NF45 and NF90 regulate HS4-dependent interleukin-13 transcription in T cells. *The Journal of biological chemistry*. 285:8256-8267.

Kim, S., Q. Li, C.V. Dang, and L.A. Lee. 2000. Induction of ribosomal genes and hepatocyte hypertrophy by adenovirus-mediated expression of c-Myc in vivo. *Proceedings of the National Academy of Sciences of the United States of America*. 97:11198-11202.

King, T.H., B. Liu, R.R. McCully, and M.J. Fournier. 2003. Ribosome structure and activity are altered in cells lacking snoRNPs that form pseudouridines in the peptidyl transferase center. *Molecular cell*. 11:425-435.

Kiss, T., E. Fayet, B.E. Jády, P. Richard, and M. Weber. 2006. Biogenesis and intranuclear trafficking of human box C/D and H/ACA RNPs. *Cold Spring Harbor symposia on quantitative biology*. 71:407-417.

Kiss-László, Z., Y. Henry, J.P. Bachellerie, M. Caizergues-Ferrer, and T. Kiss. 1996. Site-specific ribose methylation of preribosomal RNA: a novel function for small nucleolar RNAs. *Cell*. 85:1077-1088.

Klinge, S., F. Voigts-Hoffmann, M. Leibundgut, S. Arpagaus, and N. Ban. 2011. Crystal structure of the eukaryotic 60S ribosomal subunit in complex with initiation factor 6. *Science*. 334:941-948.

Klinge, S., F. Voigts-Hoffmann, M. Leibundgut, and N. Ban. 2012. Atomic structures of the eukaryotic ribosome. *Trends in biochemical sciences*. 37:189-198.

Knibiehler, B., C. Mirre, A. Navarro, and R. Rosset. 1984. Studies on chromatin organization in a nucleolus without fibrillar centres. Presence of a sub-nucleolar structure in KCo cells of Drosophila. *Cell and tissue research*. 236:279-288.

Knippschild, U., A. Gocht, S. Wolff, N. Huber, J. Löhler, and M. Stöter. 2005. The casein kinase 1 family: participation in multiple cellular processes in eukaryotes. *Cellular signalling*. 17:675-689.

Knippschild, U., D.M. Milne, L.E. Campbell, A.J. DeMaggio, E. Christenson, M.F. Hoekstra, and D.W. Meek. 1997. p53 is phosphorylated in vitro and in vivo by the delta and epsilon isoforms of casein kinase 1 and enhances the level of casein kinase 1 delta in response to topoisomerase-directed drugs. *Oncogene*. 15:1727-1736.

Krasnoselskaya-Riz, I., A. Spruill, Y.-W. Chen, D. Schuster, T. Teslovich, C. Baker, A. Kumar, and D.A. Stephan. 2002. Nuclear factor 90 mediates activation of the cellular antiviral expression cascade. *AIDS research and human retroviruses*. 18:591-604.

Kressler, D., E. Hurt, and J. Bassler. 2010. Driving ribosome assembly. *Biochimica Et Biophysica Acta-Molecular Cell Research*. 1803:673-683.

Kruse, J.-P., and W. Gu. 2009. Modes of p53 regulation. *Cell*. 137:609-622.

Kudo, N., N. Matsumori, H. Taoka, D. Fujiwara, E.P. Schreiner, B. Wolff, M. Yoshida, and S. Horinouchi. 1999. Leptomycin B inactivates CRM1/exportin 1 by covalent modification at a cysteine residue in the central conserved region. *Proceedings of the National Academy of Sciences of the United States of America*. 96:9112-9117.

Kurki, S., K. Peltonen, L. Latonen, T.M. Kiviharju, P.M. Ojala, D. Meek, and M. Laiho. 2004. Nucleolar protein NPM interacts with HDM2 and protects tumor suppressor protein p53 from HDM2-mediated degradation. *Cancer cell*. 5:465-475.

Kuwano, Y., H.H. Kim, K. Abdelmohsen, R. Pullmann, J.L. Martindale, X. Yang, and M. Gorospe. 2008. MKP-1 mRNA stabilization and translational control by RNA-binding proteins HuR and NF90. *Molecular and cellular biology*. 28:4562-4575.

la Cour, T., L. Kiemer, A. Mølgaard, R. Gupta, K. Skriver, and S. Brunak. 2004. Analysis and prediction of leucine-rich nuclear export signals. *Protein engineering, design & selection : PEDS*. 17:527-536.

Laferté, A., E. Favry, A. Sentenac, M. Riva, C. Carles, and S. Chédin. 2006. The transcriptional activity of RNA polymerase I is a key determinant for the level of all ribosome components. *Genes & development*. 20:2030-2040.

Lafontaine, D., J. Vandenhaute, and D. Tollervey. 1995. The 18S rRNA dimethylase Dim1p is required for pre-ribosomal RNA processing in yeast. *Genes & development*. 9:2470-2481.

Lafontaine, D.L., and D. Tollervey. 1998. Birth of the snoRNPs: the evolution of the modification-guide snoRNAs. *Trends in biochemical sciences*. 23:383-388.

Lamanna, A.C., and K. Karbstein. 2009. Nob1 binds the single-stranded cleavage site D at the 3'-end of 18S rRNA with its PIN domain. *Proceedings of the National Academy of Sciences of the United States of America*. 106:14259-14264.

Langland, J.O., P.N. Kao, and B.L. Jacobs. 1999. Nuclear factor-90 of activated T-cells: A double-stranded RNA-binding protein and substrate for the double-stranded RNA-dependent protein kinase, PKR. *Biochemistry*. 38:6361-6368.

Larcher, J.-C., L. Gasmi, W. Viranaicken, B. Eddé, R. Bernard, I. Ginzburg, and P. Denoulet. 2004. Ilf3 and NF90 associate with the axonal targeting element of Tau mRNA. *FASEB journal : official publication of the Federation of American Societies for Experimental Biology*. 18:1761-1763.

Lebaron, S., C. Schneider, R.W. van Nues, A. Swiatkowska, D. Walsh, B. Böttcher, S. Granneman, N.J. Watkins, and D. Tollervey. 2012. Proofreading of pre-40S ribosome maturation by a translation initiation factor and 60S subunits. *Nature structural & molecular biology*. 19:744-753.

Lebreton, A., C. Saveanu, L. Decourty, J.-C. Rain, A. Jacquier, and M. Fromont-Racine. 2006. A functional network involved in the recycling of nucleocytoplasmic pre-60S factors. *The Journal of cell biology*. 173:349-360.

Lee, C., J.P. Etchegaray, F.R. Cagampang, A.S. Loudon, and S.M. Reppert. 2001. Posttranslational mechanisms regulate the mammalian circadian clock. *Cell*. 107:855-867.

Lee, J.W., T. Hirota, E.C. Peters, M. Garcia, R. Gonzalez, C.Y. Cho, X. Wu, P.G. Schultz, and S.A. Kay. 2011. A small molecule modulates circadian rhythms through phosphorylation of the period protein. *Angewandte Chemie (International ed. in English)*. 50:10608-10611.

Léger-Silvestre, I., P. Milkereit, S. Ferreira-Cerca, C. Saveanu, J.-C. Rousselle, V. Choesmel, C. Guinefoleau, N. Gas, and P.-E. Gleizes. 2004. The ribosomal protein Rps15p is required for nuclear exit of the 40S subunit precursors in yeast. *The EMBO journal*. 23:2336-2347.

Lempiäinen, H., and D. Shore. 2009. Growth control and ribosome biogenesis. *Current opinion in cell biology*. 21:855-863.

Leung, A.K.L., L. Trinkle-Mulcahy, Y.W. Lam, J.S. Andersen, M. Mann, and A.I. Lamond. 2006. NOPdb: Nucleolar Proteome Database. *Nucleic acids research*. 34:D218-220.

Li, J., L. Yu, H. Zhang, J. Wu, J. Yuan, X. Li, and M. Li. 2009. Down-regulation of pescadillo inhibits proliferation and tumorigenicity of breast cancer cells. *Cancer science*. 100:2255-2260.

Liang, X.h., and S.T. Crooke. 2011. Depletion of key protein components of the RISC pathway impairs pre-ribosomal RNA processing. *Nucleic acids research*. 39:4875-4889.

Liang, X.h., and M.J. Fournier. 2006. The helicase Has1p is required for snoRNA release from pre-rRNA. *Molecular and cellular biology*. 26:7437-7450.

Liao, H.J., R. Kobayashi, and M.B. Mathews. 1998. Activities of adenovirus virus-associated RNAs: purification and characterization of RNA binding proteins. *Proceedings of the National Academy of Sciences of the United States of America*. 95:8514-8519.

Lin, C.Y., J. Lovén, P.B. Rahl, R.M. Paranal, C.B. Burge, J.E. Bradner, T.I. Lee, and R.A. Young. 2012. Transcriptional amplification in tumor cells with elevated c-Myc. *Cell*. 151:56-67.

Lipton, J.M., and S.R. Ellis. 2009. Diamond-Blackfan anemia: diagnosis, treatment, and molecular pathogenesis. *Hematology/oncology clinics of North America*. 23:261-282.

Lo, K.-Y., and A.W. Johnson. 2009. Reengineering ribosome export. *Molecular biology of the cell*. 20:1545-1554.

Lo, K.-Y., Z. Li, C. Bussiere, S. Bresson, E.M. Marcotte, and A.W. Johnson. 2010. Defining the pathway of cytoplasmic maturation of the 60S ribosomal subunit. *Molecular cell*. 39:196-208.

Lo, K.-Y., Z. Li, F. Wang, E.M. Marcotte, and A.W. Johnson. 2009. Ribosome stalk assembly requires the dual-specificity phosphatase Yvh1 for the exchange of Mrt4 with P0. *The Journal of cell biology*. 186:849-862.

Lohrum, M.A.E., R.L. Ludwig, M.H.G. Kubbutat, M. Hanlon, and K.H. Vousden. 2003. Regulation of HDM2 activity by the ribosomal protein L11. *Cancer cell*. 3:577-587.

Long, E.O., and I.B. Dawid. 1980. Repeated genes in eukaryotes. *Annual review of biochemistry*.

Lund, E., S. Güttinger, A. Calado, J.E. Dahlberg, and U. Kutay. 2004. Nuclear export of microRNA precursors. *Science*. 303:95-98.

Lygerou, Z., C. Allmang, D. Tollervey, and B. Séraphin. 1996. Accurate processing of a eukaryotic precursor ribosomal RNA by ribonuclease MRP in vitro. *Science*. 272:268-270.

Maggi, L.B., and J.D. Weber. 2005. Nucleolar adaptation in human cancer. *Cancer investigation*. 23:599-608.

Mais, C., J.E. Wright, J.-L. Prieto, S.L. Raggett, and B. McStay. 2005. UBF-binding site arrays form pseudo-NORs and sequester the RNA polymerase I transcription machinery. *Genes & development*. 19:50-64.

Marcel, V., S.E. Ghayad, S. Belin, G. Therizols, A.-P. Morel, E. Solano-Gonzàlez, J.A. Vendrell, S. Hacot, H.C. Mertani, M.A. Albaret, J.-C. Bourdon, L. Jordan, A. Thompson, Y. Tafer, R. Cong, P. Bouvet, J.-C. Saurin, F. Catez, A.-C. Prats, A. Puisieux, and J.-J. Diaz. 2013. p53 Acts as a Safeguard of Translational Control by Regulating Fibrillarin and rRNA Methylation in Cancer. *Cancer cell*. 24:318-330.

Marion, R.M., A. Regev, E. Segal, Y. Barash, D. Koller, N. Friedman, and E.K. O'Shea. 2004. Sfp1 is a stress- and nutrient-sensitive regulator of ribosomal protein gene expression. *Proceedings of the National Academy of Sciences of the United States of America*. 101:14315-14322.

Masliah, G., P. Barraud, and F.H.-T. Allain. 2013. RNA recognition by double-stranded RNA binding domains: a matter of shape and sequence. *Cellular and molecular life sciences : CMLS*. 70:1875-1895.

Masuda, K., Y. Kuwano, K. Nishida, K. Rokutan, and I. Imoto. 2013. NF90 in posttranscriptional gene regulation and microRNA biogenesis. *International journal of molecular sciences*. 14:17111-17121.

Matsuo, Y., S. Granneman, M. Thoms, R.-G. Manikas, D. Tollervey, and E. Hurt. 2014. Coupled GTPase and remodelling ATPase activities form a checkpoint for ribosome export. *Nature*. 505:112-116.

Mayer, C., J. Zhao, X. Yuan, and I. Grummt. 2004. mTOR-dependent activation of the transcription factor TIF-IA links rRNA synthesis to nutrient availability. *Genes & development*. 18:423-434.

McClintock, B. 1934. The relation of a particular chromosomal element to the development of the nucleoli in Zea mays. *Zeitschrift für Zellforschung und Mikroskopische Anatomie* 21:294-326

Melnikov, S., A. Ben-Shem, N. Garreau de Loubresse, L. Jenner, G. Yusupova, and M. Yusupov. 2012. One core, two shells: bacterial and eukaryotic ribosomes. *Nature structural & molecular biology*. 19:560-567.

Menne, T., B. Goyenechea, N. Sánchez-Puig, C. Wong, L. Tonkin, P. Ancliff, R. Brost, M. Costanzo, C. Boone, and A. Warren. 2007. The Shwachman-Bodian-Diamond syndrome protein mediates translational activation of ribosomes in yeast. *Nat Genet.* 39:486-495.

Merrill, M.K., and M. Gromeier. 2006. The double-stranded RNA binding protein 76:NF45 heterodimer inhibits translation initiation at the rhinovirus type 2 internal ribosome entry site. *Journal of Virology*. 80:6936-6942.

Meyer, A.E., L.A. Hoover, and E.A. Craig. 2010. The cytosolic J-protein, Jjj1, and Rei1 function in the removal of the pre-60 S subunit factor Arx1. *The Journal of biological chemistry*. 285:961-968.

Meyer, A.E., N.-J. Hung, P. Yang, A.W. Johnson, and E.A. Craig. 2007. The specialized cytosolic J-protein, Jjj1, functions in 60S ribosomal subunit biogenesis. *Proceedings of the National Academy of Sciences of the United States of America*. 104:1558-1563.

Miles, T.D., J. Jakovljevic, E.W. Horsey, P. Harnpicharnchai, L. Tang, and J.L. Woolford. 2005. Ytm1, Nop7, and Erb1 form a complex necessary for maturation of yeast 66S preribosomes. *Molecular and cellular biology*. 25:10419-10432.

Miller, G., K.I. Panov, J.K. Friedrich, L. Trinkle-Mulcahy, A.I. Lamond, and J.C. Zomerdijk. 2001. hRRN3 is essential in the SL1-mediated recruitment of RNA Polymerase I to rRNA gene promoters. *The EMBO journal*. 20:1373-1382.

Miller, O.L., and B.R. Beatty. 1969. Visualization of nucleolar genes. *Science*. 164:955-957.

Miyoshi, M., T. Okajima, T. Matsuda, M.N. Fukuda, and D. Nadano. 2007. Bystin in human cancer cells: intracellular localization and function in ribosome biogenesis. *The Biochemical journal*. 404:373-381.

Montanaro, L., D. Treré, and M. Derenzini. 2008. Nucleolus, ribosomes, and cancer. *The American journal of pathology*. 173:301-310.

Morrissey, J.P., and D. Tollervey. 1993. Yeast snR30 is a small nucleolar RNA required for 18S rRNA synthesis. *Molecular and cellular biology*. 13(4):2469-77

Moss, T. 2004. At the crossroads of growth control; making ribosomal RNA. *Current opinion in genetics & development*. 14:210-217.

Moy, T.I., and P.A. Silver. 1999. Nuclear export of the small ribosomal subunit requires the ran-GTPase cycle and certain nucleoporins. *Genes & development*. 13:2118-2133.

Moy, T.I., and P.A. Silver. 2002. Requirements for the nuclear export of the small ribosomal subunit. *Journal of cell science*. 115:2985-2995.

Mullineux, S.-T., and D.L.J. Lafontaine. 2012. Mapping the cleavage sites on mammalian pre-rRNAs: where do we stand? *Biochimie*. 94:1521-1532.

Muro, E., T.Q. Hoang, A. Jobart-Malfait, and D. Hernandez-Verdun. 2008. In nucleoli, the steady state of nucleolar proteins is leptomycin B-sensitive. *Biology of the cell / under the auspices of the European Cell Biology Organization*. 100:303-313.

Nanduri, S., B.W. Carpick, Y. Yang, B.R. Williams, and J. Qin. 1998. Structure of the double-stranded RNA-binding domain of the protein kinase PKR reveals the molecular basis of its dsRNA-mediated activation. *The EMBO journal*. 17:5458-5465.

Neplioueva, V., E.Y. Dobrikova, N. Mukherjee, J.D. Keene, and M. Gromeier. 2010. Tissue type-specific expression of the dsRNA-binding protein 76 and genome-wide elucidation of its target mRNAs. *PloS one*. 5:e11710.

Newton, K., E. Petfalski, D. Tollervey, and J.F. Cáceres. 2003. Fibrillarin is essential for early development and required for accumulation of an intron-encoded small nucleolar RNA in the mouse. *Molecular and cellular biology*. 23:8519-8527.

Ni, J., A.L. Tien, and M.J. Fournier. 1997. Small nucleolar RNAs direct site-specific synthesis of pseudouridine in ribosomal RNA. *Cell*. 89(4):565-73

Nie, Y., L. Ding, P.N. Kao, R. Braun, and J.-H. Yang. 2005. ADAR1 interacts with NF90 through double-stranded RNA and regulates NF90-mediated gene expression independently of RNA editing. *Molecular and cellular biology*. 25:6956-6963.

Nie, Z., G. Hu, G. Wei, K. Cui, A. Yamane, W. Resch, R. Wang, D.R. Green, L. Tessarollo, R. Casellas, K. Zhao, and D. Levens. 2012. c-Myc is a universal amplifier of expressed genes in lymphocytes and embryonic stem cells. *Cell*. 151:68-79.

Nigro, J.M., R. Sikorski, S.I. Reed, and B. Vogelstein. 1992. Human p53 and CDC2Hs genes combine to inhibit the proliferation of Saccharomyces cerevisiae. *Molecular and cellular biology*. 12:1357-1365.

Nissan, T.A., J. Bassler, E. Petfalski, D. Tollervey, and E. Hurt. 2002. 60S pre-ribosome formation viewed from assembly in the nucleolus until export to the cytoplasm. *The EMBO journal*. 21:5539-5547.

Nissan, T.A., K. Galani, B. Maco, D. Tollervey, U. Aebi, and E. Hurt. 2004. A pre-ribosome with a tadpole-like structure functions in ATP-dependent maturation of 60S subunits. *Molecular cell*. 15:295-301.

Nomura, M., Y. Nogi, and M. Oakes. 2004. Transcription of rDNA in the yeast Saccharomyces cerevisiae. *Molecular Biology Intelligence Unit*

O'Donohue, M.-F., V. Choesmel, M. Faubladier, G. Fichant, and P.-E. Gleizes. 2010. Functional dichotomy of ribosomal proteins during the synthesis of mammalian 40S ribosomal subunits. *The Journal of cell biology*. 190:853-866.

Occhipinti, L., Y. Chang, M. Altvater, A.M. Menet, S. Kemmler, and V.G. Panse. 2013. Non-FG mediated transport of the large pre-ribosomal subunit through the nuclear pore complex by the mRNA export factor Gle2. *Nucleic acids research*. 41:8266-8279.

Oeffinger, M., M. Dlakić, and D. Tollervey. 2004. A pre-ribosome-associated HEAT-repeat protein is required for export of both ribosomal subunits. *Genes & development*. 18:196-209.

Olson, M.O.J., and M. Dundr. 2005. The moving parts of the nucleolus. *Histochemistry and cell biology*. 123:203-216.

Ooi, S.L., D.D. Shoemaker, and J.D. Boeke. 2003. DNA helicase gene interaction network defined using synthetic lethality analyzed by microarray. *Nature genetics*. 35:277-286.

Osheim, Y.N., S.L. French, K.M. Keck, E.A. Champion, K. Spasov, F. Dragon, S.J. Baserga, and A.L. Beyer. 2004. Pre-18S ribosomal RNA is structurally compacted into the SSU processome prior to being cleaved from nascent transcripts in Saccharomyces cerevisiae. *Molecular cell*. 16:943-954.

Parker, L.M., I. Fierro-Monti, and M.B. Mathews. 2001. Nuclear factor 90 is a substrate and regulator of the eukaryotic initiation factor 2 kinase double-stranded RNA-activated protein kinase. *The Journal of biological chemistry*. 276:32522-32530.

Parrott, A.M., and M.B. Mathews. 2007. Novel rapidly evolving hominid RNAs bind nuclear factor 90 and display tissue-restricted distribution. *Nucleic acids research*. 35:6249-6258.

Parrott, A.M., M.R. Walsh, T.W. Reichman, and M.B. Mathews. 2005. RNA binding and phosphorylation determine the intracellular distribution of nuclear factors 90 and 110. *Journal of Molecular Biology*. 348:281-293.

Patel, R.C., and G.C. Sen. 1998. Requirement of PKR dimerization mediated by specific hydrophobic residues for its activation by double-stranded RNA and its antigrowth effects in yeast. *Molecular and cellular biology*. 18:7009-7019.

Patel, R.C., D.J. Vestal, Z. Xu, S. Bandyopadhyay, W. Guo, S.M. Erme, B.R. Williams, and G.C. Sen. 1999. DRBP76, a double-stranded RNA-binding nuclear protein, is phosphorylated by the interferon-induced protein kinase, PKR. *The Journal of biological chemistry*. 274:20432-20437.

Peculis, B.A., and J.A. Steitz. 1993. Disruption of U8 nucleolar snRNA inhibits 5.8S and 28S rRNA processing in the Xenopus oocyte. *Cell*. 73:1233-1245.

Pei, Y., P. Zhu, Y. Dang, J. Wu, X. Yang, B. Wan, J.O. Liu, Q. Yi, and L. Yu. 2008. Nuclear export of NF90 to stabilize IL-2 mRNA is mediated by AKT-dependent phosphorylation at Ser647 in response to CD28 costimulation. *Journal of immunology (Baltimore, Md : 1950)*. 180:222-229.

Perry, R. 1963. Selective effects of actinomycin D on the intracellular distribution of RNA synthesis in tissue culture cells. . *Exp Cell Res.*:80003-80008.

Pertschy, B., C. Saveanu, G. Zisser, A. Lebreton, M. Tengg, A. Jacquier, E. Liebminger, B. Nobis, L. Kappel, I. van der Klei, G. Högenauer, M. Fromont-Racine, and H. Bergler. 2007. Cytoplasmic recycling of 60S preribosomal factors depends on the AAA protein Drg1. *Molecular and cellular biology*. 27:6581-6592.

Pertschy, B., C. Schneider, M. Gnädig, T. Schäfer, D. Tollervey, and E. Hurt. 2009. RNA helicase Prp43 and its co-factor Pfa1 promote 20 to 18 S rRNA processing catalyzed by the endonuclease Nob1. *The Journal of biological chemistry*. 284:35079-35091.

Pestov, D.G., Y.R. Lapik, and L.F. Lau. 2008. Assays for ribosomal RNA processing and ribosome assembly. *Current Protocols in Cell ….*

Pestov, D.G., Z. Strezoska, and L.F. Lau. 2001. Evidence of p53-dependent cross-talk between ribosome biogenesis and the cell cycle: effects of nucleolar protein Bop1 on G(1)/S transition. *Molecular and cellular biology*. 21:4246-4255.

Peters, J.M., R.M. McKay, J.P. McKay, and J.M. Graff. 1999. Casein kinase I transduces Wnt signals. *Nature*. 401:345-350.

Peyroche, G., P. Milkereit, N. Bischler, H. Tschochner, P. Schultz, A. Sentenac, C. Carles, and M. Riva. 2000. The recruitment of RNA polymerase I on rDNA is mediated by the interaction of the A43 subunit with Rrn3. *The EMBO journal*. 19:5473-5482.

Pfeifer, I., R. Elsby, M. Fernandez, P.A. Faria, D.R. Nussenzveig, I.S. Lossos, B.M.A. Fontoura, W.D. Martin, and G.N. Barber. 2008. NFAR-1 and -2 modulate translation and are required for efficient host defense. *Proceedings of the National Academy of Sciences of the United States of America*. 105:4173-4178.

Phair, R.D., and T. Misteli. 2000. High mobility of proteins in the mammalian cell nucleus. *Nature*. 404:604-609.

Pierce, A.J., P. Hu, M. Han, N. Ellis, and M. Jasin. 2001. Ku DNA end-binding protein modulates homologous repair of double-strand breaks in mammalian cells. *Genes & development*. 15:3237-3242.

Pool, M.R., J. Stumm, T.A. Fulga, I. Sinning, and B. Dobberstein. 2002. Distinct modes of signal recognition particle interaction with the ribosome. *Science*. 297:1345-1348.

Poortinga, G., K.M. Hannan, H. Snelling, C.R. Walkley, A. Jenkins, K. Sharkey, M. Wall, Y. Brandenburger, M. Palatsides, R.B. Pearson, G.A. McArthur, and R.D. Hannan. 2004. MAD1 and c-MYC regulate UBF and rDNA transcription during granulocyte differentiation. *The EMBO journal*. 23:3325-3335.

Preti, M., M.-F. O'Donohue, N. Montel-Lehry, M.-L. Bortolin-Cavaillé, V. Choesmel, and P.-E. Gleizes. 2013. Gradual processing of the ITS1 from the nucleolus to the cytoplasm during synthesis of the human 18S rRNA. *Nucleic acids research*. 41:4709-4723.

Puvion-Dutilleul, F., E. Puvion, and J.P. Bachellerie. 1997. Early stages of pre-rRNA formation within the nucleolar ultrastructure of mouse cells studied by in situ hybridization with a 5'ETS leader probe. *Chromosoma*. 105:496-505.

Quin, J.E., J.R. Devlin, D. Cameron, K.M. Hannan, R.B. Pearson, and R.D. Hannan. 2014. Targeting the nucleolus for cancer intervention. *Biochimica et biophysica acta*.

Rabl, J., M. Leibundgut, S.F. Ataide, A. Haag, and N. Ban. 2011. Crystal Structure of the Eukaryotic 40S Ribosomal Subunit in Complex with Initiation Factor 1. *Science*.

Ray, P., U. Basu, A. Ray, R. Majumdar, H. Deng, and U. Maitra. 2008. The Saccharomyces cerevisiae 60 S ribosome biogenesis factor Tif6p is regulated by Hrr25p-mediated phosphorylation. *The Journal of biological chemistry*. 283:9681-9691.

Reichman, T.W., and M.B. Mathews. 2003. RNA binding and intramolecular interactions modulate the regulation of gene expression by nuclear factor 110. *RNA (New York, NY)*. 9:543-554.

Reichman, T.W., L.C. Muñiz, and M.B. Mathews. 2002. The RNA binding protein nuclear factor 90 functions as both a positive and negative regulator of gene expression in mammalian cells. *Molecular and cellular biology*. 22:343-356.

Reichman, T.W., A.M. Parrott, I. Fierro-Monti, D.J. Caron, P.N. Kao, C.-G. Lee, H. Li, and M.B. Mathews. 2003. Selective regulation of gene expression by nuclear factor 110, a member of the NF90 family of double-stranded RNA-binding proteins. *Journal of Molecular Biology*. 332:85-98.

Rena, G., J. Bain, M. Elliott, and P. Cohen. 2004. D4476, a cell-permeant inhibitor of CK1, suppresses the site-specific phosphorylation and nuclear exclusion of FOXO1a. *EMBO reports*. 5:60-65.

Rigo, F., Y. Hua, S.J. Chun, T.P. Prakash, A.R. Krainer, and C.F. Bennett. 2012. Synthetic oligonucleotides recruit ILF2/3 to RNA transcripts to modulate splicing. *Nature chemical biology*. 8:555-561.

Rodríguez-Mateos, M., J.J. García-Gómez, R. Francisco-Velilla, M. Remacha, J. de la Cruz, and J.P.G. Ballesta. 2009. Role and dynamics of the ribosomal protein P0 and its related trans-acting factor Mrt4 during ribosome assembly in Saccharomyces cerevisiae. *Nucleic acids research*. 37:7519-7532.

Romano, P.R., F. Zhang, S.L. Tan, M.T. Garcia-Barrio, M.G. Katze, T.E. Dever, and A.G. Hinnebusch. 1998. Inhibition of double-stranded RNA-dependent protein kinase PKR

by vaccinia virus E3: role of complex formation and the E3 N-terminal domain. *Molecular and cellular biology*. 18:7304-7316.

Rouquette, J., V. Choesmel, and P.-E. Gleizes. 2005. Nuclear export and cytoplasmic processing of precursors to the 40S ribosomal subunits in mammalian cells. *The EMBO journal*. 24:2862-2872.

Sakamoto, S., K. Aoki, T. Higuchi, H. Todaka, K. Morisawa, N. Tamaki, E. Hatano, A. Fukushima, T. Taniguchi, and Y. Agata. 2009. The NF90-NF45 complex functions as a negative regulator in the microRNA processing pathway. *Molecular and cellular biology*. 29:3754-3769.

Sanij, E., and R.D. Hannan. 2009. The role of UBF in regulating the structure and dynamics of transcriptionally active rDNA chromatin. *Epigenetics : official journal of the DNA Methylation Society*. 4:374-382.

Sanij, E., G. Poortinga, K. Sharkey, S. Hung, T.P. Holloway, J. Quin, E. Robb, L.H. Wong, W.G. Thomas, V. Stefanovsky, T. Moss, L. Rothblum, K.M. Hannan, G.A. McArthur, R.B. Pearson, and R.D. Hannan. 2008. UBF levels determine the number of active ribosomal RNA genes in mammals. *The Journal of cell biology*. 183:1259-1274.

Santoro, R., and I. Grummt. 2001. Molecular mechanisms mediating methylation-dependent silencing of ribosomal gene transcription. *Molecular cell*. 8:719-725.

Santos-Rosa, H., H. Moreno, G. Simos, A. Segref, B. Fahrenkrog, N. Panté, and E. Hurt. 1998. Nuclear mRNA export requires complex formation between Mex67p and Mtr2p at the nuclear pores. *Molecular and cellular biology*. 18:6826-6838.

Saunders, L.R., V. Jurecic, and G.N. Barber. 2001. The 90- and 110-kDa human NFAR proteins are translated from two differentially spliced mRNAs encoded on chromosome 19p13. *Genomics*. 71:256-259.

Saveanu, C., A. Namane, P.-E. Gleizes, A. Lebreton, J.-C. Rousselle, J. Noaillac-Depeyre, N. Gas, A. Jacquier, and M. Fromont-Racine. 2003. Sequential protein association with nascent 60S ribosomal particles. *Molecular and cellular biology*. 23:4449-4460.

Savino, T.M., J. Gébrane-Younès, J. De Mey, J.B. Sibarita, and D. Hernandez-Verdun. 2001. Nucleolar assembly of the rRNA processing machinery in living cells. *The Journal of cell biology*. 153:1097-1110.

Saxena, A., C.J. Rorie, D. Dimitrova, Y. Daniely, and J.A. Borowiec. 2006. Nucleolin inhibits Hdm2 by multiple pathways leading to p53 stabilization. *Oncogene*. 25:7274-7288.

Schäfer, T., B. Maco, E. Petfalski, D. Tollervey, B. Böttcher, U. Aebi, and E. Hurt. 2006. Hrr25-dependent phosphorylation state regulates organization of the pre-40S subunit. *Nature*. 441:651-655.

Schäfer, T., D. Strauss, E. Petfalski, D. Tollervey, and E. Hurt. 2003. The path from nucleolar 90S to cytoplasmic 40S pre-ribosomes. *The EMBO journal*. 22:1370-1380.

Scheffner, M., B.A. Werness, J.M. Huibregtse, A.J. Levine, and P.M. Howley. 1990. The E6 oncoprotein encoded by human papillomavirus types 16 and 18 promotes the degradation of p53. *Cell*. 63:1129-1136.

Schlosser, I., M. Hölzel, M. Mürnseer, H. Burtscher, U.H. Weidle, and D. Eick. 2003. A role for c-Myc in the regulation of ribosomal RNA processing. *Nucleic acids research*. 31:6148-6156.

Schmidt-Zachmann, M.S., C. Dargemont, L.C. Kühn, and E.A. Nigg. 1993. Nuclear export of proteins: the role of nuclear retention. *Cell*. 74:493-504.

Segref, A., K. Sharma, V. Doye, A. Hellwig, J. Huber, R. Lührmann, and E. Hurt. 1997. Mex67p, a novel factor for nuclear mRNA export, binds to both poly(A)+ RNA and nuclear pores. *The EMBO journal*. 16:3256-3271.

Seiser, R.M., A.E. Sundberg, B.J. Wollam, P. Zobel-Thropp, K. Baldwin, M.D. Spector, and D.E. Lycan. 2006. Ltv1 is required for efficient nuclear export of the ribosomal small subunit in Saccharomyces cerevisiae. *Genetics*. 174:679-691.

Senay, C., P. Ferrari, C. Rocher, K.-J. Rieger, J. Winter, D. Platel, and Y. Bourne. 2003. The Mtr2-Mex67 NTF2-like domain complex. Structural insights into a dual role of Mtr2 for yeast nuclear export. *The Journal of biological chemistry*. 278:48395-48403.

Senger, B., D.L. Lafontaine, J.S. Graindorge, O. Gadal, A. Camasses, A. Sanni, J.M. Garnier, M. Breitenbach, E. Hurt, and F. Fasiolo. 2001. The nucle(ol)ar Tif6p and Efl1p are required for a late cytoplasmic step of ribosome synthesis. *Molecular cell*. 8:1363-1373.

Sengupta, J., C. Bussiere, J. Pallesen, M. West, A.W. Johnson, and J. Frank. 2010. Characterization of the nuclear export adaptor protein Nmd3 in association with the 60S ribosomal subunit. *The Journal of cell biology*. 189:1079-1086.

Shabman, R.S., D.W. Leung, J. Johnson, N. Glennon, E.E. Gulcicek, K.L. Stone, L. Leung, L. Hensley, G.K. Amarasinghe, and C.F. Basler. 2011. DRBP76 associates with Ebola virus VP35 and suppresses viral polymerase function. *The Journal of infectious diseases*. 204 Suppl 3:S911-918.

Shajani, Z., M.T. Sykes, and J.R. Williamson. 2011. Assembly of bacterial ribosomes. *Annual review of biochemistry*. 80:501-526.

Shamanna, R.A., M. Hoque, A. Lewis-Antes, E.I. Azzam, D. Lagunoff, T. Pe'ery, and M.B. Mathews. 2011. The NF90/NF45 complex participates in DNA break repair via nonhomologous end joining. *Molecular and cellular biology*. 31:4832-4843.

Shamanna, R.A., M. Hoque, T. Peery, and M.B. Mathews. 2013. Induction of p53, p21 and apoptosis by silencing the NF90/NF45 complex in human papilloma virus-transformed cervical carcinoma cells. *Oncogene*. 32:5176-5185.

Shaw, J.P., P.J. Utz, D.B. Durand, J.J. Toole, E.A. Emmel, and G.R. Crabtree. 1988. Identification of a putative regulator of early T cell activation genes. *Science*. 241:202-205.

Shea, J.R., and C.P. Leblond. 1966. Number of nucleoli in various cell types of the mouse. *Journal of morphology*. 119:425-433.

Shi, L., D. Qiu, G. Zhao, B. Corthesy, S. Lees-Miller, W.H. Reeves, and P.N. Kao. 2007. Dynamic binding of Ku80, Ku70 and NF90 to the IL-2 promoter in vivo in activated T-cells. *Nucleic acids research*. 35:2302-2310.

Shim, C., W. Zhang, C.H. Rhee, and J.H. Lee. 1998. Profiling of differentially expressed genes in human primary cervical cancer by complementary DNA expression array. *Clinical cancer research : an official journal of the American Association for Cancer Research*. 4:3045-3050.

Shim, J., H. Lim, J. R Yates, and M. Karin. 2002. Nuclear export of NF90 is required for interleukin-2 mRNA stabilization. *Molecular cell*. 10:1331-1344.

Shimamura, A. 2006. Shwachman-Diamond syndrome. *Seminars in hematology*. 43:178-188.

Sloan, K.E., M.T. Bohnsack, and N.J. Watkins. 2013a. The 5S RNP couples p53 homeostasis to ribosome biogenesis and nucleolar stress. *Cell reports*. 5:237-247.

Sloan, K.E., S. Mattijssen, S. Lebaron, D. Tollervey, G.J.M. Pruijn, and N.J. Watkins. 2013b. Both endonucleolytic and exonucleolytic cleavage mediate ITS1 removal during human ribosomal RNA processing. *The Journal of cell biology*. 200:577-588.

Soudet, J., J.-P. Gelugne, K. Belhabich-Baumas, M. Caizergues-Ferrer, and A. Mougin. 2010. Immature small ribosomal subunits can engage in translation initiation in Saccharomyces cerevisiae. *The EMBO journal*. 29:80-92.

Spahn, C., R. Beckmann, N. Eswar, and P.A. Penczek. 2001. Structure of the 80S Ribosome from Saccharomyces cerevisiae—tRNA-Ribosome and Subunit-Subunit Interactions. *Cell*. 107:373-386.

Squatrito, M., M. Mancino, M. Donzelli, L.B. Areces, and G.F. Draetta. 2004. EBP1 is a nucleolar growth-regulating protein that is part of pre-ribosomal ribonucleoprotein complexes. *Oncogene*. 23:4454-4465.

St Johnston, D., N.H. Brown, J.G. Gall, and M. Jantsch. 1992. A conserved double-stranded RNA-binding domain. *Proceedings of the National Academy of Sciences of the United States of America*. 89:10979-10983.

Stage-Zimmermann, T., U. Schmidt, and P.A. Silver. 2000. Factors affecting nuclear export of the 60S ribosomal subunit in vivo. *Molecular biology of the cell*. 11:3777-3789.

Strezoska, Z., D.G. Pestov, and L.F. Lau. 2000. Bop1 is a mouse WD40 repeat nucleolar protein involved in 28S and 5. 8S RRNA processing and 60S ribosome biogenesis. *Molecular and cellular biology*. 20:5516-5528.

Strunk, B.S., and K. Karbstein. 2009. Powering through ribosome assembly. *RNA (New York, NY)*. 15:2083-2104.

Strunk, B.S., C.R. Loucks, M. Su, H. Vashisth, S. Cheng, J. Schilling, C.L. Brooks, K. Karbstein, and G. Skiniotis. 2011. Ribosome assembly factors prevent premature translation initiation by 40S assembly intermediates. *Science*. 333:1449-1453.

Stults, D.M., M.W. Killen, H.H. Pierce, and A.J. Pierce. 2007. Genomic architecture and inheritance of human ribosomal RNA gene clusters. *Genome research*. 18:13-18.

Takagi, M., M.J. Absalon, K.G. McLure, and M.B. Kastan. 2005. Regulation of p53 translation and induction after DNA damage by ribosomal protein L26 and nucleolin. *Cell*. 123:49-63.

Taylor, D., B. Devkota, A. Huang, M. Topf, E. Najayanan, A. Sali, S. Harvey, and J. Frank. 2009. Comprehensive molecular structure of the eukaryotic ribosome. *Structure*. 17:1591-1604.

Tessarz, P., H. Santos-Rosa, S.C. Robson, K.B. Sylvestersen, C.J. Nelson, M.L. Nielsen, and T. Kouzarides. 2014. Glutamine methylation in histone H2A is an RNA-polymerase-I-dedicated modification. *Nature*. 505:564-568.

Thiry, M., and D.L.J. Lafontaine. 2005. Birth of a nucleolus: the evolution of nucleolar compartments. *Trends in cell biology*. 15:194-199.

Thomas, F., and U. Kutay. 2003. Biogenesis and nuclear export of ribosomal subunits in higher eukaryotes depend on the CRM1 export pathway. *Journal of cell science*. 116:2409-2419.

Thomson, E., S. Ferreira-Cerca, and E. Hurt. 2013. Eukaryotic ribosome biogenesis at a glance. *Journal of cell science*. 126:4815-4821.

Ting, N.S., P.N. Kao, D.W. Chan, L.G. Lintott, and S.P. Lees-Miller. 1998. DNA-dependent protein kinase interacts with antigen receptor response element binding proteins NF90 and NF45. *The Journal of biological chemistry*. 273:2136-2145.

Tollervey, D., H. Lehtonen, M. Carmo-Fonseca, and E.C. Hurt. 1991. The small nucleolar RNP protein NOP1 (fibrillarin) is required for pre-rRNA processing in yeast. *The EMBO journal*. 10:573-583.

Traub, P., and M. Nomura. 1969. Studies on the assembly of ribosomes in vitro. *Cold Spring Harbor symposia on quantitative biology*. 34:63-67.

Treré, D., C. Ceccarelli, L. Montanaro, E. Tosti, and M. Derenzini. 2004. Nucleolar size and activity are related to pRb and p53 status in human breast cancer. *The journal of histochemistry and cytochemistry : official journal of the Histochemistry Society*. 52:1601-1607.

Trotta, C.R., E. Lund, L. Kahan, A.W. Johnson, and J.E. Dahlberg. 2003. Coordinated nuclear export of 60S ribosomal subunits and NMD3 in vertebrates. *The EMBO journal*. 22:2841-2851.

Tschochner, H., and E. Hurt. 2003. Pre-ribosomes on the road from the nucleolus to the cytoplasm. *Trends in cell biology*. 13:255-263.

Ulbrich, C., M. Diepholz, J. Bassler, D. Kressler, B. Pertschy, K. Galani, B. Böttcher, and E. Hurt. 2009. Mechanochemical removal of ribosome biogenesis factors from nascent 60S ribosomal subunits. *Cell*. 138:911-922.

Valenzuela, D.M., A. Chaudhuri, and U. Maitra. 1982. Eukaryotic ribosomal subunit anti-association activity of calf liver is contained in a single polypeptide chain protein of Mr = 25,500 (eukaryotic initiation factor 6). *The Journal of biological chemistry*. 257:7712-7719.

Vannini, A. 2013. A structural perspective on RNA polymerase I and RNA polymerase III transcription machineries. *Biochimica et biophysica acta*. 1829:258-264.

Vanrobays, E., J.-P. Gelugne, P.-E. Gleizes, and M. Caizergues-Ferrer. 2003. Late cytoplasmic maturation of the small ribosomal subunit requires RIO proteins in Saccharomyces cerevisiae. *Molecular and cellular biology*. 23:2083-2095.

Vanrobays, E., P.E. Gleizes, C. Bousquet-Antonelli, J. Noaillac-Depeyre, M. Caizergues-Ferrer, and J.P. Gélugne. 2001. Processing of 20S pre-rRNA to 18S ribosomal RNA in yeast requires Rrp10p, an essential non-ribosomal cytoplasmic protein. *The EMBO journal*. 20:4204-4213.

Vanrobays, E., A. Leplus, Y.N. Osheim, A.L. Beyer, L. Wacheul, and D.L.J. Lafontaine. 2008. TOR regulates the subcellular distribution of DIM2, a KH domain protein required for cotranscriptional ribosome assembly and pre-40S ribosome export. *RNA (New York, NY)*. 14:2061-2073.

Venema, J., and D. Tollervey. 1999. Ribosome synthesis in Saccharomyces cerevisiae. *Annual review of genetics*. 33:261-311.

Volarevic, S., M.J. Stewart, B. Ledermann, F. Zilberman, L. Terracciano, E. Montini, M. Grompe, S.C. Kozma, and G. Thomas. 2000. Proliferation, but not growth, blocked by conditional deletion of 40S ribosomal protein S6. *Science*. 288:2045-2047.

Vousden, K.H., and C. Prives. 2009. Blinded by the Light: The Growing Complexity of p53. *Cell*. 137:413-431.

Wagner, R. 1835. Einige Bemerkungen und Fragen über das Keimbläschen (vesicula germinativa). . *Müller's Arch. Anat. Physiol. Wissenschaftliche Med.*:373-377. .

Wahl, M.C., and W. Möller. 2002. Structure and function of the acidic ribosomal stalk proteins. *Current protein & peptide science*. 3:93-106.

Walker, J., P. Crowley, A.D. Moreman, and J. Barrett. 1993. Biochemical properties of cloned glutathione S-transferases from Schistosoma mansoni and Schistosoma japonicum. *Molecular and biochemical parasitology*. 61:255-264.

Walton, K.M., K. Fisher, D. Rubitski, M. Marconi, Q.-J. Meng, M. Sládek, J. Adams, M. Bass, R. Chandrasekaran, T. Butler, M. Griffor, F. Rajamohan, M. Serpa, Y. Chen, M. Claffey, M. Hastings, A. Loudon, E. Maywood, J. Ohren, A. Doran, and T.T. Wager. 2009. Selective inhibition of casein kinase 1 epsilon minimally alters circadian clock period. *The Journal of pharmacology and experimental therapeutics*. 330:430-439.

Wang, M., and D.G. Pestov. 2011. 5'-end surveillance by Xrn2 acts as a shared mechanism for mammalian pre-rRNA maturation and decay. *Nucleic acids research*. 39:1811-1822.

Wang, P., W. Song, B.W.-Y. Mok, P. Zhao, K. Qin, A. Lai, G.J.D. Smith, J. Zhang, T. Lin, Y. Guan, and H. Chen. 2009. Nuclear factor 90 negatively regulates influenza virus replication by interacting with viral nucleoprotein. *Journal of Virology*. 83:7850-7861.

Warner, J.R. 1999. The economics of ribosome biosynthesis in yeast. *Trends in biochemical sciences*. 24:437-440.

Warner, J.R., and R. Soeiro. 1967. Nascent ribosomes from HeLa cells. *Proceedings of the National Academy of Sciences of the United States of America*. 58:1984-1990.

Watkins, N.J., and M.T. Bohnsack. 2012. The box C/D and H/ACA snoRNPs: key players in the modification, processing and the dynamic folding of ribosomal RNA. *Wiley interdisciplinary reviews. RNA*. 3:397-414.

Weisser, M., F. Voigts-Hoffmann, J. Rabl, M. Leibundgut, and N. Ban. 2013. The crystal structure of the eukaryotic 40S ribosomal subunit in complex with eIF1 and eIF1A. *Nature structural & molecular biology*. 20:1015-1017.

West, M., J.B. Hedges, A. Chen, and A.W. Johnson. 2005. Defining the order in which Nmd3p and Rpl10p load onto nascent 60S ribosomal subunits. *Molecular and cellular biology*. 25:3802-3813

Widmann, B., F. Wandrey, L. Badertscher, E. Wyler, J. Pfannstiel, I. Zemp, and U. Kutay. 2012. The kinase activity of human Rio1 is required for final steps of cytoplasmic maturation of 40S subunits. *Molecular biology of the cell*. 23:22-35.

Wild, T., P. Horvath, E. Wyler, B. Widmann, L. Badertscher, I. Zemp, K. Kozak, G. Csucs, E. Lund, and U. Kutay. 2010. A protein inventory of human ribosome biogenesis reveals an essential function of exportin 5 in 60S subunit export. *PLoS biology*. 8:e1000522.

Wilson, D.N., and J.H. Doudna Cate. 2012. The Structure and Function of the Eukaryotic Ribosome. *Cold Spring Harbor perspectives in biology*. 4:a011536-a011536.

Wolkowicz, U.M., and A.G. Cook. 2012. NF45 dimerizes with NF90, Zfr and SPNR via a conserved domain that has a nucleotidyltransferase fold. *Nucleic acids research*. 40:9356-9368.

Woolford, J.L., and S.J. Baserga. 2013. Ribosome biogenesis in the yeast Saccharomyces cerevisiae. *Genetics*. 195:643-681.

Wu, X., J.H. Bayle, D. Olson, and A.J. Levine. 1993. The p53-mdm-2 autoregulatory feedback loop. *Genes & development*. 7:1126-1132.

Wullschleger, S., R. Loewith, and M.N. Hall. 2006. TOR signaling in growth and metabolism. *Cell*. 124:471-484.

Wyler, E., M. Zimmermann, B. Widmann, M. Gstaiger, J. Pfannstiel, U. Kutay, and I. Zemp. 2011. Tandem affinity purification combined with inducible shRNA expression as a tool to study the maturation of macromolecular assemblies. *RNA (New York, NY)*. 17:189-200.

Xu, D., A. Farmer, and Y.M. Chook. 2010. Recognition of nuclear targeting signals by Karyopherin-β proteins. *Current opinion in structural biology*. 20:782-790.

Xue, S., and M. Barna. 2012. Specialized ribosomes: a new frontier in gene regulation and organismal biology. *Nature reviews. Molecular cell biology*. 13:355-369.

Yamauchi, K., M. Yang, K. Hayashi, P. Jiang, N. Yamamoto, H. Tsuchiya, K. Tomita, A.R. Moossa, M. Bouvet, and R.M. Hoffman. 2007. Imaging of nucleolar dynamics during the cell cycle of cancer cells in live mice. *Cell cycle (Georgetown, Tex)*. 6:2706-2708.

Yanagida, M., A. Shimamoto, K. Nishikawa, Y. Furuichi, T. Isobe, and N. Takahashi. 2001. Isolation and proteomic characterization of the major proteins of the nucleolin-binding ribonucleoprotein complexes. *Proteomics*. 1:1390-1404.

Yang, J.-H., X.-C. Zhang, Z.-P. Huang, H. Zhou, M.-B. Huang, S. Zhang, Y.-Q. Chen, and L.-H. Qu. 2006. snoSeeker: an advanced computational package for screening of guide and orphan snoRNA genes in the human genome. *Nucleic acids research*. 34:5112-5123.

Yao, W., D. Roser, A. Köhler, B. Bradatsch, J. Bassler, and E. Hurt. 2007. Nuclear export of ribosomal 60S subunits by the general mRNA export receptor Mex67-Mtr2. *Molecular cell*. 26:51-62.

Yao, Y., E. Demoinet, C. Saveanu, P. Lenormand, A. Jacquier, and M. Fromont-Racine. 2010. Ecm1 is a new pre-ribosomal factor involved in pre-60S particle export. *RNA (New York, NY)*. 16:1007-1017.

Yaseen, N.R., A.L. Maizel, F. Wang, and S. Sharma. 1993. Comparative analysis of NFAT (nuclear factor of activated T cells) complex in human T and B lymphocytes. *The Journal of biological chemistry*. 268:14285-14293.

Yoon, A., G. Peng, Y. Brandenburger, Y. Brandenburg, O. Zollo, W. Xu, E. Rego, and D. Ruggero. 2006. Impaired control of IRES-mediated translation in X-linked dyskeratosis congenita. *Science*. 312:902-906.

Zeller, K.I., T.J. Haggerty, J.F. Barrett, Q. Guo, D.R. Wonsey, and C.V. Dang. 2001. Characterization of nucleophosmin (B23) as a Myc target by scanning chromatin immunoprecipitation. *The Journal of biological chemistry*. 276:48285-48291.

Zemp, I., and U. Kutay. 2007. Nuclear export and cytoplasmic maturation of ribosomal subunits. *FEBS letters*. 581:2783-2793.

Zemp, I., T. Wild, M.-F. O'Donohue, F. Wandrey, B. Widmann, P.-E. Gleizes, and U. Kutay. 2009. Distinct cytoplasmic maturation steps of 40S ribosomal subunit precursors require hRio2. *The Journal of cell biology*. 185:1167-1180.

Zhang, J., P. Harnpicharnchai, J. Jakovljevic, L. Tang, Y. Guo, M. Oeffinger, M.P. Rout, S.L. Hiley, T. Hughes, and J.L. Woolford. 2007. Assembly factors Rpf2 and Rrs1 recruit 5S rRNA and ribosomal proteins rpL5 and rpL11 into nascent ribosomes. *Genes & development*. 21:2580-2592.

Zhang, Y., and H. Lu. 2009. Signaling to p53: ribosomal proteins find their way. *Cancer cell*. 16:369-377.

Zhu, Y., M.V. Poyurovsky, Y. Li, L. Biderman, J. Stahl, X. Jacq, and C. Prives. 2009. Ribosomal protein S7 is both a regulator and a substrate of MDM2. *Molecular cell*. 35:316-326.

7. Abbreviations

AAA ATPAse	ATPase associated with diverse cellular activities
Arg	arginine
ATP	Adenosine triphosphate
ATPase	ATP hydrolyzing protein
BSA	Bovine serum albumin
CK1	casein kinase 1
DBA	Diamond-Blackfan anemia
DFC	dense fibrillar component
DMEM	Dulbecco`s Modified Eagle Medium
DMSO	dimethyl sulfoxide
DNA	deoxyribonucleic acid
dsRBD	double-stranded RNA binding domain
DTT	dithiothreitol
EDTA	ethylene diamine tetraacetic acid
EGTA	ethylene glycol tetraacetic acid
EM	electron microscopy
ETS	external transcribed spacer
FBS	fetal bovine serum
FC	fibrillar center
FG	phenylalanine-glycine
FISH	fluorescence in situ hybridization
GAP	GTPase-activating protein
GC	granular component
GFP	green fluorescent protein
Glu	glutamic acid
GDP	guanosine diphosphate
GTP	guanosine triphosphate
GTPase	GTP hydrolyzing protein
IF	immunofluorescence
ILF	interleukin enhancer binding factor
IPTG	isopropyl β-D-thiogalactopyranoside
ITS	internal transcribed spacer
HASt	N-terminal tandem HA-tag/streptavidin-binding peptide
HEAT repeat	Huntingtin/Elongation factor 3/ Protein phosphatase 2A/ Target of Rapamycin 1 repeat
HeLa	Henrietta Lacks
HEPES	N-(2-Hydroxyethyl)piperazine-N'-(2-ethanesulfonic acid)
kb	kilobase
kDa	kilodalton
KOAc	potassium acetate
LB	Luria Broth
LMB	leptomycin B
LSU	large subunit
miRNA	micro RNA
mRNA	messenger RNA
NES	nuclear export signal
NLS	nuclear localization sequence
NOR	nucleolar organizer regions

NPC	nuclear pore complex
nt	nucleotides
NTA	nitriloacetic acid
Nups	Nucleoporins
PAA	polyacrylamid gel
PAGE	polyacrylamide gel electrophoresis
PBS	phosphate buffered saline
PCR	polymerase chain reaction
PFA	paraformaldehyde
PMSF	phenylmethylsulfonyl fluoride
POL I	RNA polymerase I
POL II	RNA polymerase II
POL III	RNA polymerase III
pre-rRNA	precursor ribosomal RNA
rcf	relative centrifugal force
rDNA	ribosomal DNA
RNA	ribonucleic acid
RNAi	RNA interference
RPL	ribosomal proteins of the large subunit
rpm	revolutions per minute
RPS	ribosomal proteins of the small subunit
rRNA	ribosomal RNA
RT	room temperature
SDS	Shwachman-Bodian-Diamond syndrome
SDS	sodium dodecyl sulfate
siRNA	small interfering RNA
snoRNA	small nucleolar RNA
snoRNP	small nucleolar ribonucleoprotein
SSU	small subunit
StHA	C-terminal tandem streptavidin-binding peptide/HA-tag
TAP	tandem affinity purification
TCA	trichloro acetic acid
TOP	terminal oligopyrimidine tract
TOR	target of rapamycin
Tris	tris(hydroxymethyl)aminoethane
tRNA	transfer RNA
v/v	volume per volume
wt	wild type
w/v	weight per volume
X-DC	X-linked dyskeratosis congenital
YFP	yellow fluorescent protein
zz	two IgG binding domains of Protein A

Acknowledgements

It is a long path from starting a PhD project until the thesis is finished. Fortunately, I never had to walk alone because many people have helped me along the way, to whom I hereby would like to express my gratitude.

First and foremost, I would like to sincerely thank Prof. Ulrike Kutay for trusting me with these exciting projects and for all her support and encouragement throughout my PhD.

I am very thankful to Prof. Frédéric Allain, Prof. André Gerber, and Prof. Pierre-Emmanuel Gleizes for agreeing to serve as members of my thesis committee as well as co-examiners of this thesis, and especially for the fruitful discussions and valuable input to my project during the committee meetings.

Good science does not work without collaborations. I would like to thank Dr. Emanuel Wyler for generating PAR-CLIP data of NF90 and lots of helpful discussions about TAPs. I am especially thankful to Dr. Ivo Zemp for starting and working together with me on the CK1 project as well as teaching me many valuable things during my start in the Kutay lab. I am grateful to Dr. Marie-Françoise O'Donohue for performing experiments to further investigate the role of CK1 in rRNA processing and to Dr. Atlanta Cook for sharing NF90 constructs and helpful discussions. Many thanks to Dr. Sanjana Rao for contributing to the CK1 project by performing many kinase assays and for correcting parts of my thesis. Speaking of thesis proofreading: I am very grateful to Christian Montellese and Lukas Bammert for correcting my thesis. It is great to see that after having the pleasure to supervising you as students, you can in turn give me advice now.

I would like to extend my gratefulness to all the past and present members of the Kutay lab who have made the lab a great place to work and have fun. It would take up too much space to mention all of you but I promise that every one of you is very much appreciated. Special thanks go to Caroline Ashiono for constant technical support throughout the years.

Thanks to the IBC staff to keep the place running, especially Anton Lehmann, Nico Graf and Roland Stuber for having an open ear for my problems and – even better – a solution at hand.

Last but not least, I would like to show my gratitude to my parents and my brother, the best family one could wish for, which supported me throughout the years and taught me many important things you will not find in a text book. Words cannot express how thankful I am to Dave for being on my side for so many years as a partner and best friend and his support and patience during the sometimes rocky road of a PhD – thank you!